

# UC Berkeley

## UC Berkeley Electronic Theses and Dissertations

### Title

Computations and Moduli Spaces for Non-archimedean Varieties

### Permalink

<https://escholarship.org/uc/item/75s061fw>

### Author

Ren, Qingchun

### Publication Date

2014

Peer reviewed|Thesis/dissertation

**Computations and Moduli Spaces for Non-archimedean Varieties**

by

Qingchun Ren

A dissertation submitted in partial satisfaction of the  
requirements for the degree of  
Doctor of Philosophy

in

Mathematics

in the

Graduate Division

of the

University of California, Berkeley

Committee in charge:

Professor Bernd Sturmfels, Chair  
Professor Mark Haiman  
Professor Haiyan Huang

Spring 2014

# Computations and Moduli Spaces for Non-archimedean Varieties

Copyright 2014  
by  
Qingchun Ren

## Abstract

Computations and Moduli Spaces for Non-archimedean Varieties

by

Qingchun Ren

Doctor of Philosophy in Mathematics

University of California, Berkeley

Professor Bernd Sturmfels, Chair

Tropical geometry and non-archimedean analytic geometry study algebraic varieties over a field  $K$  with a non-archimedean valuation. One of the major goals is to classify varieties over  $K$  by intrinsic tropical properties. This thesis will contain my work at UC Berkeley and my joint work with others towards the goal.

Chapter 2 discusses some moduli spaces and their tropicalizations. The image of the complement of a hyperplane arrangement under a monomial map can be tropicalized combinatorially using matroid theory. We apply this to classical moduli spaces that are associated with complex reflection arrangements. Starting from modular curves, we visit the Segre cubic, the Igusa quartic, and moduli of marked del Pezzo surfaces of degrees 2 and 3. Our primary example is the Burkhardt quartic, whose tropicalization is a 3-dimensional fan in 39-dimensional space. This effectuates a synthesis of concrete and abstract approaches to tropical moduli of genus 2 curves.

Chapter 3 develops numerical algorithms for Mumford curves over the field of  $p$ -adic numbers. Mumford curves are foundational to subjects dealing with non-archimedean varieties, and it has various applications in number theory. We implement algorithms for tasks such as: approximating the period matrices of the Jacobians of Mumford curves; computing the Berkovich skeleta of their analytifications; and approximating points in canonical embeddings.

Chapter 4 discusses how to tropicalize del Pezzo surfaces of degree 5, 4 and 3. A generic cubic surface in  $\mathbb{P}^3$  is a Del Pezzo surface of degree 3, which is obtained by blowing up the plane at 6 points. We study its tropicalization by taking the intrinsic embedding of the surface surface minus its 27 lines. Our techniques range from controlled modifications to running gfan on the universal Cox ideal over the relevant moduli space. We classify cubic surfaces by combinatorial properties of the arrangement of 27 trees obtained from the image of the 27 lines under this tropicalization.

Chapter 5 discusses the classical Cayley–Bacharach theorem, which states that if two cubic curves on the plane intersect at 9 points, then the 9th point is uniquely determined if 8 of the points are given. The chapter derives a formula for the coordinates of the 9th point

in terms of the coordinates of the 8 given points. Furthermore, I will discuss the geometric meaning of the formula, and how it is related to del Pezzo surfaces of degree 3.

To my family

# Contents

<b>List of Figures</b>	<b>iv</b>
<b>List of Tables</b>	<b>vi</b>
<b>1 Introduction</b>	<b>1</b>
1.1 Goals . . . . .	1
1.2 Background . . . . .	4
<b>2 Tropicalization of Classical Moduli Spaces</b>	<b>10</b>
2.1 Introduction . . . . .	10
2.2 Segre Cubic, Igusa Quartic, and Kummer Surfaces . . . . .	13
2.3 Burkhardt Quartic and Abelian Surfaces . . . . .	19
2.4 Tropicalizing the Burkhardt Quartic . . . . .	25
2.5 Moduli of Genus Two Curves . . . . .	31
2.6 Marked Del Pezzo Surfaces . . . . .	37
<b>3 Algorithms for Mumford Curves</b>	<b>44</b>
3.1 Introduction . . . . .	44
3.2 Good Fundamental Domains in $\mathbb{P}^1$ and $(\mathbb{P}^1)^{an}$ . . . . .	48
3.3 Algorithms Starting With a Schottky Group . . . . .	52
3.4 From Generators in Bad Position to Generators in Good Position . . . . .	64
3.5 Future Directions: Reverse Algorithms and Whittaker Groups . . . . .	70
<b>4 Tropicalization of del Pezzo Surfaces</b>	<b>75</b>
4.1 Introduction . . . . .	75
4.2 Cox Ideals . . . . .	79
4.3 Sekiguchi Fan to Naruki Fan . . . . .	85
4.4 Modifications . . . . .	90
4.5 Tropical Cubic Surfaces and their 27 Trees . . . . .	97
<b>5 A Formula for the Cayley-Bacharach 9th Point</b>	<b>105</b>
5.1 The Formula . . . . .	105
5.2 Connection to Cubic Surfaces . . . . .	111

<b>Bibliography</b>	<b>116</b>
<b>A Appendix: Supplementary Data on the 27 Trees</b>	<b>123</b>



# List of Figures

1.1	The Berkovich projective line over $\mathbb{Q}_3$ . . . . .	6
1.2	The universal family of tropical elliptic normal curves of degree 5. . . . .	9
2.1	The Petersen graph represents the tropicalization of $\mathcal{M}_{0,5}$ . . . . .	11
2.2	Tropicalization of a Kummer surface over a snowflake tree. . . . .	17
2.3	Tropicalization of a Kummer surface over a caterpillar tree. . . . .	18
2.4	The moduli space of genus 2 tropical curves . . . . .	34
3.1	The tree in Example 3.3.12(1), and the abstract tropical curve. . . . .	59
3.2	The tree in Example 3.3.12(2), and the abstract tropical curve. . . . .	59
3.3	The tree in Example 3.3.12(3), and the abstract tropical curve. . . . .	60
3.4	The Newton polytope of the plane quartic curve in Example 3.3.17, and the corresponding tropical curve in $\mathbb{R}^2$ (drawn using the max convention). Each edge of infinite length has weight 2, and all other edges have weight 1. . . . .	65
4.1	Tropical del Pezzo surfaces of degree 4 illustrated by coloring the Clebsch graph	77
4.2	The bounded complex of the tropical del Pezzo surface in degree 4 . . . . .	78
4.3	The tropical del Pezzo surface $\text{trop}(M_{0,5})$ is the cone over the Petersen graph. . . . .	80
4.4	The 27 trees on tropical cubic surfaces of type (aaaa) . . . . .	89
4.5	The 27 trees on tropical cubic surfaces of type (aaab) . . . . .	89
4.6	The tropical divisors in Example 4.4.3. The positions of $\text{trop}(G_1 \cap H_1)$ in $\text{trop}(X_1)$ for three choices of $a$ are marked on the downward purple edge. For $a = 1$ we get $M_{0,5}$ . . . . .	93
4.7	The different possibilities for $\text{trop}(H_2) \cap \sigma$ in Example 4.4.3 . . . . .	93
4.8	The tropical conic and the tropical lines determined by the 5 points for a marked del Pezzo surface of degree 4. The diagram is drawn in $\mathbb{R}^2$ on the left and in $\mathbb{TP}^2$ on the right. The 16 trivalent trees in Figure 4.1 arise from the plane curves shown here by modifications. . . . .	94
4.9	Markings of a conic $G_1$ which produce trees of type (aaab). . . . .	98
4.10	Markings of a conic $G_1$ which produce trees of type (aaaa). . . . .	98
4.11	The tropical triangles formed by points on $G_1$ as in Figure 4.9, giving type (aaab). . . . .	99

4.12	The tropical triangles formed by points on $G_1$ as in Figure 4.10, giving type (aaaa). . . . .	99
4.13	The bounded complex of the tropical cubic surface of type (a) . . . . .	100
4.14	The 27 trees on the tropical cubic surface of type (a) . . . . .	100
4.15	The bounded complex of the tropical cubic surface of type (b) . . . . .	101
4.16	The 27 trees on the tropical cubic surface of type (b) . . . . .	101
A.1	One of the 27 trees for a type (aaaa) tropical cubic surface, with labels on the leaves. . . . .	123

# List of Tables

2.1	Orbits of cones in the tropical Burkhardt quartic . . . . .	28
2.2	Trees on four taxa and tropical curves of genus 1 . . . . .	33
2.3	Correspondence between tropical curves, cones of $\text{trop}(\mathcal{B})$ , and metric trees. . .	35
2.4	The flats of the $E_6$ reflection arrangement. . . . .	39
2.5	The Naruki complex has 76 vertices, 630 edges, 1620 triangles and 1215 tetrahedra.	39
2.6	The $f$ -vector and the number of orbits of faces of the polytope for $\mathcal{Y}$ . . . . .	40
4.1	All combinatorial types of tropical cubic surfaces . . . . .	102

## Acknowledgments

First of all, I would like to thank my advisor, Bernd Sturmfels, for guiding me through my four years as a graduate student. He is always ready to give inspiring discussions on my work and solve my problems whenever I get stuck. I would never have succeeded in my study and research without his kind support.

I am grateful to my collaborators, Ralph Morrison, Steven Sam, Gus Schrader and Kristin Shaw, for granting me authorization to include our joint works in this thesis. It is a great pleasure to work with these helpful and productive people.

During my years at Berkeley, I have been supported by Berkeley Fellowship, U.S. National Science Foundation grant DMS-0968882 and DARPA grant HR0011-12-1-0011. Also, I am grateful to the American Mathematical Society, for providing the opportunity to meet and collaborate through the Mathematics Research Communities program.

I would like to thank Federico Ardila, Matthew Baker, Natth Bejraburnin, James Blinn, Florian Block, Richard Borcherds, Melody Chan, Andrew Critch, Jonathan Dahl, Lawrence Craig Evans, Alex Fink, Samuel Gruschevsky, Nathan Ilten, Nan Li, Shaowei Lin, Diane Maclagan, Arthur Ogus, Martin Olsson, Lior Pachter, Sam Payne, Kate Poirier, Jürgen Richter-Gebert, Felipe Rincón, Jose Rodriguez, Vera Serganova, Allan Sly, Chris Swierczewski, Ngoc Tran, Marius van der Put, Cynthia Vinzant, Atilla Yilmaz and Josephine Yu for helping me on various subjects in math. Their generous help is crucial to the completion of my research projects. Especially, I would like to thank Paul Vojta for writing the standard template for this thesis.

In addition, I thank my friends Jue Chen, Long Jin, Weihua Liu and Luming Wang in the math department and Hanhan Li and Xiaodan Sun at Berkeley. Their presence reminded me that I am not alone and motivated me to move forward.

Finally, I thank my family for their encouragement on everything, and their support on making the decision on my career.

# Chapter 1

## Introduction

This chapter gives an overview of this thesis. Section 1.1 discusses the goals of my work and introduces the motivations of the problems studied in the following chapters. Section 1.2 introduces some background in tropical and non-archimedean geometry.

### 1.1 Goals

Let  $K$  be a non-archimedean valued field, such as  $\mathbb{C}\{\{t\}\}$ , the field of Puiseux series. Let  $X$  be a very affine algebraic variety over  $K$ , with an embedding  $X \hookrightarrow (K^*)^n$ . This thesis studies the *tropicalization* of  $X$ , a polyhedral complex lying in  $\mathbb{R}^n$  obtained by taking coordinate-wise valuations of points in  $X$  (see Definition 1.2.1). One drawback of tropicalizations is that they depend on the embeddings. As a result, in order to reveal the intrinsic and combinatorial properties of the variety, one usually needs to reembed the variety  $X$  into a space with higher dimension. One goal of tropical and non-archimedean analytic geometry is:

**Question 1.1.1.** Classify varieties by their intrinsic tropical properties.

For smooth curves over  $K$ , the answer to this question is well studied in the literature. Since the 1970's, the theory of semistable reductions and Berkovich analytic spaces has been well developed [3, 9, 43, 67]. The theory associates to each smooth curve  $X$  its *Berkovich skeleton*, an abstract metric graph with non-negative integer weights on each vertex. The combinatorial types of the Berkovich skeleton gives a classification of smooth curves. For surfaces and higher dimensional varieties, the notion of intrinsic tropicalization is still vague. One needs to find out nice intrinsic properties before defining the classification.

This thesis focuses on the algorithmic and computational aspect of the problem. Given a variety  $X$  expressed explicitly in terms of its defining equations, this thesis attempts to develop an algorithm which tells what class  $X$  belongs to. It is beyond the scope of this thesis to give a general algorithm that works for all  $X$ . Instead, for some specific types of varieties, the classification algorithm can be achieved. This computational problem is also

studied by number theorists. For example, finding the Berkovich skeleton of a curve over a  $p$ -adic field is the central step in studying a curve defined over a number field [17].

For elliptic curves, it is widely known that the Berkovich skeleton depends on the  $j$ -invariant: if  $\text{val}(j) < 0$ , it is a cycle of length  $-\text{val}(j)$ . Otherwise, it consists of a single point with weight 1. In the former case, the recent work [29] develops an algorithm that outputs a nice embedding  $X \hookrightarrow \mathbb{P}^2$  so that the tropical curve is in honeycomb form, which contains a cycle whose lattice length equals  $-\text{val}(j)$ .

This thesis focuses on two further cases: curves of genus 2 and 3, and del Pezzo surfaces of degree 3 and 4.

## Genus 2 and 3 curves

Chapter 2 studies covering spaces of the moduli space of genus 2 curves. Consider  $\mathcal{M}_{0,6}$ , the moduli space of 6 marked points on the line. Each point in  $\mathcal{M}_{0,6}$  corresponds to 6 distinct points  $x_1, x_2, x_3, x_4, x_5, x_6$  on  $\mathbb{P}^1$ , thus determines a genus 2 curve

$$y^2 = (x - x_1)(x - x_2)(x - x_3)(x - x_4)(x - x_5)(x - x_6).$$

In this way,  $\mathcal{M}_{0,6}$  becomes a covering space of  $\mathcal{M}_2$ , the moduli space of genus 2 curves. The group  $S_6$  acts on  $\mathcal{M}_{0,6}$  by permuting the 6 points. Therefore, the induced action on  $\mathcal{M}_2$  is trivial. We study a natural embedding  $\mathcal{M}_{0,6} \hookrightarrow \mathbb{P}^{14}$ , where  $S_6$  acts by permuting coordinates. The image of this embedding is known as the *Segre cubic threefold*. We compute the tropicalization of this threefold. It is a 3-dimensional fan, with 7 orbits of faces under the action of  $S_6$ . Our result states that the classification of genus 2 curves by the 7 possible combinatorial types of the Berkovich skeleta can be seen from the 7 orbits.

**Theorem 2.5.3.** *Let  $K$  be a complete non-archimedean field.*

(a) *There is a commutative square*

$$\begin{array}{ccc} \mathcal{M}_{0,6}(K) & \longrightarrow & \mathcal{M}_{0,6}^{\text{tr}} \\ \downarrow & & \downarrow \\ \mathcal{M}_2(K) & \longrightarrow & \mathcal{M}_2^{\text{tr}} \end{array}$$

*The left vertical map sends 6 points in  $\mathbb{P}^1$  to the genus 2 hyperelliptic curve with these ramification points. The horizontal maps send a curve (with or without marked points) to its tropical curve (with or without leaves at infinity). The right vertical map is a morphism of generalized cone complexes relating the second and fourth columns of Table 2.5.*

(b) *The top horizontal map can be described in an alternative way: under the embedding of  $\mathcal{M}_{0,6}$  into  $\mathbb{P}^{14}$  given by (2.5), take the valuations of the 15 coordinates  $m_0, m_1, \dots, m_{14}$ .*

Therefore, the 15 coordinates  $m_0, m_1, \dots, m_{14}$  play the same role as the  $j$ -invariant in the genus 1 case. Note that  $\mathcal{M}_{0,6}^{tr}$  is the space of phylogenetic trees with 6 taxa, and  $\mathcal{M}_2^{tr}$  is the space of metric graphs with genus 2 of “dumbbell” and “theta” shapes and their degenerations.

We also study the *Burkhardt quartic threefold*, another covering space of  $\mathcal{M}_2$ . It has a natural embedding into  $\mathbb{P}^{39}$  and its symmetric group is the complex reflection group  $G_{32}$ . Again, we compute the tropicalization of the Burkhardt quartic, which is also a 3-dimensional fan with 7 orbits of faces. We conjecture that an analog of Theorem 2.5.3 holds.

Chapter 3 takes an analytic approach to the problem. Instead of tropicalizing the curve, we start with generators of a *Schottky group*  $\Gamma$ , a subgroup of  $PGL(2, K)$  that satisfies certain conditions. A smooth curve is analytically isomorphic to  $(\mathbb{P}^1 \setminus \Sigma)/\Gamma$ , where  $\Sigma$  is a discontinuous subset of  $\mathbb{P}^1$ . We implemented algorithms that takes  $g$  free generators of a Schottky group and

- Finds a period matrix for the abelian variety  $\text{Jac}(C)$ ;
- Finds the Berkovich skeleton of the curve;
- Finds points in a canonical embedding of the curve  $C$  into  $\mathbb{P}^{g-1}$ .

We succeeded in recovering the quartic equation of a genus 3 curve from its Schottky group with our implementation.

## Del Pezzo surfaces

Let  $X$  be a smooth surface in  $\mathbb{P}^3$  defined by a cubic equation  $f(x_0, x_1, x_2, x_3) = 0$ . The surface can be obtained by blowing up the plane at 6 points in general position. It is classically known that there exist 27 straight lines lying in the surface. Among these lines, 15 comes from lines passing through each pair of the 6 points, 6 comes from conics passing through 5 of the 6 points, and the other 6 are exceptional divisors of the blowing up.

Chapter 4 describes our result on tropicalizations of these surfaces. One method we use is to reembed  $X$  into a 19-dimensional space whose coordinate ring is the *Cox ring*, whose definition is independent of the choice of coordinates. It is generated by 27 elements  $E, F, G$  corresponding to the 27 lines. This reembedding respects the symmetry by  $W(E_6)$ , the automorphism group of the configuration of the 27 lines. In addition, this embedding gives the *intrinsic torus* of the very affine variety obtained by removing the 27 lines from  $X$ .

Another method involves a *family* of cubic surfaces, which is a map  $\mathcal{G}' \rightarrow \mathcal{Y}'$  whose fibers are cubic surfaces. All isomorphism classes of smooth cubic surfaces appear as fibers in the family. With appropriate embeddings chosen, tropical cubic surfaces appear as subsets of the fibers of the tropicalization of this map, following the theory developed in [50]. If we exclude some special cubic surfaces (the ones with *Eckhart points*) from the family, then the fibers of the tropicalized map are exactly the tropical cubic surfaces.

The third method we use is *tropical modifications*. The process is the tropical analog of blowing up the plane at 6 points. We start with a tropical plane with 3 marked points on it (without loss of generality, we may assume that the other 3 points lie at infinity). In each step, we “blow up” the surface at a tropical line. We continue this procedure until we see all of the 27 tropical lines at infinity. Each of these is a metric tree with 10 leaves at infinity.

Using our methods, we derived the following result:

**Theorem 4.1.1.** *There are two generic types of tropical cubic surfaces. They are contractible and characterized at infinity by 27 metric trees, each having 10 leaves. The first type has 73 bounded cells, 150 edges, 78 vertices, 135 cones, 189 flaps, 216 rays, and all 27 trees are trivalent. The second type has 72 bounded cells, 148 edges, 77 vertices, 135 cones, 186 flaps, 213 rays, and three of the 27 trees have a 4-valent node. (For more data see Table 4.1.)*

A simpler case is the blowing-up of the plane at 5 points in general position. This surface can be embedded as the intersection of two quadratic hypersurfaces in  $\mathbb{P}^3$ . There is only one generic combinatorial type for the tropical surface, and we computed its face numbers.

Chapter 5 describes an independent result based on the classical Cayley–Bacharach theorem. If two cubic curves in the plane intersect at 9 points, then the 9th point is uniquely determined if 8 of the points are given. The chapter derives a formula for the coordinates of the 9th point in terms of the coordinates of the 8 given points. There is a geometric relation between the Cayley–Bacharach theorem and cubic surfaces: fix 6 of the 8 given points, and let  $S$  be the cubic surface obtained by blowing up the plane at these 6 points. Then, the factors in the formula reveals the combinatorial information: the 9th point lies on one of the 27 lines if and only if the corresponding factor vanishes. Finally, the chapter gives a formula of the coordinate of the preimage of the 9th point in  $S$  with respect to the Cox embedding.

## 1.2 Background

There are several ways to characterize a tropical variety. One may define a tropical variety as the set of non-smooth points of a polynomial in the min-plus algebra. Another approach is to define a tropical variety as the limit of the *amoeba*, the set obtained by taking coordinate-wise logarithm of points in a complex variety. In some occasions, tropical varieties are regarded as combinatorial objects in its own right. This thesis takes a fourth approach: a tropical variety is the tropicalization of an algebraic variety over a valued field with a fixed embedding into a torus. A thorough introduction to tropical geometry can be found in [62] and [64].

Let  $K$  be a field with a non-archimedean valuation  $\text{val}: K \rightarrow \mathbb{R} \cup \{\infty\}$ . One example of such a field is  $\mathbb{Q}_p$ , the field of  $p$ -adic numbers, with the valuation  $\text{val}\left(p^k \frac{a}{b}\right) = k$  for  $\text{gcd}(a, p) = \text{gcd}(b, p) = 1$ . Another example is  $\mathbb{C}\{\{t\}\}$ , the field of Puiseux series, with the valuation  $\text{val}\left(t^k \frac{a+o(1)}{b+o(1)}\right) = k$  for  $a, b \in \mathbb{C} \setminus \{0\}$ . For such a field  $K$ , let  $R = \{x \in K \mid \text{val}(x) \geq 0\}$  be its *valuation ring*. It is a local ring with maximal ideal  $\mathfrak{m} = \{x \in K \mid \text{val}(x) > 0\}$ . Let  $k = R/\mathfrak{m}$  be its *residue field*. The *absolute value* is given by  $|x| = \exp(-\text{val}(x))$ . This



absolute value induces a topology on  $K$  with metric  $d(x, y) = |x - y|$ . In the case  $K = \mathbb{Q}_p$ , the absolute value is usually replaced by  $|x|_p = p^{-\text{val}(x)}$  for convenience without affecting the induced topology.

The absolute value is exotic compared with the usual absolute values of  $\mathbb{R}$  and  $\mathbb{C}$ . For example,

$$|x + y| \leq \min(|x|, |y|), \text{ for } x, y \in K \quad (1.1)$$

This property will play a fundamental role in Chapter 3.

**Definition 1.2.1.** Let  $X$  be a very affine variety over  $K$  with an embedding  $X \hookrightarrow (K^*)^n$ . The *tropicalization map* of  $X$  with respect to this embedding is

$$\begin{aligned} \text{trop}: X &\rightarrow \text{val}(K^*)^n, \\ (x_1, x_2, \dots, x_n) &\mapsto (\text{val}(x_1), \text{val}(x_2), \dots, \text{val}(x_n)). \end{aligned}$$

The *tropicalization* of  $X$ , denoted  $\text{trop}(X)$ , is the image of the tropicalization map.

The field  $K$  is usually assumed to be algebraically closed. In this case, the group  $\text{val}(K^*)$  is a dense subset of  $\mathbb{R}$ . For simplicity, the tropicalization  $\text{trop}(X)$  is usually defined as the closure of the image of the tropicalization map in  $\mathbb{R}^n$ . This definition will be used throughout this thesis, unless specified otherwise. There are two variants of this definition: if  $X$  is an affine variety with an embedding  $X \hookrightarrow K^n$ , then  $\text{trop}(X)$  can be defined as a subset of  $(\mathbb{R} \cup \{\infty\})^n$ . On the other hand, if  $X$  is a projective variety with an embedding  $X \hookrightarrow \mathbb{P}^n$ , then  $\text{trop}(X)$  can be defined as the image of the map  $(x_0 : x_1 : \dots : x_n) \mapsto (\text{val}(x_0), \text{val}(x_1), \dots, \text{val}(x_n))$  in  $\mathbb{TP}^n = ((\mathbb{R} \cup \{\infty\})^{n+1} \setminus \{(\infty, \infty, \dots, \infty)\}) / (1, 1, \dots, 1)$ .

## Berkovich skeleta

Tropicalization is not an intrinsic way to study algebraic varieties because it depends on a specific embedding. The *Berkovich analytic space* overcomes this difficulty by taking the inverse limit of all tropicalizations, as shown by Payne in [72]:

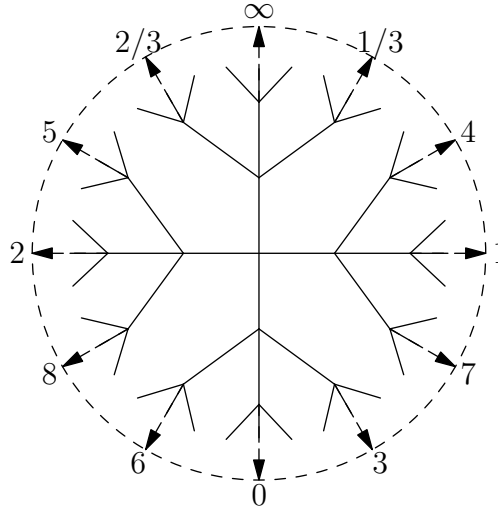
**Theorem 1.2.2.** *Let  $X$  be an affine variety over  $K$ . Then, the Berkovich analytification  $X^{an}$  is homeomorphic to the inverse limit  $\varprojlim \text{trop}(X)$ , where the limit is taken with respect to morphisms between affine embeddings of  $X$  in the form of permuting and dropping coordinates.*

In general,  $X^{an}$  is defined as the set of multiplicative seminorms on the coordinate ring of  $X$  that are compatible with the absolute value of  $K$  [9]. For the purpose of this thesis, it is sufficient to take the above theorem as a working definition. The Berkovich analytification of a projective variety is obtained by gluing the analytifications of its affine charts.

The analytic projective line  $(\mathbb{P}^1)^{an}$  is of great significance in the following chapters. As detailed in [8],  $(\mathbb{P}^1)^{an}$  consists of four types of points:

- Type 1 points are just the usual points of  $\mathbb{P}^1$ .

Figure 1.1: The Berkovich projective line over  $\mathbb{Q}_3$



- Type 2 points correspond to closed balls  $B(a, r)^+ = \{x \in K : |x - a| \leq r\}$  where  $r \in |K^\times|$ .
- Type 3 points correspond to closed balls  $B(a, r)^+$  where  $r \notin |K^\times|$ .
- Type 4 points correspond to equivalence classes of sequences of nested closed balls  $B_1^+ \supset B_2^+ \supset \dots$  such that their intersection is empty.

There is a metric on the set of Type 2 and Type 3 points, defined as follows: let  $P_1$  and  $P_2$  be two such points and let  $B(a_1, r_1)^+$  and  $B(a_2, r_2)^+$  be the corresponding closed balls.

- (1) If one of them is contained in the other, say  $B(a_1, r_1)^+$  is contained in  $B(a_2, r_2)^+$ , then the distance  $d(P_1, P_2)$  is  $\log_p(r_2/r_1)$ .
- (2) In general, there is a unique smallest closed ball  $B(a_3, r_3)^+$  containing both of them. Let  $P_3$  be the corresponding point. Then,  $d(P_1, P_2)$  is defined to be  $d(P_1, P_3) + d(P_3, P_2)$ .

The metric can be extended to Type 4 points.

This metric makes  $(\mathbb{P}^1)^{an}$  a tree with infinite branching, as we now describe. There is a unique path connecting any two points  $P_1$  and  $P_2$ . In case (1) above, the path is defined by the isometry  $t \mapsto B(a_1, p^t)^+$ ,  $t \in [\log(r_1), \log(r_2)]$ . It is straightforward to check that  $B(a_1, r_2)^+ = B(a_2, r_2)^+$ . In case (2) above, the path is the concatenation of the paths from  $P_1$  to  $P_3$  and from  $P_3$  to  $P_2$ . Then, Type 1 points become limits of Type 2 and Type 3 points with respect to this metric. More precisely, if  $x \neq \infty$ , then it lies at the limit of the path  $t \mapsto B(x, p^{-t})^+$ ,  $t \in [0, +\infty)$ . Type 1 points behave like leaves of the tree at infinity. For any two Type 1 points  $x, y$ , there is a unique path in  $(\mathbb{P}^1)^{an}$  connecting them, which has infinite length. A picture for the Berkovich projective line over  $\mathbb{Q}_3$  is shown in Figure 1.1.

Another example studied in this thesis is the minimal skeleton of the analytification of complete smooth genus  $g$  curves. The following definitions are taken from Baker, Payne and Rabinoff [9], with appropriate simplification.

- Definition 1.2.3.** (1) The *skeleton* of an open annulus  $B \setminus B' = \{x \in K : r < |x-a| < R\}$ , where  $r, R \in |K^*|$ , is the straight path between the Type 2 points corresponding to  $B(a, r)^+$  and  $B(a, R)^+$ .
- (2) Let  $C$  be a complete smooth curve over  $K$ . A *semistable vertex set*  $V$  is a finite set of Type 2 points in  $C^{an}$  such that  $C^{an} \setminus V$  is the disjoint union of open balls and open annuli. The *skeleton corresponding to  $V$*  is the union of  $V$  with all skeleta of these open annuli.
- (3) If  $\text{genus}(C) \geq 2$ , then  $C^{an}$  has a unique *minimal skeleton*. The minimal skeleton is the intersection of all skeleta, and it is a finite metric graph. We sometimes call this minimal skeleton the *abstract tropical curve* of  $C$ .

**Definition 1.2.4.** An *algebraic semistable model* of a smooth curve  $C$  over  $K$  is a flat and proper scheme  $X$  over  $R$  whose generic fiber  $X_K$  is isomorphic to  $C$  and whose special fiber  $X_k$  satisfies

- $X_k$  is a connected and reduced curve, and
- all singularities of  $X_k$  are ordinary double points.

Semistable models are related to skeleta in the following way: take a semistable model  $X$  of  $C$ . Associate a vertex for each irreducible component of  $X_k$ . For each ordinary intersection of two irreducible components in  $X_k$ , connect an edge between the two corresponding vertices. The resulting graph is combinatorially a skeleton of  $C^{an}$ . Algorithmic computation of semistable models is a hard problem in general. Some recent results are discussed in [6, §1.2] and [17, §3.1].

## Moduli spaces of tropical varieties

A *family* of algebraic varieties with Property P is a morphism  $\mathcal{F} \rightarrow \mathcal{M}$  such that the fiber over each point in  $\mathcal{M}$  is a variety with Property P. In order to study properties of such varieties, it is desirable to consider the *universal family*, which is, imprecisely speaking, a family such that there is exactly one fiber for each isomorphism class of varieties with Property P. If so, the object  $\mathcal{M}$  is called the *moduli space* of varieties with Property P. Usually, the moduli is described as an *algebraic stack*, as in the extensive treatment of  $\mathcal{M}_{g,n}$ , the moduli of genus  $g$  curves with  $n$  marked points, in [51].

Suppose that there is a uniform way of tropicalizing algebraic varieties with Property P. The fiber over each point in  $\mathcal{M}$  gives a tropical variety. The set of isomorphism classes of these tropical varieties forms a moduli space  $\mathcal{M}^{tr}$ . Thus, we define the tropicalization map

$\mathcal{M} \rightarrow \mathcal{M}^{tr}$ . For example, if  $\mathcal{M} = \mathcal{M}_{g,n}$ , then  $\mathcal{M}^{tr}$  can be taken as the moduli space of abstract tropical curves of genus  $g$ , and the tropicalization map  $\mathcal{M} \rightarrow \mathcal{M}^{tr}$  takes a point in  $\mathcal{M}$  representing a curve  $X$  to the point in  $\mathcal{M}^{tr}$  representing the Berkovich skeleton of  $X$ . The following fundamental result by Abramovich, Caporaso and Payne [3] roughly says “moduli of tropical curves is isomorphic to tropicalization of moduli of curves”:

**Theorem 1.2.5.** *The moduli space of abstract tropical curves  $\mathcal{M}_{g,n}^{tr}$  is isomorphic to the skeleton of  $\mathcal{M}_{g,n}$ , and the map  $\mathcal{M}_{g,n} \rightarrow \mathcal{M}_{g,n}^{tr}$  is a retraction.*

From the perspective of moduli space, the classification of varieties can be viewed as a partition in the moduli space  $\mathcal{M}$ . This partition is the pull back of the partition of  $\mathcal{M}^{tr}$  along the map  $\mathcal{M} \rightarrow \mathcal{M}^{tr}$ . One could evaluate the map  $\mathcal{M} \rightarrow \mathcal{M}^{tr}$  at the point representing  $X$  in order to find the intrinsic tropicalization of  $X$ . This can be done much more efficiently if  $\mathcal{M}$  is an algebraic variety and the map  $\mathcal{M} \rightarrow \mathcal{M}^{tr}$  is the same as the tropicalization map  $\mathcal{M} \rightarrow \text{trop}(\mathcal{M})$  with an appropriate choice of embedding, as in Chapters 2 and 4.

**Example 1.2.6.** Consider  $\mathcal{M} = \mathcal{M}_{0,n}$ , the moduli space of  $n$  distinct marked points on a line. Let  $\mathcal{M}_{0,n}^{tr}$  be the space of unrooted metric trees with  $n$  leaves at infinity. We define a map  $\mathcal{M}_{0,n} \rightarrow \mathcal{M}_{0,n}^{tr}$  as follows: given  $n$  marked points on  $\mathbb{P}^1$ , we take the union of the paths in  $(\mathbb{P}^1)^{an}$  between each pair of marked points.

Suppose  $n \geq 4$ . Up to a projective transformation, three of the marked points can be sent to 0, 1 and  $\infty$ . Let  $p_4, \dots, p_n$  be the other points. Then,  $\mathcal{M}_{0,n} \cong \{(p_4, \dots, p_n) | p_i \neq 0, p_i \neq 1, p_i \neq p_j\} \subset K^{n-3}$ . The tropicalization with respect to this embedding is an open subset in  $\mathbb{R}^{n-3}$ , which does not reflect the combinatorial structure of  $\mathcal{M}_{0,n}^{tr}$ .

A better way to tropicalize  $\mathcal{M}_{0,n}$  can be seen via the Grassmannian  $\text{Gr}(2, n)$ , the space of  $2 \times n$  matrices of rank 2 over  $K$  modulo elementary row operations. It has a natural *Plücker embedding* into  $\mathbb{P}^{\binom{n}{2}}$  by the  $2 \times 2$  minors. Let  $\text{Gr}(2, n)^0$  be the open subset where all Plücker coordinates are nonzero. The columns of a  $2 \times n$  matrix can be regarded as the homogeneous coordinates of  $n$  points in  $\mathbb{P}^1$ . Different  $2 \times n$  matrices may give the same  $n$  points, for the homogeneous coordinates are defined up to a constant factor. In fact,  $\mathcal{M}_{0,n}$  is isomorphic to the toric quotient  $\text{Gr}(2, n)^0 / (K^*)^{n-1}$ , where the torus  $(K^*)^{n-1}$  acts by multiplying each of the first  $n - 1$  columns of the matrix by a constant. On the tropical side, this action becomes translation along a linear subspace in  $\mathbb{R}^{\binom{n}{2}}$  of dimension  $n - 1$ . It is shown that the tropicalization of  $\text{Gr}(2, n)^0$  with respect to the Plücker embedding modulo the translation is exactly  $\mathcal{M}_{0,n}^{tr}$ .

A discussion on the role of  $\mathcal{M}_{0,n}$  in phylogenetics can be found in [61].

Moreover, suppose that the moduli space  $\mathcal{M}$  is an algebraic variety, and that embeddings of  $\mathcal{F}$  and  $\mathcal{M}$  are chosen so that the morphism  $\mathcal{F} \rightarrow \mathcal{M}$  is a coordinate projection. It induces a map of tropical varieties  $\text{trop}(\mathcal{F}) \rightarrow \text{trop}(\mathcal{M})$  which is also a coordinate projection. Let  $X$  be the fiber over a point  $p \in \mathcal{M}$ . Then, the tropicalization  $\text{trop}(X)$  is a subset of the fiber of the tropical map over  $\text{trop}(p)$ . Therefore, by tropicalizing  $\mathcal{F}$  and examining the fibers, one obtains information about tropicalizations of varieties with Property P in general. With a

suitable choice of an embedding of  $\mathcal{F}$ , one sees the tropical varieties exactly in the fibers of the tropical map.

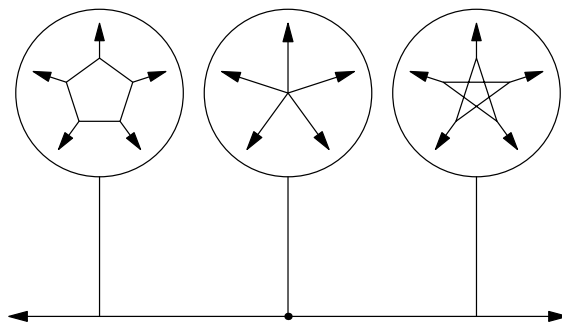


Figure 1.2: The universal family of tropical elliptic normal curves of degree 5.

**Example 1.2.7.** The family  $\mathcal{A}(5) \rightarrow \mathbb{P}^1$ , defined in Section 2.1, is a family of elliptic curves with 5 marked points. Figure 1.2 illustrates the tropicalized family  $\text{trop}(\mathcal{A}(5)) \rightarrow \mathbb{TP}^1$ . The fiber of each point in the base  $\mathbb{TP}^1$  is a tropicalization of an elliptic curve over  $K$ . The fibers come in two classes: the fiber over the origin contains a distinguished point with 5 rays, while each of the other fibers contains a cycle. The pull back of this partition is exactly the classification of the fibers of  $\mathcal{A}(5) \rightarrow \mathbb{P}^1$  by the two types of Berkovich skeleta of elliptic curves.

## Chapter 2

# Tropicalization of Classical Moduli Spaces

This chapter is joint work with Steven Sam and Bernd Sturmfels. It is published with the same title, to appear in *Mathematics in Computer Science*, Special Issue on Computational Algebraic Geometry [75].

### 2.1 Introduction

Algebraic geometry is the study of solutions sets to polynomial equations. Solutions that depend on an infinitesimal parameter can be analyzed combinatorially using min-plus algebra. This insight led to the development of tropical algebraic geometry [62]. While all algebraic varieties and their tropicalizations may be explored at various level of granularity, varieties that serve as moduli spaces are usually studied at the highest level of abstraction. This chapter does exactly the opposite: we investigate and tropicalize certain concrete moduli spaces, mostly from the 19th century repertoire [56], by means of their defining polynomials.

A first example, familiar to all algebraic geometers, is the moduli space  $\mathcal{M}_{0,n}$  of  $n$  distinct points on the projective line  $\mathbb{P}^1$ . We here regard  $\mathcal{M}_{0,n}$  as a subvariety in a suitable torus. Its tropicalization  $\text{trop}(\mathcal{M}_{0,n})$  is a simplicial fan of dimension  $n - 3$  whose points parametrize all metric trees with  $n$  labeled leaves. The cones distinguish different combinatorial types of metric trees. The defining polynomials of this (tropical) variety are the  $\binom{n}{4}$  Plücker quadrics  $p_{ij}p_{kl} - p_{ik}p_{jl} + p_{il}p_{jk}$ . These quadrics are the  $4 \times 4$ -subpfaffians of a skew-symmetric  $n \times n$ -matrix, and they form a *tropical basis* for  $\mathcal{M}_{0,n}$ . The *tropical compactification* defined by this fan is the moduli space  $\overline{\mathcal{M}}_{0,n}$  of  $n$ -pointed stable rational curves. The picture for  $n = 5$  is delightful: the tropical surface  $\text{trop}(\mathcal{M}_{0,5})$  is the cone over the *Petersen graph*, with vertices labeled by the 10 Plücker coordinates  $p_{ij}$  as in Figure 2.1.

A related example is the universal family  $\mathcal{A}(5)$  over the modular curve  $X(5)$ . The relevant combinatorics goes back to Felix Klein and his famous 1884 lectures on the icosahedron [60].

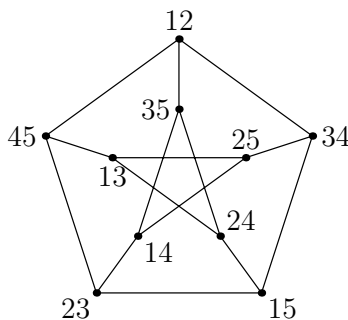


Figure 2.1: The Petersen graph represents the tropicalization of  $\mathcal{M}_{0,5}$ .

Following Fisher [39], the surface  $\mathcal{A}(5)$  sits in  $\mathbb{P}^1 \times \mathbb{P}^4$  and has the Pfaffian representation

$$\text{rank} \begin{bmatrix} 0 & -a_1x_1 & -a_2x_2 & a_2x_3 & a_1x_4 \\ a_1x_1 & 0 & -a_1x_3 & -a_2x_4 & a_2x_0 \\ a_2x_2 & a_1x_3 & 0 & -a_1x_0 & -a_2x_1 \\ -a_2x_3 & a_2x_4 & a_1x_0 & 0 & -a_1x_2 \\ -a_1x_4 & -a_2x_0 & a_2x_1 & a_1x_2 & 0 \end{bmatrix} \leq 2. \tag{2.1}$$

The base of this family is  $\mathbb{P}^1$  with coordinates  $(a_1 : a_2)$ . The tropical surface  $\text{trop}(\mathcal{A}(5))$  is a fan in  $\mathbb{TP}^1 \times \mathbb{TP}^4$ , which is combinatorially the Petersen graph in Figure 2.1. The central fiber, over the vertex of  $\mathbb{TP}^1$  given by  $\text{val}(a_1) = \text{val}(a_2)$ , is the 1-dimensional fan with rays  $e_0, e_1, e_2, e_3, e_4$ . These correspond to the edges 34-25, 12-35, 45-13, 23-14, 15-24. For  $\text{val}(a_1) < \text{val}(a_2)$ , the fiber is given by the pentagon 12-34-15-23-45-12 with these rays attached. For  $\text{val}(a_1) > \text{val}(a_2)$ , it is the pentagram 35-14-25-13-24-35 with the five rays. Each of the edges has multiplicity 5. The map from  $\text{trop}(\mathcal{A}(5))$  onto  $\mathbb{TP}^1$  is visualized in Figure 1.2.

The discriminant of our family  $\mathcal{A}(5) \rightarrow \mathbb{P}^1$  is the binary form

$$a_1^{11}a_2 - 11a_1^6a_2^6 - a_1a_2^{11}, \tag{2.2}$$

whose 12 zeros represent Klein’s icosahedron. The modular curve  $X(5)$  is  $\mathbb{P}^1$  minus these 12 points. For each  $(a_1 : a_2) \in X(5)$ , the condition (2.1) defines an elliptic normal curve in  $\mathbb{P}^4$ .

Throughout this chapter we work over an algebraically closed field  $K$  of characteristic 0. Our notation and conventions regarding tropical geometry follow [62]. For simplicity of exposition, we identify the tropical projective space  $\mathbb{TP}^n$  with its open part  $\mathbb{R}^{n+1}/\mathbb{R}(1, 1, \dots, 1)$ .

The adjective “classical” in our title has two meanings. *Classical as opposed to tropical* refers to moduli spaces that are defined over fields, the usual setting of algebraic geometry. The foundations for tropicalizing such schemes and stacks are currently being developed, notably in the work of Abramovich *et al.* [3] and Baker *et al.* [9] (see [2] for a survey). These rest on the connection to non-archimedean geometry. *Classical as opposed to modern* refers to moduli spaces that were known in the 19th century. We focus here on the varieties

featured in Hunt’s book [56], notably the Segre cubic, the Igusa quartic, the Burkhardt quartic, and their universal families. We shall also revisit the work on tropical del Pezzo surfaces by Hacking *et al.* in [50] and explain how this relates to the tropical Göpel variety of [74, §9].

Each of our moduli spaces admits a high-dimensional symmetric embedding of the form

$$\mathbb{P}^d \xrightarrow{\text{linear}} \mathbb{P}^m \xrightarrow{\text{monomial}} \mathbb{P}^n. \quad (2.3)$$

The coordinates of the first map are the linear forms defining the  $m+1$  hyperplanes in a complex reflection arrangement  $\mathcal{H}$  in  $\mathbb{P}^d$ , while the coordinates of the second map are monomials that encode the symplectic geometry of a finite vector space. The relevant combinatorics rests on the representation theory developed in [46, 47]. Each of our moduli spaces is written as the image of a map (2.3) whose coordinates are monomials in linear forms, and hence the formula in [33, Theorem 3.1] expresses its tropicalization using the matroid structure of  $\mathcal{H}$ .

Our warm-up example, the modular curve  $X(5)$ , fits the pattern (2.3) for  $d = 1, m = 11$  and  $n = 5$ . Its arrangement  $\mathcal{H} \subset \mathbb{P}^1$  is the set of 12 zeros of (2.2), but now identified with the complex reflection arrangement  $G_{16}$  as in [46, §2.2]. If we factor (2.2) into six quadrics,

$$(a_1 a_2) \cdot \prod_{i=1}^5 ((\gamma^{5-i} a_1 + (\gamma + \gamma^4) a_2)(\gamma^i a_1 + (\gamma^2 + \gamma^3) a_2)),$$

where  $\gamma$  is a primitive fifth root of unity, then these define the coordinates of  $\mathbb{P}^{11} \xrightarrow{\text{monomial}} \mathbb{P}^5$ . The image is a quadric in a plane in  $\mathbb{P}^5$ , and  $X(5)$  is now its intersection with the torus  $\mathbb{G}_m^5$ . The symmetry group  $G_{16}$  acts on  $\mathbb{P}^5$  by permuting the six homogeneous coordinates. The tropical modular curve  $\text{trop}(X(5))$  is the standard one-dimensional fan in  $\mathbb{TP}^5$ , with multiplicity five and pentagonal fibers as above. But now the full symmetry group acts on the surface  $\mathcal{A}(5) \subset \mathbb{P}^5 \times \mathbb{P}^4$  and the corresponding tropical surface by permuting coordinates.

We next discuss the organization of this chapter. In Section 2.2 we study the Segre cubic and the Igusa quartic, in their symmetric embeddings into  $\mathbb{P}^{14}$  and  $\mathbb{P}^9$ , respectively. We show that the corresponding tropical variety is the space of phylogenetic trees on six taxa, and we determine the universal family of tropical Kummer surfaces over that base. In Section 2.3 we study the Burkhardt quartic in its symmetric embedding in  $\mathbb{P}^{39}$ , and, over that base, we compute the universal family of abelian surfaces in  $\mathbb{P}^8$  along with their associated tricanonical curves of genus 2. In Section 2.4 we compute the Bergman fan of the complex reflection arrangement  $G_{32}$  and from this we derive the tropical Burkhardt quartic in  $\mathbb{TP}^{39}$ . The corresponding tropical compactification is shown to coincide with the Igusa desingularization of the Baily–Borel–Satake compactification of  $\mathcal{A}_2(3)$ . In Section 2.5 we relate our findings to the abstract tropical moduli spaces of [18, 26]. Figure 2.5 depicts the resulting correspondence between trees on six taxa, metric graphs of genus 2, and cones in the tropical Burkhardt quartic. In Section 2.6 we study the reflection arrangements of types  $E_6$  and  $E_7$ , and we show how they lead to the tropical moduli spaces of marked del Pezzo surfaces constructed by Hacking, Keel and Tevelev [50]. For  $E_7$  we recover the tropical



Göpel variety of [74, §9]. This is a six-dimensional fan which serves as the universal family of tropical cubic surfaces.

## 2.2 Segre Cubic, Igusa Quartic, and Kummer Surfaces

The moduli spaces in this section are based on the hyperplane arrangement in  $\mathbb{P}^4$  associated with the reflection representation of the symmetric group  $\Sigma_6$ . It consists of the 15 hyperplanes

$$x_i - x_j = 0 \quad (1 \leq i < j \leq 6). \quad (2.4)$$

Here  $\mathbb{P}^4$  is the projectivization of the 5-dimensional vector space  $K^6/K(1, 1, 1, 1, 1, 1)$ . The 15 linear forms in (2.4) define the map  $\mathbb{P}^4 \xrightarrow{\text{linear}} \mathbb{P}^{14}$  whose image is the 4-dimensional subspace  $\text{Cyc}_4$  of  $\mathbb{P}^{14}$  that is defined by the linear equations  $z_{ij} - z_{ik} + z_{jk} = 0$  for  $1 \leq i < j < k \leq 6$ .

The corresponding tropical linear space  $\text{trop}(\text{Cyc}_4)$ , with the coarsest fan structure, is isomorphic to both the moduli space of equidistant (rooted) phylogenetic trees with 6 leaves and the moduli space of (unrooted) phylogenetic trees with 7 leaves. The former was studied by Ardila and Klivans in [4, §4]. They develop the correspondence between ultrametrics and equidistant phylogenetic trees in [4, Theorem 3]. The latter is a tropicalization of the Grassmannian  $\text{Gr}(2, 7)$  as described in [84, §4]. From the combinatorial description given there one derives the face numbers below:

**Lemma 2.2.1.** *The tropical linear space  $\text{trop}(\text{Cyc}_4)$  is the space of ultrametrics on 6 elements, or, equivalently, the space of equidistant phylogenetic trees on 6 taxa. It is a fan over a three-dimensional simplicial complex with 56 vertices, 490 edges, 1260 triangles and 945 tetrahedra.*

We now define our two modular threefolds by way of a monomial map from  $\mathbb{P}^{14}$  to another space  $\mathbb{P}^n$ . The homogeneous coordinates on that  $\mathbb{P}^n$  will be denoted  $m_0, m_1, \dots, m_n$ , so as to highlight that they can be identified with certain modular forms, known as theta constants.

The *Segre cubic*  $\mathcal{S}$  is the cubic threefold defined in  $\mathbb{P}^5$  by the equations  $\sum_i z_i = \sum_i z_i^3 = 0$ . Now consider the closure of the image of  $\text{Cyc}_4$  under  $\mathbb{P}^{14} \xrightarrow{\text{monomial}} \mathbb{P}^{14}$  given by

$$(z_{12}z_{34}z_{56} : z_{12}z_{35}z_{46} : z_{12}z_{36}z_{45} : z_{13}z_{24}z_{56} : z_{13}z_{25}z_{46} : z_{13}z_{26}z_{45} : z_{14}z_{23}z_{56} : z_{14}z_{25}z_{36} : z_{14}z_{26}z_{35} : z_{15}z_{23}z_{46} : z_{15}z_{24}z_{36} : z_{15}z_{26}z_{34} : z_{16}z_{23}z_{45} : z_{16}z_{24}z_{35} : z_{16}z_{25}z_{34}). \quad (2.5)$$

It is isomorphic to the Segre cubic, so we also call it  $\mathcal{S}$ ; for a proof, the reader can jump ahead to (2.11) and (2.12). The prime ideal of  $\mathcal{S}$  is generated by 10 linear trinomials, like  $m_0 - m_1 + m_2$ , that come from Plücker relations among the  $x_i - x_j$ , and one cubic binomial such as  $m_0m_7m_{12} - m_2m_6m_{14}$ . For a graphical representation of this ideal we refer to Howard *et al.* [55, (1.2)]: for the connection, note that the monomials in (2.5) naturally correspond to perfect matchings of a set of size 6, which are the colored graphs in [55].

The *Igusa quartic*  $\mathcal{I}$  is the closure of the image of  $\text{Cyc}_4$  under  $\mathbb{P}^{14} \xrightarrow{\text{monomial}} \mathbb{P}^9$  given by

$$(z_{12}z_{13}z_{23}z_{45}z_{46}z_{56} : z_{12}z_{14}z_{24}z_{35}z_{36}z_{56} : z_{12}z_{15}z_{25}z_{34}z_{36}z_{46} : z_{12}z_{16}z_{26}z_{34}z_{35}z_{45} : z_{13}z_{14}z_{34}z_{25}z_{26}z_{56} : \\ z_{13}z_{15}z_{35}z_{24}z_{26}z_{46} : z_{13}z_{16}z_{36}z_{24}z_{25}z_{45} : z_{14}z_{15}z_{45}z_{23}z_{26}z_{36} : z_{14}z_{16}z_{46}z_{23}z_{25}z_{35} : z_{15}z_{16}z_{56}z_{23}z_{24}z_{34})$$

The prime ideal of  $\mathcal{I}$  is generated by the five linear forms in the column vector

$$\begin{pmatrix} 0 & m_0 & m_1 & m_2 & m_3 \\ m_0 & 0 & m_4 & m_5 & m_6 \\ m_1 & m_4 & 0 & m_7 & m_8 \\ m_2 & m_5 & m_7 & 0 & m_9 \\ m_3 & m_6 & m_8 & m_9 & 0 \end{pmatrix} \cdot \begin{pmatrix} 1 \\ -1 \\ 1 \\ -1 \\ 1 \end{pmatrix} \quad (2.6)$$

together with any of the  $4 \times 4$ -minors of the symmetric  $5 \times 5$ -matrix in (2.6). The linear forms (2.6) come from Plücker relations of degree  $(1, 1, 1, 1, 1)$  on  $\text{Gr}(3, 6)$ . We note that  $m_0, \dots, m_9$  can be written in terms of theta functions by Thomae's theorem [35, §VIII.5].

To see that this is the usual Igusa quartic, one can calculate the projective dual of the quartic hypersurface we have just described and verify that it is a cubic hypersurface whose singular locus consists of 10 nodes. The Segre cubic is the unique cubic in  $\mathbb{P}^4$  with 10 nodes.

A key ingredient in the study of modular varieties is the symplectic combinatorics of finite vector spaces. Here we consider the binary space  $\mathbb{F}_2^4$  with the symplectic form

$$\langle x, y \rangle = x_1y_3 + x_2y_4 - x_3y_1 - x_4y_2. \quad (2.7)$$

We fix the following bijection between the 15 hyperplanes (2.4) and the vectors in  $\mathbb{F}_2^4 \setminus \{0\}$ :

$$\begin{matrix} z_{12} & z_{13} & z_{14} & z_{15} & z_{16} & z_{23} & z_{24} & z_{25} & z_{26} & z_{34} & z_{35} & z_{36} & z_{45} & z_{46} & z_{56} \\ u_{0001} & u_{1100} & u_{1110} & u_{0101} & u_{0110} & u_{1101} & u_{1111} & u_{0100} & u_{0111} & u_{0010} & u_{1001} & u_{1010} & u_{1011} & u_{1000} & u_{0011} \end{matrix} \quad (2.8)$$

This bijection has the property that two vectors in  $\mathbb{F}_2^4 \setminus \{0\}$  are perpendicular with respect to (2.7) if and only if the corresponding elements of the root system  $A_5$  are perpendicular. Combinatorially, this means that the two pairs of indices are disjoint. There are precisely 35 two-dimensional subspaces  $L$  in  $\mathbb{F}_2^4$ . Of these planes  $L$ , precisely 15 are isotropic, which means that  $L = L^\perp$ . The other 20 planes naturally come in pairs  $\{L, L^\perp\}$ . Each plane is a triple in  $\mathbb{F}_2^4 \setminus \{0\}$  and we write it as a cubic monomial  $z_{ij}z_{kl}z_{mn}$ . Under this identification, the parametrization (2.5) of the Segre cubic  $\mathcal{S}$  is given by the 15 isotropic planes  $L$ , while that of the Igusa quartic  $\mathcal{I}$  is given by the 10 pairs  $L \cdot L^\perp$  of non-isotropic planes in  $\mathbb{F}_2^4$ .

The symplectic group  $\mathbf{Sp}_4(\mathbb{F}_2)$  consists of all linear automorphisms of  $\mathbb{F}_2^4$  that preserve the symplectic form (2.7). As an abstract group, this is the symmetric group on six letters:

$$\mathbf{Sp}_4(\mathbb{F}_2) \cong \Sigma_6. \quad (2.9)$$

This group isomorphism is made explicit by the bijection (2.8).

Let  $\mathcal{M}_2(2)$  denote the moduli space of smooth curves of genus 2 with a level 2 structure. In light of the isomorphism (2.9), a level 2 structure on a genus 2 curve  $C$  is an ordering

of its six Weierstrass points, and this corresponds to the choice of six labeled points on the projective line  $\mathbb{P}^1$ . The latter choices are parametrized by the moduli space  $\mathcal{M}_{0,6}$ . In what follows, we consider the *open Segre cubic*  $\mathcal{S}^\circ = \mathcal{S} \setminus \{m_0 m_1 \cdots m_{14} = 0\}$  inside the torus  $\mathbb{G}_m^{14} \subset \mathbb{P}^{14}$  and the *open Igusa quartic*  $\mathcal{I}^\circ = \mathcal{I} \setminus \{m_0 m_1 \cdots m_9 = 0\}$  inside the torus  $\mathbb{G}_m^9 \subset \mathbb{P}^9$ .

**Proposition 2.2.2.** *We have the following identification of three-dimensional moduli spaces:*

$$\mathcal{S}^\circ = \mathcal{I}^\circ = \mathcal{M}_2(2) = \mathcal{M}_{0,6}. \quad (2.10)$$

*Proof.* We already argued the last equation. The first equation is the isomorphism between the open sets  $D$  and  $D'$  in the proof of [56, Theorem 3.3.11]. A nice way to see this isomorphism is that the kernels of our two monomial maps coincide (Lemma 2.2.3). The middle equation follows from the last part of [56, Theorem 3.3.8], which concerns the Kummer functor  $\mathbf{K}_2$ . For more information on the modular interpretations of  $\mathcal{S}$  and  $\mathcal{I}$  see [35, §VIII].  $\square$

The Kummer surface associated to a point in  $\mathcal{I}^\circ$  is the intersection of the Igusa quartic  $\mathcal{I}$  with the tangent space at that point, by [56, Theorem 3.3.8]. We find it convenient to express that Kummer surface in terms of the corresponding point in  $\mathcal{S}^\circ$ . Following Dolgachev and Ortland [35, §IX.5, Proposition 6], we write the defining equation of the Segre cubic  $\mathcal{S}$  as

$$16r^3 - 4r(s_{01}^2 + s_{10}^2 + s_{11}^2) + 4s_{01}s_{10}s_{11} + rt^2 = 0. \quad (2.11)$$

This differs by normalization constants from [35, §IX.5]. See [35, §IX.5] for the transformation of this equation into the classical one, which is  $\sum_i z_i = \sum_i z_i^3 = 0$ . The embedding of the  $\mathbb{P}^4$  with coordinates  $(r : s_{01} : s_{10} : s_{11} : t)$  into our  $\mathbb{P}^{14}$  can be written as

$$\begin{aligned} r &= m_0, & s_{01} &= 2m_0 - 4m_1, & s_{10} &= 2m_0 - 4m_3, \\ s_{11} &= 4m_4 - 2m_0 - 4m_7, & t &= 8(m_1 + m_3 - m_0 - m_4 - m_7). \end{aligned} \quad (2.12)$$

This does not pick out an  $\Sigma_6$ -equivariant embedding of the space spanned by the  $r, s_{ij}$  in the permutation representation of the  $m_i$ , but it has the advantage of giving short expressions. Fixing Schrödinger coordinates  $(x_{00} : x_{01} : x_{10} : x_{11})$  on  $\mathbb{P}^3$ , the Kummer surface is now given by

$$\begin{aligned} r(x_{00}^4 + x_{01}^4 + x_{10}^4 + x_{11}^4) + s_{01}(x_{00}^2 x_{01}^2 + x_{10}^2 x_{11}^2) + s_{10}(x_{00}^2 x_{10}^2 + x_{01}^2 x_{11}^2) \\ + s_{11}(x_{00}^2 x_{11}^2 + x_{01}^2 x_{10}^2) + t(x_{00} x_{01} x_{10} x_{11}) = 0. \end{aligned} \quad (2.13)$$

This equation is the determinant of the  $5 \times 5$ -matrix in [74, Example 1.1]. Its lower  $4 \times 4$ -minors satisfy (2.11). Our notation is consistent with that for the Coble quartic in [74, (2.13)].

We now come to the tropicalization of our three-dimensional moduli spaces. We write  $e_{12}, e_{13}, \dots, e_{56}$  for the unit vectors in  $\mathbb{TP}^{14} = \mathbb{R}^{15}/\mathbb{R}(1, 1, \dots, 1)$ . These correspond to our coordinates  $z_{12}, z_{13}, \dots, z_{56}$  on the  $\mathbb{P}^{14}$  which contains  $\text{Cyc}_4 \simeq \mathbb{P}^4$ . The 56 rays of the Bergman fan  $\text{trop}(\text{Cyc}_4)$  are indexed by proper subsets  $\sigma \subsetneq \{1, 2, 3, 4, 5, 6\}$  with  $|\sigma| \geq 2$ . They are

$$E_\sigma = \sum_{\{i,j\} \subseteq \sigma} e_{ij}.$$

Cones in  $\text{trop}(\text{Cyc}_4)$  are spanned by collections of  $E_\sigma$  whose indices  $\sigma$  are nested or disjoint.

Let  $A_{\text{segre}}$  denote the  $15 \times 15$ -matrix with entries in  $\{0, 1\}$  that represents the tropicalization of the monomial map (2.5). The columns of  $A_{\text{segre}}$  are indexed by (2.8). The rows of  $A_{\text{segre}}$  are indexed by tripartitions of  $\{1, 2, \dots, 6\}$ , or by isotropic planes in  $\mathbb{F}_2^4$ . An entry is 1 if the pair that indexes the column appears in the tripartition that indexes the row, or, equivalently, if the line of  $\mathbb{F}_2^4$  that indexes the column is contained in the plane that indexes the row. Note that each row and each column of  $A_{\text{segre}}$  has precisely three nonzero entries.

We similarly define the  $10 \times 15$ -matrix  $A_{\text{igusa}}$  with entries in  $\{0, 1\}$  that represents the monomial map for the Igusa quartic. Its rows have six nonzero entries and its columns have four nonzero entries. The column labels of  $A_{\text{igusa}}$  are the same as those of  $A_{\text{segre}}$ . The rows are now labeled by bipartitions of  $\{1, 2, \dots, 6\}$ , or by pairs of non-isotropic planes in  $\mathbb{F}_2^4$ .

**Lemma 2.2.3.** *The matrices  $A_{\text{segre}}$  and  $A_{\text{igusa}}$  have the same kernel. This kernel is the 5-dimensional subspace spanned by the vectors  $E_\sigma - E_{\sigma^c}$  where  $\sigma$  runs over triples in  $\{1, 2, \dots, 6\}$ .*

This lemma can be proved by a direct computation. The multiplicative version of this fact implies the identity  $\mathcal{S}^\circ = \mathcal{I}^\circ$  as seen in Proposition 2.2.2. We have the following result.

**Theorem 2.2.4.** *The tropical Segre cubic  $\text{trop}(\mathcal{S})$  in  $\mathbb{TP}^{14}$  is the image of  $\text{trop}(\text{Cyc}_4)$  under the linear map  $A_{\text{segre}}$ . The tropical Igusa quartic  $\text{trop}(\mathcal{I})$  in  $\mathbb{TP}^9$  is the image of  $\text{trop}(\text{Cyc}_4)$  under the linear map  $A_{\text{igusa}}$ . These two 3-dimensional fans are affinely isomorphic to each other, but all maximal cones of  $\text{trop}(\mathcal{I})$  come with multiplicity two. The underlying simplicial complex has 25 vertices, 105 edges and 105 triangles. This is the tree space  $\text{trop}(\mathcal{M}_{0,6})$ .*

*Proof.* The fact that we can compute the tropicalization of the image of a linear space under a monomial map by just applying the tropicalized monomial map  $A_\bullet$  to the Bergman fan is [33, Theorem 3.1]. The fact that the two tropical threefolds are affinely isomorphic follows immediately from Lemma 2.2.3. To analyze the combinatorics of this common image fan, we set  $E_\sigma$  to be the zero vector when  $\sigma = \{i\}$  is a singleton. With this convention, we have

$$A_{\text{segre}}E_\sigma = A_{\text{segre}}E_{\sigma^c} \quad \text{and} \quad A_{\text{igusa}}E_\sigma = A_{\text{igusa}}E_{\sigma^c}$$

for all proper subsets  $\sigma$  of  $\{1, 2, \dots, 6\}$ . We conclude that the  $56 = 15 + 20 + 15 + 6$  rays of the Bergman fan  $\text{trop}(\text{Cyc}_4)$  get mapped to  $25 = 15 + 10$  distinct rays in the image fan.

The cones in  $\text{trop}(\text{Cyc}_4)$  correspond to equidistant trees, that is, rooted metric trees on six taxa. Combinatorially, our map corresponds to removing the root from the tree, so the cones in the image fan correspond to unrooted metric trees on six taxa. Specifically, each of the 945 maximal cones of  $\text{trop}(\text{Cyc}_4)$  either has one ray  $E_{\{i,j,k,\ell,m\}}$  that gets mapped to zero, or it has two rays  $E_\sigma$  and  $E_{\sigma^c}$  that become identified. Therefore its image is three-dimensional. Our map takes the 945 simplicial cones of dimension 4 in  $\text{trop}(\text{Cyc}_4)$  onto the 105 simplicial cones of dimension 3, one for each unrooted tree. The fibers involve precisely nine cones because each trivalent tree on six taxa has nine edges, each a potential root location. Combinatorially, nine rooted trivalent trees map to the same unrooted tree.

It remains to analyze the multiplicity of each maximal cone in the image. The 105 maximal cones in  $\text{trop}(\mathcal{S})$  all have multiplicity one, while the corresponding cones in  $\text{trop}(\mathcal{I})$  have multiplicity two. We first found this by a direct calculation using the software `gfan` [57], starting from the homogeneous ideals of  $\mathcal{S}$  and  $\mathcal{I}$  described above. It can also be seen by examining the images of the rays  $E_\tau$  under each matrix  $A_\bullet$  modulo the line spanned by the vector  $(1, 1, \dots, 1)$ . Each of the 15 vectors  $A_{\text{igusa}}E_{ij}$  is the sum of four unit vectors in  $\mathbb{TP}^9$ , while the 10 vectors  $A_{\text{igusa}}E_{ijk}$  are the ten unit vectors multiplied by the factor 2.  $\square$

We next discuss the tropicalization of the universal family of Kummer surfaces over  $\mathcal{S}^\circ$ . This is the hypersurface in  $\mathcal{S}^\circ \times \mathbb{P}^3$  defined by the equation (2.13). The tropicalization of this hypersurface is a five-dimensional fan whose fibers over the tree space  $\text{trop}(\mathcal{S})$  are the tropical Kummer surfaces in  $\mathbb{TP}^3$ . We computed this fan from the equations using `gfan` [57].

**Proposition 2.2.5.** *The tropicalization of the universal Kummer surface in the coordinates  $((m_0 : m_1 : \dots : m_{14}), (x_{00} : x_{01} : x_{10} : x_{11}))$  is a 5-dimensional polyhedral fan in  $\mathbb{TP}^{14} \times \mathbb{TP}^3$ . This fan has 56 rays and 1536 maximal cones, and its  $f$ -vector is  $(56, 499, 1738, 2685, 1536)$ .*

Instances of tropical Kummer surfaces can be obtained by slicing the above fan with fixed values of the 15 tropical  $m$  coordinates. Figure 2.2 shows the tropicalization of a Kummer surface over a snowflake tree (Type (7) in Table 2.5). It consists of 30 two-dimensional polyhedra, 24 unbounded and 6 bounded. The latter 6 form the facets of a parallelepiped.

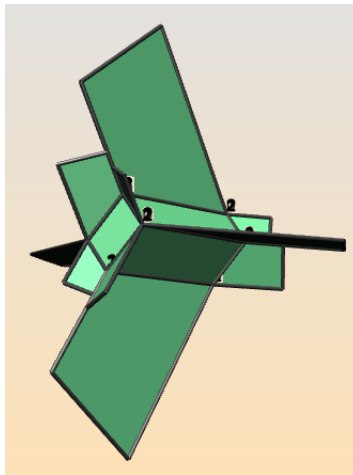


Figure 2.2: Tropicalization of a Kummer surface over a snowflake tree.

Figure 2.2 shows a tropical Kummer surface over a caterpillar tree (Type (6) in Table 2.5). It consists of 33 two-dimensional polyhedra, 24 bounded and 9 unbounded. The latter 9 polygons form a subdivision of a flat octagon. These two pictures were drawn using `polymake` [42].

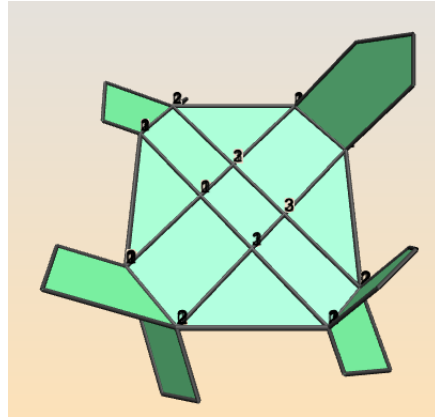


Figure 2.3: Tropicalization of a Kummer surface over a caterpillar tree.

On each Kummer surface we could now identify a tree that represents the bicanonical image of the associated genus 2 curve. Classically, one obtains a double quadric with six distinguished points by intersecting with any of the planes in the  $16_6$  configuration [74, (1.2)].

The tropical variety described in Theorem 2.2.4 defines the *tropical compactification*  $\overline{\mathcal{S}}$  of the Segre cubic  $\mathcal{S}$ . By definition, the threefold  $\overline{\mathcal{S}}$  is the closure of  $\mathcal{S}^\circ$  in the toric variety determined by the given fan structure on  $\text{trop}(\mathcal{S})$ . For details, see Tevelev’s article [89].

This tropical compactification of our moduli space (2.10) is intrinsic. To see this, we recall that the *intrinsic torus* of a very affine variety  $X \subset \mathbb{G}_m^n$  is the torus whose character lattice is the finitely generated multiplicative free abelian group  $K[X]^*/K^*$ . The following lemma can be used to find the intrinsic torus for each of the very affine varieties in this chapter.

**Lemma 2.2.6.** *Let  $m: T_1 \rightarrow T_2$  be a monomial map of tori and  $U \subset T_1$  a subvariety embedded in its intrinsic torus. Then  $\overline{m(U)} \subset \overline{m(T_1)}$  is the embedding of  $\overline{m(U)}$  in its intrinsic torus.*

*Proof.* Choose identifications  $K[T_1] = K[x_1^\pm, \dots, x_r^\pm]$  and  $K[T_2] = K[y_1^\pm, \dots, y_s^\pm]$ . By assumption, the pullback  $m^*(y_i)$  is a monomial in the  $x_j$ , which we call  $z_i$ . We have an injection of rings  $m^*: K[\overline{m(U)}] \subset K[U]$ , and hence we get an induced injection of groups  $\phi: K[\overline{m(U)}]^*/K^* \subset K[U]^*/K^*$ . Since  $K[\overline{m(U)}]$  is generated by the  $y_i$ , we conclude that  $m^*(K[\overline{m(U)}])$  is contained in the subalgebra  $K[z_1^\pm, \dots, z_s^\pm] \subset K[U]$ . Pick  $f \in K[\overline{m(U)}]^*/K^*$ . Since  $U$  is embedded in its intrinsic torus, we have  $\phi(f) = z_1^{d_1} \cdots z_s^{d_s}$  for some  $d_i \in \mathbb{Z}$ . So  $\phi(y_1^{d_1} \cdots y_s^{d_s}) = \phi(f)$  and since  $\phi$  is injective, we conclude that  $f = y_1^{d_1} \cdots y_s^{d_s}$ .  $\square$

The embedding of the Segre cubic  $\mathcal{S}$  into the 9-dimensional toric variety given by (2.5) satisfies the hypotheses of Lemma 2.2.6. Indeed,  $\mathcal{S}^\circ$  is the image of the complement of a hyperplane arrangement under a monomial map, and, by [89, §4], the intrinsic torus of an essential arrangement of  $n$  hyperplanes in  $\mathbb{P}^r$  is  $\mathbb{G}_m^{n-1}$ . The same argument works for all

moduli spaces studied in this chapter. That the ambient torus  $\mathbb{G}_m^9$  is intrinsic for the open Segre cubic  $\mathcal{S}^\circ$  can also be seen from the fact that the 15 boundary divisors  $\mathcal{S} \cap \{m_i = 0\}$  are irreducible. Indeed, by [56, §3.2.1], they are projective planes  $\mathbb{P}^2$ . Each of the ten singular points of  $\mathcal{S}$  lies on six of these planes, so each boundary plane contains four singular points.

The combinatorial structures described above have the following geometric interpretation.

**Proposition 2.2.7.** *The tropical compactification of the open Segre cubic  $\mathcal{S}^\circ$ , and hence of the other moduli spaces in (2.10), is the Deligne–Mumford compactification  $\overline{\mathcal{M}}_{0,6}$ . This threefold is the blow-up of the 10 singular points of  $\mathcal{S}$ , or of the 15 singular lines of the Igusa quartic  $\mathcal{I}$ .*

*Proof.* The first sentence is a special case of [50, Theorem 1.11]. The second is [56, Theorem 3.3.11].  $\square$

Our rationale for giving a detailed equational derivation of the familiar manifold  $\overline{\mathcal{M}}_{0,6}$  is that it sets the stage for our primary example in the next section.

## 2.3 Burkhardt Quartic and Abelian Surfaces

The Burkhardt quartic is a rational quartic threefold in  $\mathbb{P}^4$ . It can be characterized as the unique quartic hypersurface in  $\mathbb{P}^4$  with the maximal number 45 of nodal singular points [32]. It compactifies the moduli space  $\mathcal{M}_2(3)$  of genus 2 curves with level 3 structure [34, 41, 46, 56]. We identify  $\mathcal{M}_2(3)$  with a subvariety of  $\mathcal{A}_2(3)$ , the moduli space of principally polarized abelian surfaces with level 3 structure, by sending a smooth curve to its Jacobian.

All constructions in this section can be carried out over any field  $K$  of characteristic other than 2 or 3, provided  $K$  contains a primitive third root of unity  $\omega$ . In the tropical context,  $K$  will be a field with a valuation. For details on arithmetic issues see Elkies’ paper [37].

We realize the Burkhardt quartic as the image of a rational map that is given as a composition  $\mathbb{P}^3 \xrightarrow{\text{linear}} \mathbb{P}^{39} \xrightarrow{\text{monomial}} \mathbb{P}^{39}$ . We choose coordinates  $(c_0 : c_1 : c_2 : c_3)$  on  $\mathbb{P}^3$  and coordinates  $(m_0 : m_1 : \dots : m_{39})$  on the rightmost  $\mathbb{P}^{39}$ . The 40 homogeneous coordinates  $u_{ijkl}$  on the middle  $\mathbb{P}^{39}$  are indexed by the lines through the origin in the finite vector space  $\mathbb{F}_3^4$ . Each line is given by the vector whose leftmost nonzero coordinate is 1. The linear map  $\mathbb{P}^3 \hookrightarrow \mathbb{P}^{39}$  is defined as follows, where  $\omega = \frac{1}{2}(-1 + \sqrt{-3})$  is a third root of unity:

$$\begin{array}{llll}
u_{0001} = c_1 + c_2 + c_3 & u_{0010} = c_2 - c_3 + c_0 & u_{0011} = c_3 + c_0 - c_1 & u_{0012} = c_0 + c_1 - c_2 \\
u_{0100} = \sqrt{-3} \cdot c_1 & u_{0101} = c_1 + \omega^2 c_2 + \omega^2 c_3 & u_{0102} = c_1 + \omega c_2 + \omega c_3 & u_{0110} = c_2 - \omega c_3 + \omega^2 c_0 \\
u_{0111} = c_3 + c_0 - \omega c_1 & u_{0112} = c_0 + \omega^2 c_1 - c_2 & u_{0120} = c_2 - \omega^2 c_3 + \omega c_0 & u_{0121} = c_0 + \omega c_1 - c_2 \\
u_{0122} = c_3 + c_0 - \omega^2 c_1 & u_{1000} = \sqrt{-3} \cdot c_0 & u_{1001} = c_1 + \omega c_2 + \omega^2 c_3 & u_{1002} = c_1 + \omega^2 c_2 + \omega c_3 \\
u_{1010} = c_2 - c_3 + \omega c_0 & u_{1011} = c_3 + \omega c_0 - c_1 & u_{1012} = c_0 + \omega^2 c_1 - \omega^2 c_2 & u_{1020} = c_2 - c_3 + \omega^2 c_0 \\
u_{1021} = c_0 + c_1 \omega - \omega c_2 & u_{1022} = c_3 + \omega^2 c_0 - c_1 & u_{1100} = \sqrt{-3} \cdot c_3 & u_{1101} = c_1 + c_2 + \omega c_3 \\
u_{1102} = c_1 + c_2 + c_3 \omega^2 & u_{1110} = c_2 - \omega c_3 + c_0 & u_{1111} = c_3 + \omega c_0 - \omega c_1 & u_{1112} = c_0 + \omega c_1 - \omega^2 c_2
\end{array}$$

$$\begin{aligned}
u_{1120} &= c_2 - \omega^2 c_3 + c_0 & u_{1121} &= c_0 + \omega^2 c_1 - \omega c_2 & u_{1122} &= c_3 + c_0 \omega^2 - \omega^2 c_1 & u_{1200} &= \sqrt{-3} \cdot c_2 \\
u_{1201} &= c_1 + \omega^2 c_2 + c_3 & u_{1202} &= c_1 + \omega c_2 + c_3 & u_{1210} &= c_2 - \omega^2 c_3 + \omega^2 c_0 & u_{1211} &= c_3 + \omega c_0 - \omega^2 c_1 \\
u_{1212} &= c_0 + c_1 - \omega^2 c_2 & u_{1220} &= c_2 - \omega c_3 + \omega c_0 & u_{1221} &= c_0 + c_1 - \omega c_2 & u_{1222} &= c_3 + \omega^2 c_0 - \omega c_1
\end{aligned}$$

These 40 linear forms cut out the hyperplanes of the complex reflection arrangement  $G_{32}$ . We refer to the book by Hunt [56, §5] for a discussion of this arrangement and its importance for modular Siegel threefolds. Our first map  $\mathbb{P}^3 \hookrightarrow \mathbb{P}^{39}$  realizes the arrangement  $G_{32}$  as the restriction of the 40 coordinate planes in  $\mathbb{P}^{39}$  to a certain 3-dimensional linear subspace.

The monomial map  $\mathbb{P}^{39} \dashrightarrow \mathbb{P}^{39}$  is defined outside the hyperplane arrangement  $\{\prod u_{ijkl} = 0\}$  which corresponds to  $G_{32}$ . It is given by the following 40 monomials of degree four:

$$\begin{aligned}
m_0 &= u_{0001}u_{0010}u_{0011}u_{0012} & m_1 &= u_{0001}u_{1000}u_{1001}u_{1002} & m_2 &= u_{0001}u_{1010}u_{1011}u_{1012} \\
m_3 &= u_{0001}u_{1020}u_{1021}u_{1022} & m_4 &= u_{0010}u_{0100}u_{0110}u_{0120} & m_5 &= u_{0010}u_{0101}u_{0111}u_{0121} \\
m_6 &= u_{0010}u_{0102}u_{0112}u_{0122} & m_7 &= u_{0011}u_{1200}u_{1211}u_{1222} & m_8 &= u_{0011}u_{1201}u_{1212}u_{1220} \\
m_9 &= u_{0011}u_{1202}u_{1210}u_{1221} & m_{10} &= u_{0012}u_{1100}u_{1112}u_{1121} & m_{11} &= u_{0012}u_{1101}u_{1110}u_{1122} \\
m_{12} &= u_{0012}u_{1102}u_{1111}u_{1120} & m_{13} &= u_{0100}u_{1000}u_{1100}u_{1200} & m_{14} &= u_{0100}u_{1010}u_{1110}u_{1210} \\
m_{15} &= u_{0100}u_{1020}u_{1120}u_{1220} & m_{16} &= u_{0101}u_{1000}u_{1101}u_{1202} & m_{17} &= u_{0101}u_{1010}u_{1111}u_{1212} \\
m_{18} &= u_{0101}u_{1020}u_{1121}u_{1222} & m_{19} &= u_{0102}u_{1000}u_{1102}u_{1201} & m_{20} &= u_{0102}u_{1010}u_{1112}u_{1211} \\
m_{21} &= u_{0102}u_{1020}u_{1122}u_{1221} & m_{22} &= u_{0110}u_{1001}u_{1111}u_{1221} & m_{23} &= u_{0110}u_{1011}u_{1121}u_{1201} \\
m_{24} &= u_{0110}u_{1021}u_{1101}u_{1211} & m_{25} &= u_{0111}u_{1001}u_{1112}u_{1220} & m_{26} &= u_{0111}u_{1011}u_{1122}u_{1200} \\
m_{27} &= u_{0111}u_{1021}u_{1102}u_{1210} & m_{28} &= u_{0112}u_{1001}u_{1110}u_{1222} & m_{29} &= u_{0112}u_{1011}u_{1120}u_{1202} \\
m_{30} &= u_{0112}u_{1021}u_{1100}u_{1212} & m_{31} &= u_{0120}u_{1002}u_{1122}u_{1212} & m_{32} &= u_{0120}u_{1012}u_{1102}u_{1222} \\
m_{33} &= u_{0120}u_{1022}u_{1112}u_{1202} & m_{34} &= u_{0121}u_{1002}u_{1120}u_{1211} & m_{35} &= u_{0121}u_{1012}u_{1100}u_{1221} \\
m_{36} &= u_{0121}u_{1022}u_{1110}u_{1201} & m_{37} &= u_{0122}u_{1002}u_{1121}u_{1210} & m_{38} &= u_{0122}u_{1012}u_{1101}u_{1220} \\
m_{39} &= u_{0122}u_{1022}u_{1111}u_{1200}.
\end{aligned}$$

The combinatorics behind this list is as follows. The 40 monomials represent the 40 isotropic planes in the space  $\mathbb{F}_3^4$ , with respect to the symplectic inner product (2.7). The linear inclusion  $\mathbb{P}^3 \hookrightarrow \mathbb{P}^{39}$  has the property that two linearly independent vectors  $x, y$  in  $\mathbb{F}_3^4$  satisfy  $\langle x, y \rangle = 0$  if and only if the corresponding linear forms  $u_x$  and  $u_y$  are perpendicular in the root system  $G_{32}$ , using the usual Hermitian inner product (when considered over  $\mathbb{C}$ ).

Let  $\mathcal{B}$  denote the Burkhardt quartic in  $\mathbb{P}^{39}$ , that is, the closure of the image of the map above. Its homogeneous prime ideal  $I_{\mathcal{B}}$  is minimally generated by one quartic and a 35-dimensional space of linear forms in  $K[m_0, m_1, \dots, m_{39}]$ . That space has a natural generating set consisting of  $160 = 4 \cdot 40$  linear trinomials. Namely, the four coordinates  $m_{\bullet}$  that share a common parameter  $u_{ijkl}$  span a two-dimensional space modulo  $I_{\mathcal{B}}$ . For instance, the first four coordinates share the parameter  $u_{0001}$ , and they satisfy the following linear trinomials:

$$\begin{aligned}
m_0 + \omega^2 m_1 - \omega m_2 &= m_0 - \omega m_1 - \omega^2 m_3 = \\
m_0 + \omega^2 m_2 + \omega m_3 &= m_1 + \omega m_2 - \omega^2 m_3 = 0.
\end{aligned} \tag{2.14}$$

These relations are constructed as follows: Each of the 40 roots  $u_{ijkl}$  appears as a factor in precisely four of the coordinates  $m_{\bullet}$ , and these four span a two-dimensional space over  $K$ .



The 160 linear trinomials (2.14) cut out a 4-dimensional linear subspace of  $\mathbb{P}^{39}$ . We fix the following system of coordinates, analogous to (2.12), on that linear subspace  $\mathbb{P}^4$  of  $\mathbb{P}^{39}$ :

$$\begin{aligned}
 r &= 3c_0c_1c_2c_3 &= m_{13}/3 \\
 s_{01} &= -c_0(c_1^3 + c_2^3 + c_3^3) &= (\sqrt{-3} \cdot m_1 - m_{13})/3 \\
 s_{10} &= c_1(c_0^3 + c_2^3 - c_3^3) &= (-\sqrt{-3} \cdot m_4 - m_{13})/3 \\
 s_{11} &= c_2(c_0^3 - c_1^3 + c_3^3) &= (-\sqrt{-3} \cdot m_7 - m_{13})/3 \\
 s_{12} &= c_3(c_0^3 + c_1^3 - c_2^3) &= (-\sqrt{-3} \cdot m_{10} - m_{13})/3
 \end{aligned} \tag{2.15}$$

The polynomial that defines the Burkhardt quartic  $\mathcal{B} \subset \mathbb{P}^4$  is now written as

$$r(r^3 + s_{01}^3 + s_{10}^3 + s_{11}^3 + s_{12}^3) + 3s_{01}s_{10}s_{11}s_{12} = 0. \tag{2.16}$$

The Burkhardt quartic has 45 isolated singular points. For example, one of the singular points is  $(r : s_{01} : s_{10} : s_{11} : s_{12}) = (0 : 0 : 0 : 1 : 1)$ . In the  $m$ -coordinates, this point is

$$\begin{aligned}
 (0 : 0 : 0 : 0 : 0 : 0 : 0 : -\omega^2 : -\omega : 1 : \omega^2 : -1 : \omega : 0 : 0 : 0 : 0 : 0 : \\
 0 : 0 : 0 : 0 : 0 : -\omega^2 : -1 : -\omega : -1 : -\omega^2 : \omega^2 : -\omega : \omega^2 : \\
 \omega^2 : \omega^2 : 1 : \omega : 1 : \omega^2 : -\omega^2 : \omega : -\omega^2 : -\omega^2)
 \end{aligned} \tag{2.17}$$

For each singular point precisely 16 of the 40  $m$ -coordinates are zero. Each hyperplane  $m_{\bullet} = 0$  intersects the Burkhardt quartic  $\mathcal{B}$  in a tetrahedron of four planes, known as *Jacobi planes*, which contains 18 of the 45 singular points, in a configuration that is depicted in [56, Figure 5.3(b)]. The relevant combinatorics will be explained when tropicalizing in Section 2.4.

The closure of the image of the monomial map  $\mathbb{P}^{39} \dashrightarrow \mathbb{P}^{39}$ ,  $u \mapsto m$  is a toric variety  $\mathcal{T}$ . Writing  $\mathbb{P}^4$  for the linear subspace defined by the 160 trinomials like (2.14), we have

$$\mathcal{B} = \mathcal{T} \cap \mathbb{P}^4 \subset \mathbb{P}^{39}. \tag{2.18}$$

Thus we have realized the Burkhardt quartic as a linear section of the toric variety  $\mathcal{T}$ , and it makes sense to explore the combinatorial properties of  $\mathcal{T}$ . Let  $A$  denote the  $40 \times 40$  matrix representing our monomial map  $u \mapsto m$ . The columns of  $A$  are indexed by the  $u_{ijkl}$ , and hence by the lines in  $\mathbb{F}_3^4$ . The rows of  $A$  are indexed by the  $m_{\bullet}$ , and hence by the isotropic planes in  $\mathbb{F}_3^4$ . The matrix  $A$  is the 0-1 matrix that encodes incidences of lines and isotropic planes. Each row and each column has exactly four entries 1, and the other entries are 0. The matrix  $A$  has rank 25, and we computed its *Markov basis* using the software `4ti2` [1].

**Proposition 2.3.1.** (a) *The projective toric variety  $\mathcal{T}$  has dimension 24.*

(b) *Its prime ideal is minimally generated by 5136 binomials, namely 216 binomials of degree 5, 270 of degree 6, 4410 of degree 8, and 240 of degree 12.*

(c) *The Burkhardt quartic is the scheme-theoretic intersection in (2.18). This intersection is not ideal-theoretic, since there is no quartic relation on  $\mathcal{T}$  that could specialize to (2.16).*

(d) The 24-dimensional polytope of  $\mathcal{T}$ , which is the convex hull of the 40 rows of  $A$ , has precisely 13144 facets.

*Proof.* (a) follows from the fact that  $\text{rank}(A) = 25$ . The statements in (b) and (c) follow from our `4ti2` calculation. The facets in (d) were computed using the software `polymake` [42]. The scheme-theoretic intersection in (c) can be verified by taking the following five among the 216 quintic binomials that vanish on  $\mathcal{T}$ :

$$\begin{aligned} m_0m_{13}m_{22}m_{33}m_{37} - m_1m_4m_9m_{10}m_{39} & \quad m_0m_{14}m_{23}m_{33}m_{35} - m_2m_4m_9m_{10}m_{36} \\ m_0m_{16}m_{25}m_{35}m_{37} - m_1m_5m_9m_{10}m_{38} & \quad m_0m_{17}m_{26}m_{36}m_{38} - m_2m_5m_8m_{11}m_{39} \\ m_9m_{11}m_{13}m_{18}m_{20} - m_7m_{10}m_{14}m_{16}m_{21} & \end{aligned}$$

Each of these quintic binomials factors on  $\mathbb{P}^4$  as the Burkhardt quartic (2.18) times a linear form, and these five linear forms generate the irrelevant maximal ideal  $\langle r, s_{01}, s_{10}, s_{11}, s_{12} \rangle$ .  $\square$

We next explain the connection to abelian surfaces. Consider the *open Burkhardt quartic*

$$\mathcal{B}^\circ = \mathcal{B} \setminus \left\{ \prod m_i = 0 \right\} \subset \mathbb{P}^{39}.$$

In its modular interpretation ([41], [46, §3.1], [56, Lemma 5.7.1]), this threefold is the moduli space  $\mathcal{M}_2(3)$  of smooth genus 2 curves with level 3 structure. With every point  $(r : s_{01} : s_{10} : s_{11} : s_{12}) \in \mathcal{B}^\circ$  we associate an abelian surface (which is a Jacobian) following [46, §3.2]. The ambient space for this family of abelian surfaces is the projective space  $\mathbb{P}^8$  whose coordinates

$$(x_{00} : x_{01} : x_{02} : x_{10} : x_{11} : x_{12} : x_{20} : x_{21} : x_{22})$$

are indexed by  $\mathbb{F}_3^2$ . The following five polynomials represent all the affine subspaces of  $\mathbb{F}_3^2$ :

$$\begin{aligned} f &= x_{00}^3 + x_{01}^3 + x_{02}^3 + x_{10}^3 + x_{11}^3 + x_{12}^3 + x_{20}^3 + x_{21}^3 + x_{22}^3, \\ g_{01} &= 3(x_{00}x_{01}x_{02} + x_{10}x_{11}x_{12} + x_{20}x_{21}x_{22}), \\ g_{10} &= 3(x_{00}x_{10}x_{20} + x_{01}x_{11}x_{21} + x_{02}x_{12}x_{22}), \\ g_{11} &= 3(x_{00}x_{11}x_{22} + x_{01}x_{12}x_{20} + x_{10}x_{21}x_{02}), \\ g_{12} &= 3(x_{00}x_{12}x_{21} + x_{01}x_{10}x_{22} + x_{02}x_{11}x_{20}). \end{aligned}$$

Our abelian surface is the singular locus of the *Coble cubic*  $\{C = 0\}$  in  $\mathbb{P}^8$ , which is given by

$$C = rf + s_{01}g_{01} + s_{10}g_{10} + s_{11}g_{11} + s_{12}g_{12}.$$

**Theorem 2.3.2.** *The singular locus of the Coble cubic of any point in  $\mathcal{B}^\circ$  is an abelian surface  $S$  of degree 18 in  $\mathbb{P}^8$ . This equips  $S$  with an indecomposable polarization of type  $(3, 3)$ . The prime ideal of  $S$  is minimally generated by 9 quadrics and 3 cubics. The theta divisor on  $S$  is a tricanonical curve of genus 2, and this is obtained by intersecting  $S$  with the  $\mathbb{P}^4$  defined by*

$$\text{rank} \begin{pmatrix} x_{00} & x_{01}+x_{02} & x_{10}+x_{20} & x_{11}+x_{22} & x_{12}+x_{21} \\ r & s_{01} & s_{10} & s_{11} & s_{12} \end{pmatrix} \leq 1. \quad (2.19)$$

*Proof.* The first statement is classical (see [13, §10.7]). We shall explain it below using theta functions. The fact about ideal generators is due to Gunji [48, Theorem 8.3]. The representation (2.19) of the curve whose Jacobian is  $S$  is derived from [46, Theorem 3.14(d)].  $\square$

We now discuss the complex analytic view of our story. Recall (e.g. from [13, §8.1]) that a principally polarized abelian surface over  $\mathbb{C}$  is given analytically as  $S_\tau = \mathbb{C}^2/(\mathbb{Z}^2 + \tau\mathbb{Z}^2)$ , where  $\tau$  is a complex symmetric  $2 \times 2$ -matrix whose imaginary part is positive definite. The set of such matrices is the *Siegel upper half space*  $\mathfrak{H}_2$ . Fix the  $4 \times 4$  matrix  $J = \begin{bmatrix} 0 & -\text{Id}_2 \\ \text{Id}_2 & 0 \end{bmatrix}$ . Let  $\text{Sp}_4(\mathbb{Z})$  be the group of  $4 \times 4$  integer-valued matrices  $\gamma$  such that  $\gamma J \gamma^T = J$ . This acts on  $\mathfrak{H}_2$  via

$$\begin{bmatrix} A & B \\ C & D \end{bmatrix} \cdot \tau = (A\tau + B)(C\tau + D)^{-1}, \quad (2.20)$$

where  $A, B, C, D$  are  $2 \times 2$  matrices, and this descends to an action of  $\text{PSp}_4(\mathbb{Z})$  on  $\mathfrak{H}_2$ . The natural map  $\text{PSp}_4(\mathbb{Z}) \rightarrow \text{PSp}_4(\mathbb{F}_3)$  takes the residue class modulo 3 of each matrix entry. Let  $\Gamma_2(3)$  denote the kernel of this map. The action of  $\text{PSp}_4(\mathbb{Z})$  preserves the abelian surface, while  $\Gamma_2(3)$  preserves the abelian surface together with a level 3 structure. Hence  $\mathfrak{H}_2/\text{PSp}_4(\mathbb{Z})$  is the moduli space  $\mathcal{A}_2$  of principally polarized abelian surfaces, while  $\mathfrak{H}_2/\Gamma_2(3)$  is the moduli space  $\mathcal{A}_2(3)$  of principally polarized abelian surfaces with level 3 structure. The finite group  $\text{PSp}_4(\mathbb{F}_3)$  is a simple group of order 25920 and it acts naturally on  $\mathfrak{H}_2/\Gamma_2(3)$ .

The *third-order theta function* with characteristic  $\sigma \in \frac{1}{3}\mathbb{Z}^2/\mathbb{Z}^2$  is defined as

$$\begin{aligned} \Theta_3[\sigma](\tau, z) &= \exp(3\pi i \sigma^T \tau \sigma + 6\pi i \sigma^T z) \cdot \theta(3\tau, 3z + 3\tau\sigma) \\ &= \sum_{n \in \mathbb{Z}^2} \exp(3\pi i (n + \sigma)^T \tau (n + \sigma) + 6\pi i (n + \sigma)^T z). \end{aligned}$$

Here  $\theta$  is the classical Riemann theta function. For a fixed matrix  $\tau \in \mathfrak{H}_2$ , the nine third-order theta functions on  $\mathbb{C}^2$  give precisely our embedding of the abelian surface  $S_\tau$  into  $\mathbb{P}^8$ :

$$S_\tau \hookrightarrow \mathbb{P}^8, \quad z \mapsto (\Theta_3[\sigma](\tau, z))_{\sigma \in \frac{1}{3}\mathbb{Z}^2/\mathbb{Z}^2}.$$

Adopting the notation in [74, §2], for any  $(j, k) \in \{0, 1, 2\}^2$ , we abbreviate

$$u_{jk} = \Theta_3\left[\left(\frac{j}{3}, \frac{k}{3}\right)\right](\tau, 0) \quad \text{and} \quad x_{jk} = \Theta_3\left[\left(\frac{j}{3}, \frac{k}{3}\right)\right](\tau, z).$$

The nine *theta constants*  $u_{jk}$  satisfy  $u_{01} = u_{02}$ ,  $u_{10} = u_{20}$ ,  $u_{11} = u_{22}$ , and  $u_{12} = u_{21}$ . For that reason, we need only five theta constants  $u_{00}, u_{01}, u_{10}, u_{11}, u_{12}$ , which we take as homogeneous coordinates on  $\mathbb{P}^4$ . These five coordinates satisfy one homogeneous equation:

**Lemma 2.3.3.** *The closure of the image of the map  $\mathfrak{H}_2 \rightarrow \mathbb{P}^4$  given by the five theta constants is an irreducible hypersurface  $\mathcal{H}$  of degree 10. Its defining polynomial is the determinant of*

$$U = \begin{bmatrix} u_{00}^2 & u_{01}^2 & u_{10}^2 & u_{11}^2 & u_{12}^2 \\ u_{01}^2 & u_{00}u_{01} & u_{11}u_{12} & u_{10}u_{12} & u_{10}u_{11} \\ u_{10}^2 & u_{11}u_{12} & u_{00}u_{10} & u_{01}u_{12} & u_{01}u_{11} \\ u_{11}^2 & u_{10}u_{12} & u_{01}u_{12} & u_{00}u_{11} & u_{01}u_{10} \\ u_{12}^2 & u_{10}u_{11} & u_{01}u_{11} & u_{01}u_{10} & u_{00}u_{12} \end{bmatrix}.$$

*Proof.* This determinant appears in [34, (10)], [41, p. 252], and [65, §2.2].  $\square$

At this point, we have left the complex analytic world and we are back over a more general field  $K$ . The natural map  $\mathcal{H} \dashrightarrow \mathcal{B}$  is 10-to-1 and it is given explicitly by  $4 \times 4$ -minors of  $U$ .

**Corollary 2.3.4.** *Over the Hessian  $\mathcal{H}$  of the Burkhardt quartic, the Coble cubic is written as*

$$C = \det \begin{bmatrix} f(\mathbf{x}) & g_{01}(\mathbf{x}) & g_{10}(\mathbf{x}) & g_{11}(\mathbf{x}) & g_{12}(\mathbf{x}) \\ u_{01}^2 & u_{00}u_{01} & u_{11}u_{12} & u_{10}u_{12} & u_{10}u_{11} \\ u_{10}^2 & u_{11}u_{12} & u_{00}u_{10} & u_{01}u_{12} & u_{01}u_{11} \\ u_{11}^2 & u_{10}u_{12} & u_{01}u_{12} & u_{00}u_{11} & u_{01}u_{10} \\ u_{12}^2 & u_{10}u_{11} & u_{01}u_{11} & u_{01}u_{10} & u_{00}u_{12} \end{bmatrix}. \quad (2.21)$$

For  $K = \mathbb{C}$ , this expresses  $r, s_{01}, s_{10}, s_{11}, s_{12}$  as modular forms in terms of theta constants.

We note that the 10-to-1 map  $\mathcal{H} \dashrightarrow \mathcal{B}$  is analogous to the 64-to-1 map in [74, (7.1)] from the Satake hypersurface onto the Göpel variety. The formula for the Coble cubic in Corollary 2.3.4 is analogous to the expression for the Coble quartic in [74, Theorem 7.1].

In this section we have now introduced four variants of a universal abelian surface. Each of these is a five-dimensional projective variety. Our universal abelian surfaces reside

- (a) in  $\mathbb{P}^3 \times \mathbb{P}^8$  with coordinates  $(\mathbf{c}, \mathbf{x})$ ,
- (b) in  $\mathcal{B} \times \mathbb{P}^8 \subset \mathbb{P}^4 \times \mathbb{P}^8$  with coordinates  $((r : s_{ij}), \mathbf{x})$ ,
- (c) in  $\mathcal{B} \times \mathbb{P}^8 \subset \mathbb{P}^{39} \times \mathbb{P}^8$  with coordinates  $(\mathbf{m}, \mathbf{x})$ ,
- (d) in  $\mathcal{H} \times \mathbb{P}^8 \subset \mathbb{P}^4 \times \mathbb{P}^8$  with coordinates  $(\mathbf{u}, \mathbf{x})$ .

A natural commutative algebra problem is to identify explicit minimal generators for the bihomogeneous prime ideals of each of these universal abelian surfaces.

For instance, consider case (d). The ideal contains the polynomial  $\det(U)$  of bidegree  $(10, 0)$  and eight polynomials of bidegree  $(8, 2)$ , namely the partial derivatives of  $C$  with respect to the  $x_{ij}$ . However, these nine do not suffice. For instance, we have ten linearly independent ideal generators of bidegree  $(3, 3)$ , namely the  $2 \times 2$ -minors of the  $2 \times 5$ -matrix

$$\begin{bmatrix} f(\mathbf{x}) & g_{01}(\mathbf{x}) & g_{10}(\mathbf{x}) & g_{11}(\mathbf{x}) & g_{12}(\mathbf{x}) \\ f(\mathbf{u}) & g_{01}(\mathbf{u}) & g_{10}(\mathbf{u}) & g_{11}(\mathbf{u}) & g_{12}(\mathbf{u}) \end{bmatrix}.$$

These equations have been verified numerically using **Sage** [85]. For a fixed general point  $\mathbf{u} \in \mathcal{S}$ , these  $2 \times 2$ -minors give Gunji's three cubics that were mentioned in Theorem 2.3.2.

For the case (a) here is a concrete conjecture concerning the desired prime ideal.

**Conjecture 2.3.5.** *The prime ideal of the universal abelian surface in  $\mathbb{P}^3 \times \mathbb{P}^8$  is minimally generated by 93 polynomials, namely 9 polynomials of bidegree (4, 2) and 84 of bidegree (3, 3).*

The 84 polynomials of bidegree (3, 3) are obtained as the  $6 \times 6$ -subpfaffians of the matrix

$$\begin{bmatrix} 0 & -c_0x_{02} & c_0x_{01} & -c_1x_{20} & -c_2x_{22} & -c_3x_{21} & c_1x_{10} & c_3x_{12} & c_2x_{11} \\ c_0x_{02} & 0 & -c_0x_{00} & -c_3x_{22} & -c_1x_{21} & -c_2x_{20} & c_2x_{12} & c_1x_{11} & c_3x_{10} \\ -c_0x_{01} & c_0x_{00} & 0 & -c_2x_{21} & -c_3x_{20} & -c_1x_{22} & c_3x_{11} & c_2x_{10} & c_1x_{12} \\ c_1x_{20} & c_3x_{22} & c_2x_{21} & 0 & -c_0x_{12} & c_0x_{11} & -c_1x_{00} & -c_2x_{02} & -c_3x_{01} \\ c_2x_{22} & c_1x_{21} & c_3x_{20} & c_0x_{12} & 0 & -c_0x_{10} & -c_3x_{02} & -c_1x_{01} & -c_2x_{00} \\ c_3x_{21} & c_2x_{20} & c_1x_{22} & -c_0x_{11} & c_0x_{10} & 0 & -c_2x_{01} & -c_3x_{00} & -c_1x_{02} \\ -c_1x_{10} & -c_2x_{12} & -c_3x_{11} & c_1x_{00} & c_3x_{02} & c_2x_{01} & 0 & -c_0x_{22} & c_0x_{21} \\ -c_3x_{12} & -c_1x_{11} & -c_2x_{10} & c_2x_{02} & c_1x_{01} & c_3x_{00} & c_0x_{22} & 0 & -c_0x_{20} \\ -c_2x_{11} & -c_3x_{10} & -c_1x_{12} & c_3x_{01} & c_2x_{00} & c_1x_{02} & -c_0x_{21} & c_0x_{20} & 0 \end{bmatrix}. \quad (2.22)$$

This skew-symmetric  $9 \times 9$ -matrix was derived by Gruson and Sam [46, §3.2], building on the construction in [47], and it is analogous to the elliptic normal curve in (2.1). The nine principal  $8 \times 8$ -subpfaffians of (2.22) are  $x_{00}C, x_{01}C, \dots, x_{22}C$ , where  $C$  is the Coble quartic, now regarded as a polynomial in  $(\mathbf{c}, \mathbf{x})$  of bidegree (4, 3). Conjecture 2.3.5 is analogous to [74, Conjecture 8.1]. The nine polynomials of bidegree (4, 2) are  $\partial C/\partial x_{00}, \partial C/\partial x_{01}, \dots, \partial C/\partial x_{22}$ .

In the remainder of this section we recall the symmetry groups that act on our varieties. First there is the complex reflection group denoted by  $G_{32}$  in the classification of Shephard and Todd [82]. The group  $G_{32}$  is a subgroup of order 155520 in  $GL_4(K)$ . Precisely 80 of its elements are *complex reflections* of order 3. As a linear transformation on  $K^4$ , each such complex reflection has a triple eigenvalue 1 and a single eigenvalue  $\omega^{\pm 1} = \frac{1}{2}(-1 \pm \sqrt{-3})$ .

The center of  $G_{32}$  is isomorphic to the cyclic group  $\mathbb{Z}/6$ . In our coordinates  $c_0, c_1, c_2, c_3$ , the elements of the center are scalar multiplications by 6th roots of unity. Therefore, this gives an action by  $G_{32}/(\mathbb{Z}/6)$  on the hyperplane arrangement  $G_{32}$  in  $\mathbb{P}^3$ . In fact, we have

$$\frac{G_{32}}{\mathbb{Z}/6} \simeq \mathrm{PSp}_4(\mathbb{F}_3). \quad (2.23)$$

The linear map  $\mathbb{P}^3 \hookrightarrow \mathbb{P}^{39}$ ,  $c \mapsto u$ , respects the isomorphism (2.23). The group acts on the  $c$ -coordinates by the reflections on  $K^4$ , and it permutes the coordinates  $u_{ijkl}$  via its action on the lines through the origin in  $\mathbb{F}_3^4$ . Of course, the group  $\mathrm{PSp}_4(\mathbb{F}_3)$  also permutes the 40 isotropic planes in  $\mathbb{P}^{39}$ , and this action is compatible with our monomial map  $\mathbb{P}^{39} \dashrightarrow \mathbb{P}^{39}$ .

## 2.4 Tropicalizing the Burkhardt Quartic

Our goal is to understand the relationship between classical and tropical moduli spaces for curves of genus two. To this end, in this section, we study the tropicalization of the Burkhardt quartic  $\mathcal{B}$ . This is a 3-dimensional fan  $\mathrm{trop}(\mathcal{B})$  in the tropical projective torus  $\mathbb{TP}^{39}$ . We shall see that the *tropical compactification* of  $\mathcal{B}^\circ$  equals the Igusa compactification of  $\mathcal{A}_3(2)$ .

The variety  $\mathcal{B}$  is the closure of the image of the composition  $\mathbb{P}^3 \hookrightarrow \mathbb{P}^{39} \dashrightarrow \mathbb{P}^{39}$  of the linear map given by the arrangement  $G_{32}$  and the monomial map given by the  $40 \times 40$  matrix  $A$  that records incidences of isotropic planes and lines in  $\mathbb{F}_3^4$ . To be precise, recall that the source  $\mathbb{P}^{39}$  has coordinates  $e_\ell$  indexed by lines  $\ell \subset \mathbb{F}_3^4$ , the target  $\mathbb{P}^{39}$  has coordinates  $e_W$  indexed by isotropic planes  $W \subset \mathbb{F}_3^4$ , and the linear map  $A$  is defined by  $A(e_\ell) = \sum_{W \supset \ell} e_W$ . This implies the representation

$$\text{trop}(\mathcal{B}) = A \cdot \text{Berg}(G_{32}) \subset \mathbb{TP}^{39} \tag{2.24}$$

of our tropical threefold as the image under  $A$  of the *Bergman fan* of the matroid of  $G_{32}$ . By this we mean the unique coarsest fan structure on the tropical linear space given by the rank 4 matroid on the 40 hyperplanes of  $G_{32}$ . This Bergman fan is simplicial, as suggested by the general theory of [5]. We computed its cones using the software `TropLi` due to Rincón [78].

**Lemma 2.4.1.** *The Bergman complex of the rank 4 matroid of the complex root system  $G_{32}$  has 170 vertices, 1800 edges and 3360 triangles, so its Euler characteristic equals 1729. The rays and cones of the corresponding Bergman fan  $\text{Berg}(G_{32}) \subset \mathbb{TP}^{39}$  are described below.*

The Euler characteristic is the *Möbius number* of the matroid, which can also be computed as the product of the *exponents*  $n_i$  in [71, Table 2] of the complex reflection group  $G_{32}$ :

$$1 \cdot 7 \cdot 13 \cdot 19 = 1729 = 3360 - 1800 + 170 - 1.$$

See [74, (9.2)] for the corresponding formula for the Weyl group of  $E_7$  (and genus 3 curves).

We now discuss the combinatorics of  $\text{Berg}(G_{32})$ . The space  $\mathbb{TP}^{39} = \mathbb{R}^{40}/\mathbb{R}(1, 1, \dots, 1)$  is spanned by unit vectors  $e_{0001}, e_{0010}, \dots, e_{1222}$  that are labeled by the 40 lines in  $\mathbb{F}_3^4$  as before. The 170 rays of the Bergman fan correspond to the *connected flats* of the matroid of  $G_{32}$ , and these come in three symmetry classes, according to the rank of the connected flat:

- (a) 40 Bergman rays of rank 1. These are spanned by the unit vectors  $e_{0001}, e_{0010}, \dots, e_{1222}$ .
- (b) 90 Bergman rays of rank 2, such as  $e_{0001} + e_{0100} + e_{0101} + e_{0102}$ , which represents  $\{c_1, c_1+c_2+c_3, c_1+\omega c_2+\omega c_3, c_1+\omega^2 c_2+\omega^2 c_3\}$ . These are the non-isotropic planes in  $\mathbb{F}_3^4$ .
- (ä) 40 Bergman rays of rank 3, such as

$$e_{0001} + e_{0010} + e_{0011} + e_{1100} + e_{1101} + e_{1102} + e_{1110} + e_{1111} + e_{1112} + e_{1120} + e_{1121} + e_{1122}.$$

These correspond to the Hesse pencils in  $G_{32}$ , and to the hyperplanes in  $\mathbb{F}_3^4$ . Note that the 12 indices above are perpendicular to  $(0, 0, 1, 2)$  in the symplectic inner product.

The 3360 triangles of the Bergman complex of  $G_{32}$  also come in three symmetry classes:

- (aaä) Two orthogonal lines (a) together with a hyperplane (ä) that contains them both. This gives 480 triangles because each hyperplane contains 12 orthogonal pairs.

- (abä) A flag consisting of a line (a) contained in a non-isotropic plane (b) contained in a hyperplane (ä). There are 1440 such triangles since each of the 90 planes has 4·4 choices.
- (aab) Two orthogonal lines (a) together with a non-isotropic plane (b). The plane contains one of the lines and is orthogonal to the other one. The count is also 1440.

The 1800 edges of the Bergman complex come in five symmetry classes: there are 240 edges (aa) given by pairs of orthogonal lines, 360 edges (ab) given by lines in non-isotropic planes, 480 edges (aä) given by lines in hyperplanes, 360 edges (bä) given by non-isotropic planes in hyperplanes, and 360 edges ( $ab^\perp$ ) obtained by dualizing the previous pairs (bä).

Our calculations establish the following statement:

**Proposition 2.4.2.** *The Bergman complex coincides with the nested set complex for the matroid of  $G_{32}$ . In particular, the tropical compactification of the complement of the hyperplane arrangement  $G_{32}$  coincides with the wonderful compactification of de Concini–Procesi [31].*

See [38] for the relation between tropical compactifications and wonderful compactifications. We expect that Proposition 2.4.2 is true for any finite complex reflection group, but we have not made any attempts to prove this.

The wonderful compactification is obtained by blowing up the irreducible flats of lowest dimension, then blowing up the strict transforms of the irreducible flats of next lowest dimension, etc. In our case, the smallest irreducible flats are 40 points, corresponding to the Bergman rays (a) and to Family 6 in [46, Table 1]. This first blow-up  $\widehat{\mathbb{P}^3}$  is the closure of the graph of the map  $\mathbb{P}^3 \dashrightarrow \mathcal{B}$ , by [46, Proposition 3.25]. The next smallest irreducible flats are the strict transforms of 90  $\mathbb{P}^1$ 's, corresponding to the Bergman rays (b) and to Family 4 in [46, Table 1]. After that, the only remaining irreducible flats are 40 hyperplanes, corresponding to the Bergman rays (ä) and to Family 2 in [46, Table 1]. Hence the wonderful compactification  $\widetilde{\mathbb{P}^3}$  is obtained by blowing up these 90  $\mathbb{P}^1$ 's in  $\widehat{\mathbb{P}^3}$ . The 90 exceptional divisors of  $\widetilde{\mathbb{P}^3} \rightarrow \widehat{\mathbb{P}^3}$  get contracted to the 45 nodes of  $\mathcal{B}$ , so we can lift the map  $\widetilde{\mathbb{P}^3} \rightarrow \mathcal{B}$  to a map  $\widetilde{\mathbb{P}^3} \rightarrow \widetilde{\mathcal{B}}$ , where  $\widetilde{\mathcal{B}}$  denotes the blow-up of the Burkhardt quartic at its 45 singular points.

The hyperplane arrangement complement  $\mathbb{P}^3 \cap G_m^{39}$  is naturally identified with the moduli space  $\mathcal{M}_2(3)^-$  of smooth genus 2 curves with level 3 structure and the choice of a Weierstrass point (or equivalently, the choice of an odd theta characteristic). See [15] for more about  $\mathcal{M}_2(3)^-$ . Hence we have the following commutative diagram

$$\begin{array}{ccccc}
 \mathcal{M}_2(3)^- & \hookrightarrow & \widetilde{\mathbb{P}^3} & \longrightarrow & \widehat{\mathbb{P}^3} \\
 \downarrow & & \downarrow & & \downarrow \\
 \mathcal{M}_2(3) & \hookrightarrow & \widetilde{\mathcal{B}} & \longrightarrow & \mathcal{B}
 \end{array} \tag{2.25}$$

where the vertical maps are generically finite of degree 6, the right horizontal maps are blow-ups, and the moduli spaces  $\mathcal{M}_2(3)^-$  and  $\mathcal{M}_2(3)$  are realized as very affine varieties.

We now compute the tropical Burkhardt quartic (2.24), by applying the linear map  $A$  to the Bergman fan of  $G_{32}$ . Note that the image lands in the tropicalization  $\text{trop}(\mathcal{T})$  of the toric variety  $\mathcal{T} \subset \mathbb{P}^{39}$ . We regard  $\text{trop}(\mathcal{T})$  as a 24-dimensional linear subspace of  $\mathbb{TP}^{39}$ .

**Theorem 2.4.3.** *The tropical Burkhardt quartic  $\text{trop}(\mathcal{B})$  is the fan over a 2-dimensional simplicial complex with 85 vertices, 600 edges and 880 triangles. A census appears in Table 2.1.*

*Proof.* Given the  $G_{32}$ -symmetry, the following properties of the map  $A$  can be verified on representatives of  $G_{32}$ -orbits. The linear map  $A: \mathbb{TP}^{39} \rightarrow \mathbb{TP}^{39}$  has the property that the image of each vector (ä) equals twice that of the corresponding unit vector (a). For instance,

$$A(e_{0001} + e_{0010} + e_{0011} + e_{1100} + e_{1101} + e_{1102} + e_{1110} + e_{1111} + e_{1112} + e_{1120} + e_{1121} + e_{1122}) = 2Ae_{0012}.$$

Likewise, the 90 vectors (b) come in natural pairs of non-isotropic planes that are orthogonal complements. The corresponding vectors have the same image under  $A$ . For instance,

$$A(e_{0001} + e_{0100} + e_{0101} + e_{0102}) = A(e_{0010} + e_{1000} + e_{1010} + e_{1020}). \quad (2.26)$$

We refer to such a pair of orthogonal non-isotropic planes as a *plane pair*. This explains the 85 rays of  $\text{trop}(\mathcal{B})$ , namely, they are the 40 lines  $a$  and the 45 plane pairs  $\{b, b^\perp\}$  in  $\mathbb{F}_3^4$ .

The image of each cone of  $\text{Berg}(G_{32})$  under  $A$  is a simplicial cone of the same dimension. There are no non-trivial intersections of image cones. The map  $\text{Berg}(G_{32}) \rightarrow \text{trop}(\mathcal{B})$  is a proper covering of fans. The 2-to-1 covering of the rays induces a 3-to-1 or 4-to-1 covering on each higher-dimensional cone. The precise combinatorics is summarized in Table 2.1.

Dimension	Orbits in $\text{Berg}(G_{32})$	The map $A$	Orbit size in $\text{trop}(\mathcal{B})$	Cone type
1	40 (a)	2 to 1	40	(a)
	40 (ä)			
	90 (b)	2 to 1	45	(b)
2	240 (aa)	3 to 1	240	(aa)
	480 (aä)			
	360 (ab)	3 to 1	360	(ab)
	360 (bä)			
360 ( $ab^\perp$ )				
3	1440 (aab)	4 to 1	720	(aab)
	1440 (abä)			
	480 (aaä)	3 to 1	160	(aaa)

Table 2.1: Orbits of cones in the tropical Burkhardt quartic

The types of the cones are named by replacing ä with a, and  $b^\perp$  with b. In total, there are 40 vertices of type (a) and 45 vertices of type (b). There are 240 edges of type (aa), corresponding to pairs of lines  $a \perp a'$ , and 360 edges of type (ab), corresponding to inclusions  $a \subset b$ . Finally, there are 160 triangles of type (aaa) and 720 triangles of type (aab).  $\square$



**Remark 2.4.4.** There is a bijection between the 45 rays of type (b) in  $\text{trop}(\mathcal{B})$  and the 45 singular points in  $\mathcal{B}$ . Namely, each vector of type (b) can be written such that 16 of its coordinates are 1 and the other coordinates are 0. These 16 coordinates are exactly the 16 zero coordinates in the corresponding singular point. Note that the zero coordinates of the particular singular point in (2.17) form precisely the support of the vector (2.26). The number 16 arises because each of the 45 plane pairs  $\{b, b^\perp\}$  determines 16 of the 40 isotropic planes: take any vector in  $b$  and any vector in  $b^\perp$ , and these two will span an isotropic plane.  $\square$

We next consider the *tropical compactification*  $\overline{\mathcal{B}}$  of the open Burkhardt quartic  $\mathcal{B}^\circ = \mathcal{M}_2(3)$ . By definition,  $\overline{\mathcal{B}}$  is the closure of  $\mathcal{B}^\circ \subset \mathbb{G}_m^{24}$  inside of the toric variety defined by the fan  $\text{trop}(\mathcal{B})$ . This toric variety is smooth because the rays of the two types of maximal cones (aaa) and (aab) can be completed to a basis of the lattice  $\mathbb{Z}^{24}$  spanned by all 85 rays.

**Proposition 2.4.5.** *The tropical compactification  $\overline{\mathcal{B}}$  is schön in the sense of Tevelev [89]. The boundary  $\overline{\mathcal{B}} \setminus \mathcal{B}^\circ$  is a normal crossing divisor consisting of 85 irreducible smooth surfaces.*

*Proof.* Since our fan on  $\text{trop}(\mathcal{B})$  defines a smooth toric variety, it suffices to show that all initial varieties  $V(\text{in}_v(I_{\mathcal{B}}))$  are smooth and connected in the torus  $\mathbb{G}_m^{39}$  [49, Lemma 2.7]. There are six symmetry classes of initial ideals  $\text{in}_v(I_{\mathcal{B}})$ . Each of them is generated by linear binomials and trinomials together with one non-linear polynomial  $f$ , obtained from the quartic by possibly removing monomial factors. We present representatives for the six classes. The plane pair  $\{b, b^\perp\}$  appearing in three of the cases is precisely the one displayed in (2.26).

- (a) For the vertex given by the line  $(0, 0, 0, 1)$  we take the weight vector  $v = Ae_{0001} = e_0 + e_1 + e_2 + e_3$ . Then  $f = m_0m_4^3 - 3m_0m_4m_7m_{10} + m_0m_7^3 + m_0m_{10}^3 - 3\sqrt{3}m_1m_4m_7m_{10}$ . This bihomogeneous polynomial defines a smooth surface in a quotient torus  $\mathbb{G}_m^3$ .
- (b) For the vertex  $\{b, b^\perp\}$  we take the vector (2.26). This is the incidence vector of the zero coordinates in (2.17), namely  $v = e_0 + e_1 + e_2 + e_3 + e_4 + e_5 + e_6 + e_{13} + e_{14} + e_{15} + e_{16} + e_{17} + e_{18} + e_{19} + e_{20} + e_{21}$ . The resulting non-linear polynomial is  $f = -m_0m_{13} + m_1m_4$ .
- (aa) For the edge given by the orthogonal lines  $(0, 0, 0, 1)$  and  $(0, 0, 1, 0)$  in  $\mathbb{F}_3^4$ , we take  $v = 2e_0 + e_1 + e_2 + e_3 + e_4 + e_5 + e_6$ , and we get  $f = m_0m_7^3 + m_0m_{10}^3 - 3\sqrt{3}m_1m_4m_7m_{10}$ .
- (ab) For the edge given by  $(0, 0, 0, 1)$  and  $\{b, b^\perp\}$ , we take  $v = 2e_0 + 2e_1 + 2e_2 + 2e_3 + e_4 + e_5 + e_6 + e_{13} + e_{14} + e_{15} + e_{16} + e_{17} + e_{18} + e_{19} + e_{20} + e_{21}$ , and we get  $f = -m_0m_{13} + m_1m_4$ .
- (aaa) For the triangle given by  $(0, 0, 0, 1)$ ,  $(0, 0, 1, 0)$  and  $(0, 0, 1, 1)$ , we take  $v = A(e_{0001} + e_{0010} + e_{0011}) = 3e_0 + e_1 + e_2 + e_3 + e_4 + e_5 + e_6 + e_7 + e_8 + e_9$ , and we get  $f = m_0m_{10}^2 - 3\sqrt{3}m_1m_4m_7$ .
- (aab) For the triangle given by  $(0, 0, 0, 1)$ ,  $(0, 0, 1, 0)$  and  $\{b, b^\perp\}$ , we take  $v = 3e_0 + 2e_1 + 2e_2 + 2e_3 + 2e_4 + 2e_5 + 2e_6 + e_{13} + e_{14} + e_{15} + e_{16} + e_{17} + e_{18} + e_{19} + e_{20} + e_{21}$ . Here,  $f = -m_0m_{13} + m_1m_4$ .

Note that the polynomials  $f$  are the same in the cases (b), (ab) and (aab), but the varieties  $V(\text{in}_v(I_{\mathcal{B}}))$  are different because of the 35 linear relations. In cases (b) and (ab) we have both linear trinomials and linear binomials, while in case (aab) they are all binomials. In all six cases the hypersurface  $\{f = 0\}$  has no singular points with all coordinates nonzero.  $\square$

Our final goal in this section is to equate the tropical compactification  $\overline{\mathcal{B}}$  with the blown up Burkhardt quartic  $\widetilde{\mathcal{B}}$ . By [56, Theorem 5.7.2], we can identify  $\widetilde{\mathcal{B}}$  with the Igusa desingularization of the Baily–Borel–Satake compactification  $\mathcal{A}_2(3)^{\text{Sat}}$  of  $\mathcal{A}_2(3)$ . The latter can be constructed as follows. Let  $\widehat{\mathcal{B}}$  be the projective dual variety to  $\mathcal{B} \subset \mathbb{P}^4$ . The canonical birational map  $\mathcal{B} \dashrightarrow \widehat{\mathcal{B}}$  is defined outside of the 45 nodes. Since  $\mathcal{B}$  is a normal variety, this map factors through the normalization of  $\widehat{\mathcal{B}}$ , which can be identified with  $\mathcal{A}_2(3)^{\text{Sat}}$  by [40, §4]. The closure of the graph of the birational map  $\mathcal{B} \dashrightarrow \mathcal{A}_2(3)^{\text{Sat}}$  is the blow-up of  $\mathcal{B}$  at its indeterminacy locus, i.e., the 45 nodes. Using [91, Theorem 3.1], we may identify this with  $\widetilde{\mathcal{B}}$ . By symmetry, we could also view this as the closure of the image of the inverse birational map. This realizes  $\widetilde{\mathcal{B}}$  as a blow-up of  $\mathcal{A}_2(3)^{\text{Sat}}$ , and in particular, the map blows up the Satake boundary  $\mathcal{A}_2(3)^{\text{Sat}} \setminus \mathcal{A}_2(3)$  which has 40 components all isomorphic to  $\mathcal{A}_1(3)^{\text{Sat}} \cong \mathbb{P}^1$ .

**Lemma 2.4.6.** *The moduli space  $\mathcal{A}_2(3)$  coincides with the partial compactification of  $\mathcal{M}_2(3)$  given by the 1-dimensional subfan of  $\text{trop}(\mathcal{B})$  that consists of the 45 rays of type (b).*

*Proof.* Let  $M$  be the partial compactification in question. Let  $\widetilde{\mathbb{P}^3}$  be the wonderful compactification for  $G_{32}$  as described above. The preimage of the 45 rays of type (b) in  $\text{Berg}(G_{32})$  consists of 90 rays, and the resulting partial tropical compactification  $P$  of  $\mathbb{P}^3 \setminus (40 \text{ hyperplanes})$  is the complement of the strict transforms of the reflection hyperplanes in  $\widetilde{\mathbb{P}^3}$ . In the map  $P \rightarrow \mathcal{B}$ , the 90 divisors are contracted to the 45 singular points (2 divisors to each point). We have a map  $P \rightarrow M$  which maps the 90 divisors of  $P$  to the 45 divisors of  $M$ , and hence the birational map  $M \dashrightarrow \mathcal{B}$  (given by the identity map on  $\mathcal{M}_2(3)$ ) extends to a regular map  $M \rightarrow \mathcal{B}$  which contracts the 45 divisors to the 45 singular points.

By the universal property of blow-ups, there exists a map  $M \rightarrow \widetilde{\mathcal{B}}$  which takes each of the 45 divisors to one of the 45 exceptional divisors of the blow-up  $\widetilde{\mathcal{B}} \rightarrow \mathcal{B}$ . From our previous discussion, the image of the map  $P \rightarrow \widetilde{\mathcal{B}}$  equals  $\mathcal{A}_2(3)$ . Since this map factors through  $M$ , the image of the map  $M \rightarrow \widetilde{\mathcal{B}}$  is also  $\mathcal{A}_2(3)$ . This map has finite fibers: this just needs to be checked on the 45 divisors and we can reduce to considering the map  $P \rightarrow \widetilde{\mathcal{B}}$ ; in the map  $\widetilde{\mathbb{P}^3} \rightarrow \widetilde{\mathcal{B}}$ , the inverse image of an exceptional divisor is 2 disjoint copies of  $\mathbb{P}^1 \times \mathbb{P}^1$  and any surjective endomorphism of  $\mathbb{P}^1 \times \mathbb{P}^1$  has finite fibers. The map is birational and  $\mathcal{A}_2(3)$  is smooth, so, by Zariski’s Main Theorem [69, §III.9], the map is an isomorphism.  $\square$

**Theorem 2.4.7.** *The intrinsic torus of  $\mathcal{M}_2(3) = \mathcal{B}^\circ$  is the dense torus  $\mathbb{G}_m^{24}$  of the toric variety  $\mathcal{T}$  described in Proposition 2.3.1. The tropical compactification of  $\mathcal{M}_2(3)$  provided by  $\text{trop}(\mathcal{B})$  is the Igusa desingularization  $\widetilde{\mathcal{B}}$  of the Baily–Borel–Satake compactification  $\mathcal{A}_2(3)^{\text{Sat}}$  of  $\mathcal{A}_2(3)$ .*

*Proof.* The first statement follows from Lemma 2.2.6 and Proposition 2.3.1(a).

By Lemma 2.4.6,  $\overline{\mathcal{B}}$  is a compactification of  $\mathcal{A}_2(3)$ . The boundary of the compactification  $\mathcal{M}_2(3) \subset \overline{\mathcal{B}}$  is a normal crossings divisor (Proposition 2.4.5), so the same is true for the boundary of  $\mathcal{A}_2(3) \subset \overline{\mathcal{B}}$ , and hence it is toroidal. So there exists a map  $f: \overline{\mathcal{B}} \rightarrow \mathcal{A}_2(3)^{\text{Sat}}$  that is the identity on  $\mathcal{A}_2(3)$  [16, Proposition III.15.4(3)]. This map is unique and surjective.

From what we said above, the Satake boundary  $\mathcal{A}_2(3)^{\text{Sat}} \setminus \mathcal{A}_2(3)$  has 40 components all isomorphic to  $\mathbb{P}^1$ . Also,  $\overline{\mathcal{B}} \setminus \mathcal{A}_2(3)$  consists of 40 divisors. Hence the map  $f$  contracts the 40 divisors to these  $\mathbb{P}^1$ 's. By the universal property of blow-ups, there is a unique map  $\tilde{f}: \overline{\mathcal{B}} \rightarrow \tilde{\mathcal{B}}$  that commutes with the blow-up map. Then  $\tilde{f}$  is birational and surjective. We know this map is an isomorphism on  $\mathcal{A}_2(3)$  and the complement of this open subset in both domain and target are a union of  $\mathbb{P}^2$ 's. Any surjective endomorphism of  $\mathbb{P}^2$  has finite fibers, and hence  $\tilde{f}$  is an isomorphism by Zariski's Main Theorem [69, §III.9] since  $\tilde{\mathcal{B}}$  is smooth.  $\square$

## 2.5 Moduli of Genus Two Curves

The moduli space  $\mathcal{M}_{g,n}^{\text{tr}}$  of tropical curves of genus  $g$  with  $n$  marked points is a *stacky fan*. This was shown by Brannetti, Melo and Viviani [18] and Chan [26]. This space was studied by many authors. See [21, 23] for some results. Here, a *tropical curve* is a triple  $(\Gamma, w, \ell)$ , where  $\Gamma = (V, E)$  is a connected graph,  $w$  is a weight function  $V \rightarrow \mathbb{Z}_{\geq 0}$ , and  $\ell$  is a length function  $E \rightarrow \mathbb{R}_{\geq 0}$ . The *genus* of a tropical curve is the sum of weights of all vertices plus the genus of the graph  $\Gamma$ . In addition to identifications induced by graph automorphisms, two tropical curves are isomorphic if one can be obtained from another by a sequence of the following operations and their inverses:

- Removing a leaf of weight 0, together with the only edge connected to it.
- Removing a vertex of degree 2 of weight 0, and replacing the two edges connected to it with an edge whose length is the sum of the two old edges.
- Removing an edge of length 0, and combining the two vertices connected by that edge.

The weight of the new vertex is the sum of the two old vertices.

In this way, every tropical curve of genus  $\geq 2$  is uniquely represented by a *minimal skeleton*, i.e., a tropical curve with no vertices of weight 0 of degree  $\leq 2$  or edges of length 0. The moduli space of tropical curves with a fixed *combinatorial type*  $(\Gamma, w)$  is  $\mathbb{R}_{>0}^{|E|} / \text{Aut}(\Gamma)$ , where the coordinates of  $\mathbb{R}_{>0}^{|E|}$  are the lengths of the edges. The cones for all combinatorial types are glued together to form  $\mathcal{M}_g^{\text{tr}}$ . The boundary of the cone of a combinatorial type  $(\Gamma, w)$  corresponds to tropical curves with at least one edge of length 0. Contracting that edge gives a combinatorial type  $(\Gamma', w')$ . Then, the cone for  $(\Gamma', w')$  is glued along the boundary of the cone for  $(\Gamma, w)$  in the natural way. More generally, a tropical curve with *marked points* is defined similarly, but allowing rays connecting a vertex with leaves “at infinity”.

The following construction maps curves over a valued field to tropical curves. It is fundamental for [3, 9]. Our description follows [96, Lemma - Definition 2.2.4]. Let  $R$  be a complete discrete valuation ring with maximal ideal  $\mathfrak{m}$ . Let  $K$  be its field of fractions,  $k = R/\mathfrak{m}$  its residue field, and  $t \in R$  a uniformizing parameter. Fix a genus  $g$  curve  $C$  with

$n$  marked points over  $K$ . The curve  $C$  is a morphism  $\text{Spec } K \rightarrow \mathcal{M}_{g,n}$ . Since the stack  $\overline{\mathcal{M}}_{g,n}$  is proper (i.e., by the stable reduction theorem), there is a finite extension  $K'$  of  $K$  with discrete valuation ring  $R'$  such that this morphism extends uniquely to a morphism  $\text{Spec } R' \rightarrow \overline{\mathcal{M}}_{g,n}$  (we call this a *stable model* of  $C$ ). Here we renormalize the valuation on  $R'$  so that its value group is  $\mathbb{Z}$ . Reducing modulo  $\mathfrak{m}'$  gives us a point  $\text{Spec } k \rightarrow \overline{\mathcal{M}}_{g,n}$ . By definition, this is a *stable curve*  $C_k$  over  $k$ . We remark that the stable model may not be unique, but the stable curve is unique. Since such a stable curve has at worst nodal singularities, we can construct a dual graph as follows. For each genus  $h$  component of  $C_k$ , we draw a vertex of weight  $h$ . For each node of  $C_k$ , we draw an edge between the two components that meet there (this might be a loop if the node comes from a self-intersection). If a component has a marked point, then we attach a vertex at infinity to that vertex. The stable condition translates to the fact that the dual graph is a minimal skeleton as above. Finally, each node, when considered as a point in  $C_{R'}$ , is étale locally of the form  $xy = t^\ell$  for some positive integer  $\ell$ . We then assign the length  $\ell/d$  to the corresponding edge, where  $d$  is the degree of the field extension  $K \subset K'$ . In this way, we have defined a function

$$\mathcal{M}_{g,n}(K) \rightarrow \mathcal{M}_{g,n}^{\text{tr}}. \quad (2.27)$$

Here is a concrete illustration of this function for  $g = 0$  and  $n = 4$ .

**Example 2.5.1.** Let  $K = \mathbb{C}((t))$  and  $R = \mathbb{C}[[t]]$  and consider the four points in  $\mathbb{P}_K^1$  given by  $(1 : p(t))$ ,  $(1 : q(t))$ ,  $(1 : a)$ ,  $(1 : b)$  where  $a, b \in \mathbb{C}$  are generic and  $\text{val}(p(t)), \text{val}(q(t)) > 0$ . Let  $x, y$  be the coordinates on  $\mathbb{P}^1$ . Naively, this gives us four points in  $\mathbb{P}_R^1$ , but it is not a stable model since  $p(0) = q(0) = 0$  and so two points coincide in the special fiber. The fix is to blow-up the arithmetic surface  $\mathbb{P}_R^1$  at the ideal  $\langle y - p(t)x, y - q(t)x \rangle$ . We embed this blow-up into  $\mathbb{P}_R^1 \times_R \mathbb{P}_R^1$ , where the latter  $\mathbb{P}_R^1$  has coordinates  $w, z$ , as the hypersurface given by  $w(y - q(t)x) = z(y - p(t)x)$ . The special fiber is the nodal curve given by  $y(w - z) = 0$ . We wish to understand the étale local equation for the node cut out by  $y = w - z = 0$ . To do this, set  $x = z = 1$  and consider the defining equation  $y(w - 1) + p(t) - q(t)w = 0$ . Now substitute  $w' = w - 1$  and  $y' = y - q(t)$  to get  $y'w' + (p(t) - q(t)) = 0$ . Hence the dual curve is a line segment of length  $\text{val}(p(t) - q(t))$  with both vertices having weight 0.  $\square$

Evaluating the map (2.27) in general is a challenging computer algebra problem: how does one compute the metric graph from a smooth curve  $C$  that is given by explicit polynomial equations over  $K$ ? This section represents a contribution to this problem for curves of genus 2. As a warm-up for our study of genus 2 curves, let us first consider the genus 1 case.

**Example 2.5.2.** An elliptic curve  $C$  can be defined by giving four points in  $\mathbb{P}^1$ . The curve is the double cover of  $\mathbb{P}^1$  branched at those four points. This gives us a map  $\mathcal{M}_{0,4} \rightarrow \mathcal{M}_1$ , which is well-defined over our field  $K$ . The map is given explicitly by the following formula for the  $j$ -invariant of  $C$  in terms of the cross ratio  $\lambda$  of four ramification points (see [90, §3]):

$$j = 256 \frac{(\lambda^2 - \lambda + 1)^3}{\lambda^2(\lambda - 1)^2}. \quad (2.28)$$

We now pass to the tropicalization by constructing a commutative square

$$\begin{array}{ccc}
 \mathcal{M}_{0,4}(K) & \longrightarrow & \mathcal{M}_{0,4}^{\text{tr}} \\
 \downarrow & & \downarrow \\
 \mathcal{M}_1(K) & \longrightarrow & \mathcal{M}_1^{\text{tr}}
 \end{array} \tag{2.29}$$

The horizontal maps are instances of (2.27), and the left vertical map is (2.28). Our task is to define the right vertical map. The ingredients are the trees and tropical curves in Table 2.5.2:

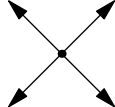
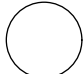
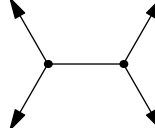
Tropical curve of genus 1	Tree with 4 leaves
• 1	
	

Table 2.2: Trees on four taxa and tropical curves of genus 1

A point in  $\mathcal{M}_{0,4}^{\text{tr}}$  can be represented by a phylogenetic tree with taxa 1, 2, 3, 4. Writing  $\nu_{ij}$  for half the distance from leaf  $i$  to leaf  $j$  in that tree, the unique interior edge has length

$$\ell = \max\{\nu_{12} + \nu_{34} - \nu_{14} - \nu_{23}, \nu_{13} + \nu_{24} - \nu_{12} - \nu_{34}, \nu_{14} + \nu_{23} - \nu_{13} - \nu_{24}\}.$$

Suppose we represent a point in  $\mathcal{M}_{0,4}$  by four scalars,  $x_1, x_2, x_3, x_4 \in K$ , as in Example 2.5.1. Then its image in  $\mathcal{M}_{0,4}^{\text{tr}}$  is the phylogenetic tree obtained by setting

$$\nu_{ij} = -\text{val}(x_i - x_j). \tag{2.30}$$

The square (2.29) becomes commutative if the right vertical map takes trees with interior edge length  $\ell > 0$  to the cycle of length  $2\ell$ , and it takes the star tree ( $\ell = 0$ ) to the node marked 1. To see this, we recall that the tropical curve contains a cycle of length  $-\text{val}(j)$ , where  $j$  is the  $j$ -invariant. This is a standard fact (see [9, §7]) from the theory of elliptic curves over  $K$ . Suppose the four given points in  $\mathbb{P}^1$  are  $0, 1, \infty, \lambda$ , and that  $\lambda$  and  $0$  are neighbors in the tree. This means  $\text{val}(\lambda) > 0$ . As desired, the length of our cycle is

$$-\text{val}(j) = -3\text{val}(\lambda^2 - \lambda + 1) + 2\text{val}(\lambda) + 2\text{val}(\lambda - 1) = 0 + 2\text{val}(\lambda) + 0 = 2\text{val}(\lambda).$$

The other case, when  $\lambda$  and 0 are not neighbors in the tree, follows from the fact that the rational function of  $\lambda$  in (2.28) is invariant under permuting the four ramification points.

In this example, the one-dimensional fan  $\mathcal{M}_{0,4}^{\text{tr}}$  serves as a moduli space for tropical elliptic curves. A variant where the fibers are elliptic normal curves is shown in Figure 1.2. In both situations, all maximal cones correspond to elliptic curves over  $K$  with bad reduction.  $\square$

Moving on to genus 2 curves, we shall now focus on the tropical spaces  $\mathcal{M}_2^{\text{tr}}$  and  $\mathcal{M}_{0,6}^{\text{tr}}$ . There are seven combinatorial types for genus 2 tropical curves. Their poset is shown in [26, Figure 4]. The seven types are drawn in the second column of Table 2.5. The stacky fan  $\mathcal{M}_2^{\text{tr}}$  is the cone over the two-dimensional cell complex shown in Figure 2.5. Note the identifications.

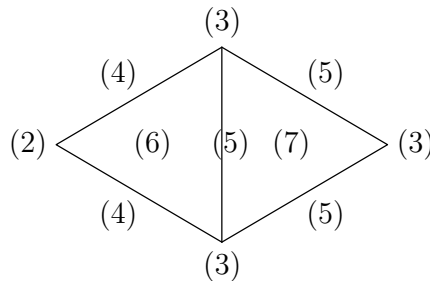


Figure 2.4: The moduli space of genus 2 tropical curves

The tropical moduli space  $\mathcal{M}_{0,6}^{\text{tr}}$  is the space of phylogenetic trees on six taxa. A concrete model, embedded in  $\mathbb{TP}^{14}$ , is the 3-dimensional fan  $\text{trop}(\mathcal{M}_{0,6})$  seen in Theorem 2.2.4. Combinatorially, it agrees with the tropical Grassmannian  $\text{Gr}(2, 6)$  as described in [84, Example 4.1], so its cones correspond to trees with six leaves. The fan  $\mathcal{M}_{0,6}^{\text{tr}}$  has one zero-dimensional cone of type (1),  $25 = 10 + 15$  rays of types (2) and (3),  $105 = 60 + 45$  two-dimensional cones of types (4) and (5), and  $105 = 90 + 15$  three-dimensional cones of types (6) and (7). The corresponding combinatorial types of trees are depicted in the last column of Table 2.5.

Table 2.5 shows that there is a combinatorial correspondence between the types of cones of the tropical Burkhardt quartic  $\text{trop}(\mathcal{B})$  in Table 2.1 and the types of cones in  $\mathcal{M}_2^{\text{tr}}$  and  $\mathcal{M}_{0,6}^{\text{tr}}$ . We seek to give a precise explanation of this correspondence in terms of algebraic geometry. At the moment we can carry this out for level 2 but we do not yet have a proof for level 3.

**Theorem 2.5.3.** *Let  $K$  be a complete non-archimedean field.*

(a) *There is a commutative square*

$$\begin{array}{ccc}
 \mathcal{M}_{0,6}(K) & \longrightarrow & \mathcal{M}_{0,6}^{\text{tr}} \\
 \downarrow & & \downarrow \\
 \mathcal{M}_2(K) & \longrightarrow & \mathcal{M}_2^{\text{tr}}
 \end{array}
 \tag{2.31}$$

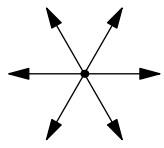
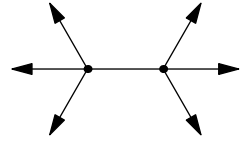
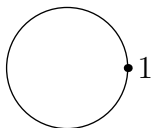
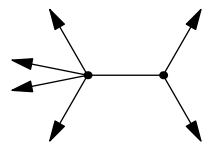
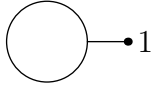
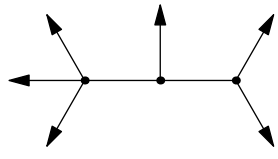
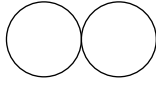
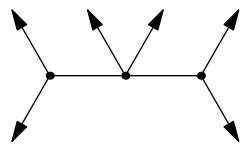
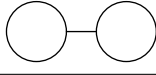
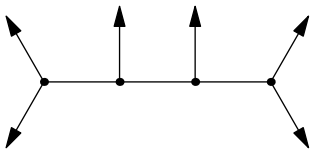
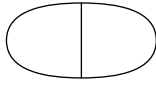
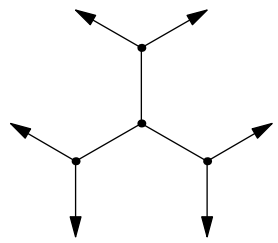
Label	Tropical curve of genus 2	Burkhardt cone	Tree with 6 leaves
(1)	$2 \bullet$	origin	
(2)	$1 \bullet \text{---} \bullet 1$	(b)	
(3)		(a)	
(4)		(ab)	
(5)		(aa)	
(6)		(aab)	
(7)		(aaa)	

Table 2.3: Correspondence between tropical curves, cones of  $\text{trop}(\mathcal{B})$ , and metric trees.

The left vertical map sends 6 points in  $\mathbb{P}^1$  to the genus 2 hyperelliptic curve with these ramification points. The horizontal maps send a curve (with or without marked points) to its tropical curve (with or without leaves at infinity). The right vertical map is a morphism of generalized cone complexes relating the second and fourth columns of Table 2.5.

- (b) The top horizontal map can be described in an alternative way: under the embedding of  $\mathcal{M}_{0,6}$  into  $\mathbb{P}^{14}$  given by (2.5), take the valuations of the 15 coordinates  $m_0, m_1, \dots, m_{14}$ .

*Proof of Theorem 2.5.3.* We start with (a). Let  $C$  be a genus 2 curve over  $K$  and let  $p_1, \dots, p_6 \in \mathbb{P}_K^1$  be the branch points of the double cover  $C \rightarrow \mathbb{P}^1$  induced from the canonical divisor. Let  $R'$  be a discrete valuation ring over which a stable model of both  $C$  and  $(\mathbb{P}^1, p_1, \dots, p_6)$  can be defined and let  $k$  be its residue field. The fact that the combinatorial types of dual graphs for  $C$  and the marked curve  $(\mathbb{P}^1, p_1, \dots, p_6)$  match up as in Table 2.5 is clear from the proof of [7, Corollary 2.5] which constructs the stable  $k$ -curve of  $C$  from that of  $(\mathbb{P}^1, p_1, \dots, p_6)$ . There is an obvious bijection of edges between the combinatorial types in all cases. We claim that the edge length coming from the étale neighborhood of nodal singularities is halved for curves of type (2) and is doubled for curves of type (3) from Table 2.5: the description and proof for the other types can be reduced to these two cases.

First consider curves of type (3). Our stable genus 0 curve consists of the union of two  $\mathbb{P}^1$ 's meeting in a point. One has 4 marked points and the other has 2 marked points. This arises from 6 distinct points in  $\mathbb{P}_{R'}^1$  such that exactly 2 of them coincide after passing to the residue field. To build a stable model (cf. Example 2.5.1), we blow up the point of intersection in the special fiber of  $\mathbb{P}_{R'}^1$  to get an arithmetic surface  $\tilde{P}_{R'}$ . Let  $E$  be the double cover of the first  $\mathbb{P}_k^1$  along the 4 marked points, and let  $E'$  be a copy of  $\mathbb{P}_k^1$  mapping to the second  $\mathbb{P}_k^1$  so that it is ramified over the 2 marked points. Over the point of intersection, both  $E$  and  $E'$  are unramified, and we glue together the two preimages (there are two ways to do this, but the choice won't matter). Then  $E \cup E'$  is a semistable (but not stable) curve which is the special fiber of an admissible double cover  $C_{R'} \rightarrow \tilde{P}_{R'}$ . Suppose that the node in the special fiber of  $\tilde{P}_{R'}$  étale locally is  $xy = t^\ell$ . In a small neighborhood of this node, there are no ramification points. Thus, a small neighborhood of each of these two points of intersection in  $C_{R'}$  is isomorphic to a small neighborhood of the node in  $\tilde{P}_{R'}$  and hence étale locally look like  $xy = t^\ell$ . Finally, we have to contract  $E'$  to a single point to get a stable curve. The result is that the two nodes become one which étale locally looks like  $xy = t^{2\ell}$ .

Now consider curves of type (2). Use the notation from the previous case. The semistable model  $C_{R'}$  over  $\text{Spec } R'$  has a hyperelliptic involution whose quotient is the union of two  $\mathbb{P}_{R'}^1$ 's. At the node of  $C_{R'}$ , which locally looks like  $R'[[x, y]]/\langle xy - t^m \rangle$  for some  $m$ , the involution negates  $x$  and  $y$  since it preserves the two components of  $C_{R'}$ . The ring of invariants is  $R'[[u, v]]/\langle uv - t^{2m} \rangle$  where  $u=x^2$ ,  $v=y^2$ . This is the local picture for the nodal genus 0 curve.

The result above can also be deduced from Caporaso's general theory in [22, §2]. For a combinatorial illustration of type (6) see Chan's Figure 1 in [27]. The two leftmost and two rightmost edges in her upstairs graph have been contracted away. What is left is a "barbell" graph with five horizontal edges of lengths  $a, a, b, c, c$ , mapping harmonically to a downstairs



graph of edge lengths  $a, 2b, c$ . Here we see both of the stretching factors represented in different parts of this harmonic morphism: a 2-edge cycle of total length  $a + a$  maps to an edge of length  $a$ , and a single edge of length  $b$  maps to an edge of length  $2b$  downstairs.

Now we consider (b). We need to argue that the internal edge lengths can be computed from the 15 quantities  $\text{val}(m_i)$ , in a manner that is consistent with the description above. For genus 1 curves this is precisely the consistency between Examples 2.5.1 and 2.5.2. We explain this for the case of the snowflake tree (7). Without loss of generality, we assume that  $\{1, 2\}$ ,  $\{3, 4\}$  and  $\{5, 6\}$  are the neighbors on the tree. If  $\nu_{ij}$  is half the distance between leaves  $i$  and  $j$ , computed from the six points as in (2.30), then, for instance,  $\text{val}(m_{13}) = -\nu_{16} - \nu_{24} - \nu_{35}$ . A direct calculation on the snowflake tree shows that the three internal edge lengths are

$$\text{val}(m_2) - \text{val}(m_{13}), \text{val}(m_6) - \text{val}(m_{13}), \text{ and } \text{val}(m_{14}) - \text{val}(m_{13}). \quad (2.32)$$

The edge lengths of the tropical curve  $\bigoplus$  are gotten by doubling these numbers.  $\square$

At present we do not know the level 3 analogues to the stretching factors  $1/2$  and  $2$  we saw in the proof above. Such lattice issues will play a role for the natural map from the tropical Burkhardt quartic onto the tropical moduli space  $\mathcal{M}_2^{\text{tr}}$ . We leave that for future research:

**Conjecture 2.5.4.** *Let  $K$  be a complete non-archimedean field. There is a commutative square*

$$\begin{array}{ccc} \mathcal{M}_2(3)(K) & \longrightarrow & \text{trop}(\mathcal{B}) \\ \downarrow & & \downarrow \\ \mathcal{M}_2(K) & \longrightarrow & \mathcal{M}_2^{\text{tr}} \end{array} \quad (2.33)$$

*The left map is the forgetful map. The top map is taking valuations of the coordinates  $m_0, \dots, m_{39}$ . The bottom map sends a curve to its tropical curve. The right map is a morphism of (stacky) fans that takes the third column of Table 2.5 to the second column.*

Here is one concrete way to evaluate the left vertical map  $\mathcal{M}_2(3) \rightarrow \mathcal{M}_2$  over a field  $K$ . We can represent an element of  $\mathcal{M}_2(3)$  by a point  $(r : s_{01} : s_{10} : s_{11} : s_{12}) \in \mathbb{P}_K^4$  that lies in the open Burkhardt quartic  $\mathcal{B}^\circ$ . The corresponding abelian surface  $S$  is the singular locus of the Coble cubic in  $\mathbb{P}_K^8$  by Theorem 2.3.2. If we intersect the abelian surface  $S$  with the linear subspace  $\mathbb{P}^4$  given by (2.19), then the result is the desired genus 2 curve  $C \in \mathcal{M}_2(K)$ . The conjecture asks about the precise relationship between the tropical curve constructed from  $C$  and the valuations of our 40 canonical coordinates  $m_0, m_1, \dots, m_{39}$  on  $\mathcal{B}^\circ$  inside  $\mathbb{P}_K^{39}$ .

## 2.6 Marked Del Pezzo Surfaces

This section is motivated by our desire to draw all combinatorial types of tropical cubic surfaces together with their 27 lines (trees). These surfaces arise in fibers of the map from a

six-dimensional fan to a four-dimensional fan. These tropical moduli spaces were characterized by Hacking, Keel and Tevelev in [50]. We now rederive their fans from first principles.

Consider a reflection arrangement of type  $E_n$  for  $n = 6, 7$ . The complement of the hyperplanes is the moduli space of  $n$  points in  $\mathbb{P}^2$  in general position (no 2 coincide, no 3 are collinear, no 6 lie on a conic) together with a cuspidal cubic through these points (none of which is the cusp). For  $n = 6$ , there is a 1-dimensional family of such curves (this family is the *parabolic curve* in [30, Definition 3.2]). For  $n = 7$  there are 24 choices. We can use maps (2.3) that come from Macdonald representations to forget the data of the cuspidal cubic.

Consider the case  $n = 6$ . Six points on a cuspidal cubic in  $\mathbb{P}^2$  are represented by a matrix

$$D = \begin{pmatrix} 1 & 1 & 1 & 1 & 1 & 1 \\ d_1 & d_2 & d_3 & d_4 & d_5 & d_6 \\ d_1^3 & d_2^3 & d_3^3 & d_4^3 & d_5^3 & d_6^3 \end{pmatrix}. \quad (2.34)$$

The maximal minors of this  $3 \times 6$ -matrix are denoted

$$[ijk] = (d_i - d_j)(d_i - d_k)(d_j - d_k)(d_i + d_j + d_k) \quad \text{for } 1 \leq i < j < k \leq 6.$$

We also abbreviate the condition for the six points to lie on a conic:

$$[\text{conic}] = [134][156][235][246] - [135][146][234][256] = (d_1 + d_2 + d_3 + d_4 + d_5 + d_6) \prod_{1 \leq i < j \leq 6} (d_i - d_j).$$

The reflection arrangement of type  $E_6$  consists of the  $36 = \binom{6}{3} + \binom{6}{2} + 1$  hyperplanes defined by the linear forms in the products above. We list the flats of this arrangement in Table 2.4. The bold numbers indicate irreducible flats. Each flat corresponds to a root subsystem, but not conversely. Root subsystems that are not parabolic, such as  $A_2^{\times 3}$ , do not come from flats.

The Bergman fan of  $E_6$  is the fan over the nested set complex [5], a 4-dimensional simplicial complex whose vertices are the  $750 = 36 + 120 + 270 + 45 + 216 + 27 + 36$  irreducible flats.

We define the *Yoshida variety*  $\mathcal{Y}$  to be the closure of the image of the rational map

$$\mathbb{P}^5 \xrightarrow{\text{linear}} \mathbb{P}^{35} \xrightarrow{\text{monomial}} \mathbb{P}^{39}, \quad (2.35)$$

where the monomial map is defined by the root subsystems of type  $A_2^{\times 3}$ . Our name for  $\mathcal{Y}$  gives credit to Masaaki Yoshida's explicit computations in [97]. (Warning: there is a closely related variety  $\mathcal{Y}$  studied in [56, §3.5]. This is not the same as our variety.) Explicitly, as shown in [30, Proposition 2.4], the map into  $\mathbb{P}^{39}$  is defined by 30 bracket monomials like  $[125][126][134][234][356][456]$  and 10 bracket monomials like  $[\text{conic}][123][456]$ . We divide each of these 40 expressions by  $\prod_{1 \leq i < j \leq 6} (d_i - d_j)$  to get a product of 9 linear forms. Thus the rational map (2.35) is given by 40 polynomials of degree 9 that factor into roots of  $E_6$ . The *tropical Yoshida variety*  $\text{trop}(\mathcal{Y})$  is the image of the Bergman fan of  $E_6$  under the linear map  $\mathbb{TP}^{35} \rightarrow \mathbb{TP}^{39}$  defined by the corresponding  $40 \times 36$ -matrix. The Yoshida variety  $\mathcal{Y}$  has 40 singular points [94, Theorem 5.7]. Its open part  $\mathcal{Y}^\circ$  is the moduli space of marked smooth

#	Codim	Size	Root subsystem	Equations of a representative flat
<b>1</b>	1	36	$A_1$	$d_1 - d_2$
<b>2</b>	2	120	$A_2$	$d_1 + d_3 + d_6, d_2 + d_4 + d_5$
<b>3</b>	2	270	$A_1 \times A_1$	$d_1 + d_4 + d_6, d_2 + d_4 + d_5$
<b>4</b>	3	270	$A_3$	$d_1 + d_4 + d_6, d_2 + d_4 + d_5, d_5 - d_6$
<b>5</b>	3	720	$A_2 \times A_1$	$d_1 + d_5 + d_6, d_2 + d_4 + d_5, d_4 - d_5$
<b>6</b>	3	540	$A_1^{\times 3}$	$d_1 + d_4 + d_6, d_2 + d_3 + d_6, d_2 + d_4 + d_5$
<b>7</b>	4	45	$D_4$	$d_5 - d_6, d_3 - d_4, d_2 + d_4 + d_6, d_1 + d_4 + d_6$
<b>8</b>	4	216	$A_4$	$d_5 - d_6, d_3 + d_4 + d_6, d_2 + d_4 + d_6, d_1 + d_4 + d_6$
<b>9</b>	4	540	$A_3 \times A_1$	$d_3 + d_4 + d_6, d_2 + d_3 + d_6, d_1 + d_4 + d_6, d_2 + d_4 + d_5$
<b>10</b>	4	120	$A_2 \times A_2$	$d_4 - d_5, d_3 + d_4 + d_5, d_2 + d_4 + d_5, d_1 + d_5 + d_6$
<b>11</b>	4	1080	$A_2 \times A_1^{\times 2}$	$d_1 + d_2 + d_5, d_2 + d_3 + d_6, d_1 + d_4 + d_6, d_2 + d_4 + d_5$
<b>12</b>	5	27	$D_5$	$d_5 - d_6, d_1 - d_4, d_1 - d_3, d_1 - d_2, d_1 + d_5 + d_6$
<b>13</b>	5	36	$A_5$	$d_5 + d_4 + d_6, d_4 - d_6, d_3 - d_5, d_2 - d_6, d_1 - d_5$
<b>14</b>	5	216	$A_4 \times A_1$	$d_6, d_4, d_3 - d_5, d_2 + d_5, d_1$
<b>15</b>	5	360	$A_2^{\times 2} \times A_1$	$d_2 + d_4 + d_5, d_2 - d_3, d_4 - d_5, d_2 + d_3 + d_6, d_1 + d_4 + d_6$

Table 2.4: The flats of the  $E_6$  reflection arrangement.

cubic surfaces [30, Theorem 3.1]. The blow-up of these points is *Naruki's cross ratio variety*  $Y_{lc}^6$  (following the notation of [50]) from [70]. The situation is analogous to Theorem 2.4.7.

As defined, we consider  $\text{trop}(\mathcal{Y})$  only as a set, but there is a unique coarsest fan structure on this set. This was shown in [50]. It is the fan over a 3-dimensional simplicial complex that was described by Naruki [70]. We call them the *Naruki fan* and *Naruki complex*, respectively. The  $76 = 36 + 40$  vertices correspond to the two types of boundary divisors on  $Y_{lc}^6$ : the 36 divisors coming from the hyperplanes of  $E_6$  (type a) and the 40 exceptional divisors of the blow-up (type b). The types of intersections of these divisors is given in [70, p.23] and is listed in Table 2.5. The divisors of type (a) correspond to root subsystems of type  $A_1$  and the divisors of type (b) correspond to root subsystems of type  $A_2^{\times 3}$ . The Naruki complex is the nested set complex on these subsystems. Its face numbers are as follows:

type	number
(a)	36
(b)	40
(aa)	270
(ab)	360
(aaa)	540
(aab)	1080
(aaaa)	135
(aaab)	1080

Table 2.5: The Naruki complex has 76 vertices, 630 edges, 1620 triangles and 1215 tetrahedra.

**Theorem 2.6.1.** *The Yoshida variety  $\mathcal{Y}$  is the intersection in  $\mathbb{P}^{39}$  of a 9-dimensional linear space and a 15-dimensional toric variety whose dense torus  $\mathbb{G}_m^{15}$  is the intrinsic torus of  $\mathcal{Y}^\circ$ . The tropical compactification  $\overline{\mathcal{Y}}$  of  $\mathcal{Y}^\circ$  induced by the Naruki fan is the cross ratio variety  $Y_{1c}^6$ .*

The polytope of the toric variety has 2232 facets. Its prime ideal is minimally generated by 8922 binomials, namely 120 of degree 3, 810 of degree 4, 2592 of degree 5, 2160 of degree 6, and 3240 of degree 8. These results, which mirror parts (b) and (d) in Proposition 2.3.1, were found using `polymake` [42] and `gfan` [57]. The prime ideal of  $\mathcal{Y}$  is minimally generated by 30 of the binomial cubics together with 30 linear forms. A natural choice of such linear forms is described in [97, §3]. It comes from 4-term Plücker relations such as  $[123][456] - [124][356] + [125][346] + [126][345]$ . There are no linear trinomial relations on  $\mathcal{Y}$ .

**Remark 2.6.2.** After our result was published, Sikirić [83] computed the  $f$ -vector and the number of orbits of faces of the polytope under the action of  $W(E_6)$ , as shown in Table 2.6.

Table 2.6: The  $f$ -vector and the number of orbits of faces of the polytope for  $\mathcal{Y}$

Dimension	#Orbits	#Faces
0 (vertices)	1	40
1	2	780
2	4	9720
3	12	83970
4	32	509544
5	84	2140560
6	189	6189210
7	336	12313755
8	442	16777012
9	412	15422760
10	282	9301770
11	136	3506895
12	50	756000
13	17	76806
14 (facets)	5	2232

The 750 rays of the Bergman fan map into  $\text{trop}(\mathcal{Y})$  as follows. Write  $m$  for the linear map  $\mathbb{TP}^{35} \rightarrow \mathbb{TP}^{39}$  and  $F_i$  for the rays representing family  $i$  of irreducible flats of Table 2.4. Then:

$$\begin{aligned}
 m(F_1) = m(F_8) = m(F_{13}) &\text{ has 36 elements (a),} \\
 m(F_2) &\text{ has 40 elements (b),} \\
 m(F_4) &\text{ has 270 elements.}
 \end{aligned}$$

All other rays map to 0 in  $\mathbb{TP}^{39}$ . Each element in  $m(F_4)$  is the sum of two vectors from  $m(F_1)$  which form a cone. The image of the Bergman fan of  $E_6$  in  $\mathbb{TP}^{39}$  is a fan with

346 = 36+40+270 rays that subdivides the Naruki fan. That fan structure on  $\text{trop}(\mathcal{Y})$  defines a modification of the Naruki variety  $Y_{\text{lc}}^6$ .

Here is the finite geometry behind (2.35). Let  $V = \mathbb{F}_2^6$  with coordinates  $x_1, \dots, x_6$ . There are two conjugacy classes of nondegenerate quadratic forms on  $V$ . Fix the non-split form

$$q(x) = x_1x_2 + x_3x_4 + x_5^2 + x_5x_6 + x_6^2.$$

Then the Weyl group  $W(E_6)$  is the subgroup of  $\text{GL}_6(\mathbb{F}_2)$  that preserves this form. Using  $q(x)$ , we define an orthogonal (in characteristic 2, this also means symplectic) form by

$$\langle x, y \rangle = q(x + y) - q(x) - q(y).$$

There is a natural bijection between the 36 positive roots of  $E_6$  and the vectors  $x \in V$  with  $q(x) \neq 0$ . There are 120 planes  $W$  such that  $q(x) \neq 0$  for all nonzero  $x \in W$ . These correspond to subsystems of type  $A_2$ . The set of 120 planes breaks up into 40 triples of pairwise orthogonal planes. These 40 triples correspond to the subsystems of type  $A_2^{\times 3}$ .

We now come to the case  $n = 7$ . The *Göpel variety*  $\mathcal{G}$  of [74] is the closed image of a map

$$\mathbb{P}^6 \xrightarrow{\text{linear}} \mathbb{P}^{62} \xrightarrow{\text{monomial}} \mathbb{P}^{134}. \tag{2.36}$$

The linear map is given by the 63 hyperplanes in the reflection arrangement  $E_7$ , and the monomial map by the 135 root subsystems of type  $A_1^{\times 7}$ . The full list of all flats of the arrangement  $E_7$  appears in [74, Table 2]. In [74, Corollary 9.2] we argued that the *tropical Göpel variety*  $\text{trop}(\mathcal{G})$  is the image of the Bergman fan of  $E_7$  under the induced linear map  $\mathbb{TP}^{62} \rightarrow \mathbb{TP}^{134}$ , and we asked how  $\text{trop}(\mathcal{G})$  would be related to the fan for  $Y_{\text{lc}}^7$  in [50, §1.14]. We call that fan the *Sekiguchi fan*, after [80]. The following theorem answers our question.

**Theorem 2.6.3.** *The Göpel variety  $\mathcal{G}$  is the intersection in  $\mathbb{P}^{134}$  of a 14-dimensional linear space and a 35-dimensional toric variety whose dense torus  $\mathbb{G}_m^{35}$  is the intrinsic torus of  $\mathcal{G}^\circ$ . The tropical compactification  $\overline{\mathcal{G}}$  of the open Göpel variety  $\mathcal{G}^\circ$  induced by the Sekiguchi fan is the Sekiguchi variety  $Y_{\text{lc}}^7$ . Hence, the Sekiguchi fan is the coarsest fan structure on  $\text{trop}(\mathcal{G})$ .*

The result about the linear space and the toric variety is [74, Theorem 6.2]. The determination of the intrinsic tori in Theorems 2.6.1 and 2.6.3 is immediate from Lemma 2.2.6. The last assertion follows from the fact that the open Göpel variety  $\mathcal{G}^\circ$  is the moduli space of marked smooth del Pezzo surfaces of degree two. For this see [30, Theorem 3.1].

The Bergman fan of type  $E_7$  has 6091 rays. They are listed in [74, Table 2]. The 6091

rays map into  $\text{trop}(\mathcal{G})$  as follows. Write  $F_i$  for family  $i$  in [74, Table 2]. Then:

$$\begin{aligned} m(F_1) = m(F_{17}) = m(F_{25}) &\text{ has 63 elements,} \\ m(F_2) = m(F_{15}) &\text{ has 336 elements,} \\ m(F_4) &\text{ has 630 elements,} \\ m(F_{24}) &\text{ has 36 elements,} \\ m(F_8) &\text{ has 2016 elements,} \\ m(F_9) &\text{ has 315 elements,} \\ m(F_{16}) &\text{ has 1008 elements.} \end{aligned}$$

Finally,  $m$  sends  $F_{26}$  to 0 (multiple of all 1's vector). The fan on the first 4 types of rays is the Sekiguchi fan as described in [50, §1.14]. The image of the Bergman fan of  $E_7$  is a refinement of the Sekiguchi fan, as follows:

- Every ray in  $m(F_8)$  is uniquely the sum of a ray in  $m(F_2)$  and a ray in  $m(F_{24})$ . This is in the image of a cone of nested set type  $A_2 \subset A_6$ .
- Every ray in  $m(F_9)$  is uniquely the sum of three rays in  $m(F_1)$ . This is in the image of a cone of nested set type  $A_1^{\times 3}$ .
- Every ray in  $m(F_{16})$  can be written uniquely as a positive sum of a ray in  $m(F_1)$  and a ray in  $m(F_{24})$ . This is in the image of a cone of nested set type  $A_1 \subset A_6$ .

The Sekiguchi fan on  $\text{trop}(\mathcal{G})$  is a fan over a 5-dimensional simplicial complex with  $1065 = 63 + 336 + 630 + 36$  vertices. It has 9 types of facets, corresponding to the 9 tubings shown in [50, Figure 2, page 200]. The significance of the Naruki fan and the Sekiguchi fan lies in the commutative diagram in [50, Lemma 5.4], which we restate here:

$$\begin{array}{ccc} \mathbb{P}^6 & \dashrightarrow & \mathcal{G}^\circ \\ \vdots & & \downarrow \\ \mathbb{P}^5 & \dashrightarrow & \mathcal{Y}^\circ \end{array} \tag{2.37}$$

The horizontal maps are those in (2.36) and (2.35). The left vertical map is defined by dropping a coordinate. The tropicalization of the right vertical map  $\mathcal{G}^\circ \rightarrow \mathcal{Y}^\circ$  is a linear projection

$$\text{trop}(\mathcal{G}) \rightarrow \text{trop}(\mathcal{Y}) \tag{2.38}$$

from the tropical Göpel variety onto the tropical Yoshida variety.

We wish to explicitly determine this map on each cone of  $\text{trop}(\mathcal{G})$ . The point is that all tropicalized generic del Pezzo surfaces of degree 3 appear in the fibers of (2.38), by the result about the universal family in [50, Theorem 1.2], and our Theorems 2.6.1 and 2.6.3. At infinity, such a del Pezzo surface is glued from 27 trees, which are exactly the tropical image of the 27 lines on a cubic surface over  $K$ . Each tree has 10 leaves, which come from

the intersections of the 27 lines. Thus, each tree represents a point of  $\mathcal{M}_{0,10}(K)$ . Thus tropicalized del Pezzo surfaces of degree 3 can be represented by a *tree arrangement* in the sense of [53, §4].

One issue with the map (2.38) is that its zero fiber is 3-dimensional. Namely, it is the union of tropicalizations of all constant coefficient cubic surfaces. The zero fiber has 27 rays, one for each line on the cubic surface, and 45 triangular cones, one for each triple of pairwise intersecting lines. This is the subtle issue of *Eckhart points*, addressed by [50, Theorem 1.19]. Cubic surfaces with Eckhart points are special, for they contribute to the points in the interior of the 45 triangular cones. Disallowing these removes the interiors of the triangular cones, and we are left with a balanced two-dimensional fan. This is the fan over a graph with 27 vertices and 135 edges, representing generic constant coefficient cubic surfaces.

In this section, we developed some tools for the classification of tropical cubic surfaces, namely as fibers of (2.38), but we did not actually carry out this classification. The solution to that problem is the topic of Chapter 4.

# Chapter 3

## Algorithms for Mumford Curves

This chapter is joint work with Ralph Morrison. It will be published with the same title in the *Journal of Symbolic Computation*, Special Issue on the Occasion of MEGA 2013 [66].

### 3.1 Introduction

Curves over non-archimedean fields are of fundamental importance to algebraic geometry and number theory. Mumford curves are a family of such curves, and are interesting from both a theoretical and computational perspective. In non-archimedean geometry, they are quotients of an open subset of the projective line by Schottky groups. In tropical geometry, which looks at the images in  $\mathbb{R}^n$  of curves under coordinate-wise valuation, these are balanced graphs with the maximal number of cycles. For instance, the tropicalization of an elliptic Mumford curve can be realized as a plane cubic in honeycomb form [29].

Let  $K$  be an algebraically closed field complete with respect to a nontrivial non-archimedean valuation. Unless otherwise stated,  $|\cdot|$  will denote a choice of norm on  $K$  coming from this valuation. Let  $R = \{x \in K \mid \text{val}(x) \geq 0\}$  be the valuation ring of  $K$ . This is a local ring with unique maximal ideal  $M = \{x \in K \mid \text{val}(x) > 0\}$ . Let  $k = R/M$  denote the residue field of  $K$ . We are most interested in the field of  $p$ -adic numbers  $\mathbb{Q}_p$ , which unfortunately is not algebraically closed. (For this case,  $R = \mathbb{Z}_p$ , the ring of  $p$ -adic integers, and  $k = \mathbb{F}_p$ , the field with  $p$  elements.) Therefore for theoretical purposes we will often consider  $K = \mathbb{C}_p$ , the complete algebraic closure of  $\mathbb{Q}_p$ . (In this case  $R$  is much larger, and  $k$  is the algebraic closure of  $\mathbb{F}_p$ .) In most of this chapter, choosing elements of  $\mathbb{C}_p$  that happen to be elements of  $\mathbb{Q}_p$  as inputs for algorithms yields an output once again in  $\mathbb{Q}_p$ . This “ $\mathbb{Q}_p$  in,  $\mathbb{Q}_p$  out” property means we may take  $K$  to be  $\mathbb{Q}_p$  for our algorithmic purposes, while still considering  $K = \mathbb{C}_p$  when more convenient for the purposes of theory. Much of the theory presented here works for other non-archimedean fields, such as the field of Puiseux series  $\mathbb{C}\{\{t\}\}$ .

We recall some standard definitions and notation for  $p$ -adic numbers; for further background on the  $p$ -adics, see [54]. For a prime  $p$ , the  $p$ -adic valuation  $\text{val}_p : \mathbb{Q}^* \rightarrow \mathbb{Z}$  is defined by  $\text{val}_p(p^v \frac{m}{n}) = v$ , where  $m$  and  $n$  are not divisible by  $p$ . The usual  $p$ -adic norm  $|\cdot|_p$  on  $\mathbb{Q}$



is defined for  $a \in \mathbb{Q}^*$  by  $|a|_p = \frac{1}{p^{\text{val}_p(a)}}$  and for 0 by  $|0|_p = 0$ . This means that large powers of  $p$  are small in absolute value, and small powers of  $p$  are large in absolute value. We will usually omit the subscript  $p$  from both  $|\cdot|_p$  and  $\text{val}_p$ .

The completion of  $\mathbb{Q}$  with respect to the  $p$ -adic norm is denoted  $\mathbb{Q}_p$ , and is called the field of  $p$ -adic numbers. Each nonzero element  $b$  of  $\mathbb{Q}_p$  can be written uniquely as

$$b = \sum_{n=v}^{\infty} a_n p^n,$$

where  $v \in \mathbb{Z}$ ,  $a_v \neq 0$  and  $a_n \in \{0, 1, \dots, p-1\}$  for all  $n$ . The  $p$ -adic valuation and norm extend to this field, and such a sum will have  $\text{val}(b) = v$  and  $|b| = \frac{1}{p^v}$ . In analog to decimal expansions, we will sometimes write

$$b = \dots a_N a_{N-1} \dots a_3 a_2 a_1 a_0 . a_{-1} a_{-2} \dots a_v,$$

where the expression trails to the left since higher powers of  $p$  are smaller in  $p$ -adic absolute value. We may approximate  $b \in \mathbb{Q}_p$  by a finite sum

$$b \approx \sum_{n=v}^N a_n p^n,$$

which will give an error of size at most  $\frac{1}{p^{N+1}}$ .

Consider the group  $PGL(2, K)$ , which acts on  $\mathbb{P}^1(K)$  by treating elements as column vectors. That is, a matrix acts on the point  $(a : b) \in \mathbb{P}^1(K)$  by acting on the vector  $\begin{pmatrix} a \\ b \end{pmatrix}$  on the left. Viewed on an affine patch, the elements of this group act as fractional linear transformations. We are interested in the action of certain subgroups of  $PGL(2, K)$  called *Schottky groups*, because a Schottky group minimally generated by  $g \geq 2$  elements will give rise to a curve of genus  $g$ .

**Definition 3.1.1.** A  $2 \times 2$  matrix is *hyperbolic* if it has two eigenvalues with different valuations. A *Schottky group*  $\Gamma \leq PGL(2, K)$  is a finitely generated subgroup such that every non-identity element is hyperbolic.

There are many equivalent definitions of Schottky groups, including the following useful characterization.

**Proposition 3.1.2.** A subgroup of  $PGL(2, K)$  is Schottky if and only if it is free, discrete, and finitely generated.

As remarked in the introduction of [67], if the matrices have entries in a locally compact field (like  $\mathbb{Q}_p$ ), the definition of Schottky is equivalent to asking that  $\Gamma$  has no elements of finite order. So if we are working with generators in  $\mathbb{Q}_p^{2 \times 2}$ , we may replace “free” with “torsion free.”

Let  $\Gamma$  be a Schottky group minimally generated by  $\gamma_1, \dots, \gamma_g$ . The above proposition implies that each element  $\gamma \in \Gamma$  can be written as a unique shortest product  $h_1 h_2 \cdots h_k$ , where each  $h_i \in \{\gamma_1, \dots, \gamma_g, \gamma_1^{-1}, \dots, \gamma_g^{-1}\}$ . This product is called the *reduced word* for  $\gamma$ .

Let  $\Sigma$  be the set of points in  $\mathbb{P}^1(K)$  that are fixed points of elements of  $\Gamma$  or limit points of the fixed points. The group  $\Gamma$  acts nicely on  $\Omega := \mathbb{P}^1(K) \setminus \Sigma$ ; for this reason we will sometimes refer to  $\Sigma$  as *the set of bad points* for  $\Gamma$ .

**Theorem 3.1.3** (Mumford, [67]). *Let  $\Gamma = \langle \gamma_1, \dots, \gamma_g \rangle$  and  $\Omega$  be as above. Then  $\Omega/\Gamma$  is analytically isomorphic to a curve of genus  $g$ . We call such a curve a Mumford curve.*

In a companion paper to [67] (see [68]), Mumford also considered abelian varieties over non-archimedean fields. He showed that these could be represented as  $(K^*)^g/Q$ , where  $Q \in (K^*)^{g \times g}$  is called a *period matrix* for the abelian variety, and represents the multiplicative subgroup generated by its columns.

Since their initial appearance in the 1970s, a rich theory behind Mumford curves has been developed, largely in the 1980s in such works as [43]. However, prior to the work in this project there have been few numerical algorithms for working with them (an exception being a treatment of hyperelliptic Mumford curves, mostly genus 2, in [58] from 2007). We have designed and implemented algorithms that accomplish Mumford curve-based tasks over  $\mathbb{Q}_p$  previously absent from the realm of computation, and have made many seemingly theoretical and opaque objects hands-on and tractable.

After discussing in Section 3.2 a technical hypothesis (“good position”) for the input for our algorithms, we present our main algorithms in Section 3.3. They accomplish the following tasks, where we denote  $\Omega/\Gamma$  by  $C$ :

- Given a Schottky group  $\Gamma$ , find a period matrix  $Q$  for the abelian variety  $\text{Jac}(C)$  (Algorithm 3.3.3).
- Given a Schottky group  $\Gamma$ , find a triple  $(G, \ell, h)$ , where
  - $G$  is a graph,
  - $\ell$  is a length function on  $G$  such that the metric graph  $(G, \ell)$  is the abstract tropical curve which is a skeleton of  $C^{an}$  (the analytification of  $C$ ), and
  - $h$  is a natural equivalence  $h : R^g \rightarrow G$  from the rose graph on  $g$  petals;

this data specifies a point in the tropical Teichmüller space described in [28] (Algorithm 3.3.9).

- Given a Schottky group  $\Gamma$ , find points in a canonical embedding of the curve  $C$  into  $\mathbb{P}^{g-1}$  (Algorithm 3.3.13).

In Section 3.4, we present an algorithm to achieve the “good position” hypothesis that allows the other algorithms to run efficiently, which in doing so verifies that the input group

is Schottky (or proves that the group is not Schottky). This is the most important result of this chapter, as the algorithms in Section 3.3 rely heavily upon it.

We take advantage of a property that makes non-archimedean valued fields like  $\mathbb{Q}_p$  special:  $|x + y| \leq \max\{|x|, |y|\}$ . As a result, the error does not accumulate in the computation. Thus we avoid a dangerous hazard present in doing numerical computation over  $\mathbb{R}$  or  $\mathbb{C}$ . The computational problems are hard in nature. Efficient computation for similar problems is not common in the literature even for genus 2 case. Our algorithms are capable of solving genus 2 and some genus 3 examples on a laptop in reasonable time (several minutes). However, they are less efficient for larger genera. The reason is that the running time grows exponentially as the requirement on the precision of the output (in terms of the number of digits) grows. One of the future goals is to find a way to reduce the running time for the algorithms.

Other future goals for Mumford curve algorithms (detailed in Section 3.5) include natural reversals of the algorithms in Section 3.3. We are also interested in a particular family of Schottky groups called *Whittaker groups*, defined in Subsection 3.5. These are the Schottky groups that give rise to hyperelliptic Mumford curves. Some computations for genus 2 curves arising from Whittaker groups were done in [58], including computation of Jacobians and finding group representations from ramification points. Two desirable algorithms in this area include:

- Given a Whittaker group  $W$ , find an affine equation for  $\Omega/W$ .
- Given a totally split hyperelliptic curve  $C$ , find a Whittaker group  $W$  such that  $C \cong \Omega/W$ .

The first can be accomplished if a particular presentation of  $W$  is available, and a brute force algorithm in [58] can compute the second if the ramification points of  $C$  are in a nice position. Future work removing these requirements and improving efficiency would make hyperelliptic Mumford curves very easy to work with computationally.

This project also looks towards understanding tropicalizations of Mumford curves, both as abstract metric graphs and as balanced polyhedral complexes in  $\mathbb{R}^n$ . For more background on tropical geometry, in particular tropical curves, tropical Jacobians, and their relationships to classical curves and Jacobians, see [3, 10, 18, 23, 26, 96].

## Supplementary Material

We made extensive use of the software package `sage` [85]. Our supplementary files can be found at [http://math.berkeley.edu/~ralph42/mumford\\_curves\\_supp.html](http://math.berkeley.edu/~ralph42/mumford_curves_supp.html). We have also included the files in the arXiv submission, and they can be obtained by downloading the source. There are minor changes in the `sage` implementation from the description of the algorithms in this chapter. The changes are made only for convenience in implementation, and they do not affect the behavior of the algorithms.

## 3.2 Good Fundamental Domains in $\mathbb{P}^1$ and $(\mathbb{P}^1)^{an}$

This section introduces *good fundamental domains* and the notion of *good position* for generators, both of which will play key roles in our algorithms for Mumford curves. Our main algorithms in Section 3.3 require as input Schottky generators in good position, without which the rate of convergence of approximations will drop drastically. For our method of putting generators into good position, see Section 3.4.

We start with the usual projective line  $\mathbb{P}^1$ , then discuss the analytic projective line  $(\mathbb{P}^1)^{an}$ . Our treatment of good fundamental domains follows Gerritzen and van der Put [43]. The notion is also discussed by Kadziela [58]. The introduction to the analytic projective line follows Baker, Payne and Rabinoff [9].

**Definition 3.2.1.** An *open ball* in  $\mathbb{P}^1$  is either a usual open ball  $B(a, r) = \{x \in K : |x - a| < r\}$  or the complement of a usual closed ball  $\mathbb{P}^1 \setminus B(a, r)^+ = \{\infty\} \cup \{x \in K : |x - a| > r\}$ . A *closed ball* is either a usual closed ball or the complement of a usual open ball.

The open balls generate a topology on  $\mathbb{P}^1$ . Both open balls and closed balls are simultaneously open and closed in this topology, as is the case for any non-archimedean field due to the ultrametric inequality  $|x + y| \leq \max\{|x|, |y|\}$ . Let  $|K^\times|$  denote the image of  $K^\times$  under  $|\cdot|$ . If  $r \in |K^\times|$ , the open ball and the closed ball of radius  $r$  are distinguished by whether there exist two points  $x, y$  in the ball such that  $|x - y|$  equals the diameter. The complement of an open ball is a closed ball, and vice versa.

**Definition 3.2.2.** A *good fundamental domain*  $F \subset \mathbb{P}^1$  corresponding to the generators  $\gamma_1, \dots, \gamma_g$  is the complement of  $2g$  open balls  $B_1, \dots, B_g, B'_1, \dots, B'_g$ , such that corresponding closed balls  $B_1^+, \dots, B_g^+, B_1'^+, \dots, B_g'^+$  are disjoint, and that  $\gamma_i(\mathbb{P}^1 \setminus B_i') = B_i^+$  and  $\gamma_i^{-1}(\mathbb{P}^1 \setminus B_i) = B_i'^+$  for all  $i$ . The *interior* of  $F$  is  $F^\circ = \mathbb{P}^1 \setminus (B_1^+ \cup \dots \cup B_g^+ \cup B_1'^+ \cup \dots \cup B_g'^+)$ . The *boundary* of  $F$  is  $F \setminus F^\circ$ .

The definition above implies that  $\gamma_i(\mathbb{P}^1 \setminus B_i'^+) = B_i$  and  $\gamma_i^{-1}(\mathbb{P}^1 \setminus B_i^+) = B_i'$  for all  $i$ .

**Example 3.2.3.** (1) Let  $K = \mathbb{C}_3$  and  $\Gamma$  be the group generated by

$$\gamma_1 = \begin{bmatrix} -5 & 32 \\ -8 & 35 \end{bmatrix}, \gamma_2 = \begin{bmatrix} -13 & 80 \\ -8 & 43 \end{bmatrix}$$

Both matrices have eigenvalues 27 and 3. The matrix  $\gamma_1$  has left eigenvectors  $\begin{pmatrix} 1 \\ 1 \end{pmatrix}$  and  $\begin{pmatrix} 4 \\ 1 \end{pmatrix}$ , and  $\gamma_2$  has left eigenvectors  $\begin{pmatrix} 2 \\ 1 \end{pmatrix}$  and  $\begin{pmatrix} 5 \\ 1 \end{pmatrix}$ . We use the convention that  $(z_1 : z_2) = z_1/z_2$ . Then,  $F = \mathbb{P}^1 \setminus (B_1 \cup B_1' \cup B_2 \cup B_2')$  where  $B_1 = B(4, 1/9)$ ,  $B_1' = B(1, 1/9)$ ,  $B_2 = B(5, 1/9)$ ,  $B_2' = B(2, 1/9)$  is a good fundamental domain relative to the generators  $\gamma_1$  and  $\gamma_2$ . One can verify as follows. First rewrite

$$\gamma_1 z = \frac{-5z + 32}{-8z + 35} = 4 + \frac{27(z - 1) - 81}{-8(z - 1) + 27}.$$

Suppose that  $z \in B'_1 = B(1, 1/9)$ . Then,  $\text{val}(27(z-1)) = 3 + \text{val}(z-1) \geq 3 + 2 = 5$ , and  $\text{val}(81) = 4$ . So  $\text{val}(27(z-1) - 81) = 4$ . Also,  $\text{val}(-8(z-1) + 27) \geq \min(\text{val}(8(z-1)), \text{val}(27)) > \min(2, 3) = 2$ . So,

$$|\gamma_1 z - 4| = \left| \frac{27(z-1) - 81}{-8(z-1) + 27} \right| > \frac{3^{-4}}{3^{-2}} = 1/9.$$

So  $\gamma_1(B'_1) \subset \mathbb{P}^1 \setminus B_1^+$ . The other three conditions can be verified similarly.

(2) Let  $K = \mathbb{C}_3$  and  $\Gamma$  be the group generated by

$$\gamma_1 = \begin{bmatrix} -79 & 160 \\ -80 & 161 \end{bmatrix}, \gamma_2 = \begin{bmatrix} -319 & 1600 \\ -80 & 401 \end{bmatrix}$$

Both matrices have eigenvalues 81 and 1. The matrix  $\gamma_1$  has left eigenvectors  $\begin{pmatrix} 1 \\ 1 \end{pmatrix}$  and  $\begin{pmatrix} 2 \\ 1 \end{pmatrix}$ , and the matrix  $\gamma_2$  has left eigenvectors  $\begin{pmatrix} 4 \\ 1 \end{pmatrix}$  and  $\begin{pmatrix} 5 \\ 1 \end{pmatrix}$ . Then,  $F = \mathbb{P}^1 \setminus (B_1 \cup B'_1 \cup B_2 \cup B'_2)$  where  $B_1 = B(2, 1/9)$ ,  $B'_1 = B(1, 1/9)$ ,  $B_2 = B(5, 1/9)$ ,  $B'_2 = B(4, 1/9)$  is a good fundamental domain relative to the generators  $\gamma_1$  and  $\gamma_2$ .

(3) Let  $K = \mathbb{C}_3$ , and let  $\Gamma$  be the group generated by

$$\gamma_1 = \begin{bmatrix} 121 & -120 \\ 40 & -39 \end{bmatrix}, \gamma_2 = \begin{bmatrix} 121 & -240 \\ 20 & -39 \end{bmatrix}, \gamma_3 = \begin{bmatrix} 401 & -1600 \\ 80 & -319 \end{bmatrix}.$$

All three generators have eigenvalues 1 and  $3^4$ . The element  $\gamma_1$  has eigenvectors  $\begin{pmatrix} 1 \\ 1 \end{pmatrix}$  and  $\begin{pmatrix} 3 \\ 1 \end{pmatrix}$ . The element  $\gamma_2$  has eigenvectors  $\begin{pmatrix} 2 \\ 1 \end{pmatrix}$  and  $\begin{pmatrix} 6 \\ 1 \end{pmatrix}$ . The element  $\gamma_3$  has eigenvectors  $\begin{pmatrix} 4 \\ 1 \end{pmatrix}$  and  $\begin{pmatrix} 5 \\ 1 \end{pmatrix}$ . Then,  $F = \mathbb{P}^1 \setminus (B_1 \cup B'_1 \cup B_2 \cup B'_2 \cup B_3 \cup B'_3)$  where  $B_1 = B(1, 1/9)$ ,  $B'_1 = B(3, 1/9)$ ,  $B_2 = B(2, 1/9)$ ,  $B'_2 = B(6, 1/9)$ ,  $B_3 = B(4, 1/9)$ ,  $B'_3 = B(5, 1/9)$  is a good fundamental domain relative to the generators  $\gamma_1$ ,  $\gamma_2$  and  $\gamma_3$ .

The following lemma follows from Definition 3.2.2 by induction (see [58, Theorem 6.2]).

**Lemma 3.2.4.** *Let  $F$  and  $\gamma_1, \dots, \gamma_g$  be as in Definition 3.2.2, and let  $\gamma \in \Gamma \setminus \{(\begin{smallmatrix} 1 & 0 \\ 0 & 1 \end{smallmatrix})\}$  and  $b \in \mathbb{P}^1(K)$ . Write the reduced word for  $\gamma$  as  $h_1 h_2 \dots h_k$ , where  $k \geq 1$  and  $h_i \in \{\gamma_1^\pm, \dots, \gamma_g^\pm\}$  for all  $i$ . Assume that  $b \notin B'_j$  if  $h_k = \gamma_j$  and  $b \notin B_j$  if  $h_k = \gamma_j^{-1}$ . Then we have*

$$\gamma b \in \begin{cases} B_i^+, & \text{if } h_1 = \gamma_i, \\ B_i'^+, & \text{if } h_1 = \gamma_i^{-1}. \end{cases}$$

*Proof.* To simplify notation we will outline the proof for the case where  $h_i \in \{\gamma_1, \dots, \gamma_g\}$  for all  $i$ , and then describe how to generalize to the case of  $h_i \in \{\gamma_1^\pm, \dots, \gamma_g^\pm\}$ .

Write  $h_i = \gamma_{a_i}$  for each  $i$ . Since  $h_k = \gamma_{a_k}$ , we know by assumption that  $b \notin B'_{a_k}$ . By Definition 3.2.2 we have  $\gamma_{a_k}(\mathbb{P}^1 \setminus B'_{a_k}) = B_{a_k}^+$ , so  $h_k b \in B_{a_k}^+$ . By the disjointness of the  $2g$  closed balls, we know that  $h_k b \notin B'_{a_{k-1}}$ , and since  $\gamma_{a_{k-1}}(\mathbb{P}^1 \setminus B'_{a_{k-1}}) = B_{a_{k-1}}^+$ , we have  $h_{k-1} h_k b \in B_{a_{k-1}}^+$ . We may continue in this fashion until we find that  $h_1 h_2 \dots h_k b \in B_{a_1}^+$ .

The only possible obstruction to the above argument in the case of  $h_i \in \{\gamma_1^\pm, \dots, \gamma_g^\pm\}$  occurs if  $h_i \dots h_k b \in B_{a_i}^+$  and  $h_{i-1} = \gamma_{a_i}$  (or, similarly, if  $h_i \dots h_k b \in B_{a_i}^+$  and  $h_{i-1} = \gamma_{a_i}^{-1}$ ), since the above argument needs  $\gamma_{a_i}$  to act on  $\mathbb{P}^1 \setminus B_{a_i}^+$ . However, this situation arises precisely when  $h_i = \gamma_{a_i}^{-1} = h_{i-1}^{-1}$ , meaning that the word is not reduced. Since we've assumed  $h_1 \dots h_k$  is reduced, we have the desired result.  $\square$

For a fixed set of generators of  $\Gamma$ , there need not exist a good fundamental domain. If there exists a good fundamental domain for some set of free generators of  $\Gamma$ , we say that the generators are *in good position*. Gerritzen and van der Put [43, §I.4] proved that there always exists a set of generators in good position. They also proved the following desirable properties for good fundamental domains.

**Theorem 3.2.5.** *Let  $\Gamma$  be a Schottky group,  $\Sigma$  its set of bad points, and  $\Omega = \mathbb{P}^1 \setminus \Sigma$ .*

- (1) *There exists a good fundamental domain for some set of generators  $\gamma_1, \dots, \gamma_g$  of  $\Gamma$ . Let  $F$  be a good fundamental domain for  $\gamma_1, \dots, \gamma_g$ , and let  $\gamma \in \Gamma$ .*
- (2) *If  $\gamma \neq \text{id}$ , then  $\gamma F^\circ \cap F = \emptyset$ .*
- (3) *If  $\gamma \notin \{\text{id}, \gamma_1, \dots, \gamma_g, \gamma_1^{-1}, \dots, \gamma_g^{-1}\}$ , then  $\gamma F \cap F = \emptyset$ .*
- (4)  $\cup_{\gamma \in \Gamma} \gamma F = \Omega$ .

The statements (2), (3), and (4) imply that  $\Omega/\Gamma$  can be obtained from  $F$  by glueing the boundary of  $F$ . More specifically,  $B_i^+ \setminus B_i$  is glued with  $B_i'^+ \setminus B_i'$  via the action of  $\gamma_i$ . We have designed the following subroutine, which takes any point  $p$  in  $\Omega$  and finds a point  $q$  in  $F$  such that they are equivalent modulo the action of  $\Gamma$ . This subroutine is useful in developing the algorithms in Section 3 and 4.

**Subroutine 3.2.6** (Reducing a point into a good fundamental domain).

**Input:** Matrices  $\gamma_1, \dots, \gamma_g$  generating a Schottky group  $\Gamma$ , a good fundamental domain  $F = \mathbb{P}^1 \setminus (B_1 \cup \dots \cup B_g \cup B_1' \cup \dots \cup B_g')$  associated to these generators, and a point  $p \in \Omega$ .

**Output:** A point  $q \in F$  and an element  $\gamma \in \Gamma$  such that  $q = \gamma p$ .

- 1: Let  $q \leftarrow p$  and  $\gamma \leftarrow \text{id}$ .
- 2: **while**  $q \notin F$  **do**
- 3:     If  $q \in B_i'$ , let  $q \leftarrow \gamma_i q$  and  $\gamma \leftarrow \gamma_i \gamma$ .
- 4:     Otherwise, if  $q \in B_i$ , let  $q \leftarrow \gamma_i^{-1} q$  and  $\gamma \leftarrow \gamma_i^{-1} \gamma$ .
- 5: **end while**
- 6: **return**  $q$  and  $\gamma$ .

*Proof.* The correctness of this subroutine is clear. It suffices to prove that the algorithm always terminates. Given  $p \in \Omega$ , if  $p \notin F$ , by Theorem 3.2.5, there exists  $\gamma^\circ = h_1 h_2 \dots h_k \in \Gamma$  (where each  $h_j$  is  $\gamma_i$  or  $\gamma_i^{-1}$  for some  $i$ ) such that  $\gamma^\circ p \in F$ . Without loss of generality, we may assume that  $\gamma^\circ$  is chosen such that  $k$  is the smallest. Steps 3,4 and Lemma 3.2.4 make sure that we always choose  $q \leftarrow h_k q$  and  $\gamma \leftarrow h_k \gamma$ . Therefore, this subroutine terminates with  $\gamma = \gamma^\circ$ .  $\square$

We can extend the definition of good fundamental domains to the analytic projective line  $(\mathbb{P}^1)^{an}$ . The notion of Berkovich analytic space is defined in Chapter 1.

**Definition 3.2.7.** Let  $\Sigma$  be a discrete subset in  $\mathbb{P}^1$ . The subtree of  $(\mathbb{P}^1)^{an}$  spanned by  $\Sigma$ , denoted  $T(\Sigma)$ , is the union of all paths connecting all pairs of points in  $\Sigma$ .

An *analytic open ball*  $B(a, r)^{an}$  is a subset of  $(\mathbb{P}^1)^{an}$  whose set of Type 1 points is just  $B(a, r)$  and whose Type 2, 3, and 4 points correspond to closed balls  $B(a', r')^+ \subset B(a, r)$  and the limit of sequences of such closed balls. An *analytic closed ball* is similar, with  $B(a, r)$  replaced with  $B(a, r)^+$ . Just as in the case of balls in  $\mathbb{P}^1$ , the analytic closed ball  $(B^+)^{an}$  is not the closure of  $B^{an}$  in the metric topology of  $(\mathbb{P}^1)^{an}$ . The complement of an analytic open ball is an analytic closed ball, and vice versa. In an analytic closed ball  $(B(a, r)^+)^{an}$  such that  $r \in |K^\times|$ , the *Gaussian point* is the Type 2 point corresponding to  $B(a, r)^+$ . An *analytic annulus* is  $B \setminus B'$ , where  $B$  and  $B'$  are analytic balls such that  $B' \subsetneq B$ . If  $B$  is an analytic open (resp. closed) ball and  $B'$  is an analytic closed (resp. open) ball, then  $B \setminus B'$  is an *analytic open annulus* (resp. *analytic closed annulus*). A special case of analytic open annulus is the complement of a point in an analytic open ball.

Any element of  $PGL(2, K)$  sends open balls to open balls and closed balls to closed balls. Thus, there is a well defined action of  $PGL(2, K)$  on  $(\mathbb{P}^1)^{an}$ .

**Definition 3.2.8.** A *good fundamental domain*  $F \subset (\mathbb{P}^1)^{an}$  corresponding to the generators  $\gamma_1, \dots, \gamma_g$  is the complement of  $2g$  analytic open balls  $B_1^{an}, \dots, B_g^{an}, B_1'^{an}, \dots, B_g'^{an}$ , such that the corresponding analytic closed balls  $(B_1^+)^{an}, \dots, (B_g^+)^{an}, (B_1'^+)^{an}, \dots, (B_g'^+)^{an}$  are disjoint, and that  $\gamma_i((\mathbb{P}^1)^{an} \setminus B_i'^{an}) = (B_i^+)^{an}$  and  $\gamma_i^{-1}((\mathbb{P}^1)^{an} \setminus B_i^{an}) = (B_i'^+)^{an}$ . The *interior* of  $F$  is  $F^\circ = (\mathbb{P}^1)^{an} \setminus ((B_1^+)^{an} \cup \dots \cup (B_g^+)^{an} \cup (B_1'^+)^{an} \cup \dots \cup (B_g'^+)^{an})$ . The *boundary* of  $F$  is  $F \setminus F^\circ$ .

Definition 3.2.8 implies that  $\gamma_i((\mathbb{P}^1)^{an} \setminus (B_i'^+)^{an}) = B_i^{an}$  and  $\gamma_i^{-1}((\mathbb{P}^1)^{an} \setminus (B_i^+)^{an}) = B_i'^{an}$ .

We now argue that there is a one-to-one correspondence between good fundamental domains in  $\mathbb{P}^1$  and good fundamental domains in  $(\mathbb{P}^1)^{an}$ . (This fact is well-known, though seldom explicitly stated in the literature; for instance, it's taken for granted in the later chapters of [43].) If  $\mathbb{P}^1 \setminus (B_1 \cup \dots \cup B_g \cup B_1' \cup \dots \cup B_g')$  is a good fundamental domain in  $\mathbb{P}^1$ , then  $(\mathbb{P}^1)^{an} \setminus (B_1^{an} \cup \dots \cup B_g^{an} \cup B_1'^{an} \cup \dots \cup B_g'^{an})$  is a good fundamental domain in  $(\mathbb{P}^1)^{an}$ . Indeed, since the closed balls  $B_1^+, \dots, B_g^+, B_1'^+, \dots, B_g'^+$  are disjoint, and the corresponding analytic closed balls consist of points corresponding to closed balls contained in  $B_1^+, \dots, B_g^+, B_1'^+, \dots, B_g'^+$  and their limits, the analytic closed balls are also disjoint. Conversely, if  $(\mathbb{P}^1)^{an} \setminus (B_1^{an} \cup \dots \cup B_g^{an} \cup B_1'^{an} \cup \dots \cup B_g'^{an})$  is a good fundamental domain in  $(\mathbb{P}^1)^{an}$ , then  $\mathbb{P}^1 \setminus (B_1 \cup \dots \cup B_g \cup B_1' \cup \dots \cup B_g')$  is a good fundamental domain in  $\mathbb{P}^1$ , because the classical statement can be obtained from the analytic statement by considering only Type 1 points. This correspondence allows us to abuse notation by not distinguishing the classical case and the analytic case. Theorem 3.2.5 is also true for analytic good fundamental domains.

### 3.3 Algorithms Starting With a Schottky Group

If we have a Schottky group  $\Gamma = \langle \gamma_1, \dots, \gamma_g \rangle$  in terms of its generators, there are many objects we wish to compute for the corresponding curve  $\Omega/\Gamma$ , such as the Jacobian of the curve, the minimal skeleton of the analytification of the curve, and a canonical embedding for the curve. In this section we present algorithms for numerically computing these three objects, given the input of a Schottky group with generators in good position. For an algorithm that puts arbitrary generators of a Schottky group into good position, see Section 3.4.

**Remark 3.3.1.** Several results in this section are concerned with the accuracy of numerical approximations. Most of our results will be of the form

$$\left| \frac{\text{estimate}}{\text{actual}} - 1 \right| = \text{size of error term} \leq \text{a small real number of the form } p^{-N},$$

where we think of  $N \gg 0$ . This is equivalent to

$$\frac{\text{estimate}}{\text{actual}} - 1 = \text{error term} = \text{a } p\text{-adic number of the form } bp^N,$$

where  $|b| \leq 1$ . So, since  $|p^N| = p^{-N}$ , the *size* of the error term is a *small* power of  $p$ , while the *error term itself* is a *large* power of  $p$  (possibly with a constant that doesn't matter much).

Rearranging the second equation gives

$$\text{estimate} = \text{actual} + \text{actual} \cdot bp^N,$$

meaning that we are considering not the *absolute* precision of our estimate, but rather the *relative* precision. In this case we would say that our estimate is of *relative precision*  $O(p^N)$ . So if we desire relative precision  $O(p^N)$ , we want the *actual* error term to be  $p^N$  (possibly with a constant term with nonnegative valuation), and the *size* of the error term to be at most  $p^{-N}$ .

#### The Period Matrix of the Jacobian

Given a Schottky group  $\Gamma = \langle \gamma_1, \dots, \gamma_g \rangle$ , we wish to find a period matrix  $Q$  so that  $\text{Jac}(\Omega/\Gamma) \cong (K^*)^g/Q$ . For previous work on this computation in the genus-2 case, see [88].

First we will set some notation. For any parameters  $a, b \in \Omega$ , we introduce the following analytic function in the unknown  $z$ , called a *theta function*:

$$\Theta(a, b; z) := \prod_{\gamma \in \Gamma} \frac{z - \gamma a}{z - \gamma b}.$$



Note that if  $\Gamma$  is defined over  $\mathbb{Q}_p$  and  $a, b, z \in \mathbb{Q}_p$ , then  $\Theta(a, b; z) \in \mathbb{Q}_p \cup \{\infty\}$ . (This is an instance of “ $\mathbb{Q}_p$  in,  $\mathbb{Q}_p$  out.”) For any  $\alpha \in \Gamma$  and  $a \in \Omega$ , we can specialize to

$$u_\alpha(z) := \Theta(a, \alpha a; z).$$

It is shown in [43, II.3] that the function  $u_\alpha(z)$  is in fact independent of the choice of  $a$ . This is because for any choice of  $a, b \in \Omega$  we have

$$\begin{aligned} \frac{\Theta(a, \alpha a; z)}{\Theta(b, \alpha b; z)} &= \prod_{\gamma \in \Gamma} \left( \frac{z - \gamma a}{z - \gamma \alpha a} \frac{z - \gamma \alpha b}{z - \gamma b} \right) = \prod_{\gamma \in \Gamma} \left( \frac{z - \gamma a}{z - \gamma b} \frac{z - \gamma \alpha b}{z - \gamma \alpha a} \right) \\ &= \prod_{\gamma \in \Gamma} \frac{z - \gamma a}{z - \gamma b} \cdot \prod_{\gamma \in \Gamma} \frac{z - \gamma \alpha b}{z - \gamma \alpha a} = \prod_{\gamma \in \Gamma} \frac{z - \gamma a}{z - \gamma b} \cdot \prod_{\gamma \in \Gamma} \frac{z - \gamma b}{z - \gamma a} \\ &= \Theta(a, b; z) \cdot \Theta(b, a; z) = 1. \end{aligned}$$

From [43, VI.2] we have a formula for the period matrix  $Q$  of  $\text{Jac}(\Omega/\Gamma)$ :

**Theorem 3.3.2.** *The period matrix  $Q$  for  $\text{Jac}(\Omega/\Gamma)$  is given by*

$$Q_{ij} = \frac{u_{\gamma_i}(z)}{u_{\gamma_i}(\gamma_j z)},$$

where  $z$  is any point in  $\Omega$ .

As shown in [43, II.3], the choice of  $z$  does not affect the value of  $Q_{ij}$ .

Theorem 3.3.2 implies that in order to compute each  $Q_{ij}$ , it suffices to find a way to compute  $\Theta(a, b; z)$ . Since a theta function is defined as a product indexed by the infinite group  $\Gamma$ , approximation will be necessary. Recall that each element  $\gamma$  in the free group generated by  $\gamma_1, \dots, \gamma_g$  can be written in a unique shortest product  $h_1 h_2 \dots h_k$  called the reduced word, where each  $h_i \in \{\gamma_1, \dots, \gamma_g, \gamma_1^{-1}, \dots, \gamma_g^{-1}\}$ . We can approximate  $\Theta(a, b; z)$  by replacing the product over  $\Gamma$  with a product over  $\Gamma_m$ , the set of elements of  $\Gamma$  whose reduced words have length  $\leq m$ . More precisely, we approximate  $\Theta(a, b; z)$  with

$$\Theta_m(a, b; z) := \prod_{\gamma \in \Gamma_m} \frac{z - \gamma a}{z - \gamma b},$$

where

$$\Gamma_m = \{h_1 h_2 \dots h_k \mid 0 \leq k \leq m, h_i \in \{\gamma_1^\pm, \dots, \gamma_g^\pm\}, h_i \neq h_{i+1}^{-1} \text{ for any } i\}.$$

With this approximation method, we are ready to describe an algorithm for computing  $Q$ .

**Algorithm 3.3.3** (Period Matrix Approximation).

**Input:** Matrices  $\gamma_1, \dots, \gamma_g \in \mathbb{Q}_p^{2 \times 2}$  generating a Schottky group  $\Gamma$  in good position, and an integer  $n$  to specify the desired relative precision.

**Output:** An approximation for a period matrix  $Q$  for  $\text{Jac}(\Omega/\Gamma)$  up to relative precision  $O(p^n)$ .

- 1: Choose suitable  $p$ -adic numbers  $a$  and  $z$  as described in Theorem 3.3.6.
- 2: Based on  $n$ , choose a suitable positive integer  $m$  as described in Remark 3.3.7.
- 3: **for**  $1 \leq i, j \leq g$  **do**
- 4:     Compute  $Q_{ij} = \Theta_m(a, \gamma_i(a); z) / \Theta_m(a, \gamma_i(a); \gamma_j(z))$
- 5: **end for**
- 6: **return**  $Q$ .

The complexity of this algorithm is in the order of the number of elements in  $\Gamma_m$ , which is exponential in  $m$ . The next issue is that to achieve certain precision in the final result, we need to know how large  $m$  needs to be. Given a good fundamental domain  $F$  for the generators  $\gamma_1, \dots, \gamma_g$ , we are able to give an upper bound on the error in our estimation of  $\Theta$  by  $\Theta_m$ . (Algorithm 3.3.3 would work even if the given generators were not in good position, but would in general require a very large  $m$  to give the desired convergence. See Example 3.3.8(4).)

To analyze the convergence of the infinite product

$$\Theta(a, \gamma_i(a); z) = \prod_{\gamma \in \Gamma} \frac{z - \gamma a}{z - \gamma \gamma_i a},$$

we need to know where  $\gamma a$  and  $\gamma \gamma_i a$  lie. We can determine this by taking the metric of  $(\mathbb{P}^1)^{an}$  into consideration. Assume that  $\infty$  lies in the interior of  $F$ . Let  $S = \{P_1, \dots, P_g, P'_1, \dots, P'_g\}$  be the set of points corresponding to the set of closed balls  $\{B_1^+, \dots, B_g^+, B'_1, \dots, B'_g\}$  from the characterization of the good fundamental domain. Let  $c$  be the smallest pairwise distance between these points. This distance  $c$  will be key for determining our choice of  $m$  in the algorithm.

**Proposition 3.3.4.** *Let  $F$ ,  $S$ , and  $c$  be as above. Suppose the reduced word for  $\gamma$  is  $h_1 h_2 \cdots h_k$ , where  $k \geq 0$ . Then  $d(\gamma P_i, S) \geq kc$  for all  $i$  unless  $h_k = \gamma_i^{-1}$ , and  $d(\gamma P'_i, S) \geq kc$  unless  $h_k = \gamma_i$ .*

*Proof.* We will prove this proposition by induction. If  $k = 0$ , there is nothing to prove. Let  $k > 0$ , and assume that the claim holds for all integers  $n$  with  $0 \leq n < k$ . Without loss of generality, we may assume  $h_1 = \gamma_1$ . Let  $B^+$  be the closed disk corresponding to  $P_i$ . By Lemma 3.2.4, we have  $\gamma(B^+) \subset B_1$ . This means  $P_1$  lies on the unique path from  $\gamma P_i$  to  $\infty$ . Since we assumed  $\infty \in F$ ,  $p_1$  lies on the unique path from  $\gamma P_i$  to any point in  $S$ . Thus,

$$\begin{aligned} d(\gamma P_i, S) &= d(\gamma P_i, P_1) \\ &= d(\gamma_1^{-1} \gamma P_i, \gamma_1^{-1} P_1) \\ &= d(h_2 h_3 \cdots h_k P_i, P'_1). \end{aligned}$$

Let  $P = P_j$  if  $h_2 = \gamma_j$  and  $P = P'_j$  if  $h_2 = \gamma_j^{-1}$ . By the same argument as above,  $P$  lies on the unique path from  $h_2 h_3 \cdots h_k P_i$  to  $P'_1$ . The reducedness of the word  $h_1 h_2 \cdots h_k$  guarantees

that  $P \neq P'_1$ . So

$$\begin{aligned} d(\gamma P_i, S) &= d(h_2 h_3 \cdots h_k P_i, P'_1) \\ &= d(h_2 h_3 \cdots h_k P_i, P) + d(P, P'_1) \\ &\geq (k-1)c + c = kc. \end{aligned}$$

The last step follows from the inductive hypothesis. The proof of the second part of this proposition is similar.  $\square$

**Proposition 3.3.5.** *Let  $F$ ,  $S$ , and  $c$  be as above. Let  $z \in F$  and  $a \in B_i^{'+} \setminus B'_i$  such that  $a$ ,  $z$ , and  $\infty$  are distinct modulo the action of  $\Gamma$ . Suppose the reduced word for  $\gamma \in \Gamma$  is  $h_1 h_2 \cdots h_k$ . If  $k \geq 2$  and  $h_k \neq \gamma_i^{-1}$ , then*

$$\left| \frac{z - \gamma a}{z - \gamma \gamma_i a} - 1 \right| \leq p^{-c(k-1)}.$$

*Proof.* Our choice of  $a$  guarantees that both  $a$  and  $\gamma_i a$  are in  $F$ . Without loss of generality, we may assume that  $h_k = \gamma_1$ . Then, both  $h_k a$  and  $h_k \gamma_i a$  are in  $B_1^+$ . So both  $\gamma a$  and  $\gamma \gamma_i a$  lie in  $h_1 h_2 \cdots h_{k-1} B_1^+$ , which is contained in some  $B = B_j$  or  $B'_j$ . By Proposition 3.3.4, the points in  $(\mathbb{P}^1)^{an}$  corresponding to the disks  $h_1 h_2 \cdots h_{k-1} B_1^+$  and  $B^+$  have distance at least  $c(k-1)$ . This implies  $\text{diam}(h_1 h_2 \cdots h_{k-1} B_1^+) \leq p^{-c(k-1)} \text{diam}(B^+)$ . Therefore,  $|\gamma a - \gamma \gamma_i a| \leq p^{-c(k-1)} \text{diam}(B^+)$ . On the other hand, since  $z \notin B$  and  $\gamma \gamma_i a \in B$ , we have  $|z - \gamma \gamma_i a| \geq \text{diam}(B^+)$ . This means that

$$\left| \frac{z - \gamma a}{z - \gamma \gamma_i a} - 1 \right| = \left| \frac{\gamma \gamma_i a - \gamma a}{z - \gamma \gamma_i a} \right| \leq \frac{p^{-c(k-1)} \text{diam}(B^+)}{\text{diam}(B^+)} = p^{-c(k-1)},$$

as claimed.  $\square$

We are now ready to prove our approximation theorem, which is a new result that allows one to determine the accuracy of an approximation of a ratio of theta functions. It is similar in spirit to [58, Theorem 6.10], which is an approximation result for a particular subclass of Schottky groups called Whittaker groups (see Subsection 3.5 of this chapter for more details). Our result is more general, as there are many Schottky groups that are not Whittaker.

**Theorem 3.3.6.** *Suppose that the given generators  $\gamma_1, \dots, \gamma_g$  of  $\Gamma$  are in good position, with corresponding good fundamental domain  $F$  and disks  $B_1, \dots, B_g, B'_1, \dots, B'_g$ . Let  $m \geq 1$ . In Algorithm 3.3.3, if we choose  $a \in B_i^{'+} \setminus B'_i$  and  $z \in B_j^{'+} \setminus B'_j$  such that  $a \neq z$ , then*

$$\left| \frac{\Theta_m(a, \gamma_i(a); z) / \Theta_m(a, \gamma_i(a); \gamma_j(z))}{\Theta(a, \gamma_i(a); z) / \Theta(a, \gamma_i(a); \gamma_j(z))} - 1 \right| \leq p^{-cm},$$

where  $c$  is the constant defined above.

*Proof.* Our choice of  $z$  guarantees that both  $z$  and  $\gamma_j z$  are in  $F$ . Thus, if  $\infty$  lies in the interior of  $F$ , then this theorem follows directly from Proposition 3.3.5. The last obstacle is to remove the assumption on  $\infty$ . We observe that  $Q_{ij}$  is a product of cross ratios:

$$\frac{\Theta(a, \gamma_i a; z)}{\Theta(a, \gamma_i a; \gamma_j z)} = \prod_{\gamma \in \Gamma} \frac{(z - \gamma a)(\gamma_j z - \gamma \gamma_i a)}{(z - \gamma \gamma_i a)(\gamma_j z - \gamma a)}.$$

Therefore, each term is invariant under any projective automorphism of  $\mathbb{P}^1$ . Under such an automorphism, any point in the interior of  $F$  can be sent to  $\infty$ .  $\square$

As a special case of this approximation theorem, suppose that we want to compute the period matrix for the tropical Jacobian of  $C$ , which is the matrix  $(\text{val}(Q_{ij}))_{g \times g}$ . We need only to compute  $Q_{ij}$  up to relative precision  $O(1)$ . Thus, setting  $m = 0$  suffices. In this case, each of the products  $\Theta_m(a, \gamma_i(a); z)$ ,  $\Theta_m(a, \gamma_i(a); \gamma_j(z))$  has only one term.

**Remark 3.3.7.** If we wish to use Algorithm 3.3.3 to compute a period matrix  $Q$  with relative precision  $O(p^n)$  (meaning that we want  $p^{-cm} \leq p^{-n}$  in Theorem 3.3.6), we must first compute  $c$ . As above,  $c$  is defined to be the minimum distance between pairs of the points  $P_1, \dots, P_g, P'_1, \dots, P'_g \in (\mathbb{P}^1)^{an}$  corresponding to the balls  $B_1, \dots, B_g, B'_1, \dots, B'_g$  that characterize our good fundamental domain. Once we have computed  $c$  (perhaps by finding a good fundamental domain using the methods of Section 3.4), then by Theorem 3.3.6 we must choose  $m$  such that  $cm \geq n$ , so  $m = \lceil n/c \rceil$  will suffice.

**Example 3.3.8.** (1) Let  $\Gamma$  be the Schottky group in Example 3.2.3(1). Choose the same good fundamental domain, with  $B_1 = B(4, 1/9)$ ,  $B'_1 = B(1, 1/9)$ ,  $B_2 = B(5, 1/9)$ , and  $B'_2 = B(2, 1/9)$ . The four balls correspond to four points in the tree  $(\mathbb{P}^1)^{an}$ . We need to find the pairwise distances between the points  $P_1, P'_1, P_2$ , and  $P'_2$  in  $(\mathbb{P}^1)^{an}$ . Since the smallest ball containing both  $B_1^+$  and  $B'_1^+$  is  $B^+(1, 1/3)$ , both  $P_1$  and  $P'_1$  are distance  $\text{val}((1/3)/(1/9)) = \text{val}(3) = 1$  from the point corresponding to  $B^+(1, 1/3)$ , so  $P_1$  and  $P'_1$  are distance 2 from one another. Similar calculations give distances of 2 between  $P_2$  and  $P'_2$ , and of 4 between  $P_1$  or  $P'_1$  and  $P_2$  or  $P'_2$ . In fact, the distance between  $P_i$  and  $P'_i$  equals the difference in the valuations of the two eigenvalues of  $\gamma_i$ . This allows us to construct the subtree of  $(\mathbb{P}^1)^{an}$  spanned by  $P_1, P_2, P'_1, P'_2$  as illustrated in Figure 3.1. The minimum distance between them is  $c = 2$ . To approximate  $Q_{11}$ , we take  $a = 10$  and  $z = 19$ . To compute  $Q$  up to relative precision  $O(p^{10})$ , we need  $2m \geq 10$  (this is the equation  $cm \geq n$  from Remark 3.3.7), so choosing  $m = 5$  works. The output of the algorithm is  $Q_{11} = (\dots 220200000100)_3$ . Similarly, we can get the other entries in the matrix  $Q$ :

$$Q = \begin{bmatrix} (\dots 220200000100)_3 & (\dots 0101010101)_3 \\ (\dots 0101010101)_3 & (\dots 220200000100)_3 \end{bmatrix}.$$

(2) Let  $\Gamma$  be the Schottky group in Example 3.2.3(2). Choose the same good fundamental domain. Again, we need  $m = 5$  for relative precision  $O(p^{10})$ . The algorithm outputs

$$Q = \begin{bmatrix} (\dots 12010021010000)_3 & (\dots 002000212200)_3 \\ (\dots 002000212200)_3 & (\dots 12010021010000)_3 \end{bmatrix}.$$

(3) Let  $\Gamma$  be the Schottky group in Example 3.2.3(3). Choose the same good fundamental domain. The minimum distance between the corresponding points in  $(\mathbb{P}^1)^{an}$  is 2, so we may take  $m = 10/2 = 5$  to have relative precision up to  $O(p^{10})$ . Our algorithm outputs

$$Q = \begin{bmatrix} (\dots 11201000010000)_3 & (\dots 12020022210)_3 & (\dots 20020002120)_3 \\ (\dots 12020022210)_3 & (\dots 10101010010000)_3 & (\dots 020201120.1)_3 \\ (\dots 20020002120)_3 & (\dots 020201120.1)_3 & (\dots 21010100010000)_3 \end{bmatrix}.$$

(4) Let  $K = \mathbb{C}_3$  and  $\Gamma$  be the group generated by

$$\gamma_1 = \begin{bmatrix} -5 & 32 \\ -8 & 35 \end{bmatrix}, \gamma_2 = \gamma_1^{100} \begin{bmatrix} -13 & 80 \\ -8 & 43 \end{bmatrix}$$

The group is the same as in part (1) of this set of examples, but the generators are not in good position. To achieve the same precision,  $m$  needs to be up to 100 times greater than in part (1), because the  $\gamma_2$  in part (1) now has a reduced word of length 101. Since the running time grows exponentially in  $m$ , it is not feasible to approximate  $Q$  using Algorithm 3.3.3 with these generators as input.

## The Abstract Tropical Curve

This subsection deals with the problem of constructing the corresponding abstract tropical curve of a Schottky group over  $K$ , together with some data on its homotopy group. This is a relatively easy task, assuming that the given generators  $\gamma_1, \dots, \gamma_g$  are in good position, and that we are also given a fundamental domain  $F = \mathbb{P}^1 \setminus (B_1 \cap \dots \cap B_g \cap B'_1 \cap \dots \cap B'_g)$ . Without loss of generality, we may assume that  $\infty \in F^\circ$ . Let  $P_1, \dots, P_g, P'_1, \dots, P'_g \in (\mathbb{P}^1)^{an}$  be the Gaussian points of the disks  $B_1^+, \dots, B_g^+, B'_1^+, \dots, B'_g^+$ .

Let  $R_g$  be the *rose graph* on  $g$  leaves (with one vertex and  $g$  loops), and let  $r_1, \dots, r_g$  be the loops. A homotopy equivalence  $h : R^g \rightarrow G$  must map  $r_1, \dots, r_g$  to  $g$  loops of  $G$  that generate  $\pi_1(G)$ , so to specify  $h$  it will suffice to label  $g$  such loops of  $G$  with  $\{s_1, \dots, s_g\}$  and orientations. It is for this reason that we call  $h$  a *marking of  $G$* .

**Algorithm 3.3.9** (Abstract Tropical Curve Construction).

**Input:** Matrices  $\gamma_1, \dots, \gamma_g \in \mathbb{Q}_p^{2 \times 2}$  generating a Schottky group  $\Gamma$ , together with a good fundamental domain  $F = \mathbb{P}^1 \setminus (B_1 \cap \dots \cap B_g \cap B'_1 \cap \dots \cap B'_g)$ .

**Output:** The triple  $(G, \ell, h)$  with  $(G, \ell)$  the abstract tropical curve as a metric graph with a  $h$  a marking presented as  $g$  labelled oriented loops of  $G$ .

- 1: Construct the subtree in  $(\mathbb{P}^1)^{an}$  spanned by  $P_1, \dots, P_g, P'_1, \dots, P'_g$ , including lengths.
- 2: Label the unique shortest path from  $P_i$  to  $P'_i$  as  $s_i$ , remembering orientation.
- 3: Identify each  $P_i$  with  $P'_i$ , and declare the length of the new edge containing  $P_i = P'_i$  to be the sum of the lengths of the edges that were joined to form it.
- 4: Define  $h$  by the labels  $s_i$ , with each  $s_i$  now an oriented loop.
- 5: **return** the resulting labeled metric graph  $(G, \ell, h)$ .

*Proof.* The proof is essentially given in [43, I 4.3].  $\square$

**Remark 3.3.10.** It's worth noting that this algorithm can be done by hand if a good fundamental domain is known. If  $P_1, P_2 \in (\mathbb{P}^1)^{an}$  are the points corresponding to the disjoint closed balls  $B(a_1, r_1)^+$  and  $B(a_2, r_2)^+$ , then the distance between  $P_1$  and  $P_2$  is just the sum of their distances from  $P_3$  corresponding to  $B(a_3, r_3)^+$ , where  $B(a_3, r_3)^+$  is the smallest closed ball containing both  $a_1$  and  $a_2$ . The distance between  $P_i$  and  $P_3$  is just  $\text{val}(r_3/r_i)$  for  $i = 1, 2$ . Once all pairwise distances are known, constructing  $(G, \ell)$  is simple. Finding  $h$  is simply a matter of drawing the orientation on the loops formed by each pair  $(P_i, P'_i)$  and labeling that loop  $s_i$ . This process is illustrated three times in Example 3.3.12.

**Remark 3.3.11.** The space parameterizing labelled metric graphs  $(G, \ell, h)$  (identifying those with markings that are homotopy equivalent) is called *Outer space*, and is denoted  $X_g$ . It is shown in [28] that  $X_g$  sits inside tropical Teichmüller space as a dense open set, so Algorithm 3.3.9 can be viewed as computing a point in tropical Teichmüller space.

**Example 3.3.12.** (1) Let  $\Gamma$  be the Schottky group in Example 3.2.3(1). Choose the same good fundamental domain, with  $B_1 = B(4, 1/9)$ ,  $B'_1 = B(1, 1/9)$ ,  $B_2 = B(5, 1/9)$ , and  $B'_2 = B(2, 1/9)$ . We have constructed the subtree of  $(\mathbb{P}^1)^{an}$  spanned by  $P_1, P_2, P'_1, P'_2$  as illustrated in Figure 3.1 in Example 3.3.8(1). After identifying  $P_1$  with  $P'_1$  and  $P_2$  with  $P'_2$ , we get the “dumbbell” graph shown in Figure 3.1, with both loops having length 2 and the connecting edge having length 2.

(2) Let  $\Gamma$  be the Schottky group in Example 3.2.3(2). Choose the same good fundamental domain. The subtree of  $(\mathbb{P}^1)^{an}$  spanned by  $P_1, P_2, P'_1, P'_2$  is illustrated in Figure 3.2. After identifying  $P_1$  with  $P'_1$  and  $P_2$  with  $P'_2$ , we get the “theta” graph shown in Figure 3.2, with two edges of length 2 and one edge of length 2.

(3) Let  $\Gamma$  be the Schottky group in Example 3.2.3(3). The subtree of  $(\mathbb{P}^1)^{an}$  spanned by  $P_1, P_2, P_3, P'_1, P'_2, P'_3$  is illustrated in Figure 3.3. After identifying  $P_1$  with  $P'_1$ ,  $P_2$  with  $P'_2$  and  $P_3$  with  $P'_3$ , we get the “honeycomb” graph shown in Figure 3.3, with interior edges of length 1 and exterior edges of length 2.

## Canonical Embeddings

From [43, VI.4], we have that

$$\omega_i(z) := w_i(z)dz = \frac{u'_{\gamma_i}(z)}{u_{\gamma_i}(z)} dz$$

are  $g$  linearly independent analytic differentials on  $\Omega$  that are invariant under the action of  $\Gamma$ . Therefore, they define  $g$  linearly independent differentials on  $C = \Omega/\Gamma$ . Gerritzen and van der Put [43, VI.4] also state that these form a basis of the space of  $\Gamma$ -invariant analytic differentials. Since the space of algebraic differentials on  $C$  has dimension  $g$ , it must be

Figure 3.1: The tree in Example 3.3.12(1), and the abstract tropical curve.

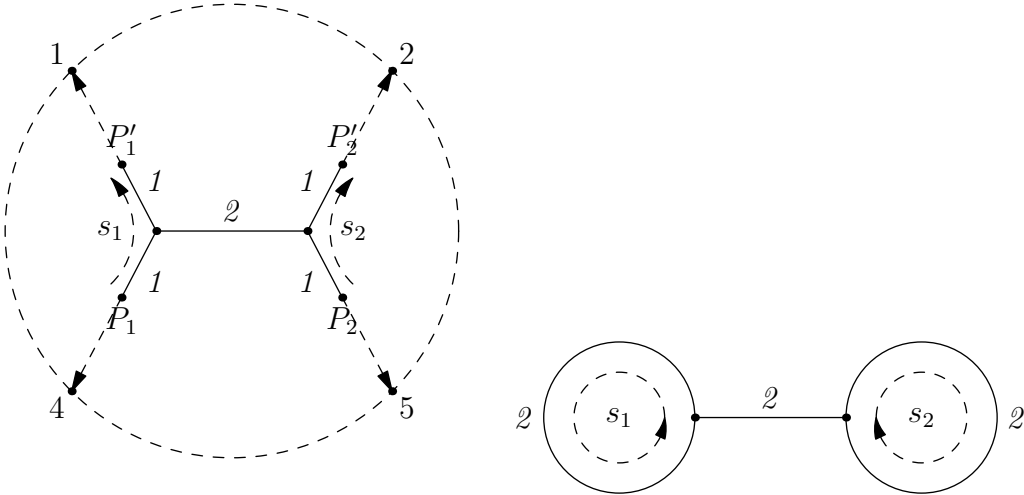


Figure 3.2: The tree in Example 3.3.12(2), and the abstract tropical curve.

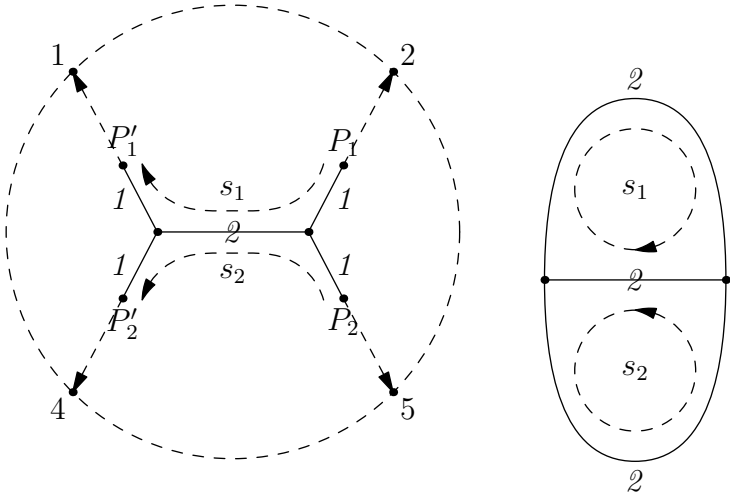
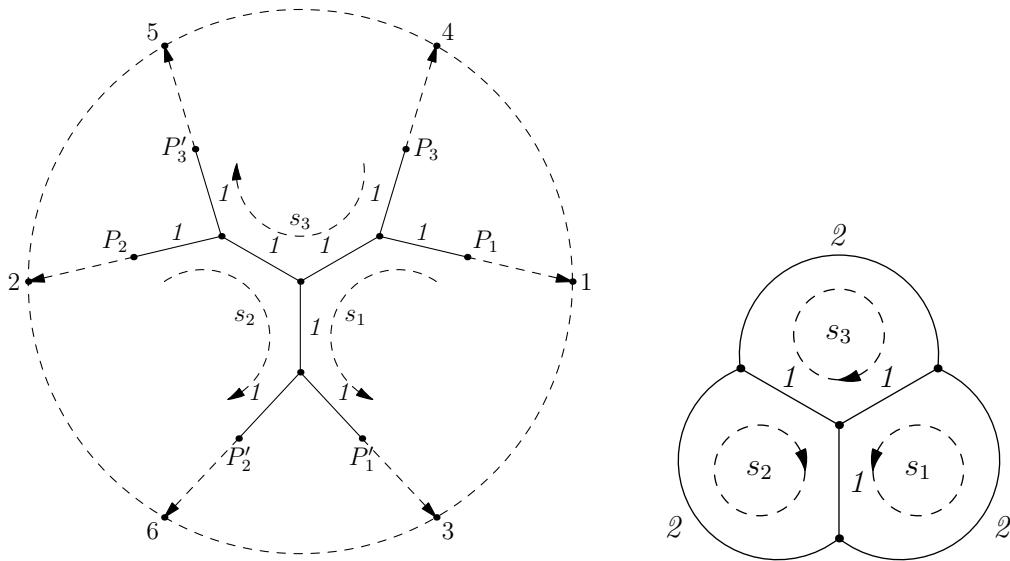


Figure 3.3: The tree in Example 3.3.12(3), and the abstract tropical curve.



generated by these  $g$  differentials. Therefore, the canonical embedding has the following form:

$$C \rightarrow \mathbb{P}^{g-1},$$

$$z \mapsto \left( \frac{u'_{\gamma_1}(z)}{u_{\gamma_1}(z)} : \dots : \frac{u'_{\gamma_g}(z)}{u_{\gamma_g}(z)} \right).$$

It therefore suffices to approximate the derivative  $u'_\alpha(z)$ . A naïve approach is to consider the approximation

$$u'_\alpha(z) \approx \frac{u_\alpha(z+h) - u_\alpha(z)}{h}.$$

We can do better by taking advantage of the product form of  $u_\alpha(z)$ :

$$\begin{aligned} u'_\alpha(z) &= \frac{d}{dz} \prod_{\gamma \in \Gamma} \frac{z - \gamma a}{z - \gamma \alpha a} \\ &= \sum_{\gamma \in \Gamma} \left( \frac{d}{dz} \left( \frac{z - \gamma a}{z - \gamma \alpha a} \right) \prod_{\gamma' \in \Gamma, \gamma' \neq \gamma} \frac{z - \gamma' a}{z - \gamma' \alpha a} \right) \\ &= u_\alpha(z) \sum_{\gamma \in \Gamma} \frac{d}{dz} \left( \frac{z - \gamma a}{z - \gamma \alpha a} \right) \left( \frac{z - \gamma a}{z - \gamma \alpha a} \right)^{-1} \\ &= u_\alpha(z) \sum_{\gamma \in \Gamma} \frac{\gamma a - \gamma \alpha a}{(z - \gamma a)(z - \gamma \alpha a)}. \end{aligned}$$



**Algorithm 3.3.13** (Canonical Embedding).

**Input:** Matrices  $\gamma_1, \dots, \gamma_g \in \mathbb{Q}_p^{2 \times 2}$  generating a Schottky group  $\Gamma$  in good position, an element  $z \in K$ , and an integer  $n$  to determine precision.

**Output:** An approximation for the image of  $z$  under *the* canonical embedding  $\Omega/\Gamma \rightarrow \mathbb{P}^{g-1}$  determined by the choice of generators.

- 1: Based on  $n$ , choose a suitable positive integer  $m$  as described in Remark 3.3.15.
- 2: **for**  $i = 1$  to  $g$  **do**
- 3:     Choose a suitable element  $a \in K$  as described in Proposition 3.3.14.
- 4:     Compute

$$w_i = \sum_{\gamma \in \Gamma_m} \frac{\gamma a - \gamma \gamma_i a}{(z - \gamma a)(z - \gamma \gamma_i a)}.$$

5: **end for**

6: **return**  $(w_1 : \dots : w_g)$ .

With appropriate choice of  $a$ , we can provide a lower bound on the precision of the result in terms of  $m$ . Fortunately, we can choose different values of  $a$  to approximate

$$\sum_{\gamma \in \Gamma} \frac{\gamma a - \gamma \gamma_i a}{(z - \gamma a)(z - \gamma \gamma_i a)}$$

for different  $\gamma_i$ . As in Proposition 3.3.5, we choose  $a \in B_i^+ \setminus B_i'$  to ensure that both  $a$  and  $\gamma_i a$  are in  $F$ .

**Proposition 3.3.14.** *If we choose  $a \in B_i^+ \setminus B_i'$  in Algorithm 3.3.13, and assuming  $z \in F$ , then*

$$\left| \sum_{\gamma \in \Gamma_m} \frac{\gamma a - \gamma \gamma_i a}{(z - \gamma a)(z - \gamma \gamma_i a)} - \frac{u'_{\gamma_i}(z)}{u_{\gamma_i}(z)} \right| \leq p^{-mc - \log_p(d)},$$

where  $c$  is the minimum pairwise distance between  $P_1, \dots, P_g, P'_1, \dots, P'_g$ , and  $d$  is the minimum diameter of  $B_1, \dots, B_g, B'_1, \dots, B'_g$ .

*Proof.* Let  $\gamma \in \Gamma$  have reduced word  $\gamma = h_1 h_2 \dots h_k$ . We have seen in the proof of Proposition 3.3.5 that  $|\gamma a - \gamma \gamma_i a| \leq p^{-(k-1)c} \text{diam}(B^+)$ ,  $|z - \gamma a| \geq \text{diam}(B^+)$  and  $|z - \gamma \gamma_i a| \geq \text{diam}(B^+)$ , where  $B$  is one of  $B_1, \dots, B_g, B'_1, \dots, B'_g$ . Thus,

$$\begin{aligned} \left| \frac{\gamma a - \gamma \gamma_i a}{(z - \gamma a)(z - \gamma \gamma_i a)} \right| &\leq \frac{p^{-(k-1)c} \text{diam}(B^+)}{\text{diam}(B^+)^2} \\ &\leq p^{-(k-1)c} d^{-1} \\ &= p^{-(k-1)c - \log_p(d)}. \end{aligned}$$

Since the difference between our approximation and the true value is the sum over terms where  $\gamma$  has reduced words of length  $\geq m + 1$ , we conclude that the error has absolute value at most  $p^{-mc - \log_p(d)}$ .  $\square$

In the last proposition, we assumed  $z \in F$ . If  $z \notin F$ , we can do an extra step and replace  $z$  by some  $\gamma z$  such that  $\gamma z \in F$ , with the help of Subroutine 3.2.6. This step does not change the end result because the theta functions are invariant under the action of  $\Gamma$ .

**Remark 3.3.15.** If we wish to use Algorithm 3.3.13 to compute a period matrix  $Q$  with accuracy up to the  $n^{\text{th}}$   $p$ -adic digit, we must first compute  $c$  and  $d$ . Recall that  $c$  is defined to be the minimum distance between pairs of the points  $P_1, \dots, P_g, P'_1, \dots, P'_g \in (\mathbb{P}^1)^{an}$  corresponding to the balls  $B_1^+, \dots, B_g^+, B_1'^+, \dots, B_g'^+$  that characterize our good fundamental domain, and  $d$  is the minimum diameter of  $B_1, \dots, B_g, B_1', \dots, B_g'$ . Once we have computed  $c$  and  $d$ , then by Proposition 3.3.14 we must choose  $m$  such that  $p^{-mc}d^{-1} \leq p^{-n}$ . We could also think of it as choosing  $m$  such that  $mc + \log_p(d) \geq n$ .

**Remark 3.3.16.** As was the case with Algorithm 3.3.3, we may run Algorithm 3.3.13 even if the input generators are not in good position, and it will approximate images of points in the canonical embedding. However, we will not have control over the rate of convergence, which will in general be very slow.

**Example 3.3.17.** Let  $\Gamma$  be the Schottky group in Example 3.2.3(3). Choose the same good fundamental domain. We will compute the image of the field element 17 under the canonical embedding (we have chosen 17 as it is in  $\Omega$  for this particular  $\Gamma$ ). The minimum diameter is  $d = 1/9$ , and the minimum distance is  $c = 2$ . To get absolute precision to the order of  $p^{-10}$ , we need  $p^{-mc}d^{-1} \leq p^{-10}$ , i.e.  $m \geq 6$ . Applying Algorithm 3.3.13 with  $m = 6$  gives us the following point in  $\mathbb{P}^2$ :

$$((\dots 2100012121)_3 : (\dots 2211022001.1)_3 : (\dots 2221222111.1)_3).$$

This point lies on the canonical embedding of the genus 3 Mumford curve  $\Omega/\Gamma$ . Any genus 3 curve is either a hyperelliptic curve or a smooth plane quartic curve. However, it is impossible for a hyperelliptic curve to have the skeleton in Figure 3.3 (see [27, Theorem 4.15]), so  $\Omega/\Gamma$  must be a smooth plane quartic curve. Its equation has the form

$$C_1x^4 + C_2x^3y + C_3x^3z + C_4x^2y^2 + C_5x^2yz + C_6x^2z^2 \\ C_7xy^3 + C_8xy^2z + C_9xyz^2 + C_{10}xz^3 + C_{11}y^4 + C_{12}y^3z + C_{13}y^2z^2 + C_{14}yz^3 + C_{15}z^4.$$

Using linear algebra over  $\mathbb{Q}_3$ , we can solve for its 15 coefficients by computing 14 points on the curve and plugging them into the equation. The result is

$$C_1 = 1, \quad C_2 = (\dots 11101)_3, \quad C_3 = (\dots 00211)_3, \\ C_4 = (\dots 1020.2)_3, \quad C_5 = (\dots 110.21)_3, \quad C_6 = (\dots 1002.1)_3, \\ C_7 = (\dots 122)_3, \quad C_8 = (\dots 222.02)_3, \quad C_9 = (\dots 222.02)_3, \\ C_{10} = (\dots 21101)_3, \quad C_{11} = (\dots 2122)_3, \quad C_{12} = (\dots 2201)_3, \\ C_{13} = (\dots 0202.2)_3, \quad C_{14} = (\dots 10102)_3, \quad C_{15} = (\dots 01221)_3.$$

For the Newton subdivision and tropicalization of this plane quartic, see the following subsection, in which we consider the interactions of the three algorithms of Section 3.3.

## Reality Check: Interactions Between The Algorithms

We close Section 3.3 by checking that the three algorithms give results consistent with one another and with some mathematical theory. We will use our running example of a genus 3 Mumford curve from Examples 3.3.8(3), 3.3.12(3), and 3.3.17, for which we have computed a period matrix of the Jacobian, the abstract tropical curve, and a canonical embedding.

First we will look at the period matrix and the abstract tropical curve, and verify that these outputs are consistent. Recall that for the period matrix  $Q$  of  $\text{Jac}(\Omega/\Gamma)$ , we have

$$Q_{ij} = \frac{u_{\gamma_i}(z)}{u_{\gamma_i}(\gamma_j z)}.$$

Motivated by this, we define

$$\begin{aligned} Q : \Gamma \times \Gamma &\rightarrow K^* \\ (\alpha, \beta) &\mapsto \frac{u_\alpha(z)}{u_\alpha(\beta z)}, \end{aligned}$$

where our choice of  $z \in \Omega$  does not affect the value of  $Q(\alpha, \beta)$ . (Note that  $Q_{ij} = Q(\gamma_i, \gamma_j)$ .) As shown in [43, VI, 2], the kernel of  $Q$  is the commutator subgroup  $[\Gamma, \Gamma]$  of  $\Gamma$ , and  $Q$  is symmetric and positive definite (meaning  $|Q(\alpha, \alpha)| < 1$  for any  $\alpha \notin \begin{bmatrix} 1 & 0 \\ 0 & 1 \end{bmatrix} \pmod{[\Gamma, \Gamma]}$ ).

Moreover, the following theorem holds (see [93, Theorem 6.4]).

**Theorem 3.3.18.** *Let  $G$  be the abstract tropical curve of  $\Omega/\Gamma$ , and let  $\pi_1(G)$  be its homotopy group, treating  $G$  as a topological space. There is a canonical isomorphism  $\phi: \Gamma \rightarrow \pi_1(G)$  such that  $\text{val}(Q(\gamma, \gamma')) = \langle \phi^{ab}(\gamma), \phi^{ab}(\gamma') \rangle$ , where  $\langle p_1, p_2 \rangle$  denotes the shared edge length of the oriented paths  $p_1$  and  $p_2$ .*

The map  $\phi$  is made very intuitive by considering the construction of  $G$  in Algorithm 3.3.9: a generator  $\gamma_i$  of  $\Gamma$  yields two points  $P_i, P'_i \in (\mathbb{P}^1)^{an}$  (corresponding to balls containing the eigenvalues of  $\gamma_i$ ), and these points are glued together in constructing  $G$ . So  $\gamma_i$  corresponds to a loop around the cycle resulting from this gluing; after abelianization, this intuition is made rigorous.

Consider the matrix  $Q$  computed in Example 3.3.8(3). Worrying only about valuations, we have

$$\text{val}(Q) = \begin{bmatrix} 4 & 1 & 1 \\ 1 & 4 & -1 \\ 1 & -1 & 4 \end{bmatrix}.$$

For  $i = 1, 2, 3$ , let  $s_i$  be the oriented loop in  $G$  arising from gluing  $P_i$  and  $P'_i$ . In light of Theorem 3.3.18, we expect to find shared edge lengths

$$\langle s_1, s_1 \rangle = \langle s_2, s_2 \rangle = \langle s_3, s_3 \rangle = 4,$$

$$\langle s_1, s_2 \rangle = \langle s_1, s_3 \rangle = 1,$$

and

$$\langle s_2, s_3 \rangle = -1.$$

That is, each cycle length should be 4, and the common edge of each distinct pair of cycles should have length 1, with the orientation of  $s_1$  agreeing with the orientation of  $s_2$  (respectively,  $s_3$ ) on the shared edge and the orientation of  $s_2$  disagreeing with the orientation of  $s_3$  on the shared edge. This is indeed what we found in Example 3.3.12(3), with edge lengths and orientations shown in Figure 3.3. This example has shown how the outputs of Algorithms 3.3.3 and 3.3.9 can be checked against one another.

We will now consider the relationship between the abstract tropical curve and the canonical embedding for this example. In particular, we will compute a tropicalization of the curve from the canonical embedding and see how this relates to the abstract tropical curve.

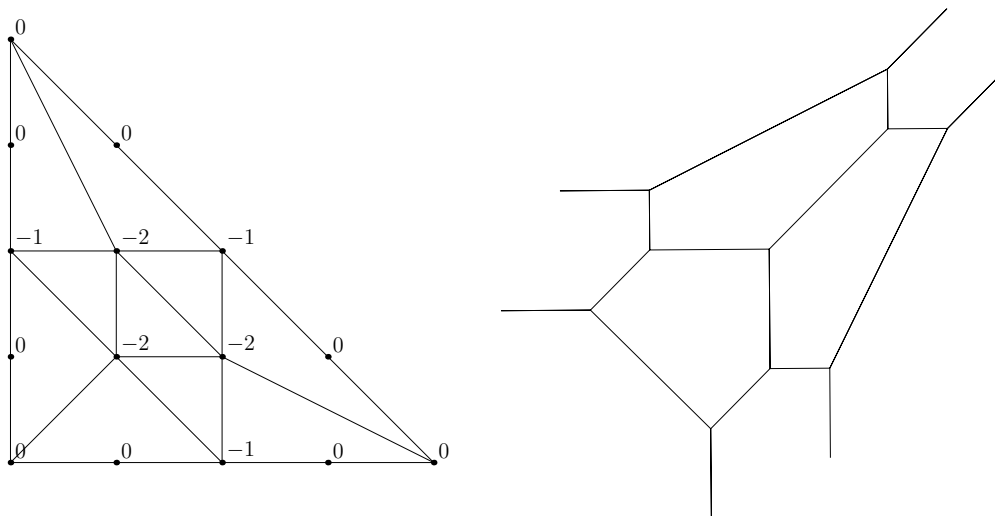
To compute the tropicalization of the curve, we will start with the quartic planar equation computed in Example 3.3.17. The *Newton polytope* of this quartic is a triangle with side length 4. We label each integral point inside or on the boundary of the Newton polytope by the valuation of the coefficient of the corresponding term, ignoring the variable  $z$ . For example, the point  $(1, 2)$  is labeled  $-2$  because the valuation of the coefficient of  $xy^2z$  is  $\text{val}(C_8) = -2$ . We then take the *lower convex hull*, giving a subdivision of the Newton polytope as shown in Figure 3.4. The tropicalization of the curve is combinatorially the dual graph of this subdivision, and using the max convention of tropical geometry it sits in  $\mathbb{R}^2$  as shown in Figure 3.4, with the common point of the three cycles at  $(0, 0)$ .

Let us compare the cycles in the tropicalization with the cycles in the abstract tropical curve. We know from [9, §6.23] that this tropicalization is faithful since all vertices are trivalent and are adjacent to at least one edge of weight one. This means that lattice lengths on the tropicalization should agree with lengths of the abstract tropical curve. Each cycle in the tropicalization has five edges, and for each cycle two edges are length  $\frac{1}{2}$  and three are length 1. This gives a length of 4, as we'd expect based on Example 3.3.12(3). Moreover, each shared edge has lattice length 1, as was the case in the abstract tropical curve. Thus we have checked the outputs of Algorithms 3.3.9 and 3.3.13 against one another.

### 3.4 From Generators in Bad Position to Generators in Good Position

The previous section describes several algorithms that compute various objects from a set of free generators of a Schottky group, assuming that the generators are in good position, and (in Algorithm 3.3.9) that a good fundamental domain is given together with the generators. This content of this section is what allows us to make this assumption. We give an algorithm (Algorithm 3.4.8) that takes an arbitrary set of free generators of a Schottky group and outputs a set of free generators that are in good position, together with a good fundamental domain. This algorithm can be modified as described in Remark 3.4.10 to perform a

Figure 3.4: The Newton polytope of the plane quartic curve in Example 3.3.17, and the corresponding tropical curve in  $\mathbb{R}^2$  (drawn using the max convention). Each edge of infinite length has weight 2, and all other edges have weight 1.



“Schottky test”; in particular, given a set of  $g$  invertible matrices generating a group  $\Gamma$ , the modified algorithm will either

- return a set of  $g$  free generators of  $\Gamma$  in good position together with a good fundamental domain, which is a certificate that  $\Gamma$  is Schottky;
- return a relation satisfied by the input matrices, which is a certificate that the generators do not freely generate the group; or
- return a non-hyperbolic, non-identity matrix  $\gamma \in \Gamma$ , which is a certificate that  $\Gamma$  is not Schottky.

Before presenting Algorithm 3.4.8, we will first develop some theory for trees, and then define useful subroutines. Our starting point is a remark in Gerritzen and van der Put’s book:

**Proposition 3.4.1.** [43, III 2.12.3] *Let  $\Gamma$  be Schottky and  $\Sigma$  and  $\Omega$  be as usual. Let  $T(\Sigma)$  be the subtree of  $(\mathbb{P}^1)^{an}$  spanned by  $\Sigma$ . Then the minimal skeleton of  $\Omega/\Gamma$  is isomorphic to  $T(\Sigma)/\Gamma$ .*

This statement is essential for our algorithm, because it helps reducing problems involving  $(\mathbb{P}^1)^{an}$  to problems involving the much simpler tree  $T(\Sigma)$ . Though  $T(\Sigma)$  is not finite, it is a finitely branching tree: it consists of vertices and edges such that each vertex is connected with finitely many edges. A good fundamental domain in  $(\mathbb{P}^1)^{an}$  can be obtained from a good fundamental domain in  $T(\Sigma)$ , defined as follows:

**Definition 3.4.2.** A *principal subtree*  $T$  of  $T(\Sigma)$  is a connected component of  $T(\Sigma) \setminus \{e\}$  for some edge  $e$  of  $T(\Sigma)$ . An *extended principal subtree* is  $T^+ = T \cup \{e\}$ .

**Definition 3.4.3.** A *good fundamental domain*  $S$  in  $T(\Sigma)$  for a set of free generators  $\gamma_1, \dots, \gamma_g$  of  $\Gamma$  is the complement of  $2g$  principal subtrees  $T_1, \dots, T_g, T'_1, \dots, T'_g$ , such that  $T_1^+, \dots, T_g^+, T_1'^+, \dots, T_g'^+$  are disjoint, and that  $\gamma_i(T(\Sigma) \setminus T_i^+) = T_i$  and  $\gamma_i^{-1}(T(\Sigma) \setminus T_i^+) = T_i'$ . The *interior* of  $S$  is  $S^\circ = T(\Sigma) \setminus (T_1^+ \cup \dots \cup T_g^+ \cup T_1'^+ \cup \dots \cup T_g'^+)$ . The *boundary* of  $S$  is  $S \setminus S^\circ$ .

In other words,  $S$  is a connected finite subtree of  $T(\Sigma)$  with  $2g$  boundary edges  $(R_i, Q_i)$  and  $(R'_i, Q'_i)$ , where  $Q_i, Q'_i \notin S$ , such that  $\gamma_i(R'_i, Q'_i) = (Q_i, R_i)$ . Given this data, the principal subtree  $T_i$  (resp.  $T'_i$ ) is the connected component of  $T(\Sigma) \setminus (R_i, Q_i)$  (resp.  $T(\Sigma) \setminus (R'_i, Q'_i)$ ) that is disjoint from  $S$ . Given a good fundamental domain  $S$  in  $T(\Sigma)$ , one can find a good fundamental domain in  $(\mathbb{P}^1)^{an}$  as follows. Without loss of generality, we may assume that the retraction of  $\infty$  to  $T(\Sigma)$  is in the interior of  $S$ . Then,  $Q_i$  and  $R_i$  correspond to two nested balls  $B(a_i, r_i)^+ \subset B(a_i, R_i)^+$ . Define  $B_i = B(a_i, \sqrt{r_i R_i})$ . Define  $B'_i$  similarly.

**Proposition 3.4.4.** *Let  $B_i, B'_i$  be as above. Then  $F = (\mathbb{P}^1)^{an} \setminus (B_1 \cup \dots \cup B_g \cup B'_1 \cup \dots \cup B'_g)$  is a good fundamental domain.*

*Proof.* Let  $Q_i, R_i$  be as above. Let  $P_i$  be the midpoint of the segment of the boundary edge  $(Q_i, R_i)$ . Then,  $P_i$  corresponds to the ball  $B_i^+$ . Let  $\pi$  denote the retraction from  $(\mathbb{P}^1)^{an}$  to  $T(\Sigma)$ . Again, we may assume  $\pi(\infty)$  is in the interior of  $S$ . For any  $P \in B_i^+$ , the unique path from  $P$  to  $\infty$  passes through  $P_i$ . Therefore,  $\pi(P)$  lies on the union of  $T_i$  with the segment  $(P_i, Q_i)$ , which is a subset of  $T_i^+$ . Hence, the condition that  $T_i^+$  and  $T_i'^+$  are disjoint implies that the retraction of the  $B_i^+$  and the  $B_i'^+$  are disjoint. Thus, the  $B_i^+$  and  $B_i'^+$  are disjoint.

Let  $(Q'_i, R'_i)$  be the boundary edge of  $T'_i$ , and let  $P'_i$  be its midpoint. Since  $\gamma_i(Q'_i, R'_i) = (R_i, Q_i)$ , it sends the midpoint  $P'_i$  to  $P_i$ . Since  $B'_i$  is a connected component in  $(\mathbb{P}^1)^{an} \setminus \{P'_i\}$ , the element  $\gamma_i$  must send  $B'_i$  to a connected component of  $(\mathbb{P}^1)^{an} \setminus \{P_i\}$ . One of the connected components in  $(\mathbb{P}^1)^{an} \setminus \{P_i\}$  is  $(\mathbb{P}^1)^{an} \setminus B_i^+$ . Since  $\gamma_i$  sends  $Q'_i \in B'_i$  to  $R_i \in (\mathbb{P}^1)^{an} \setminus B_i^+$ , it must send  $B'_i$  to  $(\mathbb{P}^1)^{an} \setminus B_i^+$ . Similarly,  $\gamma_i^{-1}$  sends  $B_i$  to  $(\mathbb{P}^1)^{an} \setminus B_i'^+$ . Thus  $F$  is a good fundamental domain in  $(\mathbb{P}^1)^{an}$ .  $\square$

One can establish properties of  $S$  similar to Theorem 3.2.5. They can be derived either combinatorially or from Proposition 3.4.4.

The following algorithm constructs a good fundamental domain  $S$  in  $T(\Sigma)$ .

**Subroutine 3.4.5** (Good Fundamental Domain Construction).

**Input:** An “agent” knowing all vertices and edges of  $T = T(\Sigma)$ , and the map  $T(\Sigma) \rightarrow T(\Sigma)/\Gamma$ , where  $\Gamma$  is defined over  $\mathbb{Q}_p$ .

**Output:** A good fundamental domain  $S$  in  $T(\Sigma)$ .

- 1: Choose a vertex  $P$  of  $T$ . Let  $P_1, \dots, P_k$  be all neighbors of  $P$  in  $T$ .
- 2: Let  $V \leftarrow \{P\}$ ,  $E \leftarrow \emptyset$ ,  $O \leftarrow \{(P, P_1), \dots, (P, P_k)\}$ ,  $I \leftarrow \emptyset$ ,  $A \leftarrow \emptyset$ .
- 3: **while**  $O \neq \emptyset$  **do**

- 4: Choose  $(Q, Q') \in O$ , remove it from  $O$  and add it to  $E$ .
- 5: Let  $Q, Q_1, \dots, Q_k$  be all neighbors of  $Q'$  in  $T$ .
- 6: Add  $Q'$  to  $V$ .
- 7: **for** each  $Q_k$  **do**
- 8:     With the help of the “agent” in the input, determine if  $(Q_k, Q')$  is conjugate to some edge  $(R, R') \in O$ , i.e.  $\gamma Q_k = R$  and  $\gamma Q' = R'$  for some  $\gamma \in \Gamma$ .
- 9:     **if so then**
- 10:         Remove  $(R, R')$  from  $O$ .
- 11:         Add  $(Q', Q_k), (R, R')$  to  $I$ .
- 12:         Add  $\gamma$  to  $A$ .
- 13:     **else**
- 14:         Add  $(Q_k, Q')$  to  $O$ .
- 15:     **end if**
- 16: **end for**
- 17: **end while**
- 18: **return**  $S = V \cup E \cup I$ . (The edges in  $I$  are the boundary edges, and  $A$  is a set of free generators of  $\Gamma$  in good position.)

*Proof.* Consider the map from  $T(\Sigma)$  to  $G = T(\Sigma)/\Gamma$ . Let  $P$  be as in Step 1. Suppose that a “fire” starts at  $P \in T(\Sigma)$  and the image of  $P$  in  $G$ . In each step, when we choose the edge  $(Q, Q')$  in Step 4 and add a vertex  $Q'$  to  $V$  in Step 5, we “propagate” the fire from  $Q$  to  $Q'$ , and “burn”  $Q'$  together with halves of all edges connecting to  $Q'$ . Also, we “burn” the corresponding part in  $G$ . Suppose two fires meet each other in  $G$ . In this case, both halves of an edge in  $G$  are burned, but it corresponds to two half burned edges in  $T(\Sigma)$ . If so, we stop the fire by removing the edges from  $O$  and adding them to  $I$  (Step 9). The algorithm terminates when the whole graph  $G$  is burned. The burned part  $S'$  of  $T(\Sigma)$  is a lifting of  $G$ . Then,  $V$  is the set of vertices of  $S'$ ,  $E$  is the set of whole edges in  $S'$ , and  $I$  is the set of half edges in  $S'$ . The fact that they form a good fundamental domain follows from the method in the proof of [43, I (4.3)].  $\square$

This algorithm requires an “agent” knowing everything about  $T(\Sigma)$ . It is hard to construct such an “agent” because  $T(\Sigma)$  is infinite. Therefore, we approximate  $T(\Sigma)$  by a finite subtree. One candidate is  $T(\Sigma_m)$ , where  $\Sigma_m$  is the set of fixed points of elements of  $\Gamma_m$ . Recall that  $\Gamma_m$  is the set of elements of  $\Gamma$  whose reduced words in terms of the given generators have lengths at most  $m$ . We take one step further: we approximate  $T(\Sigma)$  by  $T(\Gamma_m a)$ , where  $a$  is any point in  $\Sigma$ .

**Lemma 3.4.6.** *For any  $a \in K$ , we have  $T(\Gamma a) \supset T(\Sigma)$ . Furthermore, if  $a \in \Sigma$ , then  $T(\Gamma a) = T(\Sigma)$ .*

*Proof.* For any  $g \in \Gamma$ , the fixed point corresponding to the eigenvalue with larger absolute value is the limit of the sequence  $a, ga, g^2a, \dots$ . The other fixed point is the limit of the sequence  $a, g^{-1}a, g^{-2}a, \dots$ . Therefore, every point in  $\Sigma$  is either in  $\Gamma a$  or a limit point of  $\Gamma a$ . Therefore,  $T(\Gamma a) \supset T(\Sigma)$ . The second statement is clear.  $\square$

We can construct a complete list of vertices and edges in  $T(\Gamma_m a)$ . Then, the map from  $T(\Gamma_m a)$  to  $T(\Sigma)/\Gamma$  can be approximated in the following way: for each pair of vertices  $P, Q$  (resp. edges  $e, f$  in  $T(\Gamma_m a)$ ) and each given generator  $\gamma_i$ , check if  $\gamma_i P = Q$  (resp.  $\gamma_i e = f$ ). If so, then we identify them. Note that this method may not give the correct map, because two vertices  $P$  and  $Q$  in  $T(\Gamma_m a)$  may be conjugate via the action of some  $h_1 h_2 \cdots h_k \in \Gamma$ , where some intermediate step  $h_l h_{l+1} \cdots h_k P \notin T(\Gamma_m a)$ . Due to this flaw, we need a way to certify the correctness of the output.

**Subroutine 3.4.7** (Good Fundamental Domain Certification).

**Input:** Generators  $\gamma_1, \dots, \gamma_g \in \mathbb{Q}_p^{2 \times 2}$  of a Schottky group  $\Gamma$ , and a quadruple  $(V, E, I, A)$ , where  $V$  is a set of vertices in  $T(\Sigma)$ ,  $E$  and  $I$  are sets of edges of  $T(\Sigma)$ ,  $I$  contains  $k$  pairs of edges  $(P_i, Q_i), (P'_i, Q'_i)$ , where  $P_i, P'_i \in V$ ,  $Q_i, Q'_i \notin V$ , and  $A$  contains  $k$  elements  $a_i$  in  $\Gamma$ .

**Output:** TRUE if  $S = V \cup E \cup I$  is a good fundamental domain in  $T(\Sigma)$  for the set of generators  $A$ , and  $I$  is the set of boundary edges. FALSE otherwise.

- 1: If  $k \neq g$ , **return** FALSE.
- 2: If  $S$  is not connected, **return** FALSE.
- 3: If any element of  $I$  is not a terminal edge of  $S$ , **return** FALSE.
- 4: If any  $(P_i, Q_i) \neq a_i(Q'_i, P'_i)$ , **return** FALSE.
- 5: Choose  $P$  in the interior of  $S$ .
- 6: **for**  $h \in \{\gamma_1, \dots, \gamma_g, \gamma_1^{-1}, \dots, \gamma_g^{-1}\}$  **do**
- 7:     Using a variant of Subroutine 3.2.6, find point  $P' \in S$  and group element  $\gamma \in \langle a_1, \dots, a_k \rangle$  such that  $P' = \gamma(hP)$ .
- 8:     If  $P \neq P'$ , **return** FALSE.
- 9: **end for**
- 10: **return** TRUE.

*Proof.* Steps 1–4 verify that  $S$  satisfies the definition of a good fundamental domain in  $T(\Sigma)$  for the set of generators  $a_1, \dots, a_g$ . In addition, we need to verify that  $a_1, \dots, a_g$  generate the same group as the given generators  $\gamma_1, \dots, \gamma_g$ . This is done by Steps 5–9. If  $P = P'$  in Step 8, then there exists  $\gamma \in \langle a_1, \dots, a_k \rangle$  such that  $\gamma h P = P$ . We are assuming  $a_i \in \Gamma$  in the input, so  $\gamma h \in \Gamma$ . Since the action of  $\Gamma$  on  $(\mathbb{P}^1)^{an} \setminus \Sigma$  is free, we have  $\gamma h = \text{id}$ . Thus,  $h \in \langle a_1, \dots, a_k \rangle$ . If  $P = P'$  for all  $h$ , then  $\Gamma = \langle a_1, \dots, a_k \rangle$ .

Otherwise, if  $P \neq P'$  in Step 8 for some  $h$ , then there exists  $\gamma' \in \Gamma$  such that  $\gamma' P = P'$ . For any  $\gamma \in \langle a_1, \dots, a_k \rangle$  other than identity, we have  $\gamma P' \notin s^\circ$  by a variant of Lemma 3.2.4. Therefore,  $\Gamma \neq \langle a_1, \dots, a_k \rangle$ .  $\square$

If the certification fails, we choose a larger  $m$  and try again, until it succeeds. We are ready to state our main algorithm for this section:

**Algorithm 3.4.8** (Turning Arbitrary Generators into Good Generators).

**Input:** Free generators  $\gamma_1, \dots, \gamma_g \in \mathbb{Q}_p^{2 \times 2}$  of a Schottky group  $\Gamma$ .



**Output:** Free generators  $a_1, \dots, a_g$  of  $\Gamma$ , together with a good fundamental domain  $F = (\mathbb{P}^1)^{an} \setminus (B_1 \cup \dots \cup B_g \cup B'_1 \cup \dots \cup B'_g)$  for this set of generators.

- 1: Let  $m = 1$ .
- 2: Let  $a$  be a fixed point of some  $\gamma_i$ .
- 3: Compute all elements in  $\Gamma_m a$ .
- 4: Find all vertices and edges of  $T(\Gamma_m a)$ .
- 5: Approximate the map  $T(\Gamma_m a) \rightarrow T(\Sigma)/\Gamma$ .
- 6: Use Subroutine 3.4.5 to construct a subgraph  $S = V \cup E \cup I$  of  $T(\Gamma_m a)$  and a subset  $A \subset \Gamma$ .
- 7: Use Subroutine 3.4.7 to determine if  $S = V \cup E \cup I$  is a good fundamental domain in  $T(\Sigma)$ .
- 8: If not, increment  $m$  and go back to Step 2.
- 9: Compute  $B_i$  and  $B'_i$  from  $S$  using the method in Proposition 3.4.4.
- 10: **return** generators  $A$  and good fundamental domain  $F = (\mathbb{P}^1)^{an} \setminus (B_1 \cup \dots \cup B_g \cup B'_1 \cup \dots \cup B'_g)$ .

*Proof.* The correctness of the algorithm follows from the proof of Subroutine 3.4.7. It suffices to prove that the algorithm eventually terminates. Assume that we have the “agent” in Subroutine 3.4.5. Since Subroutine 3.4.5 terminates in a finite number of steps, the computation involves only finitely many vertices and edges in  $T(\Sigma)$ . If  $m$  is sufficiently large,  $T(\Sigma_m)$  will contain all vertices and edges involved in the computation. Moreover, for any pair of vertices or edges in  $T(\Sigma_m)$  that are identified in  $T(\Sigma)/\Gamma$ , there exists a sequence of actions by the given generators of  $\Gamma$  that sends one of them to the other, so there are finitely many intermediate steps. If we make  $m$  even larger so that  $T(\Sigma_m)$  contains all these intermediate steps, we get the correct approximation of the map  $T(\Sigma) \rightarrow T(\Sigma)/\Gamma$ . This data is indistinguishable from the “agent” in the computation of Subroutine 3.4.5. Thus, it will output the correct good fundamental domain.  $\square$

**Remark 3.4.9.** The performance of the algorithm depends on how “far” the given generator is from a set of generators in good position, measured by the lengths of the reduced words of the good generators in terms of the given generators. If the given generators is close to a set of generators in good position, then a relatively small  $m$  is sufficient for  $T(\Gamma_m a)$  to contain all relevant vertices. Otherwise, a larger  $m$  is needed. For example, in the genus 2 case, this algorithm terminates in a few minutes for our test cases where each given generator has a reduced word of length  $\leq 4$  in a set of good generators. However, the algorithm is not efficient on Example 3.3.8 (4), where one of the given generators has a reduced word of length 101. One possible way of speeding up the algorithm is to run the non-Euclidean Euclidean algorithm developed by Gilman [44] on the given generators.

**Remark 3.4.10.** We may relax the requirement that the input matrices freely generate a Schottky group by checking that every element in  $\Gamma_m$  not coming from the empty word is hyperbolic before Step 3. If the group is Schottky and freely generated by the input matrices, the algorithm will terminate with a good fundamental domain. Otherwise, Step 7 will never

certify a correct good fundamental domain, but the hyperbolic test will eventually fail when a non-hyperbolic matrix is generated. In particular, if the identity matrix is generated by a nonempty word, the generators are not free (though they may or may not generate a Schottky group); and if a non-identity hyperbolic matrix is generated, the group is not Schottky. Thus, Algorithm 3.4.8 is turned into a Schottky test algorithm. Again, the non-Euclidean Euclidean algorithm in [44] is a possible ingredient for a more efficient Schottky test algorithm.

### 3.5 Future Directions: Reverse Algorithms and Whittaker Groups

In this section we describe further computational questions about Mumford curves. Algorithms answering these questions would be highly desirable.

#### Reversing The Algorithms in Section 3.3

Many of our main algorithms answer questions of the form “Given  $A$ , find  $B$ ”, which we can reverse to “Given  $B$ , find  $A$ .” For instance:

- Given a period matrix  $Q$ , determine if the abelian variety  $(K^*)^g/Q$  is the Jacobian of a Mumford curve, and if it is approximate the corresponding Schottky group.
- Given an abstract tropical curve  $G$ , find a Schottky group whose Mumford curve has  $G$  as its abstract tropical curve.
- Given a polynomial representation of a curve, determine if it is a Mumford curve, and if it is approximate the corresponding Schottky group.

A particular subclass of Schottky groups called *Whittaker groups* are likely a good starting point for these questions.

#### Whittaker Groups

We will outline the construction of Whittaker groups (see [92] for more details), and discuss possible algorithms for handling computations with them. We are particularly interested in going from a matrix representation to a polynomial representation, and vice versa.

If  $s \in PGL(2, K)$  is an element of order 2, then  $s$  will have two fixed points,  $a$  and  $b$ , and is in fact determined by the pair  $\{a, b\}$  as

$$s = \begin{bmatrix} a & b \\ 1 & 1 \end{bmatrix} \begin{bmatrix} 1 & 0 \\ 0 & -1 \end{bmatrix} \begin{bmatrix} a & b \\ 1 & 1 \end{bmatrix}^{-1},$$

as long as  $\infty \neq a, b$ . Let  $s_0, \dots, s_g$  be  $g + 1$  elements of  $PGL(2, K)$  of order 2. Write their fixed points as  $\{a_0, b_0\}, \dots, \{a_g, b_g\}$ , and assume without loss of generality that  $\infty \neq a_i, b_i$  for all  $i$ . Let  $B_0, \dots, B_g$  denote small open balls containing each pair, and assume that the corresponding closed balls  $B_0^+, \dots, B_g^+$  are all disjoint. Then the group  $\Gamma := \langle s_0, \dots, s_g \rangle$  is in fact the free product  $\langle s_0 \rangle * \dots * \langle s_g \rangle$  by [92, Proposition 1].

Note that  $\Gamma$  is *not* a Schottky group, since its generators are not hyperbolic. However, we can still consider its action upon  $\mathbb{P}^1 \setminus \Sigma = \Omega$ . To fix some notation, we will choose  $a, b \in \Omega$  such that  $a \notin \Gamma b$  and  $\infty \notin \Gamma a \cup \Gamma b$  and will define

$$G(z) := \Theta(a, b; z) = \prod_{\gamma \in \Gamma} \frac{z - \gamma(a)}{z - \gamma(b)}.$$

(In our previous definition of theta functions, we took  $\Gamma$  to be Schottky, but the definition works fine for this  $\Gamma$  as well.) If we choose  $a$  and  $b$  such that  $|G(\infty) - G(s_0\infty)| < 1/2$ , then  $G$  will be invariant under  $\Gamma$ , which gives a morphism  $\Omega/\Gamma \rightarrow \mathbb{P}^1$ . This will have only one pole, so it is an isomorphism.

Now, let  $W$  be the kernel of the map  $\varphi : \Gamma \rightarrow \mathbb{Z}/2\mathbb{Z}$  defined by  $\varphi(s_i) = 1$  for all  $i$ . Then  $W = \langle s_0s_1, s_0s_2, \dots, s_0s_g \rangle$ , and is in fact free on those generators. One can show that  $W$  is a Schottky group of rank  $g$ , and we call a group that arises in this way a *Whittaker group*. We already know that  $\Omega/W$  is a curve of genus  $g$ ; in fact, we have more than that.

**Theorem 3.5.1** (Van der Put, [92]). *If  $W$  is a Whittaker group, then  $\Omega/W$  is a totally split hyperelliptic curve of genus  $g$ , with affine equation  $y^2 = \prod_{i=0}^g (x - G(a_i))(x - G(b_i))$ . Conversely, if  $X$  be a totally split hyperelliptic curve of genus  $g$  over  $K$ , then there exists a Whittaker group  $W$  such that  $X \cong \Omega/W$ , and this  $W$  is unique up to conjugation in  $PGL(2, K)$ .*

**Remark 3.5.2.** There is a natural map  $\Omega/W \rightarrow \Omega/\Gamma \cong \mathbb{P}^1$ . This is the expected morphism of degree 2 from the hyperelliptic curve to projective space, ramified at  $2g + 2$  points.

If we are content with an algorithm taking  $s_0, s_1, \dots, s_g$  as the input representing a Whittaker group  $W$  (so that  $W = \langle s_0s_1, \dots, s_0s_g \rangle$ ), the above theorem tells us how to compute the ramification points of the hyperelliptic Mumford curve  $\Omega/W$ .

**Example 3.5.3.** Let us construct an example of a Whittaker group of genus 2 with  $K = \mathbb{Q}_3$ . We need to come up with matrices  $s_0, s_1, s_2$  of order 2 with fixed points sitting inside open balls whose corresponding closed balls are disjoint. We will choose them so that the fixed points of  $s_0$  are 0 and 9; of  $s_1$  are 1 and 10; and of  $s_2$  are 2 and 11. (The smallest *open* balls containing each pair of points has radius  $\frac{1}{3}$ , and the corresponding *closed* balls of radius  $\frac{1}{3}$  are disjoint.) The eigenvalues will be 1 and  $-1$ , and the eigenvectors are the fixed points (written projectively), so we can take

$$s_0 = \begin{bmatrix} 0 & 9 \\ 1 & 1 \end{bmatrix}^{-1} \begin{bmatrix} 1 & 0 \\ 0 & -1 \end{bmatrix} \begin{bmatrix} 0 & 9 \\ 1 & 1 \end{bmatrix} = \begin{bmatrix} -1 & 0 \\ -2/9 & 1 \end{bmatrix}$$

$$s_1 = \begin{bmatrix} 1 & 10 \\ 1 & 1 \end{bmatrix}^{-1} \begin{bmatrix} 1 & 0 \\ 0 & -1 \end{bmatrix} \begin{bmatrix} 1 & 10 \\ 1 & 1 \end{bmatrix} = \begin{bmatrix} -11/9 & 20/9 \\ -2/9 & 11/9 \end{bmatrix}$$

$$s_2 = \begin{bmatrix} 2 & 11 \\ 1 & 1 \end{bmatrix}^{-1} \begin{bmatrix} 1 & 0 \\ 0 & -1 \end{bmatrix} \begin{bmatrix} 2 & 11 \\ 1 & 1 \end{bmatrix} = \begin{bmatrix} -13/9 & 44/9 \\ -2/9 & 13/9 \end{bmatrix}.$$

So the group

$$\Gamma = \left\langle \begin{bmatrix} -1 & 0 \\ -2/9 & 1 \end{bmatrix}, \begin{bmatrix} -11/9 & 20/9 \\ -2/9 & 11/9 \end{bmatrix}, \begin{bmatrix} -13/9 & 44/9 \\ -2/9 & 13/9 \end{bmatrix} \right\rangle$$

is generated by those three elements of order 2 (and is in fact the free product of the groups  $\langle s_0 \rangle$ ,  $\langle s_1 \rangle$ , and  $\langle s_2 \rangle$ ), and its subgroup

$$W = \langle s_0 s_1, s_0 s_2 \rangle = \left\langle \begin{bmatrix} 59/81 & 20/9 \\ -4/81 & 11/9 \end{bmatrix}, \begin{bmatrix} 29/81 & 44/9 \\ -8/81 & 13/9 \end{bmatrix} \right\rangle$$

is a Whittaker group of rank 2.

The quotient  $\Omega/W$  is a hyperelliptic curve of genus 2, with six points of ramification  $G(0), G(1), \dots, G(5)$ , where  $G$  is the theta function for  $\Gamma$  with suitably chosen  $a$  and  $b$ .

**Question 3.5.4.** As long as we know the 2-torsion matrices  $s_0, s_1, \dots, s_g$  that go into making a Whittaker group, we can find the ramification points of the corresponding hyperelliptic curve. But what if we don't have that data?

- If we are given  $W = \langle \gamma_1, \dots, \gamma_g \rangle$ , can we algorithmically determine whether or not  $W$  is Whittaker?
- If we know  $W = \langle \gamma_1, \dots, \gamma_g \rangle$ , can we algorithmically find  $s_0, s_1, \dots, s_g$  from  $\gamma_1, \dots, \gamma_g$ ?
- If we know  $W$  is Whittaker but cannot find  $s_0, s_1, \dots, s_g$ , is there another way to find the ramification points of  $\Omega/W$ ?

A good first family of examples to consider is Schottky groups generated by two elements. These give rise to genus 2 curves, which are hyperelliptic, so the groups must in fact be Whittaker.

Having discussed going from a Whittaker group to a set of ramification points, we now consider the other direction: going from the ramification points of a totally split hyperelliptic curve and finding the corresponding Whittaker group. This more difficult, though a brute force method was described by Kadziela in [58], and was used to compute several genus 2 examples over  $\mathbb{Q}_5$ . We will outline his approach.

After a projective transformation, we may assume that the set of fixed points of the group  $\Gamma$  is of the form

$$S = \{0, b_0, a_1, b_1, \dots, a_{g-1}, b_{g-1}, 1, \infty\},$$

where

$$0 < |b_0| < |a_1| \leq \dots \leq |b_{g-1}| < 1,$$

and where the generators of  $\Gamma$  are the 2-torsion matrices  $s_i$  with fixed points  $\{a_i, b_i\}$  (taking  $a_0 = 0$ ,  $a_g = 1$ , and  $b_g = \infty$ ). Let us choose parameters for the theta function associated to  $\Gamma$  as 0 and 1, and write

$$G(z) = \Theta(0, 1; z) = \prod_{n=0}^{\infty} L_n(z),$$

where

$$L_n(z) := \prod_{\gamma \in \Gamma, \ell(\gamma)=n} \frac{z - \gamma(0)}{z - \gamma(1)}$$

is the sub product of  $\Theta$  over all matrices in  $\Gamma$  with reduced length exactly  $n$ .

**Theorem 3.5.5** (Kadziela's Main Approximation Theorem, [58]). *Assume  $S$  and  $G$  are as above, and let  $\pi$  denote the uniformizer. Then*

$$G(0) = 0, G(1) = \infty, G(\infty) = 1,$$

and for  $z \in S - \{0, 1, \infty\}$ ,

- $G(z) \equiv 0 \pmod{\pi}$
- $G(z) \equiv \begin{cases} -4b_0 \pmod{\pi^2} & \text{if } z = b_0, \\ -2z \pmod{\pi^2} & \text{if } z \neq b_0 \end{cases}$
- $G(z) \pmod{\pi^t} = \prod_{i=0}^{t-2} L_i(z) \pmod{\pi^t} = \prod_{i=0}^{t-2} L_i(z \pmod{\pi^t})$  for  $t \geq 3$ .

Let  $X$  be a totally split hyperelliptic curve of genus  $g$ , which after projective transformation we may assume has its set of ramification points in the form

$$R = \{0, r_0, \dots, r_{2g-2}, 1, \infty\}$$

where  $0 < |r_0| < |r_1| \leq \dots \leq |r_{2g-2}| < 1$ . We know  $X \cong \Omega/W$  for some Whittaker group  $W$ . To find  $W$  it will suffice to find the fixed points  $S$  of the corresponding group  $\Gamma$ , so given  $R$  we wish to find  $S$ . We know  $S = \Theta^{-1}(R)$ , but  $\Theta$  is defined by  $S$ , and we cannot immediately invert a function we do not yet know. This means we must gradually approximate candidates for both  $S$  and  $\Theta$  that give the desired property that  $\Theta(S) = R$ . To simplify notation, we will sometimes write  $S = \{0, x_0, x_1, \dots, x_{2g-2}, 1, \infty\}$  instead of in terms of  $a_i$ 's and  $b_i$ 's.

The following algorithm follows the description in [58, §6]. Although we have not implemented it, Kadziela used a Magma implementation of it to compute several genus 2 examples over  $\mathbb{Q}_5$ .

**Algorithm 3.5.6** (From Ramification Points to Whittaker Group).

**Input:** Set of ramification points  $R = \{0, r_0, \dots, r_{2g-2}, 1, \infty\} \subset \mathbb{Q}_p \cup \{\infty\}$ , and desired degree of precision  $d \geq 3$

**Output:** The set of fixed points  $S = \{x_0, \dots, x_{2g-2}, 1, \infty\}$  of  $\Gamma$ , approximated  $\pmod{\pi^d}$ , such that  $\Omega/W$  has ramification points  $R$  for the corresponding Whittaker group of  $\Gamma$ .

- 1: Sort  $r_0, \dots, r_{2g-1}$  in increasing absolute value and rename.
- 2: **if**  $|r_0| = |r_1|$  **then**
- 3:     **return** “NOT VALID”
- 4: **end if**
- 5: Define  $x_i = 0$  for  $0 \leq i \leq 2g - 2$ . (Approximation  $\pmod{\pi}$ .)
- 6: Let  $m = \max\{k \mid r_k \equiv 0 \pmod{\pi^2}\}$ .
- 7: Set  $\ell = 0$  and GOOD=FALSE
- 8: **while** GOOD=FALSE **do**
- 9:     Set  $x_0 = -\frac{1}{4}r_i \pmod{\pi^2}$ , and all other  $x_j$ 's to the  $-\frac{1}{2}r_k \pmod{\pi^2}$ .
- 10:     Test if  $i$  is the right choice using Theorem 3.5.5; if it is, set GOOD=TRUE
- 11:     Set  $\ell = \ell + 1$ .
- 12: **end while**
- 13: **for**  $3 \leq t \leq d$  **do**
- 14:     Set DONE=FALSE.
- 15:     **while** DONE=FALSE **do**
- 16:         Choose  $\bar{v} \in (\mathcal{O}_K/\mathfrak{m}\mathcal{O}_K)^{2g-1}$ , set  $\bar{x} = (\bar{x} \pmod{\pi^{t-1}}) + \bar{v}\pi^t$ .
- 17:         Compute  $\prod_{n=0}^{t-2} L_n(x_i)$  for  $0 \leq i \leq 2g - 2$ .
- 18:         **if** this set equals  $\{r_0 \pmod{\pi^t}, \dots, r_{2g-1} \pmod{\pi^t}\}$  **then**
- 19:             Set DONE=TRUE.
- 20:         **else**
- 21:             Set DONE=FALSE.
- 22:         **end if**
- 23:     **end while**
- 24: **end for**
- 25: **return**  $x_0, \dots, x_{2g-1}$ .

This algorithm is in some sense a brute force algorithm, as for each digit's place from  $3^{rd}$  to  $d^{th}$  it might in principal try every element of  $(\mathcal{O}_K/\mathfrak{m}\mathcal{O}_K)^{2g-1}$ , essentially guessing the  $x_i$ 's digit by digit (lines 13 through 24). It is nontrivial that such a brute force method could even work, but this is made possible by Theorem 3.5.5 as it tells us how to check whether a choice of element in  $(\mathcal{O}_K/\mathfrak{m}\mathcal{O}_K)^{2g-1}$  is valid  $\pmod{\pi^m}$ . As with the other algorithms presented in this chapter, future algorithms improving the efficiency would be greatly desirable.

# Chapter 4

## Tropicalization of del Pezzo Surfaces

This chapter is joint work with Kristin Shaw and Bernd Sturmfels. It is submitted with the same title to *Advances in Mathematics*, Special Issue in Honor of Andrei Zelevinsky [76].

### 4.1 Introduction

A smooth cubic surface  $X$  in projective 3-space  $\mathbb{P}^3$  contains 27 lines. These lines are characterized intrinsically as the  $(-1)$ -curves on  $X$ , that is, rational curves of self-intersection  $-1$ . The tropicalization of an embedded surface  $X$  is obtained directly from the cubic polynomial that defines it in  $\mathbb{P}^3$ . The resulting smooth tropical surfaces are dual to unimodular triangulations of the size 3 tetrahedron. These come in many combinatorial types [62, §4.5].

Alternatively, by removing the 27 lines from the cubic surface  $X$ , we obtain a very affine surface  $X^0$ . In this chapter, we study the tropicalization of  $X^0$ , denoted  $\text{trop}(X^0)$ , via the embedding in its intrinsic torus [50]. This is an invariant of the surface  $X$ . The  $(-1)$ -curves on  $X$  now become visible as 27 *boundary trees* on  $\text{trop}(X^0)$ . This distinguishes our approach from Vigeland’s work [95] on the 27 lines on tropical cubics in  $\mathbb{TP}^3$ . It also highlights an important feature of tropical geometry [64]: there are different tropical models of a single classical variety, and the choice of model depends on what structure one wants revealed.

Throughout this chapter we work over a field  $K$  of characteristic zero that has a non-archimedean valuation. Examples include the Puiseux series  $K = \mathbb{C}\{\{t\}\}$  and the  $p$ -adic numbers  $K = \mathbb{Q}_p$ . We use the term *cubic surface* to mean a marked smooth del Pezzo surface  $X$  of degree 3. A *tropical cubic surface* is the intrinsic tropicalization  $\text{trop}(X^0)$  described above. Likewise, *tropical del Pezzo surface* refers to the tropicalization  $\text{trop}(X^0)$  for degree  $\geq 4$ . Here, the adjective “tropical” is used solely for brevity, instead of the more accurate “tropicalized” used in [62]. We do not consider non-realizable tropical del Pezzo surfaces, nor tropicalizations of surfaces defined over a field  $K$  with positive characteristic.

The moduli space of cubic surfaces is four-dimensional, and its tropical version is the four-dimensional *Naruki fan*. This was constructed combinatorially by Hacking, Keel and Tevelev [50], and it was realized in Section 2.6 as the tropicalization of the Yoshida variety

$\mathcal{Y}$  in  $\mathbb{P}^{39}$ . The Weyl group  $W(E_6)$  acts on  $\mathcal{Y}$  by permuting the 40 coordinates. The maximal cones in  $\text{trop}(\mathcal{Y}^0)$  come in two  $W(E_6)$ -orbits. We here compute the corresponding cubic surfaces:

**Theorem 4.1.1.** *There are two generic types of tropical cubic surfaces. They are contractible and characterized at infinity by 27 metric trees, each having 10 leaves. The first type has 73 bounded cells, 150 edges, 78 vertices, 135 cones, 189 flaps, 216 rays, and all 27 trees are trivalent. The second type has 72 bounded cells, 148 edges, 77 vertices, 135 cones, 186 flaps, 213 rays, and three of the 27 trees have a 4-valent node. (For more data see Table 4.1.)*

Here, by *cones* and *flaps* we mean unbounded 2-dimensional polyhedra that are affinely isomorphic to  $\mathbb{R}_{\geq 0}^2$  and  $[0, 1] \times \mathbb{R}_{\geq 0}$  respectively. The *characterization at infinity* is analogous to that for tropical planes in [53]. Indeed, by [53, Theorem 4.4], every tropical plane  $L$  in  $\mathbb{TP}^{n-1}$  is given by an arrangement of  $n$  boundary trees, each having  $n - 1$  leaves, and  $L$  is uniquely determined by this arrangement. Viewed intrinsically,  $L$  is the tropicalization of a very affine surface, namely the complement of  $n$  lines in  $\mathbb{P}^2$ . Theorem 4.1.1 offers the analogous characterization for the tropicalization of the complement of the 27 lines on a cubic surface.

Tropical geometry has undergone an explosive development during the past decade. To the outside observer, the literature is full of conflicting definitions and diverging approaches. The forthcoming text books [62, 64] offer some help, but they each stress one point of view.

An important feature of this chapter is its focus on the unity of tropical geometry. We shall develop three different techniques for computing tropical del Pezzo surfaces:

- Cox ideals, as explained in Section 4.2;
- fan structures on moduli spaces, as explained in Section 4.3;
- tropical modifications, as explained in Section 4.4.

The first approach uses the Cox ring of  $X$ , starting from the presentation given in [87]. Propositions 4.2.1 and 4.2.2 extend this to the universal Cox ideal over the moduli space. For any particular surface  $X$ , defined over a field such as  $K = \mathbb{Q}(t)$ , computing the tropicalization is a task for the software `gfan` [57]. In the second approach, we construct del Pezzo surfaces from fibers in the natural maps of moduli fans. Our success along these lines completes the program started by Hacking *et al.* [50] and further developed in Section 2.6. The third approach is to build tropical del Pezzo surfaces combinatorially from the tropical projective plane  $\mathbb{TP}^2$  by the process of modifications in the sense of Mikhalkin [63]. It mirrors the classical construction by blowing up points in the plane  $\mathbb{P}^2$ . All three approaches yield the same results. Section 4.5 presents an in-depth study of the combinatorics of tropical cubic surfaces and their trees, including an extension of Theorem 4.1.1 that includes all degenerate surfaces.



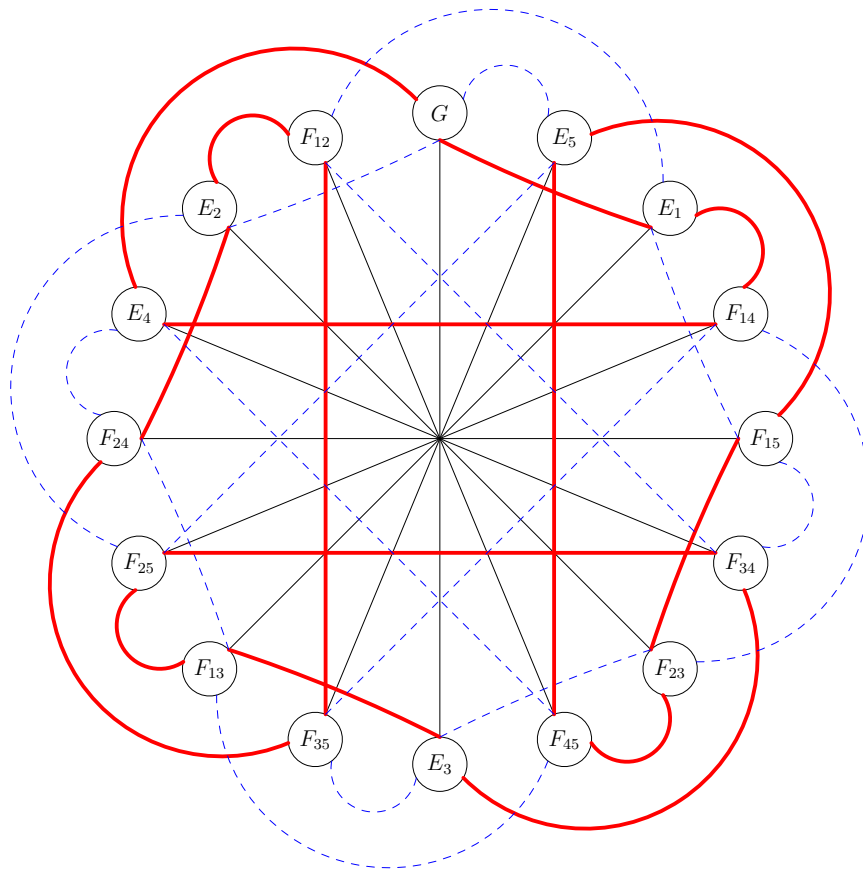


Figure 4.1: Tropical del Pezzo surfaces of degree 4 illustrated by coloring the Clebsch graph

We now illustrate the rich combinatorics in our story for a del Pezzo surface  $X$  of degree 4. Del Pezzo surfaces of degree  $d \geq 6$  are toric surfaces, so they naturally tropicalize as polygons with  $12-d$  vertices [64, Ch. 3]. On route to Theorem 4.1.1, we prove the following for  $d = 4, 5$ :

**Proposition 4.1.2.** *Among tropical del Pezzo surfaces of degree 4 and 5, each has a unique generic combinatorial type. For degree 5, this is the cone over the Petersen graph. For degree 4, the surface is contractible and characterized at infinity by 16 trivalent metric trees, each with 5 leaves. It has 9 bounded cells, 20 edges, 12 vertices, 40 cones, 32 flaps, and 48 rays.*

To understand degree 4, we consider the 5-regular *Clebsch graph* in Figure 4.1. Its 16 nodes are the  $(-1)$ -curves on  $X$ , labelled  $E_1, \dots, E_5, F_{12}, \dots, F_{45}, G$ . Edges represent intersecting pairs of  $(-1)$ -curves. In the constant coefficient case, when  $K$  has trivial valuation, the tropicalization of  $X$  is the fan over this graph. However, over fields  $K$  with non-trivial valuation,  $\text{trop}(X^0)$  is usually not a fan, but one sees the generic type from Proposition 4.1.2. Here, the Clebsch graph deforms into a trivalent graph with  $48 = 16 \cdot 3$  nodes and  $72 = 40 + 32$  edges, determined by the color coding in Figure 4.1. Each of the 16 nodes is replaced by a trivalent tree with five leaves. Incoming edges of the same color (red or blue) form a *cherry* (= two adjacent leaves) in that tree, while the black edge connects to the non-cherry leaf.

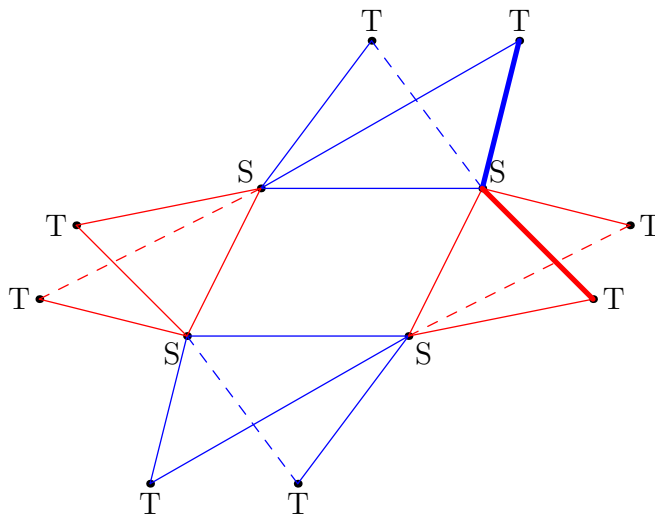


Figure 4.2: The bounded complex of the tropical del Pezzo surface in degree 4

**Corollary 4.1.3.** *For a del Pezzo surface  $X$  of degree 4, the 16 metric trees on its tropicalization  $\text{trop}(X^0)$ , obtained from the  $(-1)$ -curves on  $X$ , are identical up to relabeling.*

*Proof.* Moving from one  $(-1)$ -curve on  $X$  to another corresponds to a Cremona transformation of the plane  $\mathbb{P}^2$ . Each  $(-1)$ -curve on  $X$  has exactly five marked points arising from its intersections with the other  $(-1)$ -curves. Moreover, the Cremona transformations preserve the cross ratios among the five marked points on these 16  $\mathbb{P}^1$ 's. From this we obtain the following relabeling rules for the leaves on the 16 trees, which live in the nodes of Figure 4.1.

We start with the tree  $G$  whose leaves are labeled  $E_1, E_2, E_3, E_4, E_5$ . The tree  $F_{ij}$  is obtained by relabeling the five leaves as follows:

$$E_i \mapsto E_j, \quad E_j \mapsto E_i, \quad E_k \mapsto F_{lm}, \quad E_l \mapsto F_{km}, \quad E_m \mapsto F_{kl}. \quad (4.1)$$

Here  $\{k, l, m\} = \{1, 2, 3, 4, 5\} \setminus \{i, j\}$ . The tree  $E_i$  is obtained from the tree  $G$  by relabeling

$$E_i \mapsto G \quad \text{and} \quad E_j \mapsto F_{ij} \quad \text{where } j \neq i. \quad (4.2)$$

This explains the color coding of the graph in Figure 4.1. □

The bounded complex of  $\text{trop}(X^0)$  is shown in Figure 4.2. It consists of a central rectangle, with two triangles attached to each of its four edges. There are 12 vertices, four vertices of the rectangle, labeled **S**, and eight pendant vertices, labeled **T**. To these 12 vertices and 20 edges, we attach the flaps and cones, according to the deformed Clebsch graph structure. The link of each **S** vertex in the surface  $\text{trop}(X^0)$  is the Petersen graph (Figure 4.3), while the link of each **T** vertex is the bipartite graph  $K_{3,3}$ . The bounded complex has 16 chains **TST** consisting of two edges with different colors. These are attached by flaps to the

bounded parts of the 16 trees. The Clebsch graph (Figure 4.1) can be recovered from Figure 4.2 as follows: its nodes are the **TST** chains, and two chains connect if they share precisely one vertex. Out at infinity, **T** vertices attach along cherries, while **S** vertices attach along non-cherry leaves. Each such attachment between two of the 16 trees links to the bounded complex by a cone.

## 4.2 Cox Ideals

In this chapter we study del Pezzo surfaces over  $K$  of degrees 5, 4 and 3. Such a surface  $X$  is obtained from  $\mathbb{P}^2$  by blowing up 4, 5 or 6 general points, and we obtain moduli by varying these points. From an algebraic perspective, it is convenient to represent  $X$  by its *Cox ring*

$$\mathrm{Cox}(X) = \bigoplus_{\mathcal{L} \in \mathrm{Pic}(X)} H^0(X, \mathcal{L}). \quad (4.3)$$

The Cox ring of a del Pezzo surface  $X$  was first studied by Batyrev and Popov [11]. We shall express this ring explicitly as a quotient of a polynomial ring over the ground field  $K$ :

$$\mathrm{Cox}(X) = K[x_C : C \text{ is a } (-1)\text{-curve on } X] \text{ modulo an ideal } I_X \text{ generated by quadrics.}$$

The number of variables  $x_C$  in our three polynomial rings is 10, 16 and 27 respectively. The ideal  $I_X$  is the *Cox ideal* of the surface  $X$ . It was conjectured already in [11] that the ideal  $I_X$  is generated by quadrics. This conjecture was proved in several papers, including [86, 87].

The Cox ring encodes all maps from  $X$  to a projective space. Such a map is given by the  $\mathbb{N}$ -graded subring  $\mathrm{Cox}(X)_{[\mathcal{L}]} = \bigoplus_{m \geq 0} H^0(X, m\mathcal{L})$  for a fixed line bundle  $\mathcal{L} \in \mathrm{Pic}(X)$ . We obtain  $X \rightarrow \mathrm{Proj}(\mathrm{Cox}(X)_{[\mathcal{L}]}) \subset \mathbb{P}^N$ , where  $N = \dim(H^0(X, \mathcal{L})) - 1$ , provided  $\mathrm{Cox}(X)_{[\mathcal{L}]}$  is generated in degree 1. This holds for the anticanonical map and the blow-down map to  $\mathbb{P}^2$ .

In what follows, we give explicit generators for all relevant Cox ideals  $I_X$ . Some of this is new and of independent interest. The tropicalization of  $X^0$  we seek is defined from the ideal  $I_X$ . So, in principle, we can compute  $\mathrm{trop}(X^0)$  from  $I_X$  using the software `gfan` [57]. Recall that  $X^0$  denotes the very affine surface obtained from  $X$  by removing all  $(-1)$ -curves.

### Del Pezzo Surfaces of Degree 5

Consider four general points in  $\mathbb{P}^2$ . This configuration is projectively unique, so there are no moduli. The surface  $X$  is the moduli space  $\overline{M}_{0,5}$  of rational curves with five marked points. The Cox ideal is the *Plücker ideal* of relations among  $2 \times 2$ -minors of a  $2 \times 5$ -matrix:

$$I_X = \langle p_{12}p_{34} - p_{13}p_{24} + p_{14}p_{23}, \quad p_{12}p_{35} - p_{13}p_{25} + p_{15}p_{23}, \\ p_{12}p_{45} - p_{14}p_{25} + p_{15}p_{24}, \quad p_{13}p_{45} - p_{14}p_{35} + p_{15}p_{34}, \quad p_{23}p_{45} - p_{24}p_{35} + p_{25}p_{34} \rangle.$$

The affine variety of  $I_X$  in  $\overline{K}^{10}$  is the *universal torsor* of  $X$ , now regarded over the algebraic closure  $\overline{K}$  of the given valued field  $K$ . From the perspective of blowing up  $\mathbb{P}^2$  at 4 points,

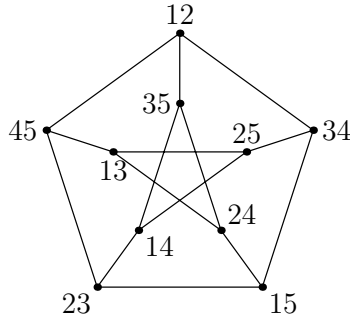


Figure 4.3: The tropical del Pezzo surface  $\text{trop}(M_{0,5})$  is the cone over the Petersen graph.

the ten variables (representing the ten  $(-1)$ -curves) fall in two groups: the four exceptional fibers, and the six lines spanned by pairs of points. For example, we may label the fibers by

$$E_1 = p_{15}, E_2 = p_{25}, E_3 = p_{35}, E_4 = p_{45},$$

and the six lines by

$$F_{12} = p_{34}, F_{13} = p_{24}, F_{14} = p_{23}, F_{23} = p_{14}, F_{24} = p_{13}, F_{34} = p_{12}.$$

The Cox ideal  $I_X$  is homogeneous with respect to the natural grading by the Picard group  $\text{Pic}(X) = \mathbb{Z}^5$ . In Plücker coordinates, this grading is given by  $\deg(p_{ij}) = e_i + e_j$ . This translates into an action of the torus  $(\bar{K}^*)^5 = \text{Pic}(X) \otimes_{\mathbb{Z}} \bar{K}^*$  on the universal torsor in  $\bar{K}^{10}$ . We remove the ten coordinate hyperplanes in  $\bar{K}^{10}$ , and we take the quotient modulo  $(\bar{K}^*)^5$ . The result is precisely the very affine del Pezzo surface we seek to tropicalize:

$$X^0 = M_{0,5} \subset (\bar{K}^*)^{10}/(\bar{K}^*)^5. \tag{4.4}$$

It is known (and easy to check with `gfan` on  $I_X$ ) that the 2-dimensional balanced fan  $\text{trop}(X^0)$  is the cone over the Petersen graph. This fan is also the moduli space of 5-marked rational tropical curves, that is, 5-leaf trees with lengths on the two bounded edges (cf. [62, §4.3]).

### Del Pezzo Surfaces of Degree 4

Consider now five general points in  $\mathbb{P}^2$ . There are two degrees of freedom. The moduli space is our previous del Pezzo surface  $M_{0,5}$ . Indeed, fixing five points in  $\mathbb{P}^2$  corresponds to fixing a point  $(p_{12}, \dots, p_{45})$  in  $M_{0,5}$ , using Cox-Plücker coordinates as in (4.4). Explicitly, if we write the five points as a  $3 \times 5$ -matrix then the  $p_{ij}$  are the Plücker coordinates of its kernel. Replacing  $K$  with the previous Cox ring, we may consider the *universal del Pezzo surface*  $\mathcal{Y}$ . The *universal Cox ring* is the quotient of a polynomial ring in  $26 = 10 + 16$  variables:

$$K[\mathcal{Y}] = \text{Cox}(M_{0,5})[E_1, E_2, E_3, E_4, E_5, F_{12}, F_{13}, \dots, F_{45}, G]/I_{\mathcal{Y}}. \tag{4.5}$$

As before,  $E_i$  represents the exceptional divisor over point  $i$ , and  $F_{ij}$  represents the line spanned by points  $i$  and  $j$ . The variable  $G$  represents the conic spanned by the five points.

**Proposition 4.2.1.** *Up to saturation with respect to the product of the 26 variables, the universal Cox ideal  $I_Y$  for degree 4 del Pezzo surfaces is generated by the following 45 trinomials:*

$$\begin{array}{lll}
\text{Base Group} & p_{12}p_{34}-p_{13}p_{24}+p_{14}p_{23} & p_{12}p_{35}-p_{13}p_{25}+p_{15}p_{23} & p_{12}p_{45}-p_{14}p_{25} + p_{15}p_{24}, \\
& p_{13}p_{45}-p_{14}p_{35} + p_{15}p_{34} & p_{23}p_{45}-p_{24}p_{35}+p_{25}p_{34} & \\
\text{Group 1} & F_{23}F_{45}-F_{24}F_{35}+F_{25}F_{34} & p_{23}p_{45}F_{24}F_{35}-p_{24}p_{35}F_{23}F_{45}-GE_1 & \\
& p_{23}p_{45}F_{25}F_{34}-p_{25}p_{34}F_{23}F_{45}-GE_1 & p_{24}p_{35}F_{25}F_{34}-p_{25}p_{34}F_{24}F_{35}-GE_1 & \\
\text{Group 2} & F_{13}F_{45}-F_{14}F_{35}+F_{15}F_{34} & p_{13}p_{45}F_{14}F_{35}-p_{14}p_{35}F_{13}F_{45}-GE_2 & \\
& p_{13}p_{45}F_{15}F_{34}-p_{15}p_{34}F_{13}F_{45}-GE_2 & p_{14}p_{35}F_{15}F_{34}-p_{15}p_{34}F_{14}F_{35}-GE_2 & \\
\text{Group 3} & F_{12}F_{45}-F_{14}F_{25}+F_{15}F_{24} & p_{12}p_{45}F_{14}F_{25}-p_{14}p_{25}F_{12}F_{45}-GE_3, & \\
& p_{12}p_{45}F_{15}F_{24}-p_{15}p_{24}F_{12}F_{45}-GE_3 & p_{14}p_{25}F_{15}F_{24}-p_{15}p_{24}F_{14}F_{25}-GE_3 & \\
\text{Group 4} & F_{12}F_{35}-F_{13}F_{25}+F_{15}F_{23} & p_{12}p_{35}F_{13}F_{25}-p_{13}p_{25}F_{12}F_{35}-GE_4 & \\
& p_{12}p_{35}F_{15}F_{23}-p_{15}p_{23}F_{12}F_{35}-GE_4 & p_{13}p_{25}F_{15}F_{23}-p_{15}p_{23}F_{13}F_{25}-GE_4 & \\
\text{Group 5} & F_{12}F_{34}-F_{13}F_{24}+F_{14}F_{23} & p_{12}p_{34}F_{13}F_{24}-p_{13}p_{24}F_{12}F_{34}-GE_5 & \\
& p_{12}p_{34}F_{14}F_{23}-p_{14}p_{23}F_{12}F_{34}-GE_5 & p_{13}p_{24}F_{14}F_{23}-p_{14}p_{23}F_{13}F_{24}-GE_5 & \\
\text{Group 1}' & p_{25}F_{12}E_2-p_{35}F_{13}E_3+p_{45}F_{14}E_4 & p_{24}F_{12}E_2-p_{34}F_{13}E_3+p_{45}F_{15}E_5 & \\
& p_{23}F_{12}E_2-p_{34}F_{14}E_4+p_{35}F_{15}E_5 & p_{23}F_{13}E_3-p_{24}F_{14}E_4+p_{25}F_{15}E_5 & \\
\text{Group 2}' & p_{15}F_{12}E_1-p_{35}F_{23}E_3+p_{45}F_{24}E_4 & p_{14}F_{12}E_1-p_{34}F_{23}E_3+p_{45}F_{25}E_5 & \\
& p_{13}F_{12}E_1-p_{34}F_{24}E_4+p_{35}F_{25}E_5 & p_{13}F_{23}E_3-p_{14}F_{24}E_4+p_{15}F_{25}E_5 & \\
\text{Group 3}' & p_{15}F_{13}E_1-p_{25}F_{23}E_2+p_{45}F_{34}E_4 & p_{14}F_{13}E_1-p_{24}F_{23}E_2+p_{45}F_{35}E_5 & \\
& p_{12}F_{13}E_1-p_{24}F_{34}E_4+p_{25}F_{35}E_5 & p_{12}F_{23}E_2-p_{14}F_{34}E_4+p_{15}F_{35}E_5 & \\
\text{Group 4}' & p_{15}F_{14}E_1-p_{25}F_{24}E_2+p_{35}F_{34}E_3 & p_{13}F_{14}E_1-p_{23}F_{24}E_2+p_{35}F_{45}E_5 & \\
& p_{12}F_{14}E_1-p_{23}F_{34}E_3+p_{25}F_{45}E_5 & p_{12}F_{24}E_2-p_{13}F_{34}E_3+p_{15}F_{45}E_5 & \\
\text{Group 5}' & p_{14}F_{15}E_1-p_{24}F_{25}E_2+p_{34}F_{35}E_3 & p_{13}F_{15}E_1-p_{23}F_{25}E_2+p_{34}F_{45}E_4 & \\
& p_{12}F_{15}E_1-p_{23}F_{35}E_3+p_{24}F_{45}E_4 & p_{12}F_{25}E_2-p_{13}F_{35}E_3+p_{14}F_{45}E_4 & 
\end{array}$$

Proposition 4.2.1 will be derived later in this section. For now, let us discuss the structure and symmetry of the generators of  $I_Y$ . We consider the 5-dimensional *demicube*, here denoted  $D_5$ . This is the convex hull of the following 16 points in the hyperplane  $\{a_0 = 0\} \subset \mathbb{R}^6$ :

$$\{(1, a_1, a_2, a_3, a_4, a_5) \in \{0, 1\}^6 : a_1 + a_2 + a_3 + a_4 + a_5 \text{ is odd}\}. \quad (4.6)$$

The group of symmetries of  $D_5$  is the Weyl group  $W(D_5)$ . It acts transitively on (4.6). There is a natural bijection between the 16 variables in the Cox ring and the vertices of  $D_5$ :

$$\begin{aligned}
E_1 &\leftrightarrow (1, 1, 0, 0, 0, 0), & E_2 &\leftrightarrow (1, 0, 1, 0, 0, 0), & \dots, & & E_5 &\leftrightarrow (1, 0, 0, 0, 0, 1), \\
F_{12} &\leftrightarrow (1, 0, 0, 1, 1, 1), & F_{13} &\leftrightarrow (1, 0, 1, 0, 1, 1), & \dots, & & F_{45} &\leftrightarrow (1, 1, 1, 1, 0, 0), \\
G &\leftrightarrow (1, 1, 1, 1, 1, 1).
\end{aligned} \quad (4.7)$$

This bijection defines the grading via the Picard group  $\mathbb{Z}^6$ . We regard the  $p_{ij}$  as scalars, so they have degree 0. Generators of  $I_{\mathcal{Y}}$  that are listed in the same group have the same  $\mathbb{Z}^6$  degrees. The action of  $W(D_5)$  on the demicube  $D_5$  gives the action on the 16 variables.

Consider now a particular smooth del Pezzo surface  $X$  of degree 4 over the field  $K$ , so the  $p_{ij}$  are scalars in  $K$  that satisfy the Plücker relations in the Base Group. The universal Cox ideal  $I_{\mathcal{Y}}$  specializes to the Cox ideal  $I_X$  for the particular surface  $X$ . That Cox ideal is minimally generated by 20 quadrics, two per group. The surface  $X^0$  is the zero set of the ideal  $I_X$  inside  $(\bar{K}^*)^{16}/(\bar{K}^*)^6$ . The torus action is obtained from (4.7), in analogy to (4.4).

*Proof of Proposition 4.1.2.* We computed  $\text{trop}(X^0)$  by applying `gfan` [57] to the ideal  $I_X$ . If  $K = \mathbb{Q}$  with the trivial valuation then the output is the cone over the *Clebsch graph* in Figure 4.1. This 5-regular graph records which pairs of  $(-1)$ -curves intersect on  $X$ . This also works over a field  $K$  with non-trivial valuation. The software `gfan` uses  $K = \mathbb{Q}(t)$ . If the vector  $(p_{12}, \dots, p_{45})$  tropicalizes into the interior of an edge in the Petersen graph then  $\text{trop}(X^0)$  is the tropical surface described in Proposition 4.1.2. Each node in Figure 4.1 is replaced by a trivalent tree on 5 nodes according to the color coding explained in Section 4.1. The surface  $\text{trop}(X^0)$  can also be determined by tropical modifications, as in Section 4.4.  $\square$

The same tropicalization method works for the universal family  $\mathcal{Y}^0$ . Its ideal  $I_{\mathcal{Y}}$  is given by the 45 polynomials in 26 variables listed above, and  $\mathcal{Y}^0$  is the zero set of  $I_{\mathcal{Y}}$  in the 15-dimensional torus  $(\bar{K}^*)^{10}/(\bar{K}^*)^5 \times (\bar{K}^*)^{16}/(\bar{K}^*)^6$ . The tropical universal del Pezzo surface  $\text{trop}(\mathcal{Y}^0)$  is a 4-dimensional fan in  $\mathbb{R}^{26}/\mathbb{R}^{11}$ . We compute it by applying `gfan` to the *universal Cox ideal*  $I_{\mathcal{Y}}$ . The Gröbner fan structure on  $\text{trop}(I_{\mathcal{Y}})$  has f-vector  $(76, 630, 1620, 1215)$ . It is isomorphic to the *Naruki fan* described in Table 2.5 and discussed further in Section 4.3.

### Del Pezzo Surfaces of Degree 3 (Cubic Surfaces)

There exists a cuspidal cubic through any six points in  $\mathbb{P}^2$ . See e.g. (2.34) and [74, (4.4)]. Hence any configuration of six points in  $\mathbb{P}^2$  can be represented by the columns of a matrix

$$D = \begin{pmatrix} 1 & 1 & 1 & 1 & 1 & 1 \\ d_1 & d_2 & d_3 & d_4 & d_5 & d_6 \\ d_1^3 & d_2^3 & d_3^3 & d_4^3 & d_5^3 & d_6^3 \end{pmatrix}. \quad (4.8)$$

The maximal minors of the matrix  $D$  factor into linear forms,

$$[ijk] = (d_i - d_j)(d_i - d_k)(d_j - d_k)(d_i + d_j + d_k), \quad (4.9)$$

and so does the condition for the six points to lie on a conic:

$$\begin{aligned} [\text{conic}] &= [134][156][235][246] - [135][146][234][256] \\ &= (d_1 + d_2 + d_3 + d_4 + d_5 + d_6) \cdot \prod_{1 \leq i < j \leq 6} (d_i - d_j). \end{aligned} \quad (4.10)$$

The linear factors in these expressions form the root system of type  $E_6$ . This corresponds to an arrangement of 36 hyperplanes in  $\mathbb{P}^5$ . Similarly, the arrangement of type  $E_7$  consists

of 63 hyperplanes in  $\mathbb{P}^6$ , as in [74, (4.4)]. To be precise, for  $m = 6, 7$ , the roots for  $E_m$  are

$$\begin{aligned} d_i + d_j & \quad \text{for} \quad 1 \leq i < j \leq m, \\ d_i + d_j + d_k & \quad \text{for} \quad 1 \leq i < j < k \leq m, \\ d_{i_1} + d_{i_2} + \cdots + d_{i_6} & \quad \text{for} \quad 1 \leq i_1 < i_2 < \cdots < i_6 \leq m. \end{aligned} \quad (4.11)$$

Linear dependencies among these linear forms specify a matroid of rank  $m$ , also denoted  $E_m$ .

The moduli space of marked cubic surfaces is the 4-dimensional *Yoshida variety*  $\mathcal{Y}$  defined in Section 2.6. It coincides with the subvariety  $\mathcal{Y}^0$  of  $(\bar{K}^*)^{26}/(\bar{K}^*)^{11}$  cut out by the 45 trinomials listed in Proposition 4.1.2. The universal family for cubic surfaces is denoted by  $\mathcal{G}^0$ . This is the open part of the *Göpel variety*  $\mathcal{G} \subset \mathbb{P}^{134}$  constructed in [74, §5]. The base of this 6-dimensional family is the 4-dimensional  $\mathcal{Y}^0$ . The map  $\mathcal{G}^0 \rightarrow \mathcal{Y}^0$  was described in [50]. Thus the ring  $K[\mathcal{Y}]$  in (4.5) is the natural base ring for the universal Cox ring for degree 3 surfaces.

At this point it is essential to avoid confusing notation. To aim for a clear presentation, we use the uniformization of  $\mathcal{Y}$  by the  $E_6$  hyperplane arrangement. Namely, we take  $R = \mathbb{Z}[d_1, d_2, d_3, d_4, d_5, d_6]$  instead of  $K[\mathcal{Y}]$  as the base ring. We write  $\mathcal{X}$  for the universal cubic surface over  $R$ . The *universal Cox ring* is a quotient of the polynomial ring over  $R$  in 27 variables, one for each line on the cubic surface. Using variable names as in [87, §5], we write

$$\text{Cox}(\mathcal{X}) = R[E_1, E_2, \dots, E_6, F_{12}, F_{13}, \dots, F_{56}, G_1, G_2, \dots, G_6]/I_{\mathcal{X}}. \quad (4.12)$$

This ring is graded by the Picard group  $\mathbb{Z}^7$ , similarly to (4.7). The role of the 5-dimensional demicube  $D_5$  is now played by the 6-dimensional *Gosset polytope* with 27 vertices, here also denoted by  $E_6$ . The symmetry group of this polytope is the Weyl group  $W(E_6)$ .

**Proposition 4.2.2.** *Up to saturation by the product of all 27 variables and all 36 roots, the universal Cox ideal  $I_{\mathcal{X}}$  is generated by 270 trinomials. These are clustered by  $\mathbb{Z}^7$ -degrees into 27 groups of 10 generators, one for each line on the cubic surface. For instance, the 10 generators of  $I_{\mathcal{X}}$  that correspond to the line  $G_1$  involve the 10 lines that meet  $G_1$ . They are*

$$\begin{aligned} & (d_3 - d_4)(d_1 + d_3 + d_4)E_2F_{12} + (d_2 - d_4)(d_1 + d_2 + d_4)E_3F_{13} - (d_2 - d_3)(d_1 + d_2 + d_3)E_4F_{14}, \\ & (d_3 - d_5)(d_1 + d_3 + d_5)E_2F_{12} + (d_2 - d_5)(d_1 + d_2 + d_5)E_3F_{13} - (d_2 - d_3)(d_1 + d_2 + d_3)E_5F_{15}, \\ & (d_3 - d_6)(d_1 + d_3 + d_6)E_2F_{12} + (d_2 - d_6)(d_1 + d_2 + d_6)E_3F_{13} - (d_2 - d_3)(d_1 + d_2 + d_3)E_6F_{16}, \\ & (d_5 - d_4)(d_1 + d_4 + d_5)E_2F_{12} - (d_2 - d_5)(d_1 + d_2 + d_5)E_4F_{14} + (d_2 - d_4)(d_1 + d_2 + d_4)E_5F_{15}, \\ & (d_4 - d_6)(d_1 + d_4 + d_6)E_2F_{12} + (d_2 - d_6)(d_1 + d_2 + d_6)E_4F_{14} - (d_2 - d_4)(d_1 + d_2 + d_4)E_6F_{16}, \\ & (d_5 - d_6)(d_1 + d_5 + d_6)E_2F_{12} + (d_2 - d_6)(d_1 + d_2 + d_6)E_5F_{15} - (d_2 - d_5)(d_1 + d_2 + d_5)E_6F_{16}, \\ & (d_4 - d_5)(d_1 + d_4 + d_5)E_3F_{13} - (d_3 - d_5)(d_1 + d_3 + d_5)E_4F_{14} + (d_3 - d_4)(d_1 + d_3 + d_4)E_5F_{15}, \\ & (d_4 - d_6)(d_1 + d_4 + d_6)E_3F_{13} - (d_3 - d_6)(d_1 + d_3 + d_6)E_4F_{14} + (d_3 - d_4)(d_1 + d_3 + d_4)E_6F_{16}, \\ & (d_5 - d_6)(d_1 + d_5 + d_6)E_3F_{13} - (d_3 - d_6)(d_1 + d_3 + d_6)E_5F_{15} + (d_3 - d_5)(d_1 + d_3 + d_5)E_6F_{16}, \\ & (d_6 - d_5)(d_1 + d_5 + d_6)E_4F_{14} + (d_4 - d_6)(d_1 + d_4 + d_6)E_5F_{15} - (d_4 - d_5)(d_1 + d_4 + d_5)E_6F_{16}. \end{aligned}$$

The remaining 260 trinomials are obtained by applying the action of  $W(E_6)$ . The variety defined by  $I_{\mathcal{X}}$  in  $\mathbb{P}^5 \times (\bar{K}^*)^{27}/(\bar{K}^*)^7$  is 6-dimensional. It is the universal family  $\mathcal{X}^0$ .

*Proof of Propositions 4.2.1 and 4.2.2.* We consider the prime ideal in [74, §6] that defines the embedding of the Göpel variety  $\mathcal{G}$  into  $\mathbb{P}^{134}$ . By [74, Theorem 6.2],  $\mathcal{G}$  is the ideal-theoretic intersection of a 35-dimensional toric variety  $\mathcal{T}$  and a 14-dimensional linear space  $L$ . The latter is cut out by a canonical set of 315 linear trinomials, indexed by the 315 isotropic planes in  $(\mathbb{F}_2)^6$ . Pulling these linear forms back to the Cox ring of  $\mathcal{T}$ , we obtain 315 quartic trinomials in 63 variables, one for each root of  $E_7$ . Of these 63 roots, precisely 27 involve the unknown  $d_7$ . We identify these with the  $(-1)$ -curves on the cubic surface via

$$d_i - d_7 \mapsto E_i, \quad d_i + d_j + d_7 \mapsto F_{ij}, \quad -d_j + \sum_{i=1}^7 d_i \mapsto G_j. \quad (4.13)$$

Moreover, of the 315 quartics, precisely 270 contain a root involving  $d_7$ . Their images under the map (4.13) are the 270 Cox relations listed above. Our construction ensures that they generate the correct Laurent polynomial ideal on the torus of  $\mathcal{T}$ . This proves Proposition 4.2.2.

The derivation of Proposition 4.2.1 is similar, but now we use the substitution

$$d_i - d_6 \mapsto E_i, \quad d_i + d_j + d_6 \mapsto F_{ij}, \quad \sum_{i=1}^6 d_i \mapsto G.$$

We consider the 45 quartic trinomials that do not involve  $d_7$ . Of these, precisely 5 do not involve  $d_6$  either. They translate into the 5 Plücker relations for  $M_{0,5}$ . With this identification, the remaining 40 quartics translate into the ten groups listed after Proposition 4.2.1.

For an alternative argument, in degree 3, we may consider the base ring

$$R = K[d_1, d_2, \dots, d_6, (d_1 - d_2)^{-1}, (d_1 + d_2 + d_3)^{-1}, \dots, (d_1 + d_2 + d_3 + d_4 + d_5 + d_6)^{-1}].$$

Then, our ideal  $I$  can be regarded as an ideal in the ring  $R[E., F., G.]$ . We need to show that the ideal is prime.

Consider the family  $\text{Proj}(R[E., F., G.]/I) \rightarrow \text{Spec}R$ . The base  $\text{Spec}R$  is the variety of 6 points in  $\mathbb{P}^2$  in general position. Up to the grading, the fibers are smooth cubic surfaces, which are reduced. We claim that the family is flat. If so, then  $\text{Proj}(R[E., F., G.]/I)$  is also reduced, by [45, 11.3.13].

By [52, III 9.9], it suffices to show that the Hilbert polynomials for all fibers are the same. To show this, we compute a Gröbner basis of  $I$  over the fraction field  $\text{Frac}(R) = K(d_1, d_2, d_3, d_4, d_5, d_6)$ . By abuse of notation, we also write  $I$  for  $\text{Frac}(R)[E., F., G.] \cdot I$ . Then, we look at the coefficients of the leading terms in the Gröbner basis and observe that only products of the 36 roots in  $E_6$  appear. Therefore, it remains a Gröbner basis when  $d_1, d_2, \dots, d_6$  are specialized to any point in  $\text{Spec}R$ . Since the Hilbert polynomial is determined by the leading terms, we conclude that the Hilbert polynomials are all same.

The irreducibility of  $\text{Proj}(R[E., F., G.]/I)$  follows from the fact that the generic fiber

$$\text{Proj}(\text{Frac}(R)[E., F., G.]/I)$$



is irreducible, also by a standard theorem on flat families. Hence, the ideal  $I$  is prime.

The degree 4 case is similar.  $\square$

We now fix a  $K$ -valued point in the base  $\mathcal{Y}^0$ , by replacing the unknowns  $d_i$  with scalars in  $K$ . In order for the resulting surface  $X$  to be smooth, we require  $(d_1 : d_2 : d_3 : d_4 : d_5 : d_6)$  to be in the complement of the 36 hyperplanes for  $E_6$ . The corresponding specialization of  $I_{\mathcal{X}}$  is the Cox ideal  $I_X$  of  $X$ . Seven of the ten trinomials in each degree are redundant over  $K$ . Only three are needed to generate  $I_X$ . Hence, the Cox ideal  $I_X$  is minimally generated by 81 quadrics in the  $E_i, F_{ij}$  and  $G_i$ . Its variety is the surface  $X^0 = V(I_X) \subset (\bar{K}^*)^{27}/(\bar{K}^*)^7$ .

**Proposition 4.2.3.** *Each of the marked 27 trees on a tropical cubic surface has an involution.*

*Proof.* Every line  $L$  on a cubic surface  $X$  over  $K$ , with its ten marked points, admits a double cover to  $\mathbb{P}^1$  with five markings. The preimage of one of these marked points is the pair of markings on  $L$  given by two other lines forming a tritangent with  $L$ . Tropically, this gives a double cover from the 10-leaf tree for  $L$  to a 5-leaf tree with leaf labelings given by these pairs. The desired involution on the 10-leaf tree exchanges elements in each pair.  $\square$

For instance, for the tree that corresponds to the line  $L = G_1$ , the involution equals

$$E_2 \leftrightarrow F_{12}, \quad E_3 \leftrightarrow F_{13}, \quad E_4 \leftrightarrow F_{14}, \quad E_5 \leftrightarrow F_{15}, \quad E_6 \leftrightarrow F_{16}.$$

Indeed, this involution fixes the 10 Cox relations displayed in Proposition 4.2.2. This will be seen more clearly in Figures 4.4 and 4.5, where the involution reflects about a vertical axis. The corresponding 5-leaf tree is the tropicalization of the line in

$$\text{Proj}(K[E_2F_{12}, E_3F_{13}, E_4F_{14}, E_5F_{15}, E_6F_{16}]) \simeq \mathbb{P}^4$$

that is the intersection of the 10 hyperplanes defined by the polynomials in Proposition 4.2.2.

We aim to compute  $\text{trop}(X^0)$  by applying `gfan` to the ideal  $I_X$ . This works well for  $K = \mathbb{Q}$  with the trivial valuation. Here the output is the cone over the *Schläfli graph* which records which pairs of  $(-1)$ -curves intersect on  $X$ . This is a 10-regular graph with 27 nodes. However, for  $K = \mathbb{Q}(t)$ , our `gfan` calculations did not terminate. Future implementations of tropical algorithms will surely succeed; see also Conjecture 4.5.3. To get the tropical cubic surfaces, and to prove Theorem 4.1.1, we used the alternative method explained in Section 4.3.

### 4.3 Sekiguchi Fan to Naruki Fan

In the previous section we discussed the computation of tropical del Pezzo surfaces directly from their Cox ideals. This worked well for degree 4. However, using the current implementation in `gfan`, this computation did not terminate for degree 3. We here discuss an alternative method that did succeed. In particular, we present the proof of Theorem 4.1.1.

The successful computation uses the following commutative diagram of balanced fans:

$$\begin{array}{ccc}
 \text{Berg}(E_7) & \longrightarrow & \text{trop}(\mathcal{G}^0) \\
 \downarrow & & \downarrow \\
 \text{Berg}(E_6) & \longrightarrow & \text{trop}(\mathcal{Y}^0)
 \end{array} \tag{4.14}$$

This diagram was first derived by Hacking *et al.* [50], in their study of moduli spaces of marked del Pezzo surfaces. Combinatorial details were worked out in Section 2.6. The material that follows completes the program that was suggested at the very end of Section 2.6.

The notation  $\text{Berg}(E_m)$  denotes the *Bergman fan* of the rank  $m$  matroid defined by the (36 resp. 63) linear forms listed in (4.11). Thus,  $\text{Berg}(E_6)$  is a tropical linear space in  $\mathbb{TP}^{35}$ , and  $\text{Berg}(E_7)$  is a tropical linear space in  $\mathbb{TP}^{62}$ . Coordinates are labeled by roots.

The list (4.11) fixes a choice of injection of root systems  $E_6 \hookrightarrow E_7$ . This defines coordinate projections  $\mathbb{R}^{63} \rightarrow \mathbb{R}^{36}$  and  $\mathbb{TP}^{62} \dashrightarrow \mathbb{TP}^{35}$ , namely by deleting coordinates with index 7. This projection induces the vertical map from  $\text{Berg}(E_7)$  to  $\text{Berg}(E_6)$  on the left in (4.14).

On the right in (4.14), we see the 4-dimensional *Yoshida variety*  $\mathcal{Y} \subset \mathbb{P}^{62}$  and the 6-dimensional *Göpel variety*  $\mathcal{G} \subset \mathbb{P}^{134}$ . Explicit parametrizations and equations for these varieties were presented in [74] and Chapter 2. The corresponding very affine varieties  $\mathcal{G}^0 \subset (\bar{K}^*)^{36}/\bar{K}^*$  and  $\mathcal{Y}^0 \subset (\bar{K}^*)^{63}/\bar{K}^*$  are moduli spaces of marked del Pezzo surfaces [50]. Their tropicalizations  $\text{trop}(\mathcal{G}^0)$  and  $\text{trop}(\mathcal{Y}^0)$  are known as the *Sekiguchi fan* and *Naruki fan*, respectively. The modular interpretation in [50] ensures the existence of the vertical map  $\text{trop}(\mathcal{G}^0) \rightarrow \text{trop}(\mathcal{Y}^0)$ .

The two horizontal maps in (4.14) are surjective and (classically) linear. The linear map  $\text{Berg}(E_7) \rightarrow \text{trop}(\mathcal{G}^0)$  is given by the  $135 \times 63$  matrix  $A$  in [74, §6]. The corresponding toric variety is the object of [74, Theorem 6.1]. The map  $\text{Berg}(E_6) \rightarrow \text{trop}(\mathcal{Y}^0)$  is given by the  $40 \times 36$ -matrix in Theorem 2.6.1. We record the following computational result. It refers to the natural simplicial fan structure on  $\text{Berg}(E_m)$  described by Ardila *et al.* in [5].

**Lemma 4.3.1.** *The Bergman fans of  $E_6$  and  $E_7$  have dimensions 5 and 6. Their f-vectors are*

$$\begin{aligned}
 f_{\text{Berg}(E_6)} &= (1, 750, 17679, 105930, 219240, 142560), \\
 f_{\text{Berg}(E_7)} &= (1, 6091, 315399, 3639804, 14982660, 24607800, 13721400).
 \end{aligned}$$

*The moduli fans  $\text{trop}(\mathcal{Y}^0)$  and  $\text{trop}(\mathcal{G}^0)$  have dimensions 4 and 6. Their f-vectors are*

$$\begin{aligned}
 f_{\text{trop}(\mathcal{Y}^0)} &= (1, 76, 630, 1620, 1215), \\
 f_{\text{trop}(\mathcal{G}^0)} &= (1, 1065, 27867, 229243, 767025, 1093365, 547155).
 \end{aligned}$$

*Proof.* The f-vector for the Naruki fan  $\text{trop}(\mathcal{Y}^0)$  appears in Table 2.5. For the other three fans, only the numbers of rays (namely 750, 6091 and 1065) were known from Section 2.6. The main new result in Lemma 4.3.1 is the computation of all 57273155 cones in  $\text{Berg}(E_7)$ .

The fans  $\text{Berg}(E_6)$  and  $\text{trop}(\mathcal{G}^0)$  are subsequently derived from  $\text{Berg}(E_7)$  using the maps in (4.14).

We now describe how  $f_{\text{Berg}(E_7)}$  was found. We did not use the theory of tubings in [5]. Instead, we carried out a brute force computation based on [38] and [78]. Recall that a point  $\mathbf{x}$  lies in the Bergman fan of a matroid if and only if the minimum is obtained twice on each circuit. We computed all circuits of the rank 7 matroid on the 63 vectors in the root system  $E_7$ . That matroid has precisely 100662348 circuits. Their cardinalities range from 3 to 8. This furnishes a subroutine for deciding whether a given point lies in the Bergman fan.

Our computations were mostly done in `sage` [85] and `java`. We achieved speed by exploiting the action of the Weyl group  $W(E_7)$  given by the two generators in [74, (4.2)]. The two matrices derived from these two generators using [74, (4.3)] act on the space  $\mathbb{R}^7$  with coordinates  $d_1, d_2, \dots, d_7$ . This gives subroutines for the action of  $W(E_7)$  on  $\mathbb{R}^{63}$ , e.g. for deciding whether two given sequences of points are conjugate with respect to this action.

Let  $\mathbf{r}_1, \dots, \mathbf{r}_{6091}$  denote the rays of  $\text{Berg}(E_7)$ , as in [50, Table 2] and Section 2.6. They form 11 orbits under the action of  $W(E_7)$ . For each orbit, we take the representative  $\mathbf{r}_i$  with smallest label. For each pair  $i < j$  such that  $\mathbf{r}_i$  is a representative, our program checks if  $\mathbf{r}_i + \mathbf{r}_j$  lies in  $\text{Berg}(E_7)$ , using the precomputed list of circuits. If yes, then  $\mathbf{r}_i$  and  $\mathbf{r}_j$  span a 2-dimensional cone in  $\text{Berg}(E_7)$ . This process gives representatives for the  $W(E_7)$ -orbits of 2-dimensional cones. The list of all 2-dimensional cones are produced by applying the action of  $W(E_7)$  on the result. For each orbit, we keep only the lexicographically smallest representative  $(\mathbf{r}_i, \mathbf{r}_j)$ .

Next, for each triple  $i < j < k$  such that  $(\mathbf{r}_i, \mathbf{r}_j)$  is a representative, we check if  $\mathbf{r}_i + \mathbf{r}_j + \mathbf{r}_k$  lies in  $\text{Berg}(E_7)$ . If so, then  $\{\mathbf{r}_i, \mathbf{r}_j, \mathbf{r}_k\}$  spans a 3-dimensional cone in  $\text{Berg}(E_7)$ . The list of all 3-dimensional cones can be found by applying the action of  $W(E_7)$  on the result. As before, we fix the lexicographically smallest representatives. Repeating this process for dimensions 4, 5 and 6, we obtain the list of all cones in  $\text{Berg}(E_7)$ , and hence the f-vector of this fan.

We now describe the procedure to derive  $\text{trop}(\mathcal{G}^0)$  by applying the top horizontal map  $\phi : \text{Berg}(E_7) \rightarrow \text{trop}(\mathcal{G}^0)$ . Each ray  $\mathbf{r}$  in  $\text{Berg}(E_7)$  maps to either (a)  $\mathbf{0}$ , (b) a ray of  $\text{trop}(\mathcal{G}^0)$ , or (c) a positive linear combination of 2 or 3 rays, as listed in Section 2.6. For each ray in case (c), our program iterates through all pairs and triples of rays in  $\text{trop}(\mathcal{G}^0)$  and writes the image explicitly as a positive linear combination of rays. With this data, we give a first guess of  $\text{trop}(\mathcal{G}^0)$  as follows: for each maximal cone  $\sigma = \text{span}(\mathbf{r}_{i_1}, \dots, \mathbf{r}_{i_6})$  of  $\text{Berg}(E_7)$ , we write  $\phi(\mathbf{r}_{i_1}), \dots, \phi(\mathbf{r}_{i_6})$  as linear combinations of the rays of  $\text{trop}(\mathcal{G}^0)$  and take  $\sigma' \subset \mathbb{TP}^{134}$  to be the cone spanned by all rays of  $\text{trop}(\mathcal{G}^0)$  that appear in the linear combinations. From this we get a list of 6-dimensional cones  $\sigma'$ . Let  $\Phi \subset \mathbb{TP}^{134}$  be the union of these cones.

To certify that  $\Phi = \text{trop}(\mathcal{G}^0)$  we need to show (1) for each  $\sigma \in \text{Berg}(E_7)$ , we have  $\phi(\sigma) \subset \sigma'$  for some cone  $\sigma' \subset \Phi$ ; (2) each cone  $\sigma' \subset \Phi$  is the union of some  $\phi(\sigma)$  for  $\sigma \in \text{Berg}(E_7)$ ; and (3) the intersection of any two cones  $\sigma'_1, \sigma'_2$  in  $\Phi$  is a face of both  $\sigma'_1$  and  $\sigma'_2$ . The claim (1) follows from the procedure of constructing  $\Phi$ . For (2), one only needs to verify the cases where  $\sigma'$  is one of the 9 representatives by the action of  $W(E_7)$ . For each of these, our program produces a list of  $\phi(\sigma)$ , and we check manually that  $\sigma'$  is indeed the intersection. For (3), one only needs to iterate through the cases where  $\sigma'_1$  is a

representative, and the procedure is straightforward. Therefore, our procedure shows that  $\Phi$  is exactly  $\text{trop}(\mathcal{G}^0)$ . Then the  $f$ -vector is obtained from the list of all cones in the fan  $\Phi$ .

Finally, we recover the list of all cones in  $\text{Berg}(\mathbb{E}_6)$  and  $\text{trop}(\mathcal{Y}^0)$  by following the same procedure with the left vertical map and the bottom horizontal map.  $\square$

**Remark 4.3.2.** We see from Lemma 4.3.1 that the Euler characteristic of  $\text{Berg}(\mathbb{E}_7)$  equals

$$\begin{aligned} 1 - 6091 + 315399 - 3639804 + 14982660 - 24607800 + 13721400 \\ = 765765 = 1 \cdot 5 \cdot 7 \cdot 9 \cdot 11 \cdot 13 \cdot 17. \end{aligned}$$

This is the product of all exponents of  $W(\mathbb{E}_7)$ , thus confirming the prediction in [74, (9.2)].

The Naruki fan  $\text{trop}(\mathcal{Y}^0)$  is studied in Section 2.6. Under the action of  $W(\mathbb{E}_6)$  through  $\text{Berg}(\mathbb{E}_6)$ , it has two classes of rays, labelled type (a) and type (b). It also has two  $W(\mathbb{E}_6)$ -orbits of maximal cones: there are 135 type (aaaa) cones, each spanned by four type (a) rays, and 1080 type (aaab) cones, each spanned by three type (a) rays and one type (b) ray.

The map  $\text{trop}(\mathcal{G}^0) \rightarrow \text{trop}(\mathcal{Y}^0)$  tropicalizes the morphism  $\mathcal{G}^0 \rightarrow \mathcal{Y}^0$  between very affine  $K$ -varieties of dimension 6 and 4. That morphism is the universal family of cubic surfaces. In order to tropicalize these surfaces, we examine the fibers of the map  $\text{trop}(\mathcal{G}^0) \rightarrow \text{trop}(\mathcal{Y}^0)$ . The next lemma concerns the subdivision of  $\text{trop}(\mathcal{Y}^0)$  induced by this map. By definition, this is the coarsest subdivision such that each cone in  $\text{trop}(\mathcal{G}^0)$  is sent to a union of cones.

**Lemma 4.3.3.** *The subdivision induced by the map  $\text{trop}(\mathcal{G}^0) \rightarrow \text{trop}(\mathcal{Y}^0)$  is the barycentric subdivision on type (aaaa) cones. For type (aaab) cones, each cone in the subdivision is a cone spanned by the type (b) ray and a cone in the barycentric subdivision of the (aaa) face. Thus each (aaaa) cone is divided into 24 cones, and each (aaab) cone is divided into 6 cones.*

*Proof.* The map  $\pi : \text{trop}(\mathcal{G}^0) \rightarrow \text{trop}(\mathcal{Y}^0)$  can be defined via the commutative diagram (4.14): for  $\mathbf{x} \in \text{trop}(\mathcal{G}^0)$ , take any point in its preimage in  $\text{Berg}(\mathbb{E}_7)$ , then follow the left vertical map and the bottom horizontal map to get  $\pi(\mathbf{x})$  in  $\text{trop}(\mathcal{Y}^0)$ . It is well-defined because the kernel of the map  $\text{Berg}(\mathbb{E}_7) \rightarrow \text{trop}(\mathcal{G}^0)$  is contained in the kernel of the composition  $\text{Berg}(\mathbb{E}_7) \rightarrow \text{Berg}(\mathbb{E}_6) \rightarrow \text{trop}(\mathcal{Y}^0)$ . With this, we can compute the image in  $\text{trop}(\mathcal{Y}^0)$  of any cone in  $\text{trop}(\mathcal{G}^0)$ . For each orbit of cones in  $\text{trop}(\mathcal{Y}^0)$ , pick a representative  $\sigma$ , and examine all cones in  $\text{trop}(\mathcal{G}^0)$  that map into  $\sigma$ . Their images reveal the subdivision of  $\sigma$ .  $\square$

Lemma 4.3.3 shows that each (aaaa) cone of the Naruki fan  $\text{trop}(\mathcal{Y}^0)$  is divided into 24 subcones, and each (aaab) cone is divided into 6 subcones. Thus, the total number of cones in the subdivision is  $24 \times 135 + 6 \times 1080 = 9720$ . For the base points in the interior of a cone, the fibers are contained in the same set of cones in  $\text{trop}(\mathcal{G}^0)$ . The fiber changes continuously as the base point changes. Therefore, moving the base point around the interior of a cone simply changes the metric but not the combinatorial type of marked tropical cubic surface.

**Corollary 4.3.4.** *The map  $\text{trop}(\mathcal{G}^0) \rightarrow \text{trop}(\mathcal{Y}^0)$  has at most two combinatorial types of generic fibers up to relabeling.*

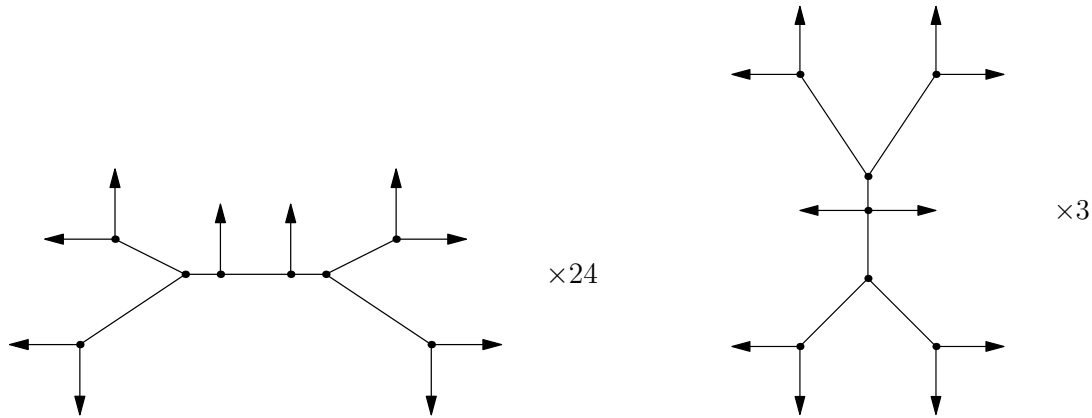


Figure 4.4: The 27 trees on tropical cubic surfaces of type (aaaa)

*Proof.* We fixed an inclusion  $E_6 \hookrightarrow E_7$  in (4.11). The action of  $\text{Stab}_{E_6}(W(E_7))$  on the fans is compatible with the entire commutative diagram (4.14). Hence, the fibers over two points that are conjugate under this action have the same combinatorial type. We verify that the 9720 cones form exactly two orbits under this action. One orbit consists of the cones in the type (aaaa) cones, and the other consists of the cones in the type (aaab) cones. Therefore, there are at most two combinatorial types, one for each orbit.  $\square$

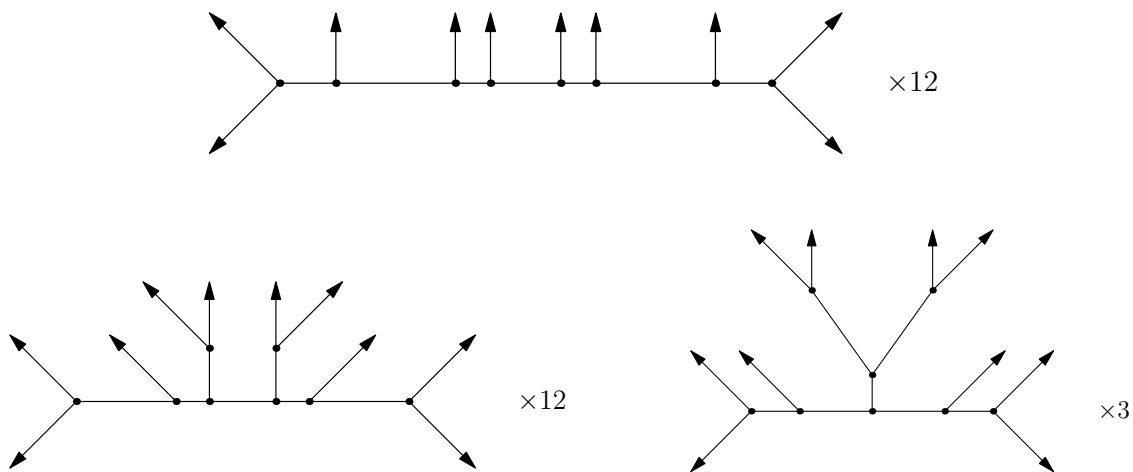


Figure 4.5: The 27 trees on tropical cubic surfaces of type (aaab)

We can now derive our classification theorem for tropical cubic surfaces.

*Proof of Theorem 4.1.1.* We compute the two types of fibers of  $\pi : \text{trop}(\mathcal{G}^0) \rightarrow \text{trop}(\mathcal{Y}^0)$ . In what follows we explain this for a cone  $\sigma$  of type (aaaa). The computation for type

(aaab) is similar. Let  $\mathbf{r}_1, \mathbf{r}_2, \mathbf{r}_3, \mathbf{r}_4$  denote the rays that generate  $\sigma$ . We fix the vector  $\mathbf{x} = \mathbf{r}_1 + 2\mathbf{r}_2 + 3\mathbf{r}_3 + 4\mathbf{r}_4$  that lies in the interior of a cone in the barycentric subdivision.

The fiber  $\pi^{-1}(\mathbf{x})$  is found by an explicit computation. First we determine the directions of the rays. They arise from rays of  $\text{trop}(\mathcal{G}^0)$  that are mapped to zero by  $\pi$ . There are 27 such ray directions in  $\pi^{-1}(\mathbf{x})$ . These are exactly the image of the 27 type  $A_1$  rays in  $\text{Berg}(E_7)$  that correspond to the roots in  $E_7 \setminus E_6$ . We label them by  $E_i, F_{ij}, G_j$  as in (4.13). Next, we compute the vertices of  $\pi^{-1}(\mathbf{x})$ . They are contained in 4-dimensional cones  $\sigma' = \text{pos}\{\mathbf{R}_1, \mathbf{R}_2, \mathbf{R}_3, \mathbf{R}_4\}$  with  $\mathbf{x} \in \pi(\sigma')$ . The coordinates of each vertex in  $\mathbb{TP}^{134}$  is computed by solving  $y_1\pi(\mathbf{R}_1) + y_2\pi(\mathbf{R}_2) + y_3\pi(\mathbf{R}_3) + y_4\pi(\mathbf{R}_4) = \mathbf{x}$  for  $y_1, y_2, y_3, y_4$ .

The part of the fiber contained in each cone in  $\text{trop}(\mathcal{G}^0)$  is spanned by the vertices and the  $E_i, F_{ij}, G_j$  rays it contains. Iterating through the list of cones and looking at this data, we get a list that characterizes the polyhedral complex  $\pi^{-1}(\mathbf{x})$ . In particular, that list verifies that  $\pi^{-1}(\mathbf{x})$  is 2-dimensional and has the promised f-vector. For each of the 27 ray directions  $E_i, F_{ij}, G_j$ , there is a tree at infinity. It is the link of the corresponding point at infinity  $\pi^{-1}(\mathbf{x}) \subset \mathbb{TP}^{134}$ . The combinatorial types of these 27 trees are shown in Figure 4.4. The metric on each tree can be computed as follows: the length of a bounded edge equals the lattice distance between the two vertices in the corresponding flap.

The surface  $\pi^{-1}(\mathbf{x})$  is homotopy equivalent to its bounded complex. We check directly that the bounded complex is contractible. This can also be inferred from Theorem 4.4.4.  $\square$

**Remark 4.3.5.** We may replace  $\mathbf{x} = \mathbf{r}_1 + 2\mathbf{r}_2 + 3\mathbf{r}_3 + 4\mathbf{r}_4$  with a generic point  $\mathbf{x} = x_1\mathbf{r}_1 + x_2\mathbf{r}_2 + x_3\mathbf{r}_3 + x_4\mathbf{r}_4$ , where  $x_1 < x_2 < x_3 < x_4$ . This lies in the same cone in the barycentric subdivision, so the combinatorics of  $\pi^{-1}(\mathbf{x})$  remains the same. Repeating the last step over the field  $\mathbb{Q}(x_1, x_2, x_3, x_4)$  instead of  $\mathbb{Q}$ , we write the length of each bounded edge in the 27 trees in terms of the parameters. Each length either equals  $x_1, x_2, x_3, x_4$  or is  $x_i - x_j$  for some  $i, j$ . The complete data on the 27 trees are given in Appendix A.

## 4.4 Modifications

In Section 4.2 we computed tropical varieties from polynomial ideals, along the lines of the book by Maclagan and Sturmfels [62]. We now turn to tropical geometry as a self-contained subject in its own right. This is the approach presented in the book by Mikhalkin and Rau [64]. Central to that approach is the notion of tropical modifications. In this section we explain how to construct our tropical del Pezzo surfaces from the flat plane  $\mathbb{R}^2$  by modifications. This leads to proofs of Proposition 4.1.2 and Theorem 4.1.1 purely within tropical geometry.

*Modification* is an operation that relates topologically different tropical models of the same variety. This operation was first defined by Mikhalkin in [63]; see also [64, Chapter 5]. Here we work with a variant known as *open modifications*. These were introduced in the context of Bergman fans of matroids in [81]. They were also used by Brugallé and Lopez de Medrano [19] to study intersections and inflection points of tropical plane curves.

We fix a tropical cycle  $Y$  in  $\mathbb{R}^n$ , as in [64]. An *open modification* is a map  $p : Y' \rightarrow Y$  where  $Y' \subset \mathbb{R}^{n+1}$  is a new tropical variety to be described below. One should think of  $Y'$  as being an embedding of the complement of a divisor in  $Y$  into a higher-dimensional torus.

Consider a piecewise integer affine function  $g : Y \rightarrow \mathbb{R}$ . The graph

$$\Gamma_g(Y) = \{(y, g(y)) \mid y \in Y\} \subset \mathbb{R}^{n+1}$$

is a polyhedral complex which does not usually satisfy the balancing condition. There is a canonical way to turn  $\Gamma_g(Y)$  into a balanced complex. If  $\Gamma_g(Y)$  is unbalanced around a codimension one face  $E$ , then we attach to it a new unbounded facet  $F_E$  in direction  $-e_{n+1}$ . (We here use the max convention, as in [64]). The facet  $F_E$  can be equipped with a unique weight  $w_{F_E} \in \mathbb{Z}$  such that the complex obtained by adding  $F_E$  is balanced at  $E$ . The resulting tropical cycle is  $Y' \subset \mathbb{R}^{n+1}$ . By definition, the *open modification* of  $Y$  given by  $g$  is the map  $p : Y' \rightarrow Y$ , where  $p$  comes from the projection  $\mathbb{R}^{n+1} \rightarrow \mathbb{R}^n$  with kernel  $\mathbb{R}e_{n+1}$ .

The *tropical divisor*  $\text{Div}_Y(g)$  consists of all points  $y \in Y$  such that  $p^{-1}(y)$  is infinite. This is a polyhedral complex. It inherits weights on its top-dimensional faces from those of  $Y'$ . A tropical cycle is *effective* if the weights of its top-dimensional faces are positive. Therefore, the cycle  $Y'$  is effective if and only if  $Y$  and the divisor  $\text{Div}_Y(g)$  are effective. Given a tropical variety  $Y$  and an effective divisor  $\text{Div}_Y(g)$ , we say the *modification*  $p : Y' \rightarrow Y$  is *along*  $\text{Div}_Y(g)$ . See [63, 64, 81] for details and examples concerning divisors and modifications.

Open tropical modifications are related to re-embeddings of classical varieties as follows. Fix a very affine  $K$ -variety  $X \subset (\bar{K}^*)^n$  and  $Y = \text{trop}(X) \subset \mathbb{R}^n$ . Given a polynomial function  $f \in K[X]$ , let  $D$  be its divisor in  $X$ . Then  $X \setminus D$  is isomorphic to the graph of the restriction of  $f$  to  $X \setminus D$ . In this manner, the function  $f$  gives a closed embedding of  $X \setminus D$  into  $(\bar{K}^*)^{n+1}$ .

**Proposition 4.4.1.** *Let  $X \subset (\bar{K}^*)^n$ ,  $f \in K[X]$ ,  $D = \text{div}_X(f)$ ,  $X' = X \setminus D \subset (\bar{K}^*)^{n+1}$ ,  $Y = \text{trop}(X) \subset \mathbb{R}^n$ ,  $Y' = \text{trop}(X') \subset \mathbb{R}^{n+1}$ , and suppose that all facets of  $Y$  have weight one. There exists a piecewise integer affine function  $g : Y \rightarrow \mathbb{R}$  such that  $\text{Div}_Y(g) = \text{trop}(D)$  and the coordinate projection  $Y' \rightarrow Y$  is the open modification of  $Y$  along that divisor.*

*Proof.* That  $Y'$  maps onto  $Y$  under the coordinate projection  $p : \mathbb{R}^{n+1} \rightarrow \mathbb{R}^n$  is clear since the tropicalization map is coordinate-wise. We next show that the fiber over a point  $y \in Y$  is either a single point or a half-line in the  $-e_{n+1}$  direction. This is a simple application of the balancing condition and the assumption that  $Y$  has weight one facets. Firstly,  $Y'$  induces a polyhedral subdivision  $\mathcal{S}(Y)$  of  $Y$  via the coordinate projection  $p$ . Let  $F$  be a facet of this subdivision, then  $p^{-1}(F)$  must be a unique facet of  $Y'$  since all facets of  $Y$  are of weight one.

Now, let  $E$  be an open codimension one face in  $\mathcal{S}(Y)$ , and let  $F_1, \dots, F_l$  be the facets of  $\mathcal{S}(Y)$  that contain  $E$ . The preimage of  $E$  cannot consist of more than one codimension one face of  $Y'$ , since otherwise these faces would be adjacent to some collection of facets of  $Y'$  whose projections would necessarily overlap with  $F_1, \dots, F_l$ , again violating the weight one condition. Therefore, the preimage of  $E$  is either a single face of codimension one in  $Y'$  or it is a facet of  $Y'$  which is parallel to  $e_{n+1}$ . Moreover, it cannot be a bounded facet since then there would be another codimension one face in the preimage of  $E$ . Also, since

$f \in K[X]$  is a regular function,  $Y'$  cannot have any unbounded faces in the  $+e_{n+1}$  direction. Thus the only other possible preimage  $p^{-1}(E)$  is an unbounded face in the  $-e_{n+1}$  direction. This occurs if and only if  $E \subset \text{trop}(D)$ . Therefore, we have determined all facets of  $Y'$ , by taking their closure we obtain  $Y'$ . Finally, we obtain the piecewise integer affine function  $g$  by taking  $g(y) = p^{-1}(y)$  for  $y \in Y \setminus \text{trop}(D)$  and then extending by continuity to the rest of  $Y$ . Then  $Y'$  is the tropical modification along the function  $g$  which was described above.  $\square$

Any two tropical rational functions  $g$  and  $g'$  that define the same tropical divisor on  $Y$  must differ by a map which is integer affine on  $Y$ . This leads to the following conclusion.

**Corollary 4.4.2.** *Under the assumptions of Proposition 4.4.1, the tropicalization of  $X' = X \setminus D \subset \mathbb{R}^{n+1}$  is determined uniquely by those of  $D$  and  $X$ , up to an integer affine map.*

It is generally not the case that  $\text{trop}(X')$  is determined by the tropical hypersurface of  $f \in K[X]$ , as the tropicalization of the divisor  $D = \text{div}_X(f)$  may differ from the stable intersection of  $\text{trop}(X')$  and the tropical hypersurface. Examples 4.2 and 4.3 of [19] demonstrate both this and that Proposition 4.4.1 can fail without the weight one hypothesis.

Suppose now that  $X' \subset (\bar{K}^*)^{n+k}$  is obtained from  $X \subset (\bar{K}^*)^n$  by taking the graph of a list of  $k \geq 2$  polynomials  $f_1, f_2, \dots, f_k$ . This gives us a sequence of projections

$$X' = X_k \rightarrow X_{k-1} \rightarrow \dots \rightarrow X_2 \rightarrow X_1 \rightarrow X_0 = X, \tag{4.15}$$

where  $X_i \subset (\bar{K}^*)^{n+i}$  is obtained from  $X$  by taking the graph of  $(f_1, \dots, f_i)$ . We further get a corresponding sequence of projections of the tropicalizations:

$$\text{trop}(X') = \text{trop}(X_k) \rightarrow \text{trop}(X_{k-1}) \rightarrow \dots \rightarrow \text{trop}(X_0) = \text{trop}(X). \tag{4.16}$$

We may ask if it is possible to recover  $\text{trop}(X') \subset \mathbb{R}^{n+k}$  just from  $\text{trop}(X)$  and its  $k$  tropical divisors  $\text{trop}(D_i)$ . For example, this is possible in the special case when  $\text{trop}(X) = \mathbb{R}^n$  and the arrangement of divisors  $\text{trop}(D_i)$  intersect properly, meaning the intersection of any  $k$  of the tropical divisors is always of codimension  $k$ . However, in general, iterating modifications to recover  $\text{trop}(X')$  can be a delicate procedure. In most cases, the outcome is not solely determined by the configuration of tropical divisors in  $\text{trop}(X)$ , even if the divisors intersect pairwise properly. We illustrate this by deriving the degree 5 del Pezzo surface  $\text{trop}(M_{0,5})$ .

**Example 4.4.3.** This is a variation on [81, Example 2.29]. Let  $X = (\bar{K}^*)^2$  and consider the functions  $f(x) = x_1 - 1$ ,  $g(x) = x_2 - 1$  and  $h(x) = ax_1 - x_2$ , for some constant  $a \in K^*$  with  $\text{val}(a) = 0$ . Denote  $\text{div}_X(f)$  by  $F$ , and analogously for  $G$  and  $H$ . The tropicalization of each divisor is a line through the origin in  $\mathbb{R}^2$ . The directions of  $\text{trop}(F)$ ,  $\text{trop}(G)$ , and  $\text{trop}(H)$  are  $(1, 0)$ ,  $(0, 1)$ , and  $(1, 1)$  respectively. Let  $X' \subset (\bar{K}^*)^5$  denote the graph of  $X$  along the three functions  $f, g$ , and  $h$ , in that order. This defines a sequence of projections,

$$X' \longrightarrow X_2 \longrightarrow X_1 \longrightarrow X = (\bar{K}^*)^2.$$



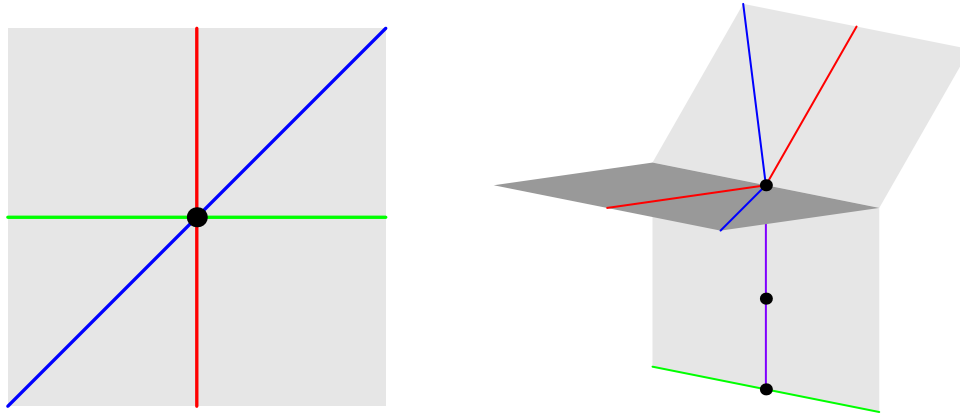


Figure 4.6: The tropical divisors in Example 4.4.3. The positions of  $\text{trop}(G_1 \cap H_1)$  in  $\text{trop}(X_1)$  for three choices of  $a$  are marked on the downward purple edge. For  $a = 1$  we get  $M_{0,5}$ .

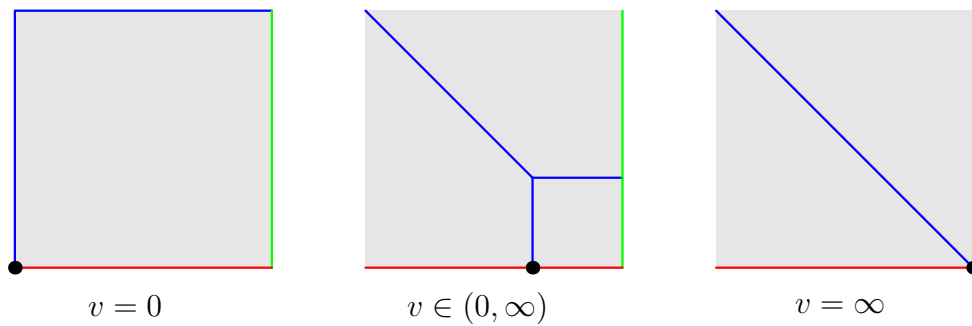


Figure 4.7: The different possibilities for  $\text{trop}(H_2) \cap \sigma$  in Example 4.4.3

Here,  $X_2 = \{(x_1, x_2, x_1 - 1, x_2 - 1)\} \subset (\bar{K}^*)^4$ . The tropical plane  $\text{trop}(X_2)$  contains the cone  $\sigma = \{0\} \times \{0\} \times (-\infty, 0] \times (-\infty, 0]$ , corresponding to points with  $\text{val}(x_1) = \text{val}(x_2) = 0$ . Let  $H_2$  denote the graph of  $f$  and  $g$  restricted to  $H$ . This is a line in 4-space, namely,

$$H_2 = \{(x_1, ax_1, x_1 - 1, ax_1 - 1)\} \subset X_2 \subset (\bar{K}^*)^4.$$

The tropical line  $\text{trop}(H_2)$  depends on the valuation of  $a - 1$ . It can be determined from

$$\text{trop}(G_1 \cap H_1) = \left\{ \left( 0, 0, -\text{val}\left(\frac{1}{a} - 1\right) \right) \right\}.$$

Here,  $H_1, G_1$  denote the graph of  $f$  restricted to  $H$  and  $G$ , respectively. Figure 4.6 shows the possibilities for  $\text{trop}(G_1 \cap H_1)$  in  $\text{trop}(X_1)$ . Figure 4.7 shows  $\text{trop}(H_2) \cap \sigma$  in  $\text{trop}(X_2)$ .

We can prescribe any value  $v \in (0, \infty)$  for the valuation of  $\frac{1}{a} - 1$ , for instance by taking  $\frac{1}{a} = 1 + t^v$  when  $K = \mathbb{C}\{\{t\}\}$ . In these cases, the tropical plane  $\text{trop}(X')$  is not a fan. However, it becomes a fan when  $v$  moves to either endpoint of the interval  $[0, -\infty]$ . For instance,  $v = 0$  happens when the constant term of  $\frac{1}{a}$  is not equal to 1 and  $\text{trop}(X')$  is the

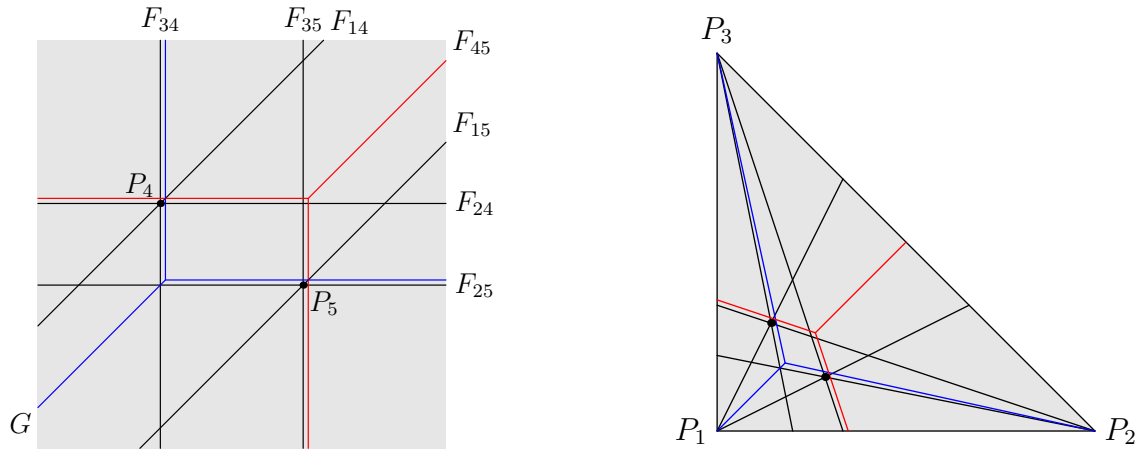


Figure 4.8: The tropical conic and the tropical lines determined by the 5 points for a marked del Pezzo surface of degree 4. The diagram is drawn in  $\mathbb{R}^2$  on the left and in  $\mathbb{TP}^2$  on the right. The 16 trivalent trees in Figure 4.1 arise from the plane curves shown here by modifications.

fan obtained from  $\mathbb{R}^2$  by *stable modification* along the three tropical divisors, shown on the left in Figure 4.6. The other extreme is when  $a = 1$ . Here,  $F, G, H$  are concurrent lines in  $(\bar{K}^*)^2$ , and  $\text{trop}(H_2)$  contains a ray in the direction  $e_3 + e_4$ . Upon modification, we obtain the fan over the Petersen graph in Figure 4.3. This is the tropicalization of the degree 5 del Pezzo surface in (4.4). Thus beginning from the tropical divisors  $\text{trop}(F), \text{trop}(G)$ , and  $\text{trop}(H)$  in  $\mathbb{R}^2$ , we recover  $\text{trop}(M_{0,5})$  if we also insist that they represent concurrent lines in  $(\bar{K}^*)^2$ .  $\diamond$

In Example 4.4.3, knowing simply the position of the three tropical divisors in  $\mathbb{R}^2$  was not sufficient to determine  $\text{trop}(X')$ . However, if we insist that the initial divisors  $F, G, H$  in  $(\bar{K}^*)^2$  are concurrent, then the tropical surface in  $\mathbb{R}^5$  is unique; it must be the Petersen fan.

We now explain how this extends to a del Pezzo surface  $X$  of degree  $d \leq 4$ . As before, we write  $X^0$  for the complement of the  $(-1)$ -curves in  $X$ . Then  $X' = X^0$  is obtained from  $(\bar{K}^*)^2$  by taking the graphs of the polynomials  $f_1, \dots, f_k$  of the curves in  $(\bar{K}^*)^2$  that give rise to  $(-1)$ -curves on  $X$ . More precisely, fix  $p_1 = (1 : 0 : 0)$ ,  $p_2 = (0 : 1 : 0)$ ,  $p_3 = (0 : 0 : 1)$ ,  $p_4 = (1 : 1 : 1)$ , and take  $p_5, \dots, p_{9-d}$  to be general points in  $\mathbb{P}^2$ . If  $d = 4$  then there is only one extra point  $p_5$ , we have  $k = 8$  in (4.15), and  $f_1, \dots, f_8$  are the polynomials defining

$$F_{14}, F_{15}, F_{24}, F_{25}, F_{34}, F_{35}, F_{45}, G. \tag{4.17}$$

For  $d = 3$ , there are two extra points  $p_5, p_6$  in  $X$ , we have  $k = 18$ , and  $f_1, \dots, f_{18}$  represent

$$F_{14}, F_{15}, F_{16}, F_{24}, F_{25}, F_{26}, F_{34}, F_{35}, F_{36}, F_{45}, F_{46}, F_{56}, G_1, G_2, G_3, G_4, G_5, G_6. \tag{4.18}$$

We write  $P_i = \text{trop}(p_i) \in \mathbb{TP}^2$  for the image of the point  $p_i$  under tropicalization. The tropical points  $P_1, P_2, \dots$  are in *general position* if any two lie in a unique tropical line, these

lines are distinct, any five lie in a unique tropical conic, and these conics are distinct in  $\mathbb{TP}^2$ . A configuration in general position for  $d = 4$  is shown in Figure 4.8. Our next result implies that the colored Clebsch graph in Figure 4.1 can be read off from Figure 4.8 alone. For  $d = 3$ , in order to recover the tropical cubic surface from the planar configuration, the points  $P_i$  must satisfy further genericity assumptions, to be revealed in the proof of the next theorem.

**Theorem 4.4.4.** *Fix  $d \in \{3, 4, 5\}$  and points  $p_1, \dots, p_{9-d}$  in  $\mathbb{P}^2$  whose tropicalizations  $P_i$  are sufficiently generic in  $\mathbb{TP}^2$ . The tropical del Pezzo surface  $\text{trop}(X^0)$  can be constructed from  $\mathbb{TP}^2$  by a sequence of open modifications that is determined by the points  $P_1, \dots, P_{9-d}$ .*

*Proof.* The sequence of modifications we use to go from  $\mathbb{R}^2$  to  $\text{trop}(X^0)$  is determined if we know, for each  $i$ , the correct divisor on each  $(-1)$ -curve  $C$  in the tropical model  $\text{trop}(X_i)$ . Then, the preimage of  $C$  in the next surface  $\text{trop}(X_{i+1})$  is the modification  $C'$  of the curve  $C$  along that divisor. With this, Theorem 4.4.4 follows from Proposition 4.4.1, applied to both the  $i$ -th surface and its  $(-1)$ -curves. The case of degree  $d = 5$  was covered in Example 4.4.3. From the metric tree that represents the boundary divisor  $C$  of  $X^0$  we can derive the corresponding trees on each intermediate surface  $\text{trop}(X_i)$  by deleting leaves. Thus, to establish Theorem 4.4.4, it suffices to prove the following claim: *the final arrangement of the (16 or 27) metric trees on  $\text{trop}(X^0)$  is determined by the locations of the points  $P_i$  in  $\mathbb{TP}^2$ .*

Consider first the case  $d = 4$ . The points  $P_4$  and  $P_5$  determine an arrangement of plane tropical curves (4.17) as shown in Figure 4.8. The conic  $G$  through all five points looks like an “inverted tropical line”, with three rays in directions  $P_1, P_2, P_3$ . By the genericity assumption, the points  $P_4$  and  $P_5$  are located on distinct rays of  $G$ . These data determine a trivalent metric tree with five leaves, which we now label by  $E_1, E_2, E_3, E_4, E_5$ . Namely,  $P_4$  forms a cherry together with the label of its ray, and ditto for  $P_5$ . For instance, in Figure 4.8, the cherries on the tree  $G$  are  $\{E_1, E_4\}$  and  $\{E_2, E_5\}$ , while  $E_3$  is the non-cherry leaf. This is precisely the tree sitting on the node labeled  $G$  in Figure 4.1. The lengths of the two bounded edges of the tree  $G$  are the distances from  $P_4$  resp.  $P_5$  to the unique vertex of the conic  $G$  in  $\mathbb{R}^2$ . Thus the metric tree  $G$  is easily determined from  $P_4$  and  $P_5$ . The other 15 metric trees can also be determined in a similar way from the configuration of points and curves in  $\mathbb{R}^2$  and by performing a subset of the necessary modifications. Alternatively, we may use the transition rules (4.1) and (4.2) to obtain the other 15 trees from  $G$ . This proves the above claim, and hence Theorem 4.4.4, for del Pezzo surfaces of degree  $d = 4$ .

Consider now the case  $d = 3$ . Here the arrangement of tropical plane curves in  $\mathbb{R}^2 \subset \mathbb{TP}^2$  consists of three lines at infinity,  $F_{12}, F_{13}, F_{23}$ , nine straight lines,  $F_{14}, F_{15}, \dots, F_{36}$ , three honest tropical lines,  $F_{45}, F_{46}, F_{56}$ , three conics that are “inverted tropical lines”  $G_4, G_5, G_6$ , and three conics with one bounded edge,  $G_1, G_2, G_3$ . Each of these looks like a tree already in the plane, and it gets modified to a 10-leaf tree, like to ones in Figures 4.4 and 4.5. We claim that these labeled metric trees are uniquely determined by the positions of  $P_4, P_5, P_6$  in  $\mathbb{R}^2$ .

Consider one of the 9 straight lines in our arrangement, say,  $F_{14}$ . If the points  $P_4, P_5, P_6$  are generically chosen, 7 of the 10 leaves on the tree  $F_{ij}$  can be determined from the diagram

in  $\mathbb{R}^2$ . These come from the 7 markings on the line  $F_{14}$  given by  $E_1, E_4, F_{23}, F_{25}, F_{26}, F_{35}, F_{36}$ . The markings  $E_1$  and  $F_{23}$  are the points at infinity, the marking  $E_4$  is the location of point  $P_4$ , and the markings  $F_{25}, F_{26}, F_{35}, F_{36}$  are the points of intersection with those lines. Under our hypothesis, these 7 marked points on the line  $F_{14}$  will be distinct. With this,  $F_{14}$  is already a metric caterpillar tree with 7 leaves. The three markings which are missing are  $G_1, G_4$  and  $F_{56}$ . Depending on the positions of  $P_4, P_5, P_6$ , the intersection points of these three curves with the line  $F_{14}$  may coincide with previously marked points. Whenever this happens, the position of the additional marking on the tree  $F_{14}$  can be anywhere on the already attached leaf ray. Again, the actual position of the point on that ray may be determined by performing modifications along those curves. Alternatively, we use the involution given in Corollary 4.2.3. The involution on the ten leaves of the desired tree  $F_{14}$  is

$$E_1 \leftrightarrow \underline{G_4}, \quad E_4 \leftrightarrow \underline{G_1}, \quad F_{23} \leftrightarrow \underline{F_{56}}, \quad F_{25} \leftrightarrow F_{36}, \quad F_{26} \leftrightarrow F_{35}.$$

Since the involution exchanges each of the three unknown leaves with one of the seven known leaves, we can easily construct the final 10-leaf tree from the 7-leaf caterpillar.

A similar argument works the other six lines  $F_{ij}$ , and the conics  $G_4, G_5, G_6$ . In these cases, 8 of the 10 marked points on a tree are determined from the arrangement in the plane, provided the choice of points is generic. Finally, the conics  $G_1, G_2, G_3$  are dual to subdivisions of lattice parallelograms of area 1. They may contain a bounded edge. Suppose no point  $P_j$  lies on the bounded edge of the conic  $G_i$ , then the positions of all 10 marked points of the tree are visible from the arrangement in the plane. If  $G_i$  does contain a marked point  $P_j$  on its bounded edge, then the tropical line  $F_{ij}$  intersects  $G_i$  in either a bounded edge or a single point with intersection multiplicity 2, depending on the dual subdivision of  $G_i$ . In the first case the position of the marked point  $F_{ij}$  is easily determined from the involution; the distance from a vertex of the bounded edge of  $G_i$  to the marked point  $F_{ij}$  must be equal to the distance from  $P_j$  to the opposite vertex of the bounded edge of  $G_i$ .

If  $G_i \cap F_{ij}$  is a single point of intersection multiplicity two, then  $P_j$  and  $F_{ij}$  form a cherry on the tree  $G_i$  which is invariant under the involution. We claim that this cherry attaches to the rest of the tree at a 4-valent vertex. The involution on the 10-leaf tree can also be seen as a tropical double cover from our 10-leaf tree to a 5-leaf tree,  $h : T \rightarrow t$ , where the 5-leaf tree  $t$  is labeled with the pair of markings interchanged by the involution. As mentioned in Corollary 4.2.3, this double cover comes from the classical curve in the del Pezzo surface  $X$ . In particular, the double cover locally satisfies the tropical translation of the Riemann-Hurwitz condition [12, Definition 2.2]. In our simple case of a degree 2 map between two trees, this local condition for a vertex  $v$  of  $T$  is  $\deg(v) - d_{h,v}(\deg(h(v)) - 2) - 2 \geq 0$ , where  $\deg$  denotes the valency of a vertex, and  $d_{h,v}$  denotes the local degree of the map  $h$  at  $v$ . Suppose the two leaves did not attach at a four valent vertex, then they form a cherry, this cherry attaches to the rest of the tree by an edge  $e$  which is adjacent to another vertex  $v$  of the tree. The Riemann-Hurwitz condition is violated at  $v$ , since  $\deg(v) = \deg(h(v)) = 3$  and  $d_{h,v} = 2$ .

We conclude that the tree arrangement can be recovered from the position of the points  $P_1, P_2, \dots$  in  $\mathbb{R}^2$ . Therefore it is also compute to recover the tropical del Pezzo surface

$\text{trop}(X^0)$  by open modifications. In each case, we recover the corresponding final 10 leaf tree from the arrangement in  $\mathbb{TP}^2$  plus our knowledge of the involution in Corollary 4.2.3.  $\square$

**Remark 4.4.5.** Like in the case  $d = 4$ , knowledge of transition rules among the 27 metric trees on  $\text{trop}(X^0)$  can greatly simplify their reconstruction. We give such a rule in Proposition 4.5.2.

In this section we gave a geometric construction of tropical del Pezzo surfaces of degree  $d \geq 3$ , starting from a configuration of points  $P_1, \dots, P_{9-d}$  in the tropical plane  $\mathbb{TP}^2$ . The lines and conics in  $\mathbb{TP}^2$  that correspond to the  $(-1)$ -curves are transformed, by a sequence of open modifications, into the trees that make up the boundary of the del Pezzo surface. Knowing these well-specified modifications of curves ahead of time allows us to carry out a unique sequence of open modifications of surfaces, starting with  $\mathbb{R}^2$ . In each step, going from right to left in (4.15), we modify the surface along a divisor given by one of the trees.

This gives a geometric construction for the bounded complex in a tropical del Pezzo surface: it is the preimage under (4.15) of the bounded complex in the arrangement in  $\mathbb{R}^2$ . For instance, Figure 4.2 is the preimage of the parallelogram and the four triangles in Figure 4.8.

The same modification approach can be used to construct (the bounded complexes of) any tropical plane in  $\mathbb{TP}^n$  from its tree arrangement. This provides a direct link between the papers [53] and [81]. That link should be useful for readers of the text books [62] and [64].

## 4.5 Tropical Cubic Surfaces and their 27 Trees

This section is devoted to the combinatorial structure of tropical cubic surfaces. Throughout,  $X$  is a smooth del Pezzo surface of degree 3, without Eckhart points, and  $X^0$  the very affine surface obtained by removing the 27 lines from  $X$ . Going well beyond the summary statistics of Theorem 4.1.1, we now offer an in-depth study of the combinatorics of the surface  $\text{trop}(X^0)$ .

We begin with the construction of  $\text{trop}(X^0)$  from six points in  $\mathbb{TP}^2$ , as in Section 4.4. The points  $P_5$  and  $P_6$  are general in  $\mathbb{R}^2 \subset \mathbb{TP}^2$ . The first four points are the coordinate points

$$P_1 = (0 : -\infty : -\infty), P_2 = (-\infty : 0 : -\infty), P_3 = (-\infty : -\infty : 0), P_4 = (0 : 0 : 0). \quad (4.19)$$

Theorem 4.4.4 tells us that  $\text{trop}(X^0)$  is determined by the locations of  $P_5$  and  $P_6$  when the points are generically chosen. There are two generic types, namely (aaaa) and (aaab), as shown in Figures 4.4 and 4.5. This raises the question of how the type can be decided from the positions of  $P_5$  and  $P_6$ . To answer that question, we shall use *tropical convexity* [62, §5.2]. Recall that there are five generic types of tropical triangles, depicted e.g. in [24, Figure 6(i)]. The unique 2-cell in such a tropical triangle has either 3, 4, 5 or 6 vertices. Two of these have 4 vertices, but only one type contains a parallelogram. That is the type which gives (aaaa).

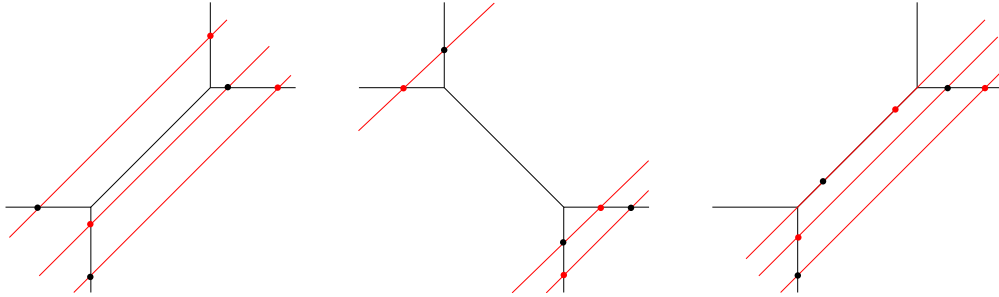


Figure 4.9: Markings of a conic  $G_1$  which produce trees of type (aaab).

**Theorem 4.5.1.** *Suppose that the tropical cubic surface constructed as in Theorem 4.4.4 has one of the two generic types. Then it has type (aaaa) if and only if the 2-cell in the tropical triangle spanned by  $P_4, P_5$  and  $P_6$  is a parallelogram. In all other cases, it has type (aaab).*

Note that the condition that the six points  $P_i$  are in general position is not sufficient to imply that the tropical cubic surface is generic. In some cases, the corresponding point in the Naruki fan  $\text{trop}(\mathcal{Y}^0)$  will lie on the boundary of the subdivision induced by the map from  $\text{trop}(\mathcal{G}^0)$ , as described in Section 4.3 and below. If so, the tropical cubic surface is degenerate.

*Proof of Theorem 4.5.1.* The tree arrangements for the two types of generic surfaces consist of distinct combinatorial types, i.e. there is no overlap in Figures 4.4 and 4.5. Therefore, when the tropical cubic surface is generic, it is enough to determine the combinatorial type of a single tree. We do this for the conic  $G_1$ . Given our choices of points (4.19) in  $\mathbb{TP}^2$ , the tropical conic  $G_1$  is dual to the Newton polygon with vertices  $(0, 0)$ ,  $(1, 0)$ ,  $(0, 1)$ , and  $(1, 1)$ . The triangulation has one interior edge, either of slope 1 or of slope  $-1$ . We claim the following:

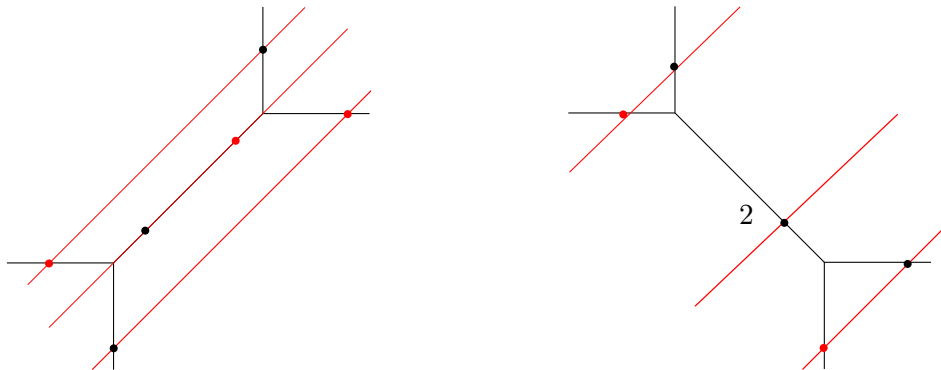


Figure 4.10: Markings of a conic  $G_1$  which produce trees of type (aaaa).

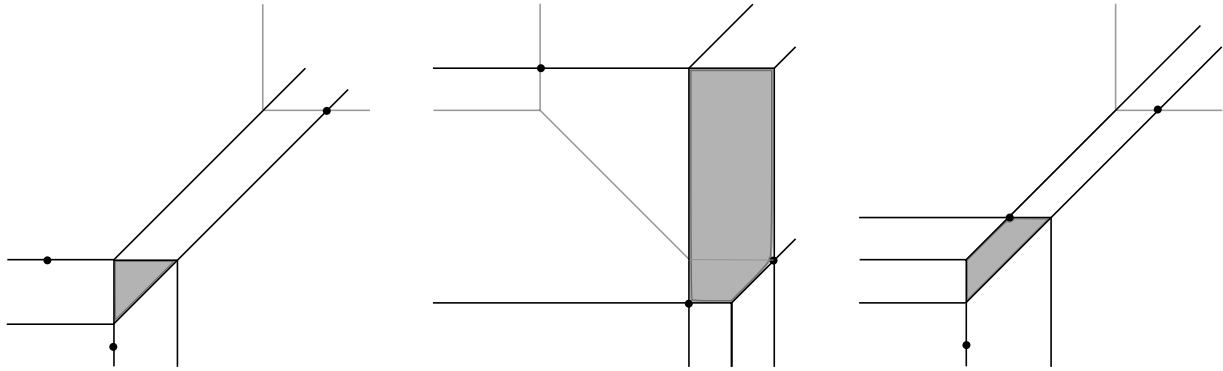


Figure 4.11: The tropical triangles formed by points on  $G_1$  as in Figure 4.9, giving type (aaab).

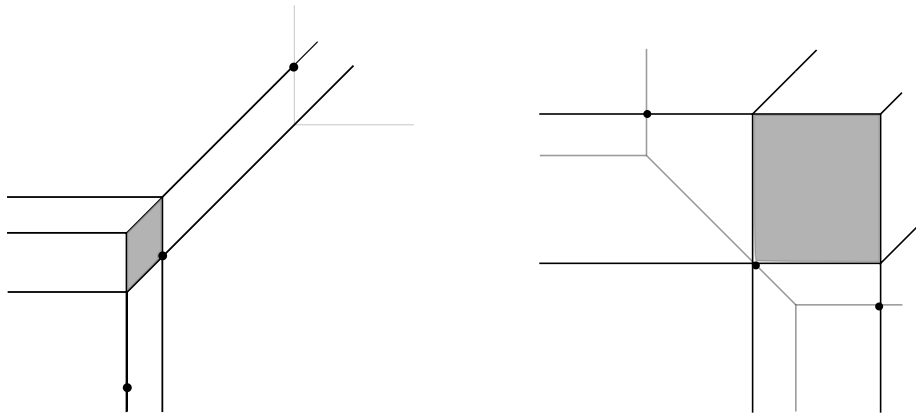


Figure 4.12: The tropical triangles formed by points on  $G_1$  as in Figure 4.10, giving type (aaaa).

*The tropical cubic surface  $\text{trop}(X^0)$  has type (aaaa) if and only if the following holds:*

1. *The bounded edge of the conic  $G_1$  has slope  $-1$  and contains a marked point  $P_j$ , or*
2. *the bounded edge of the conic  $G_1$  has slope  $1$  and contains a marked point  $P_j$ , and the other two points  $P_j, P_k$  lie on opposite sides of the line spanned by the bounded edge.*

To show this, we follow the proof of Theorem 4.4.4. For each configuration of  $P_4, P_5, P_6$  on the conic  $G_1$ , we draw lines with slope 1 through these points. These are the tropical lines  $F_{14}, F_{15}, F_{16}$ . Each intersects  $G_1$  at one further point. These are the images of  $E_4, E_5, E_6$  under the tree involution, *i.e.* the points labeled  $F_{14}, F_{15}, F_{16}$  on the tree  $G_1$ . Together with  $E_2, E_3, F_{12}$  and  $F_{13}$  lying at infinity of  $\mathbb{TP}^2$ , we can reconstruct a tree with 10 leaves. Then, we can identify the type of the tree arrangement. We did this for all possible configurations up to symmetry. Some of the results are shown in Figures 4.9 and 4.10. The claim follows.

To derive the theorem from the claim, we must consider the tropical convex hull of the points  $P_4, P_5, P_6$  in the above cases. As an example, the 2-cells of the tropical triangle corresponding to the trees in Figures 4.9 and 4.10 are shown in Figures 4.11 and 4.12 respectively.

The markings of  $G_1$  producing a type (aaaa) tree always give parallelograms. Finally, if the marking of a conic produces a type (aaab) tree then the 2-cell may have 3, 4, 5, or 6 vertices. However, if it has 4 vertices, then it is a trapezoid with only one pair of parallel edges.  $\square$

We next discuss some relations among the 27 boundary trees of a tropical cubic surface  $X$ . Any pair of disjoint  $(-1)$ -curves on  $X$  meets exactly five other  $(-1)$ -curves. Thus, two 10-leaf trees  $T$  and  $T'$  representing disjoint  $(-1)$ -curves have exactly five leaf labels in common. Let  $t$  and  $t'$  denote the 5-leaf trees constructed from  $T$  and  $T'$  as in the proof of Proposition 4.2.3. Thus  $T$  double-covers  $t$ , and  $T'$  double-covers  $t'$ . Given a subset  $E$  of the leaf labels of a tree  $T$ , we write  $T|_E$  for the subtree of  $T$  that is spanned by the leaves labeled with  $E$ .

**Proposition 4.5.2.** *Let  $T$  and  $T'$  be the trees corresponding to disjoint  $(-1)$ -curves on a cubic surface  $X$ , and  $E$  the set of five leaf labels common to  $T$  and  $T'$ . Then  $t = T'|_E$  and  $t' = T|_E$ .*

*Proof.* The five lines that meet two disjoint  $(-1)$ -curves  $C$  and  $C'$  define five points on  $C$  and five tritangent planes containing  $C'$ . The cross-ratios among the former are equal to the cross-ratios among the latter modulo  $C'$ . The proposition follows by taking valuations.  $\square$

Proposition 4.5.2 suggests a combinatorial method for recovering the entire arrangement of 27 trees on  $\text{trop}(X^0)$  from a single tree  $T$ . Namely, for any tree  $T'$  that is disjoint from  $T$ , we can recover both  $t'$  and  $T'|_E$ . Moreover, for any of the 10 trees  $T_i$  that are disjoint from both  $T$  and  $T'$ , with labels  $E_i$  common with  $T$ , we can determine  $T'|_{E_i}$  as well. Then  $T'$  is an amalgamation of  $t'$ ,  $T'|_E$ , and the 10 subtrees  $T'|_{E_i}$ . This amalgamation process is reminiscent of a tree building algorithm in phylogenetics known as *quartet puzzling* [20].

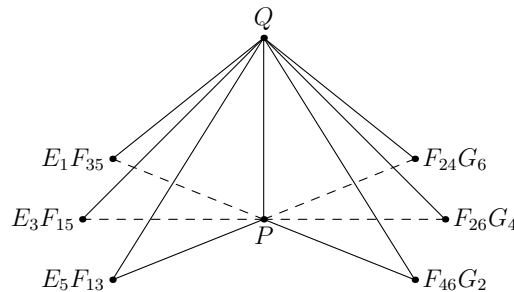


Figure 4.13: The bounded complex of the tropical cubic surface of type (a)

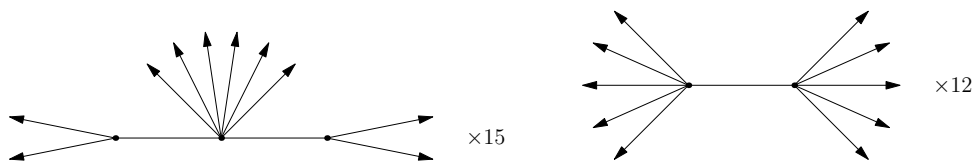


Figure 4.14: The 27 trees on the tropical cubic surface of type (a)



We next examine tropical cubic surfaces of non-generic types. These surfaces are obtained from non-generic fibers of the vertical map on the right in (4.14). We use the subdivision of the Naruki fan  $\text{trop}(\mathcal{Y}^0)$  described in Lemma 4.3.3. There are five types of rays in this subdivision. We label them (a), (b),  $(a_2)$ ,  $(a_3)$ ,  $(a_4)$ . A ray of type  $(a_k)$  is a positive linear combination of  $k$  rays of type (a). The new rays  $(a_2)$ ,  $(a_3)$ ,  $(a_4)$  form the barycentric subdivision of an (aaaa) cone. With this, the maximal cones in the subdivided Naruki fan are called  $(aa_2a_3a_4)$  and  $(aa_2a_3b)$ . They are known as the generic types (aaaa) and (aaab) in the previous sections. A list of all 24 cones, up to symmetry, is presented in the first column of Table 4.1.

The fiber of  $\text{trop}(\mathcal{G}^0) \rightarrow \text{trop}(\mathcal{Y}^0)$  over any point in the interior of a maximal cone is a tropical cubic surface. However, some special fibers have dimension 3. Such fibers contain infinitely many tropical cubic surfaces, including those with Eckhart points. Removing such Eckhart points is a key issue in [50]. We do this by considering the *stable fiber*, i.e. the limit of the generic fibers obtained by perturbing the base point by an infinitesimal. Alternatively, the tree arrangement of the stable fiber is found by setting some edge lengths to 0 in Remark 4.3.5. We computed representatives for all stable fibers. Our results are shown in Table 4.1.

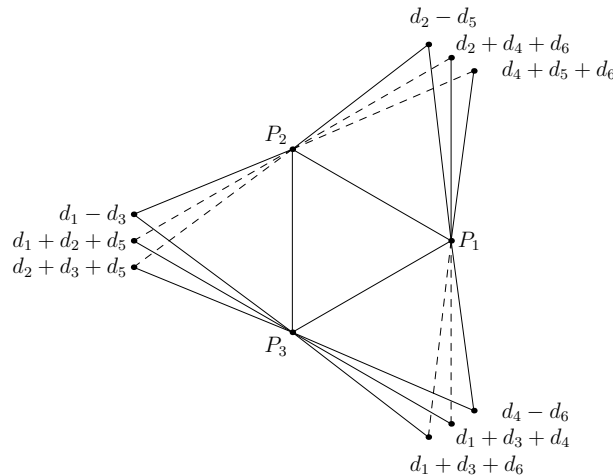


Figure 4.15: The bounded complex of the tropical cubic surface of type (b)

We explain the two simplest non-trivial cases. The 36 type (a) rays in the Naruki fan are in bijection with the 36 positive roots of  $E_6$ . Figure 4.13 shows the bounded cells in

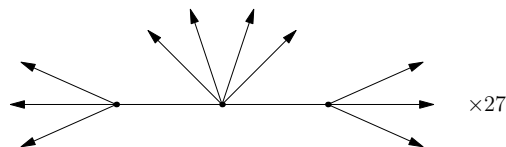


Figure 4.16: The 27 trees on the tropical cubic surface of type (b)

Type	#cones	Vertices	Edges	Rays	Triangles	Squares	Flaps	Cones
0	1	1	0	27	0	0	0	135
(a)	36	8	13	69	6	0	42	135
(a <sub>2</sub> )	270	20	37	108	14	4	81	135
(a <sub>3</sub> )	540	37	72	144	24	12	117	135
(a <sub>4</sub> )	1620	59	118	177	36	24	150	135
(b)	40	12	21	81	10	0	54	135
(aa <sub>2</sub> )	540	23	42	114	13	7	87	135
(aa <sub>3</sub> )	1620	43	82	156	22	18	129	135
(aa <sub>4</sub> )	540	68	133	195	33	33	168	135
(a <sub>2</sub> a <sub>3</sub> )	1620	43	82	156	22	18	129	135
(a <sub>2</sub> a <sub>4</sub> )	810	71	138	201	32	36	174	135
(a <sub>3</sub> a <sub>4</sub> )	540	68	133	195	33	33	168	135
(ab)	360	26	48	123	16	7	96	135
(a <sub>2</sub> b)	1080	45	86	162	24	18	135	135
(a <sub>3</sub> b)	1080	69	135	198	34	33	171	135
(aa <sub>2</sub> a <sub>3</sub> )	3240	46	87	162	21	21	135	135
(aa <sub>2</sub> a <sub>4</sub> )	1620	74	143	207	31	39	180	135
(aa <sub>3</sub> a <sub>4</sub> )	1620	74	143	207	31	39	180	135
(a <sub>2</sub> a <sub>3</sub> a <sub>4</sub> )	1620	74	143	207	31	39	180	135
(aa <sub>2</sub> b)	2160	48	91	168	23	21	141	135
(aa <sub>3</sub> b)	3240	75	145	210	32	39	183	135
(a <sub>2</sub> a <sub>3</sub> b)	3240	75	145	210	32	39	183	135
(aa <sub>2</sub> a <sub>3</sub> a <sub>4</sub> )	3240	77	148	213	30	42	186	135
(aa <sub>2</sub> a <sub>3</sub> b)	6480	78	150	216	31	42	189	135

Table 4.1: All combinatorial types of tropical cubic surfaces

the stable fiber over the (a) ray corresponding to root  $r = d_1 + d_3 + d_5$ . It consists of six triangles sharing a common edge. The two shared vertices are labeled by  $P$  and  $Q$ . Recall the identification of the roots of  $E_6$  involving  $d_7$  with the 27  $(-1)$ -curves from (4.13). Then, considering  $E_i, F_{ij}$  and  $G_i$  as roots of  $E_6$ , exactly 15 of them are orthogonal to  $r$ . The other 12 roots are

$$E_1, F_{35}; \quad E_3, F_{15}; \quad E_5, F_{13}; \quad F_{24}, G_6; \quad F_{26}, G_4; \quad F_{46}, G_2. \quad (4.20)$$

These form a *Schläfli double six*. The 36 double six configurations on a cubic surface are in bijection with the 36 positive roots of  $E_6$ . Each of the six pairs forms an  $A_2$  subroot system with  $d_1 + d_3 + d_5$ . The non-shared vertices in the (a) surface are labeled by these pairs.

The 12 rays labeled by (4.20) emanate from  $Q$ , and the other 15 rays emanate from  $P$ . Each other vertex has 7 outgoing rays, namely its labels in Figure 4.13 and the 5 roots orthogonal to both of these. Figure 4.14 shows the resulting  $27 = 12 + 15$  trees at infinity.

The 40 type (b) rays in the Naruki fan are in bijection with the type  $A_2^{\times 3}$  subroot systems in  $E_6$ . Figure 4.15 illustrates the stable fiber over a point lying on the ray corresponding to

$$\begin{aligned} d_1 - d_3, d_1 + d_2 + d_5, d_2 + d_3 + d_5, \\ d_2 - d_5, d_2 + d_4 + d_6, d_4 + d_5 + d_6, \\ d_4 - d_6, d_1 + d_3 + d_4, d_1 + d_3 + d_6. \end{aligned} \tag{4.21}$$

This is the union of three type  $A_2$  subroot systems that are pairwise orthogonal. The bounded complex consists of 10 triangles. The central triangle  $P_1P_2P_3$  has 3 other triangles attached to each edge. The 9 pendant vertices are labeled with the roots in (4.21). The 3 vertices in the triangles attached to the same edge are labeled with 3 roots in a type  $A_2$  subroot system.

Each of  $P_1, P_2$  and  $P_3$  is connected with 9 rays, labeled with the roots in  $E_7 \setminus E_6$  that are orthogonal to a type  $A_2$  subroot system in (4.21). Each of the other vertices is connected with 6 rays. The labels of these rays are the roots in  $E_7 \setminus E_6$  that are orthogonal to the label of that vertex but are not orthogonal to the other two vertices in the same group.

All of the 27 trees are isomorphic, as shown in Figure 4.16. In each tree, the 10 leaves are partitioned into  $10 = 4 + 3 + 3$ , by orthogonality with the type  $A_2$  subroot systems in (4.21). The bounded part of the tree is connected by two flaps to two edges containing the same  $P_i$ .

We close this chapter with a brief discussion of open questions and future directions. One obvious question is whether our construction can be extended to del Pezzo surfaces of degree  $d = 2$  and  $d = 1$ . In principle, this should be possible, but the complexity of the algebraic and combinatorial computations will be very high. In particular, the analogues of Theorem 4.4.4 for 7 and 8 points in  $\mathbb{TP}^2$  are likely to require rather complicated genericity hypotheses.

For  $d = 4$ , we were able compute the Naruki fan  $\text{trop}(\mathcal{Y}^0)$  without any prior knowledge, by just applying the software `gfan` to the 45 trinomials in Proposition 4.2.1. We believe that the same will work for  $d = 3$ , and that even the tropical basis property [62, §2.6] will hold:

**Conjecture 4.5.3.** *The 270 trinomial relations listed in Proposition 4.2.2 form a tropical basis.*

This chapter did not consider embeddings of del Pezzo surfaces into projective spaces. However, it would be very interesting to study these via the results obtained here. For cubic surfaces in  $\mathbb{P}^3$ , we should see a shadow of Table 4.1 in  $\mathbb{TP}^3$ . Likewise, for complete intersections of two quadrics in  $\mathbb{P}^4$ , we should see a shadow of Figures 4.1 and 4.2 in  $\mathbb{TP}^4$ . One approach is to start with the following modifications of the ambient spaces  $\mathbb{TP}^3$  resp.  $\mathbb{TP}^4$ . Consider a graded component in (4.3) with  $\mathcal{L}$  very ample. Let  $N + 1$  be the number of monomials in  $E_i, F_{ij}, G_k$  that lie in  $H^0(X, \mathcal{L})$ . The map given by these monomials embeds  $X$  into a linear subspace of  $\mathbb{P}^N$ . The corresponding tropical surfaces in  $\mathbb{TP}^N$  should be isomorphic to the tropical del Pezzo surfaces constructed here. In particular, if  $\mathcal{L} = -K$  is the anticanonical bundle, then the subspace has dimension  $d$ , and the ambient dimensions are  $N = 44$  for  $d = 3$ , and  $N = 39$  for  $d = 4$ . In the former case, the 45 monomials (like  $E_1F_{12}G_2$  or  $F_{12}F_{34}F_{56}$ ) correspond to Eckhart triangles. In the latter case, the 40 monomials

(like  $E_1E_2F_{12}G$  or  $E_1F_{12}F_{13}F_{45}$ ) are those of degree  $(4, 2, 2, 2, 2, 2)$  in the grading (4.7). The tropicalizations of these *combinatorial anticanonical embeddings*,  $X \subset \mathbb{P}^3 \subset \mathbb{P}^{44}$  for  $d = 3$  and  $X \subset \mathbb{P}^4 \subset \mathbb{P}^{39}$  for  $d = 4$ , should agree with our surfaces here. This will help in resolving the mysteries regarding the 27 tropical lines on a cubic surface in  $\mathbb{TP}^3$  uncovered by Vigeland [95].

One last consideration concerns cubic surfaces defined over  $\mathbb{R}$ . A cubic surface equipped with a real structure induces another involution on the 27 metric trees corresponding to real  $(-1)$ -curves. These trees already come partitioned by combinatorial type, depending on the type of tropical cubic surface. One could ask which trees can result from real lines, and whether the tree arrangement reveals Segre's partition of real lines on cubic surfaces into hyperbolic and elliptic types [79]. For example, for the (aaaa) and (aaab) types, if the involution on the trees from the real structure is the trivial one, then the trees with combinatorial type occurring exactly three times always correspond to hyperbolic real lines.

## Chapter 5

# A Formula for the Cayley-Bacharach 9th Point

This chapter is based on my final project in the course Math 255: *Algebraic curves*, which was taught in Fall 2011 at Berkeley.

### 5.1 The Formula

In this chapter,  $K$  is an algebraically closed field of characteristic 0 (not necessarily with a valuation). The goal of this chapter is to give an explicit formula for  $P_9$  in terms of the coordinates of the other 8 points in the classical Cayley-Bacharach theorem:

**Theorem 5.1.1.** (*Cayley–Bacharach*) *Let  $C_1, C_2$  be two cubic curves (not necessarily irreducible) in  $\mathbb{P}^2$  over  $K$ . Suppose that they intersect in 9 distinct points  $P_1, P_2, \dots, P_9$ . Then any cubic curve that contains  $P_1, P_2, \dots, P_8$  also contains  $P_9$ .*

The proof of the theorem is given as an exercise in [59, Exercise 3.13]. Proofs of various versions of the theorem are given in [36]. Let  $P_1 = (x_1 : y_1 : z_1), P_2 = (x_2 : y_2 : z_2), \dots, P_8 = (x_8 : y_8 : z_8)$  be 8 distinct points in general position. Consider the linear system of cubic curves which contain  $P_1, P_2, \dots, P_8$ . Its dimension is at least  $\# \text{degrees of freedom} - \# \text{constraints} = 10 - 8 = 2$ . Choose two linearly independent elements  $C_1, C_2$ , and let  $P_9$  be their 9th intersection point. In this way,  $P_9$  is uniquely determined by  $P_1, P_2, \dots, P_8$ .

**Lemma 5.1.2.** *Regard the quotients  $y_9/x_9, z_9/x_9$  as functions in  $x_1, y_1, z_1, \dots, x_8, y_8, z_8$ . Then,  $y_9/x_9, z_9/x_9 \in \mathbb{Q}(x_1, y_1, z_1, \dots, x_8, y_8, z_8)$ .*

*Proof.* Let  $L = \mathbb{Q}(x_1, y_1, z_1, \dots, x_8, y_8, z_8)$ . Let  $F_1, F_2 \in L[x, y, z]$  be two linearly independent cubics that pass through  $P_1, P_2, \dots, P_8$ . Since  $P_9$  is an intersection point of  $F_1$  and  $F_2$ , we see that  $y_9/x_9$  and  $z_9/x_9$  are in the algebraic closure of  $L$ . Let  $L'$  be a finite Galois extension of  $L$  that contains  $y_9/x_9$  and  $z_9/x_9$ . Every  $\sigma \in \text{Gal}(L'/L)$  fixes  $F_1$  and  $F_2$ , thus fixes their

intersection. All other points  $P_1, \dots, P_8$  are fixed, so  $P_9$  must also be fixed. Therefore,  $y_9/x_9, z_9/x_9$  are fixed by the Galois group, thus they are in  $L$ .  $\square$

This chapter gives a formula for the coordinates of  $P_9$  in Theorem 5.1.6. Before stating the formula, let us define some notations:

**Definition 5.1.3.** *The Plücker coordinates of the eight given points are*

$$[ijk] = \det \begin{pmatrix} x_i & y_i & z_i \\ x_j & y_j & z_j \\ x_k & y_k & z_k \end{pmatrix}.$$

**Definition 5.1.4.** *The polynomial  $C(P_1, P_2, \dots, P_6) \in K[x, y, z]$  is defined as follows:*

$$C(P_1, P_2, \dots, P_6) = \det \begin{pmatrix} x_1^2 & x_1y_1 & x_1z_1 & y_1^2 & y_1z_1 & z_1^2 \\ x_2^2 & x_2y_2 & x_2z_2 & y_2^2 & y_2z_2 & z_2^2 \\ x_3^2 & x_3y_3 & x_3z_3 & y_3^2 & y_3z_3 & z_3^2 \\ x_4^2 & x_4y_4 & x_4z_4 & y_4^2 & y_4z_4 & z_4^2 \\ x_5^2 & x_5y_5 & x_5z_5 & y_5^2 & y_5z_5 & z_5^2 \\ x_6^2 & x_6y_6 & x_6z_6 & y_6^2 & y_6z_6 & z_6^2 \end{pmatrix}$$

**Definition 5.1.5.** *The polynomial  $D(P_1; P_2, \dots, P_8) \in K[x, y, z]$  is defined as follows:*

$$D(P_1; P_2, \dots, P_8) = \det \begin{pmatrix} x_2^3 & x_2^2y_2 & x_2^2z_2 & x_2y_2^2 & x_2y_2z_2 & x_2z_2^2 & y_2^3 & y_2^2z_2 & y_2z_2^2 & z_2^3 \\ x_3^3 & x_3^2y_3 & x_3^2z_3 & x_3y_3^2 & x_3y_3z_3 & x_3z_3^2 & y_3^3 & y_3^2z_3 & y_3z_3^2 & z_3^3 \\ \dots & \dots & \dots & \dots & \dots & \dots & \dots & \dots & \dots & \dots \\ x_8^3 & x_8^2y_8 & x_8^2z_8 & x_8y_8^2 & x_8y_8z_8 & x_8z_8^2 & y_8^3 & y_8^2z_8 & y_8z_8^2 & z_8^3 \\ 3x_1^2 & 2x_1y_1 & 2x_1z_1 & y_1^2 & y_1z_1 & z_1^2 & 0 & 0 & 0 & 0 \\ 0 & x_1^2 & 0 & 2x_1y_1 & x_1z_1 & 0 & 3y_1^2 & 2y_1z_1 & z_1^2 & 0 \\ 0 & 0 & x_1^2 & 0 & x_1y_1 & 2x_1z_1 & 0 & y_1^2 & 2y_1z_1 & 3z_1^2 \end{pmatrix}$$

The geometric interpretation of  $C(P_1, P_2, \dots, P_6)$  and  $D(P_1; P_2, \dots, P_8)$  are as follows. If  $P_1, P_2, \dots, P_6$  lie on a conic, then the system of linear equations  $F(x_i, y_i, z_i) = 0, 1 \leq i \leq 6$ , where  $F$  is a conic with 6 unknown coefficients, has a nontrivial solution. Consequently,  $C(P_1, P_2, \dots, P_6) = 0$ . The converse is also true. Similarly,  $D(P_1; P_2, \dots, P_8) = 0$  if and only if there exists a cubic curve that passes through  $P_1, P_2, \dots, P_8$  and is singular at  $P_1$ .

Of course, there are choices of homogeneous coordinates of the points, up to constant factors. Whenever we write  $[ijk]$ ,  $C(P_1, P_2, \dots, P_6)$  and  $D(P_1; P_2, \dots, P_8)$ , we assume that the choices of homogeneous coordinates are fixed. For simplicity, we write

$$\begin{aligned} C_x &= C(P_1, P_4, P_5, P_6, P_7, P_8), \\ C_y &= C(P_2, P_4, P_5, P_6, P_7, P_8), \\ C_z &= C(P_3, P_4, P_5, P_6, P_7, P_8), \\ D_x &= D(P_1; P_2, P_3, P_4, P_5, P_6, P_7, P_8), \\ D_y &= D(P_2; P_3, P_1, P_4, P_5, P_6, P_7, P_8), \\ D_z &= D(P_3; P_1, P_2, P_4, P_5, P_6, P_7, P_8). \end{aligned}$$

Now we are ready to state the main theorem:

**Theorem 5.1.6.** *The Cayley-Bacharach 9th point equals*

$$P_9 = C_x D_y D_z P_1 + D_x C_y D_z P_2 + D_x D_y C_z P_3, \quad (5.1)$$

or equivalently, its coordinates are the rational functions

$$\begin{aligned} x_9 &= C_x D_y D_z x_1 + D_x C_y D_z x_2 + D_x D_y C_z x_3, \\ y_9 &= C_x D_y D_z y_1 + D_x C_y D_z y_2 + D_x D_y C_z y_3, \\ z_9 &= C_x D_y D_z z_1 + D_x C_y D_z z_2 + D_x D_y C_z z_3. \end{aligned}$$

It is worth noting that one may derive a formula following the geometric construction of Cayley [25]. However, this formula would be too complicated for any further derivation related to the Cox ring of del Pezzo surfaces of degree 3 in Section 5.2. Another attempt is to find the cubics  $F_1$  and  $F_2$  in the proof of Lemma 5.1.2, intersect them and solve for the 9th point. However, this approach is not feasible due to the large number of variables and terms in the computation.

The polynomials  $C(P_1, P_2, \dots, P_6)$  and  $D(P_1; P_2, \dots, P_8)$  can be written neatly in terms of the Plücker coordinates. A formula that expresses  $C(P_1, P_2, \dots, P_6)$  in terms of the  $[ijk]$  is given by [25] and [73, Equation 7.3], see also Equation 4.10:

$$C(P_1, P_2, \dots, P_6) = -[123][145][246][356] + [124][135][236][456].$$

A similar formula for  $D(P_1; P_2, \dots, P_8)$  was suggested to us by Jürgen Richter-Gebert [77]. This equation can be verified by symbolic computation.

$$\begin{aligned} D(P_7; P_1, P_2, P_3, P_4, P_5, P_6, P_8) = & \\ & -3(-[647][857][473][428][178][123][573][526][176] \\ & + [647][857][478][128][173][423][573][526][176] \\ & + [647][857][473][428][178][576][126][173][523] \\ & + [657][847][573][528][178][123][473][426][176] \\ & - [657][847][578][128][173][523][473][426][176] \\ & - [657][847][573][528][178][476][126][173][423]). \end{aligned}$$

The following lemma follows from the above formulas:

**Lemma 5.1.7.** *Let  $T$  be a projective transformation on  $\mathbb{P}^2$ , expressed as a 3 by 3 matrix. Fix the homogeneous coordinates of  $T(P_i)$  to be the product of the matrix  $T$  with the fixed homogeneous coordinates of  $P_i$ . Then*

$$\begin{aligned} C(T(P_1), T(P_2), \dots, T(P_6)) &= \det(T)^4 C(P_1, P_2, \dots, P_6), \\ D(T(P_1); T(P_2), \dots, T(P_8)) &= \det(T)^9 D(P_1; P_2, \dots, P_8). \end{aligned}$$

*Proof of Theorem 5.1.6.* The ring  $K[x, y, z]$  is  $\mathbb{Z}^8$ -graded with  $\deg(x_i) = \deg(y_i) = \deg(z_i) = \mathbf{e}_i$ . It is straightforward to check that the right hand side of (5.1) is homogeneous of multidegree  $(9, 9, 9, 8, 8, 8, 8, 8)$ . Therefore, it is independent from the choice of homogeneous coordinates, up to a constant factor. Moreover, by Lemma 5.1.7, it is also preserved by projective transformations on  $\mathbb{P}^2$ , up to a constant factor. Therefore, it suffices to prove (5.1) for the simpler case  $P_1 = (1 : 0 : 0)$ ,  $P_2 = (0 : 1 : 0)$ ,  $P_3 = (0 : 0 : 1)$ ,  $P_4 = (1 : 1 : 1)$ ,  $P_5 = (1 : a : b)$ ,  $P_6 = (1 : c : d)$ ,  $P_7 = (1 : e : f)$ ,  $P_8 = (1 : g : h)$ .

Let  $u = y_9/x_9$  and  $v = z_9/x_9$ . By linear algebra, the condition that  $F(x_9, y_9, z_9) = 0$  whenever  $F(x_i, y_i, z_i) = 0$ ,  $1 \leq i \leq 8$  is equivalent to the condition that the following matrix does not have full rank:

$$\begin{pmatrix} 1 & 0 & 0 & 0 & 0 & 0 & 0 & 0 & 0 & 0 \\ 0 & 0 & 0 & 0 & 0 & 0 & 1 & 0 & 0 & 0 \\ 0 & 0 & 0 & 0 & 0 & 0 & 0 & 0 & 0 & 1 \\ 1 & 1 & 1 & 1 & 1 & 1 & 1 & 1 & 1 & 1 \\ 1 & a & b & a^2 & ab & b^2 & a^3 & a^2b & ab^2 & b^3 \\ 1 & c & d & c^2 & cd & d^2 & c^3 & c^2d & cd^2 & d^3 \\ 1 & e & f & e^2 & ef & f^2 & e^3 & e^2f & ef^2 & f^3 \\ 1 & g & h & g^2 & gh & h^2 & g^3 & g^2h & gh^2 & h^3 \\ 1 & u & v & u^2 & uv & v^2 & u^3 & u^2v & uv^2 & v^3 \end{pmatrix} \quad (5.2)$$

This is true if and only if each of its ten 9 by 9 minors are 0. Therefore, we get 10 equations in  $u, v$  whose coefficients are polynomials in  $a, b, \dots, h$ . Each equation is of the form

$$A_1u^2v + A_2uv^2 + A_3v^2 + A_4uv + A_5v^2 + A_6u + A_7v = 0, \quad (5.3)$$

where  $A_1, A_2, \dots, A_7 \in \mathbb{Z}[a, b, c, d, e, f, g, h]$ . Under our new assumption, the formula in Theorem 5.1.6 becomes  $P_9 = (1 : u : v)$ , where

$$u = \frac{D_x C_y}{C_x D_y},$$

$$v = \frac{D_x C_z}{C_x D_z}$$

It suffices to verify that this particular set of values of  $u$  and  $v$  satisfies the 10 equations (5.3), i.e.

$$\begin{aligned} & -A_1 C_y^2 C_z D_x^2 D_z + A_2 C_y C_z^2 D_x^2 D_y + A_3 C_x C_y^2 D_x D_z^2 - A_4 C_x C_y C_z D_x D_y D_z \\ & + A_5 C_x C_z^2 D_x D_y^2 + A_6 C_x^2 C_y D_y D_z^2 - A_7 C_x^2 C_z D_y^2 D_z = 0. \end{aligned}$$



The amount of computation needed to multiply out each term on the left hand side is still too large for a standard computer. To make it faster, we rewrite it in the following form:

$$\begin{aligned} & \frac{C_z D_x \frac{-A_1 C_y D_z + A_2 C_z D_y}{C_x} + A_3 C_y D_z^2}{D_y} - A_4 C_z D_z \\ & + \frac{C_z D_y \frac{A_5 C_z D_x - A_7 C_x D_z}{C_y} + A_6 C_x D_z^2}{D_x} = 0. \end{aligned}$$

After computing  $-A_1 C_y D_z + A_2 C_z D_y$ , one verifies that the result is divisible by  $C_x$ . Similarly, all other fractions in the above expression leave integral quotients. Therefore, the sizes of the intermediate results are limited. The final verification is carried out symbolically in `sage` [85].  $\square$

The formula in Theorem 5.1.6 is defined up to a common factor. The following proposition gives the simplest form:

**Proposition 5.1.8.** *Let*

$$P_9 = (x_9, y_9, z_9)^T = (C_x D_y D_z P_1 + D_x C_y D_z P_2 + D_x D_y C_z P_3) / [123]. \quad (5.4)$$

*Then,  $x_9, y_9, z_9 \in K[x, y, z]$ , and  $\gcd(x_9, y_9, z_9) = 1$ .*

**Remark 5.1.9.** With respect to the grading defined in the proof of Theorem 5.1.6, the right hand side of (5.4) is homogeneous of degree  $(8, 8, 8, 8, 8, 8, 8, 8)$ . The formula is invariant under the action of  $S_8$  that permutes the 8 given points, though it is not obvious in the expression.

*Proof.* Define  $F_x = C_x D_y D_z x_1 + D_x C_y D_z x_2 + D_x D_y C_z x_3$ , and  $F_y, F_z$  similarly. The variety of  $F_x$  in  $K^{24}$  is the union of irreducible hypersurfaces, one for each irreducible factor of  $F_x$ . In order to prove that  $[123]$  divides  $F_x$ , it suffices to prove that the variety of  $[123]$  is contained in the variety of  $F_x$ . That is,  $F_x = 0$  whenever the points  $P_1, P_2, P_3$  are collinear. Similarly, one needs to show that  $F_y = F_z = 0$  whenever  $[123] = 0$ . Since (5.1) is preserved by projective transformations on  $\mathbb{P}^2$ , without loss of generality, we may assume that  $P_1 = (1 : 0 : 0)$ ,  $P_2 = (0 : 1 : 0)$  and  $P_3 = (1 : 1 : 0)$ . For the special case, it can be verified with `sage` that  $F_x = F_y = F_z = 0$ . Therefore,  $[123]$  divides  $F_x, F_y$  and  $F_z$ , thus  $x_9, y_9, z_9 \in K[x, y, z]$ .

For the second statement, let

$$A = \begin{pmatrix} x_1 & x_2 & x_3 \\ y_1 & y_2 & y_3 \\ z_1 & z_2 & z_3 \end{pmatrix}.$$

Then,  $\det(A)A^{-1}$  has entries in  $K[x_1, y_1, z_1, \dots, x_3, y_3, z_3]$ . Then,

$$\det(A)A^{-1}P_9 = \det(A)A^{-1}(C_x D_y D_z P_1 + D_x C_y D_z P_2 + D_x D_y C_z P_3) / [123] = \begin{pmatrix} C_x D_y D_z \\ D_x C_y D_z \\ D_x D_y C_z \end{pmatrix}.$$

Therefore,  $\gcd(x_9, y_9, z_9)$  divides  $\gcd(C_x D_y D_z, D_x C_y D_z, D_x D_y C_z)$ . If  $\gcd(x_9, y_9, z_9) \neq 1$ , then it has an irreducible factor  $f$ . All of  $C_x D_y D_z, D_x C_y D_z, D_x D_y C_z$  vanish on the hypersurface in  $K^{24}$  cut out by  $f$ . Let  $(P_1, P_2, \dots, P_8)$  be a generic point on this hypersurface. Up to symmetry, three cases may occur: (a)  $C_x = C_y = 0$ ; (b)  $C_x = D_x = 0$ ; (c)  $D_x = D_y = 0$ .

First, we want to exclude some special cases: (1) Two of the points are the same; (2) Four of the points lie on a line; (3) Three of the points lie on a line, and three of the points lie on another line; (4) Seven of the points lie on a conic; (5) Three of the points lie on a line, and six of the points lie on a conic. All of these are codimension 2 conditions, so they do not occur to a generic point on the hypersurface  $V(f)$ . Now, we claim contradiction in each case:

(a) If  $C_x = C_y = 0$ , then there is a conic  $\mathcal{C}_1$  passing through  $P_1, P_4, P_5, P_6, P_7, P_8$  and a conic  $\mathcal{C}_2$  passing through  $P_2, P_4, P_5, P_6, P_7, P_8$ . If  $\mathcal{C}_1 = \mathcal{C}_2$ , then it passes through seven of the eight points. We have already excluded this case. If  $\mathcal{C}_1 \neq \mathcal{C}_2$ , then these two conics intersect at five points  $P_4, P_5, P_6, P_7, P_8$ . By Bézout's theorem, they must share a line  $\mathcal{L}$ . Then,  $\mathcal{C}_1$  is the union of two lines, which implies either (2) or (3). Therefore, this case is impossible.

(b) If  $C_x = D_x = 0$ , then there is a conic  $\mathcal{C}_1$  passing through  $P_1, P_4, P_5, P_6, P_7, P_8$  and a cubic  $\mathcal{C}_2$  passing through  $P_1, P_2, P_3, P_4, P_5, P_6, P_7, P_8$  that is singular at  $P_1$ . They intersect at six points  $P_1, P_4, P_5, P_6, P_7, P_8$  with multiplicity  $\geq 2$  at  $P_1$ . By Bézout's's theorem, two cases may occur: (b1)  $\mathcal{C}_1 \subset \mathcal{C}_2$ ; (b2)  $\mathcal{C}_1$  and  $\mathcal{C}_2$  share a line. For (b1), let  $\mathcal{C}_2 = \mathcal{C}_1 \cup \mathcal{L}$ . The line  $\mathcal{L}$  cannot pass through  $P_1$  because we excluded (5). Therefore,  $\mathcal{C}_1$  is singular at  $P_1$ , so it is the union of two lines, which implies either (2) or (3). For (b2),  $\mathcal{C}_1$  is the union of two lines, which also implies (2) or (3). Therefore, this case is impossible.

(c) If  $D_x = D_y = 0$ , then there is a cubic  $\mathcal{C}_1$  passing through  $P_1, P_2, P_3, P_4, P_5, P_6, P_7, P_8$  that is singular at  $P_1$  and a cubic  $\mathcal{C}_2$  passing through  $P_1, P_2, P_3, P_4, P_5, P_6, P_7, P_8$  that is singular at  $P_2$ . They intersect at these eight points with multiplicity 2 at  $P_1$  and  $P_2$ . By Bézout's's theorem, three cases may occur: (c1)  $\mathcal{C}_1 = \mathcal{C}_2$ ; (c2)  $\mathcal{C}_1$  and  $\mathcal{C}_2$  share a conic; (c3)  $\mathcal{C}_1$  and  $\mathcal{C}_2$  share a line. For (c1), the cubic is singular at two points, thus it cannot be irreducible. So this case is reduced to either (c2) or (c3). For (c2), let  $\mathcal{C}_1 = \mathcal{C} \cup \mathcal{L}_1$  and  $\mathcal{C}_2 = \mathcal{C} \cup \mathcal{L}_2$ . If the conic  $\mathcal{C}$  is the union of two lines, then  $\mathcal{C}_1$  is the union of three lines. Then, either (2) or (3) occurs. If  $\mathcal{C}$  is smooth, then both  $\mathcal{L}_1$  and  $\mathcal{L}_2$  must contain  $P_1$  and  $P_2$ . So  $\mathcal{L}_1 = \mathcal{L}_2$ . Then, either  $\mathcal{L}_1$  contains 4 given points or  $\mathcal{C}$  contains 7 given points. Both cases are excluded. For (c3), let  $\mathcal{C}_1 = \mathcal{C}'_1 \cup \mathcal{L}$  and  $\mathcal{C}_2 = \mathcal{C}'_2 \cup \mathcal{L}$ . For the same reason, both  $\mathcal{C}'_1$  and  $\mathcal{C}'_2$  are smooth. By Bézout's's theorem, they intersect at at most four points. The other four must lie on  $\mathcal{L}$ , which is (2). Therefore, this case is impossible.

Therefore, there cannot be such an irreducible factor  $f$ . Thus,  $\gcd(x_9, y_9, z_9) = 1$ .  $\square$

**Remark 5.1.10.** The *Newton polytope* of a polynomial  $f = \sum c_{\alpha_1, \alpha_2, \dots, \alpha_n} x_1^{\alpha_1} x_2^{\alpha_2} \cdots x_n^{\alpha_n}$  in  $n$  variables ( $c_{\alpha_1, \alpha_2, \dots, \alpha_n} \neq 0$ ) is the convex hull of  $\{(\alpha_1, \alpha_2, \dots, \alpha_n)\}$  in  $\mathbb{R}^n$ . Suppose that  $P_1 = (1 : 0 : 0), P_2 = (0 : 1 : 0), P_3 = (0 : 0 : 1), P_4 = (1 : 1 : 1)$ . Then,  $C_x C_y, C_z, D_x, D_y, D_z$  are polynomials in 12 variables  $x_i, y_i, z_i, 5 \leq i \leq 8$ . It is verified with `polymake` [42] that their Newton polytopes are isometric. The f-vector for the Newton polytope is

$$(120, 1980, 7430, 11470, 8720, 3460, 700, 60).$$

That is, the polytope has 120 vertices, 1980 edges, 7430 2-dimensional faces, etc.

The tropical polynomial for  $f$  is

$$f^{\text{tr}} = \min\{\text{val}(c_{\alpha_1, \alpha_2, \dots, \alpha_n}) + \alpha_1 x_1^{\text{tr}} + \alpha_2 x_2^{\text{tr}} + \dots + \alpha_n x_n^{\text{tr}}\}.$$

Suppose that  $(x_1^{\text{tr}}, \dots, x_n^{\text{tr}}) \in \mathbb{R}^n$  is generic, in the sense that the minimum is attained only once. One sufficient condition is that all  $\text{val}(c_{\alpha_1, \alpha_2, \dots, \alpha_n}) = 0$  and  $(\text{val}(x_1), \dots, \text{val}(x_n))$  is not orthogonal to any edge of the Newton polytope. If so, the valuation of  $f$  is uniquely determined by

$$\text{val}(f) = f^{\text{tr}}(\text{val}(x_1), \dots, \text{val}(x_n)).$$

One further question is to find a tropical version of Theorem 5.1.6.

## 5.2 Connection to Cubic Surfaces

### Cox Coordinates

In this subsection, let  $P_1, P_2, \dots, P_6$  be six points in  $\mathbb{P}^2$  in general position. By blowing up the plane at  $P_1, P_2, \dots, P_6$ , we obtain a del Pezzo surface  $S$  of degree 3. Section 4.2 describes the Cox embedding

$$S \hookrightarrow \text{Proj}(K[E_1, \dots, E_6, F_{12}, \dots, F_{56}, G_1, \dots, G_6]) / (K^*)^6,$$

with the ideal given in Proposition 4.2.2. The quotient by  $(K^*)^6$  is due to the  $\mathbb{Z}^7$ -grading

$$\begin{aligned} \deg(E_i) &= e_i + e_7, \\ \deg(F_{ij}) &= (e_1 + e_2 + \dots + e_7) - e_i - e_j, \\ \deg(G_i) &= (e_1 + e_2 + \dots + e_7) + e_i \end{aligned}$$

The coordinates  $E, F, G$  correspond to the divisors of  $S$  given by the 27 lines. The exceptional divisors of the blowing-up map  $\phi: S \rightarrow \mathbb{P}^2$  are exactly  $E_1, E_2, \dots, E_6$ .

Up to a projective transformation, we may assume that the coordinates of  $P_1, P_2, \dots, P_6$  are the columns of the matrix (4.8):

$$\begin{pmatrix} 1 & 1 & 1 & 1 & 1 & 1 \\ d_1 & d_2 & d_3 & d_4 & d_5 & d_6 \\ d_1^3 & d_2^3 & d_3^3 & d_4^3 & d_5^3 & d_6^3 \end{pmatrix}$$

Lemma 5.2.1 and Proposition 5.2.2 allow us to go back and forth between the Cox coordinates of a point in  $S$  and its image under the blowing-up map.

**Lemma 5.2.1.** *Let  $P'$  be a point in  $S$  with Cox coordinates  $(E, F, G)$ , and  $P = \phi(P')$  be its image under the blowing-up map. Then, up to a “+/-” sign before each term, the coordinates of  $P$  are*

$$P = (d_2 - d_3)E_2E_3F_{23}P_1 + (d_1 - d_3)E_1E_3F_{13}P_2 + (d_1 - d_2)E_1E_2F_{12}P_3. \quad (5.5)$$

*Proof.* Let  $L$  be the line in  $\mathbb{P}^2$  passing through  $P_1$  and  $P_2$ . Then, the pull back divisor  $\phi^*(L) = E_1 + E_2 + F_{12}$ . Note that this divisor has degree  $(3, 1, 1, 1, 1, 1, 1)$ . Therefore,  $\phi^*(\mathcal{O}_{\mathbb{P}^2}(1)) = \mathcal{O}_S(E_i + E_j + F_{ij}) = \mathcal{O}_S(3, 1, 1, 1, 1, 1, 1)$ . Let  $\mathcal{L}$  denote this line sheaf. Its global section  $H^0(X, \mathcal{L})$  is a 3-dimensional vector space over  $K$  generated by  $E_1E_2F_{12}$ ,  $E_2E_3F_{23}$  and  $E_1E_3F_{13}$  in the Cox coordinates.

Let  $\phi': S \rightarrow \mathbb{P}^2$  be the map given by (5.5). The coordinates of  $P$  is a linear combination of  $E_1E_2F_{12}$ ,  $E_2E_3F_{23}$  and  $E_1E_3F_{13}$ . Thus,  $\phi$  and  $\phi'$  are projective morphisms corresponding to the same very ample sheaf  $\mathcal{L}$ . Hence, they differ only by a linear automorphism of  $\mathbb{P}^2$ . Since a linear automorphism of  $\mathbb{P}^2$  is determined at 4 generic points, it suffices to show that  $\phi$  and  $\phi'$  coincide at  $P'_1, P'_2, P'_3, P'_4$ , namely,  $\phi'(P'_i) = P_i$  for  $i = 1, 2, 3, 4$ , where  $P'_i$  is a generic point in the exceptional divisor  $E_i$ .

For  $P'_1$ , the coordinate  $E_1 = 0$ . Then,  $\phi'(P'_1) = (d_2 - d_3)E_2E_3F_{23}P_1$ , which equals  $P_1$  up to the choice of homogeneous coordinates. The situation is similar for  $P'_2$  and  $P'_3$ . In order to show  $\phi'(P'_4) = P_4$ , it suffices to show that

$$\frac{[P12]}{[412]} = \frac{[P23]}{[423]} = \frac{[P13]}{[413]},$$

where  $P = \phi'(P'_4)$ . By symmetry, it suffices to show the first equality. It follows from (5.5) that

$$\begin{aligned} [P12] &= (d_1 - d_2)E_1E_2F_{12}[312], \\ [P23] &= (d_2 - d_3)E_2E_3F_{23}[123]. \end{aligned}$$

Then, it suffices to show that

$$\frac{(d_1 - d_2)E_1E_2F_{12}}{[412]} = \frac{(d_2 - d_3)E_2E_3F_{23}}{[423]}.$$

This follows from the first equation in Proposition 4.2.2 by setting  $E_4 = 0$ .  $\square$

**Proposition 5.2.2.** *Let  $P \in \mathbb{P}^2 \setminus \{P_1, P_2, \dots, P_6\}$ , and let  $P'$  be its preimage in  $S$  under the blowing-up map. Up to a “+/-” sign and the  $\mathbb{Z}^7$ -grading, the Cox coordinates of  $P'$  are*

$$\begin{aligned} E_i &= 1, \\ F_{ij} &= [ijP]/(d_i - d_j), \\ G_i &= C(P_{i_1}, P_{i_2}, P_{i_3}, P_{i_4}, P_{i_5}, P)/\prod_{1 \leq j < k \leq 5} (d_{i_j} - d_{i_k}), \\ &\text{where } \{i_1, i_2, i_3, i_4, i_5\} = \{1, 2, 3, 4, 5, 6\} \setminus \{i\}. \end{aligned}$$

*Proof.* Let  $Q \in S$  be the point with the above Cox coordinates. It can be verified by straightforward computation that  $Q$  satisfy the 270 relations in Proposition 4.2.2. It remains to show that  $\phi(Q) = P$ . By Lemma 5.2.1, it suffices to verify that (5.5) holds. This can also be done by straightforward computation.  $\square$

**Remark 5.2.3.** Assume in addition that  $P = (1 : d : d^3)$ . In the proof of Proposition 4.2.2, another set of Cox coordinates is given in (4.13):

$$\begin{aligned} E_i &= d_i - d, \\ F_{ij} &= d_i + d_j + d, \\ G_i &= -d_i + \sum_{j=1}^6 d_j + d. \end{aligned}$$

This is equivalent to the one given by Proposition 5.2.2 up to the  $\mathbb{Z}^7$ -grading.

Now let us return to Cayley-Bacharach theorem. Let  $P_7, P_8$  be two other generic points in  $\mathbb{P}^2$ , and  $P_9$  be the Cayley-Bacharach 9th point. The linear system of cubics vanishing at  $P_1, P_2, \dots, P_6$  has dimension 4. Choose a basis  $f_1, f_2, f_3, f_4$ . Let  $f$  be the rational map  $(f_1 : f_2 : f_3 : f_4)$  from  $\mathbb{P}^2$  to  $\mathbb{P}^3$ . Then, the closure of its image in  $\mathbb{P}^3$  is isomorphic to  $S$ . In fact,  $f$  is the inverse of the blowing-up map  $\phi$  on  $\mathbb{P}^2 \setminus \{P_1, P_2, \dots, P_6\}$ . The following proposition was suggested by James Blinn [14].

**Proposition 5.2.4.** *The points  $f(P_7), f(P_8), f(P_9)$  are collinear.*

*Proof.* Let  $W = \{u_1 f_1 + u_2 f_2 + u_3 f_3 + u_4 f_4 \mid u_i \in K\}$ . Consider  $W$  as the dual of the space  $\mathbb{P}^3$  where the image of  $f: \mathbb{P}^2 \dashrightarrow \mathbb{P}^3$  lies in: each  $(c_1 : c_2 : c_3 : c_4) \in \mathbb{P}^3$  corresponds to a codimension 1 subspace  $\{c_1 u_1 + c_2 u_2 + c_3 u_3 + c_4 u_4 = 0\} \subset W$ . Then,  $f(P_7) = (f_1(P_7) : f_2(P_7) : f_3(P_7) : f_4(P_7))$  corresponds to the subspace  $\{u_1 f_1(P_7) + u_2 f_2(P_7) + u_3 f_3(P_7) + u_4 f_4(P_7) = 0\}$ , which is the space of homogeneous cubics that vanish at  $P_1, P_2, \dots, P_7$ . Let  $W_7$  denote this subspace. Similarly, we define  $W_8, W_9$ . Then  $W_7 \cap W_8$  is the subspace of homogeneous cubics that vanish at  $P_1, P_2, \dots, P_8$ . Since any cubic curve that contains  $P_1, P_2, \dots, P_8$  also contains  $P_9$ , we have  $W_7 \cap W_8 \subset W_9$ . Therefore,  $W_7 \cap W_8 \cap W_9$  has dimension at least 1. Dually in  $\mathbb{P}^3$ , this means  $f(P_7), f(P_8), f(P_9)$  are collinear.  $\square$

Thus,  $f(P_9)$  can be constructed by finding the third intersection point of  $S$  and the line passing through  $f(P_7)$  and  $f(P_8)$ . The following proposition gives the Cox coordinates of the point  $f(P_9)$  in terms of the coordinates of  $P_1, P_2, \dots, P_8$ .

**Proposition 5.2.5.** *Up to a “+/-” sign and the  $\mathbb{Z}^7$ -grading, the Cox coordinates of  $f(P_9)$*

are

$$E_i = D(P_i; P_{i_1}, P_{i_2}, P_{i_3}, P_{i_4}, P_{i_5}, P_7, P_8) / \left( \prod_{j=1}^5 (d_i - d_{i_j})^2 \prod_{1 \leq j < k \leq 5} (d_{i_j} - d_{i_k}) \right),$$

$$\text{where } \{i_1, i_2, i_3, i_4, i_5\} = \{1, 2, 3, 4, 5, 6\} \setminus \{i\},$$

$$F_{ij} = C(P_{i_1}, P_{i_2}, P_{i_3}, P_{i_4}, P_7, P_8) / \prod_{1 \leq j < k \leq 4} (d_{i_j} - d_{i_k}),$$

$$\text{where } \{i_1, i_2, i_3, i_4\} = \{1, 2, 3, 4, 5, 6\} \setminus \{i, j\},$$

$$G_i = [i78].$$

*Proof.* Let  $Q \in S$  be the point with the above Cox coordinates. It can be verified by straightforward computation that  $Q$  satisfy the 270 relations in Proposition 4.2.2. It remains to show that  $\phi(Q) = P_9$ . By Lemma 5.2.1, this is equivalent to  $P = P_9$  in (5.5). After plugging in the expressions for  $E_1, E_2, E_3, F_{12}, F_{13}, F_{23}$ , this becomes exactly Theorem 5.1.6.  $\square$

### An analog in $\mathbb{P}^3$

Three quadratic surfaces in  $\mathbb{P}^3$  in general position intersect in 8 distinct points  $Q_1, \dots, Q_8$ . The coordinates of  $Q_8$  are uniquely determined by the coordinates of  $Q_1, \dots, Q_7$ . Plaumann, Sturmfels and Vinzant [73, Proposition 7.1] give a formula for the 8th intersection points of three quadratic surfaces in  $\mathbb{P}^3$  in terms of coordinates of the other 7 intersection points. Proposition 5.2.6 gives its general form.

**Proposition 5.2.6.** *Let  $Q_i = (w_i : x_i : y_i : z_i)$ , such that the linear system of quadratics that vanish at  $Q_1, Q_2, \dots, Q_7$  has dimension 3. Then any quadratic surface that contains  $Q_1, Q_2, \dots, Q_7$  also contains*

$$Q_8 = \frac{[1567]}{B_1} Q_1 + \frac{[2567]}{B_2} Q_2 + \frac{[3567]}{B_3} Q_3 + \frac{[4567]}{B_4} Q_4,$$

where

$$[1567] = \det \begin{pmatrix} w_1 & x_1 & y_1 & z_1 \\ w_5 & x_5 & y_5 & z_5 \\ w_6 & x_6 & y_6 & z_6 \\ w_7 & x_7 & y_7 & z_7 \end{pmatrix},$$

$$B_1 = \det \begin{pmatrix} w_2^2 & w_2x_2 & w_2y_2 & w_2z_2 & x_2^2 & x_2y_2 & x_2z_2 & y_2^2 & y_2z_2 & z_2^2 \\ w_3^2 & w_3x_3 & w_3y_3 & w_3z_3 & x_3^2 & x_3y_3 & x_3z_3 & y_3^2 & y_3z_3 & z_3^2 \\ \dots & \dots & \dots & \dots & \dots & \dots & \dots & \dots & \dots & \dots \\ w_7^2 & w_7x_7 & w_7y_7 & w_7z_7 & x_7^2 & x_7y_7 & x_7z_7 & y_7^2 & y_7z_7 & z_7^2 \\ 2w_1 & x_1 & y_1 & z_1 & 0 & 0 & 0 & 0 & 0 & 0 \\ 0 & w_1 & 0 & 0 & 2x_1 & y_1 & z_1 & 0 & 0 & 0 \\ 0 & 0 & w_1 & 0 & 0 & x_1 & 0 & 2y_1 & z_1 & 0 \\ 0 & 0 & 0 & w_1 & 0 & 0 & x_1 & 0 & y_1 & 2z_1 \end{pmatrix},$$

and the other terms are defined similarly.

*Proof.* The proof is analogous to the proof of Theorem 5.1.6. First notice that the formula is invariant under projective transformations on  $\mathbb{P}^3$ , up to a constant factor in the homogeneous coordinates of  $Q_8$ . Then, without loss of generality, we may assume that  $Q_1 = (1 : 0 : 0 : 0)$ ,  $Q_2 = (0 : 1 : 0 : 0)$ ,  $Q_3 = (0 : 0 : 1 : 0)$ ,  $Q_4 = (0 : 0 : 0 : 1)$  and  $Q_5 = (1 : 1 : 1 : 1)$ . The special case follows from [73, Proposition 7.1].  $\square$

Note that  $[1567] = 0$  if and only if  $Q_1, Q_5, Q_6, Q_7$  lie on a plane, and  $B_1 = 0$  if and only if there exists a quadratic surface  $S$  containing  $Q_1, Q_2, \dots, Q_7$  that is singular at  $Q_1$ . This is analogous to the geometric interpretation of  $C$  and  $D$ .

There is a similar geometric construction for the 3-dimensional analog. Consider the rational map  $g$  from  $\mathbb{P}^3$  to  $\mathbb{P}^5$  defined by  $(w : x : y : z) \mapsto (wx : wy : wz : xy : xz : yz)$ . It is regular on  $\mathbb{P}^3 \setminus \{Q_1, Q_2, Q_3, Q_4\}$ . Take the closure  $V$  of its image in  $\mathbb{P}^5$ .

**Proposition 5.2.7.** *The points  $f(Q_5), f(Q_6), f(Q_7), f(Q_8)$  lie on a plane.*

*Proof.* The proof is similar to the 2-dimensional analog.  $\{wx, wy, wz, xy, xz, yz\}$  form a basis of the vector space of homogeneous quadratics in  $x, y, z, w$  that vanish at  $Q_1, Q_2, Q_3, Q_4$ . Let  $W = \{u_1wx + u_2wy + u_3wz + u_4xy + u_5xz + u_6yz \mid u_i \in K\}$ . Consider  $W$  as the dual of the space  $\mathbb{P}^5$  where the image of  $g: \mathbb{P}^3 \dashrightarrow \mathbb{P}^5$  lies in: each  $(c_1 : c_2 : c_3 : c_4 : c_5 : c_6) \in \mathbb{P}^5$  corresponds to a codimension 1 subspace  $\{c_1u_1 + c_2u_2 + c_3u_3 + c_4u_4 + c_5u_5 + c_6u_6 = 0\} \subset W$ . Then,  $f(Q_5) = (w_5x_5 : w_5y_5 : w_5z_5 : x_5y_5 : x_5z_5 : y_5z_5)$  corresponds to the subspace  $\{u_1w_5x_5 + u_2w_5y_5 + u_3w_5z_5 + u_4x_5y_5 + u_5x_5z_5 + u_6y_5z_5 = 0\}$ , which is the space of homogeneous quadratics that vanish at  $Q_1, Q_2, Q_3, Q_4, Q_5$ . Let  $W_5$  denote this subspace. Similarly, we define  $W_6, W_7, W_8$ . Then  $W_5 \cap W_6 \cap W_7$  is the subspace of homogeneous quadratics that vanish at  $Q_1, Q_2, \dots, Q_7$ . Since any quadratic surface that contains  $Q_1, Q_2, \dots, Q_7$  also contains  $Q_8$ , we have  $W_5 \cap W_6 \cap W_7 \subset W_8$ . Therefore,  $W_5 \cap W_6 \cap W_7 \cap W_8$  has dimension at least 3. Dually in  $\mathbb{P}^5$ , this means  $f(Q_5), f(Q_6), f(Q_7), f(Q_8)$  lie on a plane.  $\square$

**Remark 5.2.8.** The 3-dimensional variety  $V$  is the blowing-up of  $\mathbb{P}^3$  at 4 points  $Q_1, Q_2, Q_3, Q_4$ . It contains 8 planes: 4 planes correspond to the 4 blown up points, and 4 planes correspond to the planes passing through 3 of the 4 chosen points.

# Bibliography

- [1] 4ti2 team: *4ti2-A software package for algebraic, geometric and combinatorial problems on linear spaces*, [www.4ti2.de](http://www.4ti2.de).
- [2] Dan Abramovich: *Moduli of algebraic and tropical curves*, Colloquium De Giorgi 2010-2012, 35–47, Scuola Normale Superiore, 2013.
- [3] Dan Abramovich, Lucia Caporaso and Sam Payne: *The tropicalization of the moduli space of curves*, [arXiv:1212:0373](https://arxiv.org/abs/1212.0373).
- [4] Federico Ardila and Caroline Klivans: *The Bergman complex of a matroid and phylogenetic trees*, Journal of Combinatorial Theory, Series B **96.1** (2006), 38–49.
- [5] Federico Ardila, Victor Reiner and Lauren Williams: *Bergman complexes, Coxeter arrangements, and graph associahedra*, Séminaire Lotharingien de Combinatoire **54** (2006) B54Aj.
- [6] Kai Arzdorf and Stefan Wewers: *Another proof of the semistable reduction theorem*, [arXiv:1211.4624](https://arxiv.org/abs/1211.4624).
- [7] Dan Avritzer and Herbert Lange: *The moduli spaces of hyperelliptic curves and binary forms*, Mathematische Zeitschrift **242.4** (2002), 615–632.
- [8] Matthew Baker: *An introduction to Berkovich analytic spaces and non-archimedean potential theory on curves*, notes from the 2007 Arizona Winter School on  $p$ -adic geometry, [http://people.math.gatech.edu/~mbaker/pdf/aws07mb\\_v4.pdf](http://people.math.gatech.edu/~mbaker/pdf/aws07mb_v4.pdf).
- [9] Matthew Baker, Sam Payne and Joseph Rabinoff: *Nonarchimedean geometry, tropicalization, and metrics on curves*, [arXiv:1104.0320](https://arxiv.org/abs/1104.0320).
- [10] Matthew Baker and Joseph Rabinoff: *The skeleton of the Jacobian, the Jacobian of the skeleton, and lifting meromorphic functions from tropical to algebraic curves*, [arxiv:1308.3864](https://arxiv.org/abs/1308.3864).
- [11] Victor Batyrev and Oleg Popov: *The Cox ring of a del Pezzo surface*, Arithmetic of higher-dimensional algebraic varieties, 85–103, Progress in Mathematics, Birkhäuser, Boston, 2004.



- [12] Benoit Bertrand, Erwan Brugallé and Grigory Mikhalkin: *Tropical open Hurwitz numbers*, Rendiconti del Seminario Matematico della Università di Padova **125** (2011), 151–171.
- [13] Christina Birkenhake and Herbert Lange: *Complex abelian varieties*, Grundlehren der mathematischen Wissenschaften **302**, Springer, 2004.
- [14] James Blinn: *personal communication* (2011).
- [15] Michele Bolognesi: *On Weddle surfaces and their moduli*, Advances in Geometry **7** (2007), 113–144.
- [16] Armand Borel and Lizhen Ji: *Compactifications of symmetric and locally symmetric spaces*, Springer, 2006.
- [17] Irene Bouw and Stefan Wewers: *Computing  $L$ -functions and semistable reduction of superelliptic curves*, arXiv:1211.4459.
- [18] Silvia Brannetti, Margarida Melo and Filippo Viviani: *On the tropical Torelli map*, Advances in Mathematics **226.3** (2011), 2546–2586.
- [19] Erwan Brugallé and Lucia López de Medrano: *Inflection points of real and tropical plane curves*, Journal of Singularities **4** (2012), 74–103.
- [20] David Bryant and Mike Steel: *Constructing optimal trees from quartets*, Journal of Algorithms **38.1** (2001), 237–259.
- [21] Lucia Caporaso: *Geometry of tropical moduli spaces and linkage of graphs*, Journal of Combinatorial Theory, Series A **119.3** (2012), 579–598.
- [22] Lucia Caporaso: *Gonality of algebraic curves and graphs*, arXiv:1201.6246.
- [23] Lucia Caporaso: *Algebraic and tropical curves: comparing their moduli spaces*, Handbook of Moduli, Volume I, 119–160, Advanced Lectures in Mathematics **24**, 2013.
- [24] Dustin Cartwright, Mathias Häbich, Bernd Sturmfels and Annette Werner: *Mustafin varieties*, Selecta Mathematica **17.4** (2011), 757–793.
- [25] Arthur Cayley: *On the construction of the ninth point of intersection of the cubics which pass through eight given points*, Quarterly Journal of Pure and Applied Mathematics **5** (1862), 222–233.
- [26] Melody Chan: *Combinatorics of the tropical Torelli map*, Algebra and Number Theory **6** (2012), 1133–1169.
- [27] Melody Chan: *Tropical hyperelliptic curves*, Journal of Algebraic Combinatorics **37.2** (2013), 331–359.

- [28] Melody Chan, Margarida Melo and Filippo Viviani: *Tropical Teichmüller and Siegel spaces*, Proceedings of the CIEM workshop in tropical geometry, 45–85, AMS Contemporary Mathematics **589**, 2013.
- [29] Melody Chan and Bernd Sturmfels: *Elliptic curves in honeycomb form*, Proceedings of the CIEM workshop in tropical geometry, 87–107, AMS Contemporary Mathematics **589**, 2013.
- [30] Elisabetta Colombo, Bert van Geemen and Eduard Looijenga: *Del Pezzo moduli via root systems*, Algebra, Arithmetic, and Geometry, 291–337, Springer, 2009.
- [31] Corrado De Concini and Claudio Procesi: *Wonderful models of subspace arrangements*, Selecta Mathematica, New Series **1.3** (1995), 459–494.
- [32] Aise Johan De Jong, Nicholas Ian Shepherd-Barron and Antonius Van de Ven: *On the Burkhardt quartic*, Mathematische Annalen **286.1** (1990), 309–328.
- [33] Alicia Dickenstein, Eva Feichtner and Bernd Sturmfels: *Tropical discriminants*, Journal of the American Mathematical Society **20.4** (2007), 1111–1133.
- [34] Igor Dolgachev and David Lehavi: *On isogenous principally polarized abelian surfaces*, Curves and Abelian Varieties, 51–69, Contemporary Mathematics **465**, American Mathematical Society, 2008.
- [35] Igor Dolgachev and David Ortland: *Point Sets in Projective Spaces and Theta Functions*, Astérisque **165**, Société mathématique de France, 1988.
- [36] David Eisenbud, Mark Green and Joe Harris: *Cayley-Bacharach theorems and conjectures*, Bulletin of the American Mathematical Society **33** (1996), 295–324.
- [37] Noam Elkies: *The identification of three moduli spaces*, arXiv:math/9905195.
- [38] Eva Maria Feichtner and Bernd Sturmfels: *Matroid polytopes, nested sets and Bergman fans*, Portugaliae Mathematica **62.4** (2005), 437–468.
- [39] Tom Fisher: *Pfaffian presentations of elliptic normal curves*, Transactions of the American Mathematical Society **362.5** (2010), 2525–2540.
- [40] Eberhard Freitag and Riccardo Salvati Manni: *The Burkhardt group and modular forms*, Transformation groups **9.1** (2004), 25–45.
- [41] Eberhard Freitag and Riccardo Salvati Manni: *The Burkhardt group and modular forms 2*, Transformation groups **9.3** (2004), 237–256.
- [42] Ewgenij Gawrilow and Michael Joswig: *Polymake: a framework for analyzing convex polytopes*, Polytopes-Combinatorics and Computation, 43–73, Oberwolfach Seminars, 2000.

- [43] Lothar Gerritzen and Marius Van der Put: *Schottky Groups and Mumford Curves*, Lecture Notes in Mathematics **817**, Springer, 1980.
- [44] Jane Gilman: *The non-Euclidean Euclidean algorithm*, Advances in Mathematics **250** (2014), 227–241.
- [45] Alexandre Grothendieck (assisted by Jean Dieudonné): *Éléments de Géométrie Algébrique: IV. Étude Locale des Schémas et des Morphismes de Schémas, Troisième Partie*, Publications Mathématiques de l’IHÉS **28**, 1966.
- [46] Laurent Gruson and Steven V Sam: *Alternating trilinear forms on a 9-dimensional space and degenerations of (3, 3)-polarized Abelian surfaces*, arXiv:1301.5276.
- [47] Laurent Gruson, Steven V Sam and Jerzy Weyman: *Moduli of Abelian varieties, Vinberg  $\theta$ -groups, and free resolutions*, Commutative Algebra, 419–469, Springer, 2013.
- [48] Keiichi Gunji: *Defining equations of the universal abelian surfaces with level three structure*, manuscripta mathematica **119.1** (2006), 61–96.
- [49] Paul Hacking: *The homology of tropical varieties*, Collectanea Mathematica **59.3** (2008), 263–273.
- [50] Paul Hacking, Sean Keel and Jenia Tevelev: *Stable pair, tropical, and log canonical compactifications of moduli spaces of del Pezzo surfaces*, Inventiones Mathematicae **178.1** (2009), 173–227.
- [51] Joe Harris and Ian Morrison: *Moduli of Curves*, Springer New York, 1998.
- [52] Robin Hartshorne: *Algebraic Geometry*, Springer-Verlag, New York, 1977.
- [53] Sven Herrmann, Anders Jensen, Michael Joswig and Bernd Sturmfels: *How to draw tropical planes*, Electronic Journal of Combinatorics **16.2** (2009) R6.
- [54] Jan Holly: *Pictures of ultrametric spaces, the  $p$ -adic numbers, and valued fields*, American Mathematical Monthly **108.8** (2001), 721–728.
- [55] Benjamin Howard, John J Millson, Andrew Snowden and Ravi Vakil: *The ideal of relations for the ring of invariants of  $n$  points on the line*, Journal of the European Mathematical Society **14.1** (2012), 1–60.
- [56] Bruce Hunt: *The geometry of some special arithmetic quotients*, Springer Berlin, 1996.
- [57] Anders Jensen: *Gfan, a software system for Gröbner fans and tropical varieties* (2009), <http://home.imf.au.dk/jensen/software/gfan/gfan.html>.
- [58] Samuel Kadziela: *Rigid analytic uniformization of hyperelliptic curves*, 2007, Ph.D. Thesis, University of Illinois at Urbana Champaign.

- [59] Frances Kirwan: *Complex Algebraic Curves*, London Mathematical Society Student Texts **23**, Cambridge University Press, Cambridge, 1992.
- [60] Felix Klein: *Vorlesungen über das Ikosaeder und die Auflösung der Gleichungen vom fünften Grade*, Teubner, Leipzig, 1884.
- [61] Dan Levy and Lior Pachter: *The neighbor-net algorithm*, Advances in Applied Mathematics **47.2** (2011), 240–258.
- [62] Diane Maclagan and Bernd Sturmfels: *Introduction to Tropical Geometry*, book in preparation, <http://homepages.warwick.ac.uk/staff/D.Maclagan/papers/TropicalBook.html>.
- [63] Grigory Mikhalkin: *Tropical geometry and its applications*, International Congress of Mathematicians **II**, 827–852, European Mathematical Society, Zürich, 2006.
- [64] Grigory Mikhalkin and Johannes Rau: *Tropical Geometry*, in preparation.
- [65] Hisasi Morikawa: *On the relation for two-dimensional theta constants of level three*, Journal of the Mathematical Society of Japan **20.1-2** (1968), 248–262.
- [66] Ralph Morrison and Qingchun Ren: *Algorithms for Mumford curves*, [arxiv:1309.5243](https://arxiv.org/abs/1309.5243).
- [67] David Mumford: *An analytic construction of degenerating curves over complete local rings*, Compositio Mathematica **24.2** (1972), 129–174.
- [68] David Mumford: *An analytic construction of degenerating abelian varieties over complete rings*, Compositio Mathematica **24.3** (1972), 239–272.
- [69] David Mumford: *The Red Book of Varieties and Schemes, second, expanded edition*, Lecture Notes in Mathematics **1358**, Springer-Verlag, Berlin, 1999.
- [70] Isao Naruki: *Cross ratio variety as a moduli space of cubic surfaces*, Proceedings of the London Mathematical Society **s3-45.1** (1982), 1–30.
- [71] Peter Orlik and Louis Solomon: *Unitary reflection groups and cohomology*, Inventiones Mathematicae **59.1** (1980), 77–94.
- [72] Sam Payne: *Analytification is the limit of all tropicalizations*, Mathematical Research Letters **16.3** (2009), 543–556.
- [73] Daniel Plaumann, Bernd Sturmfels and Cynthia Vinzant: *Quartic curves and their bitangents*, Journal of Symbolic Computation **46** (2011), 712–733.
- [74] Qingchun Ren, Steven V Sam, Gus Schrader and Bernd Sturmfels: *The universal Kummer threefold*, Experimental Mathematics **22.3** (2013), 327–362.

- [75] Qingchun Ren, Steven V Sam and Bernd Sturmfels: *Tropicalization of classical moduli spaces*, Mathematics in Computer Science, Special Issue on Computational Algebraic Geometry, to appear, [arXiv:1303.1132](https://arxiv.org/abs/1303.1132).
- [76] Qingchun Ren, Kristin Shaw and Bernd Sturmfels: *Tropicalization of Del Pezzo surfaces*, [arXiv:1402.5651](https://arxiv.org/abs/1402.5651).
- [77] Jürgen Richter-Gebert: *Personal communication* (2011).
- [78] Felipe Rincón: *Computing tropical linear spaces*, Journal of Symbolic Computation **51** (2013), 86–98.
- [79] Beniamino Segre: *The non-singular cubic surfaces: A new method of investigation with special reference to questions of reality*, Oxford University Press, London, 1942.
- [80] Jiro Sekiguchi: *Cross ratio varieties for root systems II: The case of the root system of type  $E_7$* , Kyushu Journal of Mathematics **54.1** (2000), 7–37.
- [81] Kristin Shaw: *A tropical intersection product in matroidal fans*, SIAM Journal on Discrete Mathematics **27.1** (2013), 459–491.
- [82] Geoffrey Shephard and John Todd: *Finite unitary reflection groups*, Canadian Journal of Mathematics **6.2** (1954), 274–301.
- [83] Mathieu Dutour Sikirić: *Polyhedral (software)*, <http://drobilica.irb.hr/~mathieu/Polyhedral/index.html>.
- [84] David Speyer and Bernd Sturmfels: *The tropical Grassmannian*, Advances in Geometry **4.3** (2004), 389–411.
- [85] William Stein and others: *Sage mathematics software* (2014), The Sage Development Team, <http://www.sagemath.org>.
- [86] Mike Stillman, Damiano Testa and Mauricio Velasco: *Gröbner bases, monomial group actions, and the Cox rings of del Pezzo surfaces*, Journal of Algebra **316.2** (2007), 777–801.
- [87] Bernd Sturmfels and Zhiqiang Xu: *Sagbi bases of Cox-Nagata rings*, Journal of the European Mathematical Society **12** (2010), 429–459.
- [88] Jeremy Teitelbaum:  *$p$ -adic periods of genus two Mumford-Schottky curves*, Journal für die Reine und Angewandte Mathematik **385** (1988), 117–151.
- [89] Jenia Tevelev: *Compactifications of subvarieties of tori*, American Journal of Mathematics **129** (2007), 1087–1104.

- [90] Jenia Tevelev: *Moduli spaces and invariant theory*, Lecture Notes, University of Massachusetts, Spring 2011, <https://www.math.umass.edu/~tevelev/moduli797.pdf>.
- [91] Gerard van der Geer: *Note on abelian schemes of level three*, *Mathematische Annalen* **278.1** (1987), 401–408.
- [92] Marius van der Put:  *$p$ -adic Whittaker groups*, *Groupe de Travail d'Analyse Ultramétrique* **6**, 1978–1979.
- [93] Marius van der Put: *Discrete groups, Mumford curves and theta functions*, *Annales de la faculté des sciences de Toulouse* **s6-1.3** (1992), 399–438.
- [94] Bert van Geemen: *A linear system on Naruki's moduli space of marked cubic surfaces*, *International Journal of Mathematics* **13.2** (2002), 183–208.
- [95] Magnus Dehli Vigeland: *Smooth tropical surfaces with infinitely many tropical lines*, *Arkiv för Matematik* **48.1** (2010), 177–206.
- [96] Filippo Viviani: *Tropicalizing vs compactifying the Torelli morphism*, *Contemporary Mathematics* **605** (2013), 181–210.
- [97] Masaaki Yoshida: *A  $W(E_6)$ -equivariant projective embedding of the moduli space of cubic surfaces*, [arXiv:math/0002102](https://arxiv.org/abs/math/0002102).

# Appendix A

## Appendix: Supplementary Data on the 27 Trees

The following represents the 27 metric trees for each generic type of tropical cubic surfaces. The bounded edges in the trees are represented by the *split systems*. For each bounded edge  $e$  in a tree  $T$ , there are exactly two connected components in  $T \setminus \{e\}$ . This gives a partition of the set of leaves into two subsets. The labels of these leaves are listed in the two brackets in each row of the data. For example, the first tree in the data represents the tree in Figure A.1.

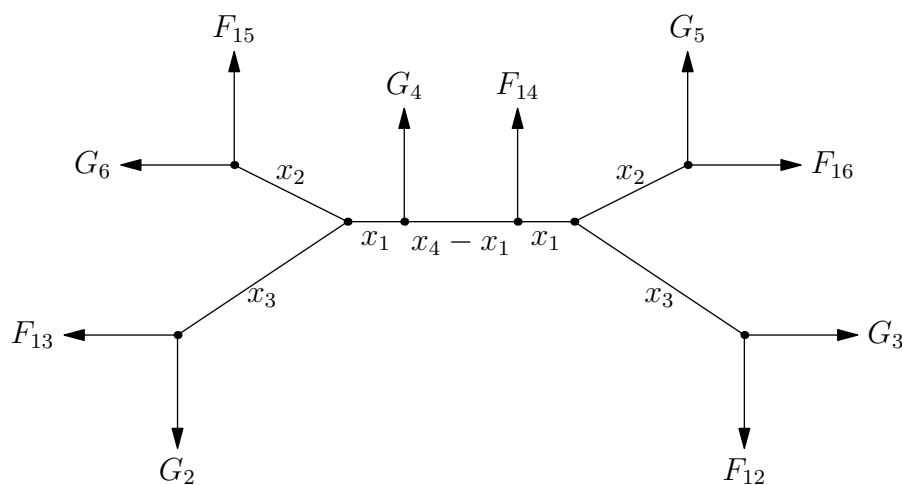


Figure A.1: One of the 27 trees for a type (aaaa) tropical cubic surface, with labels on the leaves.

**Type (aaaa)**

-----Tree (E1)-----

involution: F12<-->G2 F13<-->G3 F14<-->G4 F15<-->G5 F16<-->G6  
[F12, G3 ] [G2 , F13, F14, G4 , F15, G5 , F16, G6 ] length: x3  
[G2 , F13] [F12, G3 , F14, G4 , F15, G5 , F16, G6 ] length: x3  
[F15, G6 ] [F12, G2 , F13, G3 , F14, G4 , G5 , F16] length: x2  
[G5 , F16] [F12, G2 , F13, G3 , F14, G4 , F15, G6 ] length: x2  
[F12, G3 , G5 , F16] [G2 , F13, F14, G4 , F15, G6 ] length: x1  
[G2 , F13, F15, G6 ] [F12, G3 , F14, G4 , G5 , F16] length: x1  
[F12, G3 , F14, G5 , F16] [G2 , F13, G4 , F15, G6 ] length: -x1 + x4

-----Tree (E2)-----

involution: F12<-->G1 F23<-->G3 F24<-->G4 F25<-->G5 F26<-->G6  
[F12, G3 ] [G1 , F23, F24, G4 , F25, G5 , F26, G6 ] length: x3  
[G1 , F23] [F12, G3 , F24, G4 , F25, G5 , F26, G6 ] length: x3  
[F24, G6 ] [F12, G1 , F23, G3 , G4 , F25, G5 , F26] length: x4  
[G4 , F26] [F12, G1 , F23, G3 , F24, F25, G5 , G6 ] length: x4  
[F12, G3 , G4 , F26] [G1 , F23, F24, F25, G5 , G6 ] length: x1  
[G1 , F23, F24, G6 ] [F12, G3 , G4 , F25, G5 , F26] length: x1  
[F12, G3 , G4 , F25, F26] [G1 , F23, F24, G5 , G6 ] length: -x1 + x2

-----Tree (E3)-----

involution: F13<-->G1 F23<-->G2 F34<-->G4 F35<-->G5 F36<-->G6  
[F13, G2 ] [G1 , F23, F34, G4 , F35, G5 , F36, G6 ] length: x3  
[G1 , F23] [F13, G2 , F34, G4 , F35, G5 , F36, G6 ] length: x3  
[F34, G5 ] [F13, G1 , F23, G2 , G4 , F35, F36, G6 ] length: x1  
[G4 , F35] [F13, G1 , F23, G2 , F34, G5 , F36, G6 ] length: x1  
[F13, G2 , G4 , F35] [G1 , F23, F34, G5 , F36, G6 ] length: x2  
[G1 , F23, F34, G5 ] [F13, G2 , G4 , F35, F36, G6 ] length: x2  
[F13, G2 , G4 , F35, G6 ] [G1 , F23, F34, G5 , F36] length: -x2 + x4

-----Tree (E4)-----

involution: F14<-->G1 F24<-->G2 F34<-->G3 F45<-->G5 F46<-->G6  
[F24, G6 ] [F14, G1 , G2 , F34, G3 , F45, G5 , F46] length: x4  
[G2 , F46] [F14, G1 , F24, F34, G3 , F45, G5 , G6 ] length: x4  
[F34, G5 ] [F14, G1 , F24, G2 , G3 , F45, F46, G6 ] length: x1  
[G3 , F45] [F14, G1 , F24, G2 , F34, G5 , F46, G6 ] length: x1  
[F24, F34, G5 , G6 ] [F14, G1 , G2 , G3 , F45, F46] length: x2  
[G2 , G3 , F45, F46] [F14, G1 , F24, F34, G5 , G6 ] length: x2  
[F14, F24, F34, G5 , G6 ] [G1 , G2 , G3 , F45, F46] length: -x2 + x3



## -----Tree (E5)-----

involution: F15<-->G1 F25<-->G2 F35<-->G3 F45<-->G4 F56<-->G6  
 [F15, G6 ] [G1 , F25, G2 , F35, G3 , F45, G4 , F56] length: x2  
 [G1 , F56] [F15, F25, G2 , F35, G3 , F45, G4 , G6 ] length: x2  
 [F35, G4 ] [F15, G1 , F25, G2 , G3 , F45, F56, G6 ] length: x1  
 [G3 , F45] [F15, G1 , F25, G2 , F35, G4 , F56, G6 ] length: x1  
 [F15, F35, G4 , G6 ] [G1 , F25, G2 , G3 , F45, F56] length: x3  
 [G1 , G3 , F45, F56] [F15, F25, G2 , F35, G4 , G6 ] length: x3  
 [F15, G2 , F35, G4 , G6 ] [G1 , F25, G3 , F45, F56] length: -x3 + x4

## -----Tree (E6)-----

involution: F16<-->G1 F26<-->G2 F36<-->G3 F46<-->G4 F56<-->G5  
 [F16, G5 ] [G1 , F26, G2 , F36, G3 , F46, G4 , F56] length: x2  
 [G1 , F56] [F16, F26, G2 , F36, G3 , F46, G4 , G5 ] length: x2  
 [F26, G4 ] [F16, G1 , G2 , F36, G3 , F46, F56, G5 ] length: x4  
 [G2 , F46] [F16, G1 , F26, F36, G3 , G4 , F56, G5 ] length: x4  
 [F16, F26, G4 , G5 ] [G1 , G2 , F36, G3 , F46, F56] length: x1  
 [G1 , G2 , F46, F56] [F16, F26, F36, G3 , G4 , G5 ] length: x1  
 [F16, F26, F36, G4 , G5 ] [G1 , G2 , G3 , F46, F56] length: -x1 + x3

## -----Tree (F12)-----

involution: E1<-->G2 E2<-->G1 F34<-->F56 F35<-->F46 F36<-->F45  
 [E1 , F35] [G2 , E2 , G1 , F34, F56, F46, F36, F45] length: x4  
 [G2 , F46] [E1 , E2 , G1 , F34, F56, F35, F36, F45] length: x4  
 [E2 , F34] [E1 , G2 , G1 , F56, F35, F46, F36, F45] length: x2  
 [G1 , F56] [E1 , G2 , E2 , F34, F35, F46, F36, F45] length: x2  
 [E1 , E2 , F34, F35] [G2 , G1 , F56, F46, F36, F45] length: x1  
 [G2 , G1 , F56, F46] [E1 , E2 , F34, F35, F36, F45] length: x1  
 [E1 , E2 , F34, F35, F36] [G2 , G1 , F56, F46, F45] length: -x1 + x3

## -----Tree (F13)-----

involution: E1<-->G3 E3<-->G1 F24<-->F56 F25<-->F46 F26<-->F45  
 [E1 , F26] [G3 , E3 , G1 , F24, F56, F25, F46, F45] length: x1  
 [G3 , F45] [E1 , E3 , G1 , F24, F56, F25, F46, F26] length: x1  
 [E3 , F24] [E1 , G3 , G1 , F56, F25, F46, F26, F45] length: x2  
 [G1 , F56] [E1 , G3 , E3 , F24, F25, F46, F26, F45] length: x2  
 [E1 , E3 , F24, F26] [G3 , G1 , F56, F25, F46, F45] length: x3  
 [G3 , G1 , F56, F45] [E1 , E3 , F24, F25, F46, F26] length: x3  
 [E1 , E3 , F24, F46, F26] [G3 , G1 , F56, F25, F45] length: -x3 + x4

## -----Tree (F14)-----

involution: E1<-->G4 E4<-->G1 F23<-->F56 F25<-->F36 F26<-->F35

[E1 , F35]	[G4 , E4 , G1 , F23, F56, F25, F36, F26]	length: $-x_1 + x_4$
[G4 , F26]	[E1 , E4 , G1 , F23, F56, F25, F36, F35]	length: $-x_1 + x_4$
[E4 , F56]	[E1 , G4 , G1 , F23, F25, F36, F26, F35]	length: $-x_2 + x_3$
[G1 , F23]	[E1 , G4 , E4 , F56, F25, F36, F26, F35]	length: $-x_2 + x_3$
[E1 , G4 , F26, F35]	[E4 , G1 , F23, F56, F25, F36]	length: $x_1$
[E4 , G1 , F23, F56]	[E1 , G4 , F25, F36, F26, F35]	length: $x_2$

-----Tree (F15)-----

involution: E1<-->G5	E5<-->G1	F23<-->F46	F24<-->F36	F26<-->F34	
[E1 , F26]	[G5 , E5 , G1 , F23, F46, F24, F36, F34]				length: $x_1$
[G5 , F34]	[E1 , E5 , G1 , F23, F46, F24, F36, F26]				length: $x_1$
[E5 , F46]	[E1 , G5 , G1 , F23, F24, F36, F26, F34]				length: $x_3$
[G1 , F23]	[E1 , G5 , E5 , F46, F24, F36, F26, F34]				length: $x_3$
[E1 , E5 , F46, F26]	[G5 , G1 , F23, F24, F36, F34]				length: $x_2$
[G5 , G1 , F23, F34]	[E1 , E5 , F46, F24, F36, F26]				length: $x_2$
[E1 , E5 , F46, F24, F26]	[G5 , G1 , F23, F36, F34]				length: $-x_2 + x_4$

-----Tree (F16)-----

involution: E1<-->G6	E6<-->G1	F23<-->F45	F24<-->F35	F25<-->F34	
[E1 , F35]	[G6 , E6 , G1 , F23, F45, F24, F25, F34]				length: $x_4$
[G6 , F24]	[E1 , E6 , G1 , F23, F45, F35, F25, F34]				length: $x_4$
[E6 , F45]	[E1 , G6 , G1 , F23, F24, F35, F25, F34]				length: $x_3$
[G1 , F23]	[E1 , G6 , E6 , F45, F24, F35, F25, F34]				length: $x_3$
[E1 , E6 , F45, F35]	[G6 , G1 , F23, F24, F25, F34]				length: $x_1$
[G6 , G1 , F23, F24]	[E1 , E6 , F45, F35, F25, F34]				length: $x_1$
[E1 , E6 , F45, F35, F25]	[G6 , G1 , F23, F24, F34]				length: $-x_1 + x_2$

-----Tree (F23)-----

involution: E2<-->G3	E3<-->G2	F14<-->F56	F15<-->F46	F16<-->F45	
[E2 , F16]	[G3 , E3 , G2 , F14, F56, F15, F46, F45]				length: $x_1$
[G3 , F45]	[E2 , E3 , G2 , F14, F56, F15, F46, F16]				length: $x_1$
[E3 , F15]	[E2 , G3 , G2 , F14, F56, F46, F16, F45]				length: $x_4$
[G2 , F46]	[E2 , G3 , E3 , F14, F56, F15, F16, F45]				length: $x_4$
[E2 , E3 , F15, F16]	[G3 , G2 , F14, F56, F46, F45]				length: $x_2$
[G3 , G2 , F46, F45]	[E2 , E3 , F14, F56, F15, F16]				length: $x_2$
[E2 , E3 , F14, F15, F16]	[G3 , G2 , F56, F46, F45]				length: $-x_2 + x_3$

-----Tree (F24)-----

involution: E2<-->G4	E4<-->G2	F13<-->F56	F15<-->F36	F16<-->F35	
[E2 , F16]	[G4 , E4 , G2 , F13, F56, F15, F36, F35]				length: $x_1$
[G4 , F35]	[E2 , E4 , G2 , F13, F56, F15, F36, F16]				length: $x_1$
[E4 , F56]	[E2 , G4 , G2 , F13, F15, F36, F16, F35]				length: $x_3$

[G2 , F13]	[E2 , G4 , E4 , F56, F15, F36, F16, F35]	length: x3
[E2 , E4 , F56, F16]	[G4 , G2 , F13, F15, F36, F35]	length: x2
[G4 , G2 , F13, F35]	[E2 , E4 , F56, F15, F36, F16]	length: x2
[E2 , E4 , F56, F36, F16]	[G4 , G2 , F13, F15, F35]	length: -x2 + x4

-----Tree (F25)-----

involution: E2<-->G5	E5<-->G2	F13<-->F46	F14<-->F36	F16<-->F34	
[E2 , F34]	[G5 , E5 , G2 , F13, F46, F14, F36, F16]				length: -x1 + x2
[G5 , F16]	[E2 , E5 , G2 , F13, F46, F14, F36, F34]				length: -x1 + x2
[E5 , F13]	[E2 , G5 , G2 , F46, F14, F36, F16, F34]				length: -x3 + x4
[G2 , F46]	[E2 , G5 , E5 , F13, F14, F36, F16, F34]				length: -x3 + x4
[E2 , G5 , F16, F34]	[E5 , G2 , F13, F46, F14, F36]				length: x1
[E5 , G2 , F13, F46]	[E2 , G5 , F14, F36, F16, F34]				length: x3

-----Tree (F26)-----

involution: E2<-->G6	E6<-->G2	F13<-->F45	F14<-->F35	F15<-->F34	
[E2 , F34]	[G6 , E6 , G2 , F13, F45, F14, F35, F15]				length: x2
[G6 , F15]	[E2 , E6 , G2 , F13, F45, F14, F35, F34]				length: x2
[E6 , F45]	[E2 , G6 , G2 , F13, F14, F35, F15, F34]				length: x3
[G2 , F13]	[E2 , G6 , E6 , F45, F14, F35, F15, F34]				length: x3
[E2 , E6 , F45, F34]	[G6 , G2 , F13, F14, F35, F15]				length: x1
[G6 , G2 , F13, F15]	[E2 , E6 , F45, F14, F35, F34]				length: x1
[E2 , E6 , F45, F14, F34]	[G6 , G2 , F13, F35, F15]				length: -x1 + x4

-----Tree (F34)-----

involution: E3<-->G4	E4<-->G3	F12<-->F56	F15<-->F26	F16<-->F25	
[E3 , F15]	[G4 , E4 , G3 , F12, F56, F26, F16, F25]				length: x4
[G4 , F26]	[E3 , E4 , G3 , F12, F56, F15, F16, F25]				length: x4
[E4 , F56]	[E3 , G4 , G3 , F12, F15, F26, F16, F25]				length: x3
[G3 , F12]	[E3 , G4 , E4 , F56, F15, F26, F16, F25]				length: x3
[E3 , E4 , F56, F15]	[G4 , G3 , F12, F26, F16, F25]				length: x1
[G4 , G3 , F12, F26]	[E3 , E4 , F56, F15, F16, F25]				length: x1
[E3 , E4 , F56, F15, F16]	[G4 , G3 , F12, F26, F25]				length: -x1 + x2

-----Tree (F35)-----

involution: E3<-->G5	E5<-->G3	F12<-->F46	F14<-->F26	F16<-->F24	
[E3 , F24]	[G5 , E5 , G3 , F12, F46, F14, F26, F16]				length: x2
[G5 , F16]	[E3 , E5 , G3 , F12, F46, F14, F26, F24]				length: x2
[E5 , F46]	[E3 , G5 , G3 , F12, F14, F26, F16, F24]				length: x3
[G3 , F12]	[E3 , G5 , E5 , F46, F14, F26, F16, F24]				length: x3
[E3 , E5 , F46, F24]	[G5 , G3 , F12, F14, F26, F16]				length: x1
[G5 , G3 , F12, F16]	[E3 , E5 , F46, F14, F26, F24]				length: x1

[E3 , E5 , F46, F26, F24]      [G5 , G3 , F12, F14, F16]      length:  $-x_1 + x_4$

-----Tree (F36)-----

involution: E3<-->G6 E6<-->G3 F12<-->F45 F14<-->F25 F15<-->F24  
 [E3 , F15]      [G6 , E6 , G3 , F12, F45, F14, F25, F24]      length:  $-x_2 + x_4$   
 [G6 , F24]      [E3 , E6 , G3 , F12, F45, F14, F25, F15]      length:  $-x_2 + x_4$   
 [E6 , F45]      [E3 , G6 , G3 , F12, F14, F25, F15, F24]      length:  $-x_1 + x_3$   
 [G3 , F12]      [E3 , G6 , E6 , F45, F14, F25, F15, F24]      length:  $-x_1 + x_3$   
 [E3 , G6 , F15, F24]      [E6 , G3 , F12, F45, F14, F25]      length:  $x_2$   
 [E6 , G3 , F12, F45]      [E3 , G6 , F14, F25, F15, F24]      length:  $x_1$

-----Tree (F45)-----

involution: E4<-->G5 E5<-->G4 F12<-->F36 F13<-->F26 F16<-->F23  
 [E4 , F23]      [G5 , E5 , G4 , F12, F36, F13, F26, F16]      length:  $x_2$   
 [G5 , F16]      [E4 , E5 , G4 , F12, F36, F13, F26, F23]      length:  $x_2$   
 [E5 , F13]      [E4 , G5 , G4 , F12, F36, F26, F16, F23]      length:  $x_4$   
 [G4 , F26]      [E4 , G5 , E5 , F12, F36, F13, F16, F23]      length:  $x_4$   
 [E4 , E5 , F13, F23]      [G5 , G4 , F12, F36, F26, F16]      length:  $x_1$   
 [G5 , G4 , F26, F16]      [E4 , E5 , F12, F36, F13, F23]      length:  $x_1$   
 [E4 , E5 , F12, F13, F23]      [G5 , G4 , F36, F26, F16]      length:  $-x_1 + x_3$

-----Tree (F46)-----

involution: E4<-->G6 E6<-->G4 F12<-->F35 F13<-->F25 F15<-->F23  
 [E4 , F23]      [G6 , E6 , G4 , F12, F35, F13, F25, F15]      length:  $x_2$   
 [G6 , F15]      [E4 , E6 , G4 , F12, F35, F13, F25, F23]      length:  $x_2$   
 [E6 , F12]      [E4 , G6 , G4 , F35, F13, F25, F15, F23]      length:  $x_1$   
 [G4 , F35]      [E4 , G6 , E6 , F12, F13, F25, F15, F23]      length:  $x_1$   
 [E4 , E6 , F12, F23]      [G6 , G4 , F35, F13, F25, F15]      length:  $x_3$   
 [G6 , G4 , F35, F15]      [E4 , E6 , F12, F13, F25, F23]      length:  $x_3$   
 [E4 , E6 , F12, F25, F23]      [G6 , G4 , F35, F13, F15]      length:  $-x_3 + x_4$

-----Tree (F56)-----

involution: E5<-->G6 E6<-->G5 F12<-->F34 F13<-->F24 F14<-->F23  
 [E5 , F13]      [G6 , E6 , G5 , F12, F34, F24, F14, F23]      length:  $x_4$   
 [G6 , F24]      [E5 , E6 , G5 , F12, F34, F13, F14, F23]      length:  $x_4$   
 [E6 , F12]      [E5 , G6 , G5 , F34, F13, F24, F14, F23]      length:  $x_1$   
 [G5 , F34]      [E5 , G6 , E6 , F12, F13, F24, F14, F23]      length:  $x_1$   
 [E5 , E6 , F12, F13]      [G6 , G5 , F34, F24, F14, F23]      length:  $x_2$   
 [G6 , G5 , F34, F24]      [E5 , E6 , F12, F13, F14, F23]      length:  $x_2$   
 [E5 , E6 , F12, F13, F23]      [G6 , G5 , F34, F24, F14]      length:  $-x_2 + x_3$

-----Tree (G1)-----

involution: E2<-->F12 E3<-->F13 E4<-->F14 E5<-->F15 E6<-->F16  
 [E2 , F16] [F12, E3 , F13, E4 , F14, E5 , F15, E6 ] length: x1  
 [F12, E6 ] [E2 , E3 , F13, E4 , F14, E5 , F15, F16] length: x1  
 [E3 , F15] [E2 , F12, F13, E4 , F14, E5 , E6 , F16] length: x4  
 [F13, E5 ] [E2 , F12, E3 , E4 , F14, F15, E6 , F16] length: x4  
 [E2 , E3 , F15, F16] [F12, F13, E4 , F14, E5 , E6 ] length: x2  
 [F12, F13, E5 , E6 ] [E2 , E3 , E4 , F14, F15, F16] length: x2  
 [E2 , E3 , F14, F15, F16] [F12, F13, E4 , E5 , E6 ] length: -x2 + x3

-----Tree (G2)-----

involution: E1<-->F12 E3<-->F23 E4<-->F24 E5<-->F25 E6<-->F26  
 [E1 , F26] [F12, E3 , F23, E4 , F24, E5 , F25, E6 ] length: x1  
 [F12, E6 ] [E1 , E3 , F23, E4 , F24, E5 , F25, F26] length: x1  
 [E3 , F24] [E1 , F12, F23, E4 , E5 , F25, E6 , F26] length: x2  
 [F23, E4 ] [E1 , F12, E3 , F24, E5 , F25, E6 , F26] length: x2  
 [E1 , E3 , F24, F26] [F12, F23, E4 , E5 , F25, E6 ] length: x3  
 [F12, F23, E4 , E6 ] [E1 , E3 , F24, E5 , F25, F26] length: x3  
 [E1 , E3 , F24, E5 , F26] [F12, F23, E4 , F25, E6 ] length: -x3 + x4

-----Tree (G3)-----

involution: E1<-->F13 E2<-->F23 E4<-->F34 E5<-->F35 E6<-->F36  
 [E1 , F35] [F13, E2 , F23, E4 , F34, E5 , E6 , F36] length: x4  
 [F13, E5 ] [E1 , E2 , F23, E4 , F34, F35, E6 , F36] length: x4  
 [E2 , F34] [E1 , F13, F23, E4 , E5 , F35, E6 , F36] length: x2  
 [F23, E4 ] [E1 , F13, E2 , F34, E5 , F35, E6 , F36] length: x2  
 [E1 , E2 , F34, F35] [F13, F23, E4 , E5 , E6 , F36] length: x1  
 [F13, F23, E4 , E5 ] [E1 , E2 , F34, F35, E6 , F36] length: x1  
 [E1 , E2 , F34, F35, F36] [F13, F23, E4 , E5 , E6 ] length: -x1 + x3

-----Tree (G4)-----

involution: E1<-->F14 E2<-->F24 E3<-->F34 E5<-->F45 E6<-->F46  
 [E2 , F34] [E1 , F14, F24, E3 , E5 , F45, E6 , F46] length: x2  
 [F24, E3 ] [E1 , F14, E2 , F34, E5 , F45, E6 , F46] length: x2  
 [E5 , F46] [E1 , F14, E2 , F24, E3 , F34, F45, E6 ] length: x3  
 [F45, E6 ] [E1 , F14, E2 , F24, E3 , F34, E5 , F46] length: x3  
 [E2 , F34, F45, E6 ] [E1 , F14, F24, E3 , E5 , F46] length: x1  
 [F24, E3 , E5 , F46] [E1 , F14, E2 , F34, F45, E6 ] length: x1  
 [E1 , F24, E3 , E5 , F46] [F14, E2 , F34, F45, E6 ] length: -x1 + x4

-----Tree (G5)-----

involution: E1<-->F15 E2<-->F25 E3<-->F35 E4<-->F45 E6<-->F56  
 [E1 , F35] [F15, E2 , F25, E3 , E4 , F45, E6 , F56] length: x4

[F15, E3 ]	[E1 , E2 , F25, F35, E4 , F45, E6 , F56]	length: x4
[E4 , F56]	[E1 , F15, E2 , F25, E3 , F35, F45, E6 ]	length: x3
[F45, E6 ]	[E1 , F15, E2 , F25, E3 , F35, E4 , F56]	length: x3
[E1 , F35, F45, E6 ]	[F15, E2 , F25, E3 , E4 , F56]	length: x1
[F15, E3 , E4 , F56]	[E1 , E2 , F25, F35, F45, E6 ]	length: x1
[E1 , F25, F35, F45, E6 ]	[F15, E2 , E3 , E4 , F56]	length: -x1 + x2

-----Tree (G6)-----

involution: E1<-->F16 E2<-->F26 E3<-->F36 E4<-->F46 E5<-->F56		
[E1 , F26]	[F16, E2 , E3 , F36, E4 , F46, E5 , F56]	length: x1
[F16, E2 ]	[E1 , F26, E3 , F36, E4 , F46, E5 , F56]	length: x1
[E4 , F56]	[E1 , F16, E2 , F26, E3 , F36, F46, E5 ]	length: x3
[F46, E5 ]	[E1 , F16, E2 , F26, E3 , F36, E4 , F56]	length: x3
[E1 , F26, F46, E5 ]	[F16, E2 , E3 , F36, E4 , F56]	length: x2
[F16, E2 , E4 , F56]	[E1 , F26, E3 , F36, F46, E5 ]	length: x2
[E1 , F26, E3 , F46, E5 ]	[F16, E2 , F36, E4 , F56]	length: -x2 + x4

## Type (aaab)

-----Tree (E1)-----

involution: F12<-->G2 F13<-->G3 F14<-->G4 F15<-->G5 F16<-->G6		
[F13, G5 ]	[F12, G2 , G3 , F14, G4 , F15, F16, G6 ]	length: x2
[G3 , F15]	[F12, G2 , F13, F14, G4 , G5 , F16, G6 ]	length: x2
[F12, G3 , F15]	[G2 , F13, F14, G4 , G5 , F16, G6 ]	length: x4
[G2 , F13, G5 ]	[F12, G3 , F14, G4 , F15, F16, G6 ]	length: x4
[F12, G3 , F15, F16]	[G2 , F13, F14, G4 , G5 , G6 ]	length: x1
[G2 , F13, G5 , G6 ]	[F12, G3 , F14, G4 , F15, F16]	length: x1
[F12, G3 , G4 , F15, F16]	[G2 , F13, F14, G5 , G6 ]	length: -x1 + x3

-----Tree (E2)-----

involution: F12<-->G1 F23<-->G3 F24<-->G4 F25<-->G5 F26<-->G6		
[F12, F23]	[G1 , G3 , F24, G4 , F25, G5 , F26, G6 ]	length: x1
[G1 , G3 ]	[F12, F23, F24, G4 , F25, G5 , F26, G6 ]	length: x1
[F25, G6 ]	[F12, G1 , F23, G3 , F24, G4 , G5 , F26]	length: x3
[G5 , F26]	[F12, G1 , F23, G3 , F24, G4 , F25, G6 ]	length: x3
[F24, G5 , F26]	[F12, G1 , F23, G3 , G4 , F25, G6 ]	length: x4
[G4 , F25, G6 ]	[F12, G1 , F23, G3 , F24, G5 , F26]	length: x4
[F12, F23, G4 , F25, G6 ]	[G1 , G3 , F24, G5 , F26]	length: x2

-----Tree (E3)-----

involution: F13<-->G1 F23<-->G2 F34<-->G4 F35<-->G5 F36<-->G6		
[F13, G5 ]	[G1 , F23, G2 , F34, G4 , F35, F36, G6 ]	length: x2

[G1 , F35]	[F13, F23, G2 , F34, G4 , G5 , F36, G6 ]	length: x2
[F13, G2 , G5 ]	[G1 , F23, F34, G4 , F35, F36, G6 ]	length: x4
[G1 , F23, F35]	[F13, G2 , F34, G4 , G5 , F36, G6 ]	length: x4
[F13, G2 , G5 , G6 ]	[G1 , F23, F34, G4 , F35, F36]	length: x1
[G1 , F23, F35, F36]	[F13, G2 , F34, G4 , G5 , G6 ]	length: x1
[F13, G2 , F34, G5 , G6 ]	[G1 , F23, G4 , F35, F36]	length: -x1 + x3

-----Tree (E4)-----

involution: F14<-->G1	F24<-->G2	F34<-->G3	F45<-->G5	F46<-->G6	
[F14, F34]	[G1 , F24, G2 , G3 , F45, G5 , F46, G6 ]	length: x1			
[G1 , G3 ]	[F14, F24, G2 , F34, F45, G5 , F46, G6 ]	length: x1			
[F14, F34, G6 ]	[G1 , F24, G2 , G3 , F45, G5 , F46]	length: x4			
[G1 , G3 , F46]	[F14, F24, G2 , F34, F45, G5 , G6 ]	length: x4			
[F14, G2 , F34, G6 ]	[G1 , F24, G3 , F45, G5 , F46]	length: x2			
[G1 , F24, G3 , F46]	[F14, G2 , F34, F45, G5 , G6 ]	length: x2			
[F14, G2 , F34, G5 , G6 ]	[G1 , F24, G3 , F45, F46]	length: -x2 + x3			

-----Tree (E5)-----

involution: F15<-->G1	F25<-->G2	F35<-->G3	F45<-->G4	F56<-->G6	
[F15, G3 ]	[G1 , F25, G2 , F35, F45, G4 , F56, G6 ]	length: -x1 + x2			
[G1 , F35]	[F15, F25, G2 , G3 , F45, G4 , F56, G6 ]	length: -x1 + x2			
[F25, G6 ]	[F15, G1 , G2 , F35, G3 , F45, G4 , F56]	length: x3			
[G2 , F56]	[F15, G1 , F25, F35, G3 , F45, G4 , G6 ]	length: x3			
[F25, G4 , G6 ]	[F15, G1 , G2 , F35, G3 , F45, F56]	length: x4			
[G2 , F45, F56]	[F15, G1 , F25, F35, G3 , G4 , G6 ]	length: x4			
[F15, G1 , F35, G3 ]	[F25, G2 , F45, G4 , F56, G6 ]	length: x1			

-----Tree (E6)-----

involution: F16<-->G1	F26<-->G2	F36<-->G3	F46<-->G4	F56<-->G5	
[F16, F36]	[G1 , F26, G2 , G3 , F46, G4 , F56, G5 ]	length: x1			
[G1 , G3 ]	[F16, F26, G2 , F36, F46, G4 , F56, G5 ]	length: x1			
[F26, G5 ]	[F16, G1 , G2 , F36, G3 , F46, G4 , F56]	length: x3			
[G2 , F56]	[F16, G1 , F26, F36, G3 , F46, G4 , G5 ]	length: x3			
[F16, F36, G4 ]	[G1 , F26, G2 , G3 , F46, F56, G5 ]	length: x4			
[G1 , G3 , F46]	[F16, F26, G2 , F36, G4 , F56, G5 ]	length: x4			
[F16, G2 , F36, G4 , F56]	[G1 , F26, G3 , F46, G5 ]	length: x2			

-----Tree (F12)-----

involution: E1<-->G2	E2<-->G1	F34<-->F56	F35<-->F46	F36<-->F45	
[E1 , F34]	[G2 , E2 , G1 , F56, F35, F46, F36, F45]	length: x3			
[G2 , F56]	[E1 , E2 , G1 , F34, F35, F46, F36, F45]	length: x3			
[E2 , F46]	[E1 , G2 , G1 , F34, F56, F35, F36, F45]	length: x2			

[G1 , F35]	[E1 , G2 , E2 , F34, F56, F46, F36, F45]	length: x2
[E1 , F34, F36]	[G2 , E2 , G1 , F56, F35, F46, F45]	length: x4
[G2 , F56, F45]	[E1 , E2 , G1 , F34, F35, F46, F36]	length: x4
[E1 , G1 , F34, F35, F36]	[G2 , E2 , F56, F46, F45]	length: x1

-----Tree (F13)-----

involution: E1<-->G3	E3<-->G1	F24<-->F56	F25<-->F46	F26<-->F45	
[E1 , E3 ]	[G3 , G1 , F24, F56, F25, F46, F26, F45]				length: x1
[G3 , G1 ]	[E1 , E3 , F24, F56, F25, F46, F26, F45]				length: x1
[E1 , E3 , F25]	[G3 , G1 , F24, F56, F46, F26, F45]				length: x4
[G3 , G1 , F46]	[E1 , E3 , F24, F56, F25, F26, F45]				length: x4
[E1 , E3 , F56, F25]	[G3 , G1 , F24, F46, F26, F45]				length: x2
[G3 , G1 , F24, F46]	[E1 , E3 , F56, F25, F26, F45]				length: x2
[E1 , E3 , F56, F25, F26]	[G3 , G1 , F24, F46, F45]				length: -x2 + x3

-----Tree (F14)-----

involution: E1<-->G4	E4<-->G1	F23<-->F56	F25<-->F36	F26<-->F35	
[E4 , F26]	[E1 , G4 , G1 , F23, F56, F25, F36, F35]				length: x2
[G1 , F35]	[E1 , G4 , E4 , F23, F56, F25, F36, F26]				length: x2
[E4 , F56, F26]	[E1 , G4 , G1 , F23, F25, F36, F35]				length: x4
[G1 , F23, F35]	[E1 , G4 , E4 , F56, F25, F36, F26]				length: x4
[E4 , F56, F25, F26]	[E1 , G4 , G1 , F23, F36, F35]				length: x1
[G1 , F23, F36, F35]	[E1 , G4 , E4 , F56, F25, F26]				length: x1
[E1 , E4 , F56, F25, F26]	[G4 , G1 , F23, F36, F35]				length: -x1 + x3

-----Tree (F15)-----

involution: E1<-->G5	E5<-->G1	F23<-->F46	F24<-->F36	F26<-->F34	
[E1 , F34]	[G5 , E5 , G1 , F23, F46, F24, F36, F26]				length: x3
[G5 , F26]	[E1 , E5 , G1 , F23, F46, F24, F36, F34]				length: x3
[E1 , F36, F34]	[G5 , E5 , G1 , F23, F46, F24, F26]				length: x4
[G5 , F24, F26]	[E1 , E5 , G1 , F23, F46, F36, F34]				length: x4
[E1 , F23, F36, F34]	[G5 , E5 , G1 , F46, F24, F26]				length: x1
[G5 , F46, F24, F26]	[E1 , E5 , G1 , F23, F36, F34]				length: x1
[E1 , E5 , F23, F36, F34]	[G5 , G1 , F46, F24, F26]				length: -x1 + x2

-----Tree (F16)-----

involution: E1<-->G6	E6<-->G1	F23<-->F45	F24<-->F35	F25<-->F34	
[E1 , F34]	[G6 , E6 , G1 , F23, F45, F24, F35, F25]				length: x3
[G6 , F25]	[E1 , E6 , G1 , F23, F45, F24, F35, F34]				length: x3
[E6 , F24]	[E1 , G6 , G1 , F23, F45, F35, F25, F34]				length: x2
[G1 , F35]	[E1 , G6 , E6 , F23, F45, F24, F25, F34]				length: x2
[E6 , F45, F24]	[E1 , G6 , G1 , F23, F35, F25, F34]				length: x4



[G1 , F23, F35] [E1 , G6 , E6 , F45, F24, F25, F34] length: x4  
 [E1 , G1 , F23, F35, F34] [G6 , E6 , F45, F24, F25] length: x1

-----Tree (F23)-----

involution: E2<-->G3 E3<-->G2 F14<-->F56 F15<-->F46 F16<-->F45  
 [E2 , F46] [G3 , E3 , G2 , F14, F56, F15, F16, F45] length: x2  
 [G3 , F15] [E2 , E3 , G2 , F14, F56, F46, F16, F45] length: x2  
 [E3 , F14] [E2 , G3 , G2 , F56, F15, F46, F16, F45] length: x3  
 [G2 , F56] [E2 , G3 , E3 , F14, F15, F46, F16, F45] length: x3  
 [E3 , F14, F16] [E2 , G3 , G2 , F56, F15, F46, F45] length: x4  
 [G2 , F56, F45] [E2 , G3 , E3 , F14, F15, F46, F16] length: x4  
 [E2 , G2 , F56, F46, F45] [G3 , E3 , F14, F15, F16] length: x1

-----Tree (F24)-----

involution: E2<-->G4 E4<-->G2 F13<-->F56 F15<-->F36 F16<-->F35  
 [E4 , F13] [E2 , G4 , G2 , F56, F15, F36, F16, F35] length: x3  
 [G2 , F56] [E2 , G4 , E4 , F13, F15, F36, F16, F35] length: x3  
 [F15, F35] [E2 , G4 , E4 , G2 , F13, F56, F36, F16] length: x1  
 [F36, F16] [E2 , G4 , E4 , G2 , F13, F56, F15, F35] length: x1  
 [E2 , F15, F35] [G4 , E4 , G2 , F13, F56, F36, F16] length: x4  
 [G4 , F36, F16] [E2 , E4 , G2 , F13, F56, F15, F35] length: x4  
 [E2 , E4 , F13, F15, F35] [G4 , G2 , F56, F36, F16] length: x2

-----Tree (F25)-----

involution: E2<-->G5 E5<-->G2 F13<-->F46 F14<-->F36 F16<-->F34  
 [E2 , F46] [G5 , E5 , G2 , F13, F14, F36, F16, F34] length: x2  
 [G5 , F13] [E2 , E5 , G2 , F46, F14, F36, F16, F34] length: x2  
 [F14, F34] [E2 , G5 , E5 , G2 , F13, F46, F36, F16] length: x1  
 [F36, F16] [E2 , G5 , E5 , G2 , F13, F46, F14, F34] length: x1  
 [E2 , E5 , F46] [G5 , G2 , F13, F14, F36, F16, F34] length: x4  
 [G5 , G2 , F13] [E2 , E5 , F46, F14, F36, F16, F34] length: x4  
 [E2 , E5 , F46, F36, F16] [G5 , G2 , F13, F14, F34] length: x3

-----Tree (F26)-----

involution: E2<-->G6 E6<-->G2 F13<-->F45 F14<-->F35 F15<-->F34  
 [F14, F34] [E2 , G6 , E6 , G2 , F13, F45, F35, F15] length: x1  
 [F35, F15] [E2 , G6 , E6 , G2 , F13, F45, F14, F34] length: x1  
 [E2 , F35, F15] [G6 , E6 , G2 , F13, F45, F14, F34] length: x4  
 [G6 , F14, F34] [E2 , E6 , G2 , F13, F45, F35, F15] length: x4  
 [E2 , E6 , F35, F15] [G6 , G2 , F13, F45, F14, F34] length: x2  
 [G6 , G2 , F14, F34] [E2 , E6 , F13, F45, F35, F15] length: x2  
 [E2 , E6 , F45, F35, F15] [G6 , G2 , F13, F14, F34] length: -x2 + x3

## -----Tree (F34)-----

involution: E3<-->G4 E4<-->G3 F12<-->F56 F15<-->F26 F16<-->F25  
 [E4 , F26] [E3 , G4 , G3 , F12, F56, F15, F16, F25] length: x2  
 [G3 , F15] [E3 , G4 , E4 , F12, F56, F26, F16, F25] length: x2  
 [E4 , F56, F26] [E3 , G4 , G3 , F12, F15, F16, F25] length: x4  
 [G3 , F12, F15] [E3 , G4 , E4 , F56, F26, F16, F25] length: x4  
 [E4 , F56, F26, F25] [E3 , G4 , G3 , F12, F15, F16] length: x1  
 [G3 , F12, F15, F16] [E3 , G4 , E4 , F56, F26, F25] length: x1  
 [E3 , E4 , F56, F26, F25] [G4 , G3 , F12, F15, F16] length: -x1 + x3

## -----Tree (F35)-----

involution: E3<-->G5 E5<-->G3 F12<-->F46 F14<-->F26 F16<-->F24  
 [E3 , F14] [G5 , E5 , G3 , F12, F46, F26, F16, F24] length: x3  
 [G5 , F26] [E3 , E5 , G3 , F12, F46, F14, F16, F24] length: x3  
 [E3 , F14, F16] [G5 , E5 , G3 , F12, F46, F26, F24] length: x4  
 [G5 , F26, F24] [E3 , E5 , G3 , F12, F46, F14, F16] length: x4  
 [E3 , F12, F14, F16] [G5 , E5 , G3 , F46, F26, F24] length: x1  
 [G5 , F46, F26, F24] [E3 , E5 , G3 , F12, F14, F16] length: x1  
 [E3 , E5 , F12, F14, F16] [G5 , G3 , F46, F26, F24] length: -x1 + x2

## -----Tree (F36)-----

involution: E3<-->G6 E6<-->G3 F12<-->F45 F14<-->F25 F15<-->F24  
 [E3 , F14] [G6 , E6 , G3 , F12, F45, F25, F15, F24] length: x3  
 [G6 , F25] [E3 , E6 , G3 , F12, F45, F14, F15, F24] length: x3  
 [E6 , F24] [E3 , G6 , G3 , F12, F45, F14, F25, F15] length: x2  
 [G3 , F15] [E3 , G6 , E6 , F12, F45, F14, F25, F24] length: x2  
 [E6 , F45, F24] [E3 , G6 , G3 , F12, F14, F25, F15] length: x4  
 [G3 , F12, F15] [E3 , G6 , E6 , F45, F14, F25, F24] length: x4  
 [E3 , G3 , F12, F14, F15] [G6 , E6 , F45, F25, F24] length: x1

## -----Tree (F45)-----

involution: E4<-->G5 E5<-->G4 F12<-->F36 F13<-->F26 F16<-->F23  
 [E4 , F13] [G5 , E5 , G4 , F12, F36, F26, F16, F23] length: -x2 + x3  
 [G5 , F26] [E4 , E5 , G4 , F12, F36, F13, F16, F23] length: -x2 + x3  
 [F12, F23] [E4 , G5 , E5 , G4 , F36, F13, F26, F16] length: x1  
 [F36, F16] [E4 , G5 , E5 , G4 , F12, F13, F26, F23] length: x1  
 [E5 , F12, F23] [E4 , G5 , G4 , F36, F13, F26, F16] length: x4  
 [G4 , F36, F16] [E4 , G5 , E5 , F12, F13, F26, F23] length: x4  
 [E4 , G5 , F13, F26] [E5 , G4 , F12, F36, F16, F23] length: x2

## -----Tree (F46)-----

involution: E4<-->G6 E6<-->G4 F12<-->F35 F13<-->F25 F15<-->F23  
 [E4 , F13] [G6 , E6 , G4 , F12, F35, F25, F15, F23] length: x3  
 [G6 , F25] [E4 , E6 , G4 , F12, F35, F13, F15, F23] length: x3  
 [F12, F23] [E4 , G6 , E6 , G4 , F35, F13, F25, F15] length: x1  
 [F35, F15] [E4 , G6 , E6 , G4 , F12, F13, F25, F23] length: x1  
 [E4 , E6 , F13] [G6 , G4 , F12, F35, F25, F15, F23] length: x4  
 [G6 , G4 , F25] [E4 , E6 , F12, F35, F13, F15, F23] length: x4  
 [E4 , E6 , F35, F13, F15] [G6 , G4 , F12, F25, F23] length: x2

-----Tree (F56)-----

involution: E5<-->G6 E6<-->G5 F12<-->F34 F13<-->F24 F14<-->F23  
 [E6 , F24] [E5 , G6 , G5 , F12, F34, F13, F14, F23] length: x2  
 [G5 , F13] [E5 , G6 , E6 , F12, F34, F24, F14, F23] length: x2  
 [F12, F23] [E5 , G6 , E6 , G5 , F34, F13, F24, F14] length: x1  
 [F34, F14] [E5 , G6 , E6 , G5 , F12, F13, F24, F23] length: x1  
 [E5 , F12, F23] [G6 , E6 , G5 , F34, F13, F24, F14] length: x4  
 [G6 , F34, F14] [E5 , E6 , G5 , F12, F13, F24, F23] length: x4  
 [E5 , E6 , F12, F24, F23] [G6 , G5 , F34, F13, F14] length: x3

-----Tree (G1)-----

involution: E2<-->F12 E3<-->F13 E4<-->F14 E5<-->F15 E6<-->F16  
 [E3 , F14] [E2 , F12, F13, E4 , E5 , F15, E6 , F16] length: x3  
 [F13, E4 ] [E2 , F12, E3 , F14, E5 , F15, E6 , F16] length: x3  
 [E3 , F14, F16] [E2 , F12, F13, E4 , E5 , F15, E6 ] length: x4  
 [F13, E4 , E6 ] [E2 , F12, E3 , F14, E5 , F15, F16] length: x4  
 [E2 , F13, E4 , E6 ] [F12, E3 , F14, E5 , F15, F16] length: x1  
 [F12, E3 , F14, F16] [E2 , F13, E4 , E5 , F15, E6 ] length: x1  
 [E2 , F13, E4 , F15, E6 ] [F12, E3 , F14, E5 , F16] length: -x1 + x2

-----Tree (G2)-----

involution: E1<-->F12 E3<-->F23 E4<-->F24 E5<-->F25 E6<-->F26  
 [E1 , E3 ] [F12, F23, E4 , F24, E5 , F25, E6 , F26] length: x1  
 [F12, F23] [E1 , E3 , E4 , F24, E5 , F25, E6 , F26] length: x1  
 [E4 , F26] [E1 , F12, E3 , F23, F24, E5 , F25, E6 ] length: x2  
 [F24, E6 ] [E1 , F12, E3 , F23, E4 , E5 , F25, F26] length: x2  
 [E1 , E3 , F25] [F12, F23, E4 , F24, E5 , E6 , F26] length: x4  
 [F12, F23, E5 ] [E1 , E3 , E4 , F24, F25, E6 , F26] length: x4  
 [E1 , E3 , E4 , F25, F26] [F12, F23, F24, E5 , E6 ] length: x3

-----Tree (G3)-----

involution: E1<-->F13 E2<-->F23 E4<-->F34 E5<-->F35 E6<-->F36  
 [E1 , F34] [F13, E2 , F23, E4 , E5 , F35, E6 , F36] length: x3

[F13, E4 ]	[E1 , E2 , F23, F34, E5 , F35, E6 , F36]	length: x3
[E1 , F34, F36]	[F13, E2 , F23, E4 , E5 , F35, E6 ]	length: x4
[F13, E4 , E6 ]	[E1 , E2 , F23, F34, E5 , F35, F36]	length: x4
[E1 , F23, F34, F36]	[F13, E2 , E4 , E5 , F35, E6 ]	length: x1
[F13, E2 , E4 , E6 ]	[E1 , F23, F34, E5 , F35, F36]	length: x1
[E1 , F23, F34, E5 , F36]	[F13, E2 , E4 , F35, E6 ]	length: -x1 + x2

-----Tree (G4)-----

involution: E1<-->F14 E2<-->F24 E3<-->F34 E5<-->F45 E6<-->F46		
[E1 , F34]	[F14, E2 , F24, E3 , E5 , F45, E6 , F46]	length: -x1 + x3
[F14, E3 ]	[E1 , E2 , F24, F34, E5 , F45, E6 , F46]	length: -x1 + x3
[E2 , F46]	[E1 , F14, F24, E3 , F34, E5 , F45, E6 ]	length: x2
[F24, E6 ]	[E1 , F14, E2 , E3 , F34, E5 , F45, F46]	length: x2
[E2 , E5 , F46]	[E1 , F14, F24, E3 , F34, F45, E6 ]	length: x4
[F24, F45, E6 ]	[E1 , F14, E2 , E3 , F34, E5 , F46]	length: x4
[E1 , F14, E3 , F34]	[E2 , F24, E5 , F45, E6 , F46]	length: x1

-----Tree (G5)-----

involution: E1<-->F15 E2<-->F25 E3<-->F35 E4<-->F45 E6<-->F56		
[E1 , E3 ]	[F15, E2 , F25, F35, E4 , F45, E6 , F56]	length: x1
[F15, F35]	[E1 , E2 , F25, E3 , E4 , F45, E6 , F56]	length: x1
[E1 , F25, E3 ]	[F15, E2 , F35, E4 , F45, E6 , F56]	length: x4
[F15, E2 , F35]	[E1 , F25, E3 , E4 , F45, E6 , F56]	length: x4
[E1 , F25, E3 , F56]	[F15, E2 , F35, E4 , F45, E6 ]	length: x2
[F15, E2 , F35, E6 ]	[E1 , F25, E3 , E4 , F45, F56]	length: x2
[E1 , F25, E3 , E4 , F56]	[F15, E2 , F35, F45, E6 ]	length: -x2 + x3

-----Tree (G6)-----

involution: E1<-->F16 E2<-->F26 E3<-->F36 E4<-->F46 E5<-->F56		
[E1 , E3 ]	[F16, E2 , F26, F36, E4 , F46, E5 , F56]	length: x1
[F16, F36]	[E1 , E2 , F26, E3 , E4 , F46, E5 , F56]	length: x1
[E2 , F46]	[E1 , F16, F26, E3 , F36, E4 , E5 , F56]	length: x2
[F26, E4 ]	[E1 , F16, E2 , E3 , F36, F46, E5 , F56]	length: x2
[E2 , F46, E5 ]	[E1 , F16, F26, E3 , F36, E4 , F56]	length: x4
[F26, E4 , F56]	[E1 , F16, E2 , E3 , F36, F46, E5 ]	length: x4
[E1 , F26, E3 , E4 , F56]	[F16, E2 , F36, F46, E5 ]	length: x3